# Identification of genetic regulators of transcellular chaperone signalling in *C. elegans*

**Jay Jo Miles**

Submitted in accordance with the requirements for the degree of
Doctor of Philosophy

The University of Leeds
School of Molecular and Cellular Biology

April 2020

The candidate confirms that the work submitted is their own, except where work which has formed part of jointly authored publications has been included. The contribution of the candidate and the other authors to this work has been explicitly indicated below. The candidate confirms that appropriate credit has been given within the thesis where reference has been made to the work of others.

Some of the work shown in **Chapter 6** of the thesis has appeared in publication as follows:

Miles J., van Oosten-Hawle P.; 2020. Tissue-specific RNAi tools to identify components for systemic stress signalling. *J. Vis. Exp.* 159, e61357

My contribution to this work was to perform tissue-specific RNAi screening and associated data analysis in the *hsp-90*$^{int}$ hp-RNAi strain. The contribution of Patricija van Oosten-Hawle to this work was its conceptualisation and methodology; writing, reviewing and editing the article; and performing experimental work other than the tissue-specific RNAi screen, which included generation of the hairpin RNAi construct and tissue-specific knockdown strains as well as Q44 aggregation assays.

# Acknowledgements

I am very grateful to Dr Patricija van Oosten-Hawle for the opportunity to be part of her research group; her supervision throughout the project I have enjoyed working on for the past three-and-a-half years; and her support and guidance. One's supervisor is arguably one of the strongest influences on whether a PhD is a positive experience, and I have enjoyed my time working in the van Oosten-Hawle group immensely. I would like to thank the other members of the group for their friendship and support, and for being so enjoyable to work with. In particular, I would like to acknowledge Sarah Good and Daniel O'Brien. I suspect that karaoke in the worm room is a memory that will last a lifetime (in a good way). Thanks also to colleagues in Garstang 8.53 for making it such a friendly working environment. I am grateful to my co-supervisor Professor David Westhead for his advice on bioinformatic analysis, his perspectives on my project, and his feedback and advice on draft work for my thesis. In addition, I would like to acknowledge Professor Ian Hope for his support.

I would like to thank the Medical Research Council for funding this research in the form of a Discovery Medicine North (DiMeN) Doctoral Training Programme scholarship, and Dr Emily Goodall as the DiMeN DTP co-ordinator. I would also like to thank Dr Richard Morimoto (Northwestern University, USA) for kindly gifting the AM722 and AM994 *C. elegans* strains.

Finally, I would like to acknowledge and thank my family and friends, without whose support this would not have been possible.

# Abstract

The maintenance of a functional proteome is key to cellular health. Because of this, cells have developed highly conserved protective mechanisms termed stress responses, which act to promote proteostasis. Stress responses have conventionally been considered from a cell-autonomous perspective. However, increasing evidence shows that they can also act in a cell-non-autonomous manner to influence systemic proteostasis. An example of this is transcellular chaperone signalling (TCS) in the nematode *C. elegans*, which is activated by tissue-specific perturbations in expression of the chaperone *hsp-90*. Activation of TCS by tissue-specific depletion of *hsp-90* leads to inter-tissue upregulation of the chaperone *hsp-70* and confers organismal benefits such as improved heat stress resistance. However, the mechanisms underlying TCS activation in this manner are currently not well characterised.

In order to better understand TCS, this study took a dual approach using strains in which *hsp-90* is constitutively knocked down either in the intestine or pan-neuronally. Firstly, the organismal effects of TCS activation were investigated through whole-organism transcriptome profiling, enabling identification of genes which are differentially expressed in these strains. The second approach aimed to identify genes required for transcellular *hsp-70* upregulation, which might indicate a specific intercellular pathway. This involved a forward genetic screen with whole-genome sequencing and SNP mapping in the strain harbouring intestine-specific *hsp-90* knockdown. To further investigate genes identified by these approaches, a tissue-specific RNAi screen was then performed in the same strain. This confirmed 29 genes as tissue-specific modulators of TCS, subsequently denoted TCS cross (X)-Tissue (*txt*) genes. Furthermore, bioinformatics in combination with functional genetic analysis and survival assays identified a potential mechanism for *hsf-1*-independent *hsp-70* upregulation, in a proposed pathway involving the PDZ domain protein *C50D2.3* and the transcription factor *ceh-58*. This brings us closer to understanding the signalling pathways underlying TCS, and the potential benefits of activating organismal proteostasis mechanisms.

# Table of Contents

# List of Figures

# List of Tables

# Abbreviations

| | |
|---|---|
| Aß | Amyloid beta |
| bp | Base pairs |
| CFP | Cyan fluorescent protein |
| CGC | *Caenorhabditis* genetics centre |
| DAE | DAF-16-associated element |
| DBE | DAF-16-binding element |
| DCV | Dense core vesicle |
| DEG | Differentially expressed gene |
| dsRNA | Double-stranded RNA |
| ECM | Extracellular matrix |
| EDTA | Ethylenediamine tetra-acetic acid |
| EMS | Ethyl methanesulfonate |
| ER | Endoplasmic reticulum |
| ETC | Electron transport chain |
| FC | Fold-change |
| FDR | False discovery rate |
| gDNA | Genomic DNA |
| GO | Gene ontology |
| GPCR | G protein-coupled receptor |
| HLH | Helix-loop-helix |
| hp-RNAi | Hairpin RNAi |
| HS | Heat shock |
| HSE | Heat shock element |
| HSP | Heat shock protein |
| HSR | Heat shock response |
| ILS | Insulin-like signalling |
| IPR | Intracellular pathogen response |
| IPTG | Isopropyl ß-d-1-thiogalactopyranoside |
| LB | Lysogeny broth |
| NGM | Nematode growth medium |
| PCR | Polymerase chain reaction |
| polyQ | Polyglutamine |

| | |
|---|---|
| PTM | Post-translational modification |
| qRT-PCR | Quantitative reverse transcription PCR |
| RFP | Red fluorescent protein |
| RIN | RNA integrity number |
| RNAi | RNA interference |
| RNA-Seq | RNA sequencing |
| ROS | Reactive oxygen species |
| SC | Subcellular |
| SCV | Small clear vesicle |
| SEM | Standard error of the mean |
| sHSP | Small heat shock protein |
| SNP | Single nucleotide polymorphism |
| TCS | Transcellular chaperone signalling |
| TF | Transcription factor |
| TM | Transmembrane |
| UPR | Unfolded protein response |
| $UPR^{ER}$ | UPR of the endoplasmic reticulum |
| $UPR^{Mt}$ | UPR of the mitochondria |
| WGS | Whole-genome sequencing |
| YFP | Yellow fluorescent protein |

*"In every object there is inexhaustible meaning;*
*the eye sees in it what the eye brings means of seeing."*

Thomas Carlyle (Attrib.)

# Chapter 1. Introduction

## 1.1 Overview and context

Stress, considered in the sense of the perturbation of homeostasis, is something with which all organisms must contend (Chrousos et al. 1988; Chrousos 2009). Stressors may come in a variety of forms including physical, chemical, physiological, immunological and psychological. To ensure survival, organisms have developed stress responses: mechanisms which detect and respond to various stressors in order to maintain organismal health, and which are often conserved between species (Lindquist & Craig 1988; Jovaisaite et al. 2014; Loboda et al. 2016). The key stressor considered in this thesis is the perturbation of protein homeostasis (proteostasis). Proteostasis, or the maintenance of a functional proteome, encompasses a wide range of processes including the synthesis, folding, maintenance and degradation of all the proteins needed for an organism to function (Balch et al. 2008). The perturbation of proteostasis can be stressful for several reasons – there may be insufficient or surplus levels of specific proteins, which may adversely affect the efficiency of cellular pathways; or proteins may occupy non-native folding states which promote aggregation. If left unrectified, defects in proteostasis can lead to diseases such as cystic fibrosis or Alzheimer's disease in humans (Powers et al. 2009). However, several stress responses such as the heat shock response (HSR) and the unfolded protein responses of the endoplasmic reticulum or mitochondria ($UPR^{ER}$ and $UPR^{Mt}$) function to detect proteostatic imbalances and restore proteostasis (Åkerfeld et al. 2010; Walter & Ron 2011; Shpilka & Haynes 2018). This can be achieved through decreasing protein synthesis, increasing levels of protein-folding chaperone proteins, or increasing the degradation of surplus or misfolded proteins (Balch et al. 2008).

Conventionally, these responses to proteotoxic stress have been considered at the cell-autonomous level. However, increasing evidence shows that they also utilise cell-non-autonomous signalling pathways (Durieux et al. 2011; Taylor & Dillin 2013; van Oosten-Hawle et al. 2013), and that this signalling has implications for other processes such as longevity and the immune response. One such cell-non-autonomous stress response is transcellular chaperone signalling (TCS) in the nematode *Caenorhabditis elegans*, which is activated by tissue-specific perturbations in the chaperone protein *hsp-90* (van Oosten-Hawle et al. 2013).

Activation of TCS not only causes cell-non-autonomous upregulation of chaperone proteins in non-targeted tissues, but can also confer benefits such as increased stress resistance or an improved protein-folding environment (van Oosten-Hawle et al. 2013; O'Brien et al. 2018). This indicates that activation of cell-non-autonomous stress signalling can result in whole-organism benefits, raising intriguing possibilities concerning stress responses in humans. However, the mechanisms underlying TCS remain unclear. To better understand this cell-non-autonomous process, this research aimed to both characterise the organismal consequences of TCS activation and to identify genes involved in its intercellular signalling pathways. The research was carried out in *C. elegans* as although there is evidence that cell-non-autonomous stress signalling occurs in mammals (Fawcett et al. 1994; Williams et al. 2014), TCS has not yet been specifically shown to occur in other organisms. In addition, this species possesses only one cytosolic *hsp-90* (Brehme et al. 2014), negating the potential problem of redundancy.

## 1.2 *C. elegans* as a model organism

Since the pioneering work of Sidney Brenner in the early 1970s, the nematode *Caenorhabditis elegans* has become one of the most thoroughly characterised model organisms available (Brenner 1974; Sulston & Brenner 1974). By the mid-1980s, the complete *C. elegans* cell lineage was described and the structure of the entire nervous system recorded (Sulston & Horvitz 1976; Sulston et al. 1983; White et al. 1986). In 1998 the species became the first multicellular organism to have its entire genome sequenced (The *C. elegans* Sequencing Consortium 1998). The popularity of this organism as a model for genetics, development and neurobiology owes much to its ease of propagation and genetic tractability, and its utility as an intermediate between *in vitro* studies and more complex *in vivo* systems. Its relative simplicity enables the study of basic cellular mechanisms whilst still set in the context of a multi-tissue organism, a feature which has been key to this research on cell-non-autonomous proteostasis.

### 1.2.1 Key anatomical features and life cycle

*C. elegans* are transparent nematodes which feed on bacteria and can be isolated in the field from rotting plant matter (Félix & Duveau 2012). They grow to a maximum length of roughly 1mm, which whilst advantageous for large-scale propagation necessitates microscopy for visualisation. Their transparency is highly useful, as both internal anatomical features and the expression of transgenic fluorescent proteins can be viewed *in vivo* in real-time. Despite their small size, they possess distinct digestive, reproductive, nervous, muscular and epidermal systems (**Fig. 1.1**). Bacteria are ingested through the mouth and undergo grinding in the pharynx, before passing through the intestine and excretion via the anus. The intestine, a tube formed from ten pairs of large epithelial cells, is an important tissue in the immune response due to its exposure to ingested bacteria; it can be colonised by pathogenic species such as *Pseudomonas aeruginosa* or *Enterococcus faecalis* (Tan et al. 1999; Garsin et al. 2001).

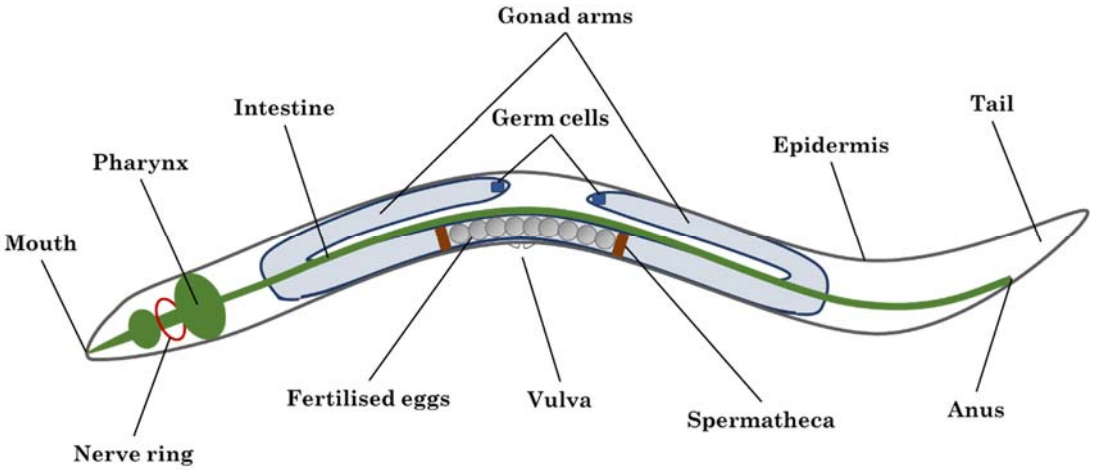


**Figure 1.1 Selected anatomical features of adult hermaphrodite *C. elegans*.** Bacterial food source is ingested through the mouth and undergoes grinding in the pharynx, before passing through the intestine and excretion via the anus. The intestine lies alongside the gonad, which consists of two arms that meet at a central vulva. Proliferating germ cells at the tips of the gonad arms develop into oocytes as they progress towards the vulva, and are fertilised upon passing through the spermatheca.

In mature *C. elegans*, the nervous system comprises 302 neurons in hermaphrodites and 385 in males (White et al. 1986; Sammut et al. 2015). Many neuronal cell bodies are grouped together in ganglia near the pharynx or rectum, with the main neuropil forming a nerve ring around the pharynx and other nerve processes extending longitudinally through the animal as dorsal and ventral nerve cords. At 25°C, wild-type *C. elegans* eggs develop into gravid adults in approximately 3 days, allowing many generations to be studied over a short timescale (Brenner 1974). In conditions favourable for reproductive development, namely abundant food and low population density, an egg will hatch into the first larval stage (L1) and progress through stages L2-L4 before development into a reproductively fertile adult (**Fig. 1.2**). However, in the absence of food, animals arrest development; either remaining in L1 stage if no food is available upon hatching, or developing into a long-lived, stress-resistant alternative L3 stage termed 'dauer' (Cassada & Russell 1975; Hong et al. 1998). Animals in dauer state may subsequently resume development and progress to L4 if conditions improve.

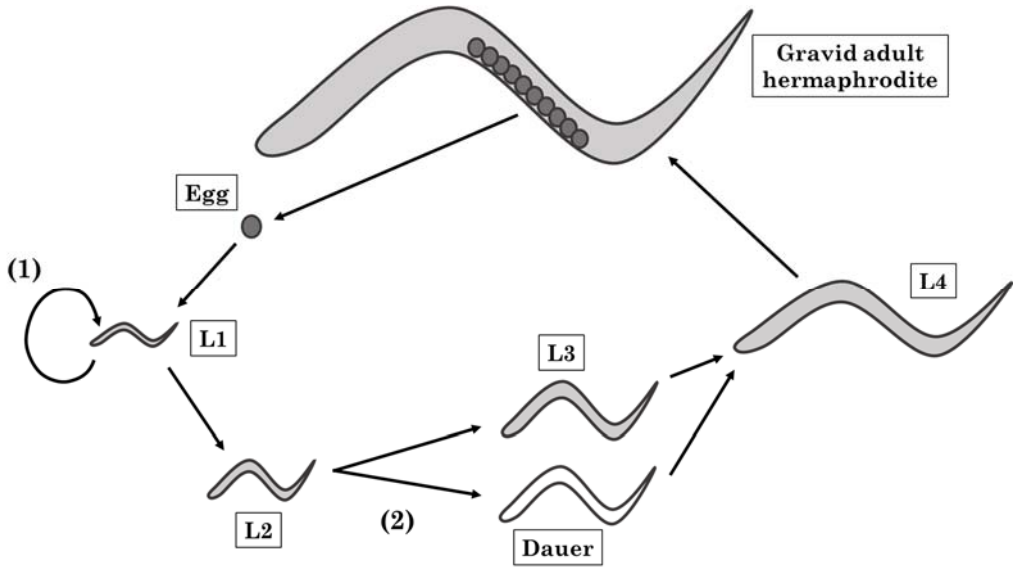


**Figure 1.2 Life cycle of self-fertilising *C. elegans* hermaphrodite**. Eggs hatch into L1 stage, where they arrest in the absence of food (**1**). If conditions are favourable, larvae progress through development into reproductively fertile adults. If not, larvae progress from L2 into an alternative L3 stage called dauer state (**2**).

*C. elegans* are sexually androdioecious. The species consists of hermaphrodites, which are diploid for the X chromosome (XX), and males, which are haploid for it (XO) (Nigon & Dougherty 1949). The gonad, which consists of two arms in hermaphrodites and one in males, lies alongside the intestine. Germline cells proliferate at the ends of gonad arms in response to signals from distal tip cells (DTCs), which maintain the proliferating cells in a pre-meiotic state (Kimble & White 1981). Germ cells mature as they progress along the gonad arms. In males or L4 hermaphrodites, germ cells undergo spermatogenesis, whilst in adult hermaphrodites they undergo oogenesis (Hirsh et al. 1976; L'Hernault 2009). Sperm produced by L4 hermaphrodites are stored in the spermatheca, and subsequently used to fertilise eggs produced during the adult stage. Alternatively, oocytes produced by a hermaphrodite may be fertilised by mating with a male, which benefits the population through greater genetic variability (**Fig. 1.3**). However, males occur at very low frequencies in wild-type populations, generally at a rate below 0.2% (Nigon & Dougherty 1949; Hodgkin et al. 1979). In a wild-type population of self-fertilising hermaphrodites, males will only rarely arise, as generation of an XO egg requires spontaneous non-disjunction of the X chromosome (Anderson et al. 2010). However, elevated temperature leads to a higher rate of non-disjunction, increasing the prevalence of male progeny (Nigon & Dougherty 1949; Rose & Baillie 1979).

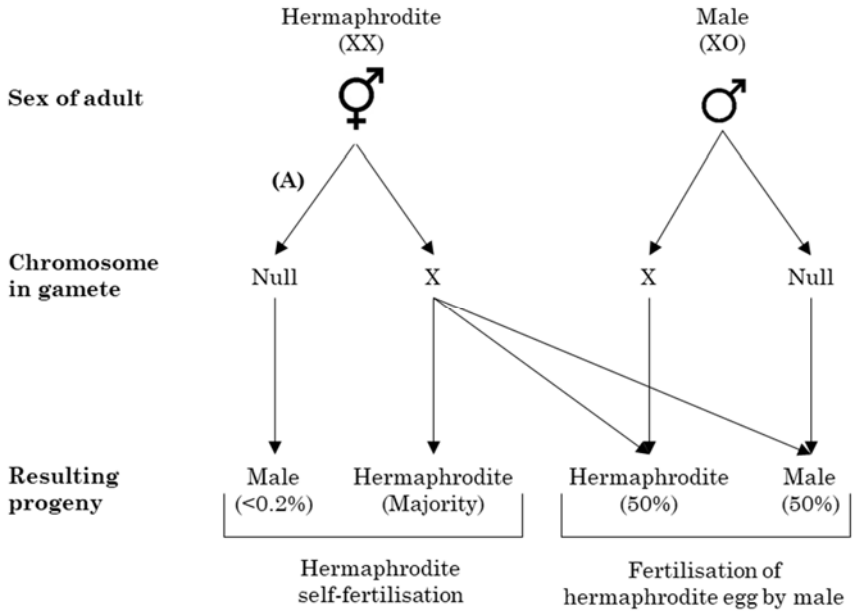


**Figure 1.3 Sex determination of *C. elegans* progeny**. Self-fertilisation of eggs in hermaphrodites produces a majority of hermaphrodite progeny, but males can also arise infrequently through spontaneous X chromosome non-disjunction (**A**). Eggs fertilised by mating with a male have an equal probability of being hermaphrodite or male.

### 1.2.2 Manipulating gene expression in *C. elegans*

The *C. elegans* genome contains approximately 20,000 protein-coding genes and is over 100 megabases long (WormBase release WS277, 2020; The *C. elegans* Sequencing Consortium 1998). Both males and hermaphrodites are diploid for the five autosomal chromosomes (Nigon & Dougherty 1949), in which genes tend to be clustered more densely in the central regions and more sparsely in the arms (Brenner 1974; Kamath et al. 2003). Mutations can be introduced to the genome with relative ease. This may be done randomly, by exposure to mutagens such as ethyl methanesulfonate (EMS); or through targeted genome editing using a method such as CRISPR-Cas9. Alternatively, DNA constructs containing transgenes may be injected directly into the proliferating germline, where they are taken up into oocyte nuclei (Stinchcomb et al. 1985). Transgenes taken up in this manner are then expressed as heritable extrachromosomal arrays, although the exogenous DNA will only be transmitted to a fraction of progeny. Since hermaphrodites are capable of self-fertilising, populations carrying a mutation of interest can be maintained by phenotype selection without the need for mating.

A key feature of *C. elegans* biology which enables temporally controlled gene knockdown is systemic RNA interference (RNAi), in which application of transcript-specific double-stranded RNA (dsRNA) results in silencing of the relevant transcript throughout the organism (Fire et al. 1998; Tabara et al. 1998; Timmons & Fire 1998). This silencing is post-transcriptional and mediated by sequence-specific mRNA degradation (Montgomery et al. 1998). Such RNAi can be applied by feeding with bacteria which express the RNAi construct, creating transgenic animals which express RNAi under an endogenous promoter, soaking animals in a solution of RNAi, or injecting it directly into tissues. Applied RNAi is transmitted throughout the organism in a manner dependent on the protein SID-1, a transmembrane dsRNA transporter which facilitates cellular dsRNA uptake (Winston et al. 2002; Feinberg & Hunter 2003). Animals lacking functional SID-1, such as *sid-1* (pk3321) mutants, are unable to take up exogenous RNAi or transmit dsRNA between tissues (Winston et al. 2002). The requirement for SID-1 in systemic RNAi facilitates the creation of transgenic strains displaying tissue-specific gene knockdown. If dsRNA is expressed under the control of a tissue-specific promoter in animals lacking functional SID-1, gene silencing will be restricted to the tissue in which dsRNA is expressed (Jose et al. 2009). Furthermore, RNAi by bacterial feeding can also be restricted to specific tissues. Transgenic overexpression of SID-1 under the control of a tissue-specific promoter, in a *sid-1* mutant background, facilitates uptake of ingested dsRNA into only the tissue expressing functional SID-1 (Jose et al. 2009). However, not all tissues are equally susceptible to systemic RNAi transmission, with neuronally-expressed genes more difficult to silence (Tavernarakis et al. 2000; Timmons et al. 2001; Kamath et al. 2001). This is thought to be due to reduced expression of SID-1 in most neurons, and indeed neuronal overexpression of *sid-1* renders these cells sensitive to RNAi by feeding (Winston et al. 2002; Calixto et al. 2010).

## 1.3 Proteostasis in *C. elegans*

### 1.3.1 The importance of a functional proteostasis network

In a dynamic environment, maintaining or restoring conditions for normal cellular function is vitally important. As proteins are involved in the vast majority of cellular activities, the production and maintenance of a functional proteome is a key aspect of this. This is referred to as protein homeostasis (proteostasis). Since protein function is determined by structure, molecular challenges such as extreme temperature or pH, reactive oxygen species, radiation, chemicals, or infection can adversely impact the proteome. Even in an optimal environment it is necessary to constantly regulate protein folding and maintenance, as misfolded proteins can give rise to a wide variety of deleterious conditions such as Alzheimer's disease or cystic fibrosis in humans (Cohen & Kelly 2003). Protein structure is therefore controlled at every stage by a network of molecular mechanisms referred to as the proteostasis network. This network regulates the production of new proteins to meet cellular needs, their maintenance in functional conformations, and the degradation of those which are irreparably misfolded or aggregated. Proteins may be degraded through one of several mechanisms, including the ubiquitin-proteasome system (UPS) (Hershko & Ciechanover 1998; Nandi et al. 2006) or autophagy (Seglen & Bohley 1992; Meléndez & Levine 2009).

Regulation of protein conformation is a key element of proteostasis and is mediated by proteins called molecular chaperones. Chaperone-mediated protein folding can occur post-translationally, if existing proteins occupy non-native conformations; or co-translationally, as nascent polypeptide chains are produced (Fink 1999; Hartl et al. 2011). Chaperones often recognise and bind to exposed hydrophobic amino acids in unfolded or partly folded polypeptides. Once bound, they then mediate folding of the polypeptide chain via ATP hydrolysis, often in conjunction with cofactors such as co-chaperones (Kim et al. 2013(a)). However, increased protein misfolding during challenges such as heat stress leads to a higher requirement for chaperone proteins (Wallace et al. 2015; Poppek & Grune 2006). Cells have therefore developed conserved pathways termed stress responses, one function of which is to increase expression of chaperone proteins when activated by specific stimuli. Such stress responses include the heat shock response (HSR) (Åkerfeld et al. 2010), unfolded protein response of the endoplasmic reticulum ($UPR^{ER}$) (Walter & Ron 2011), and

unfolded protein response of the mitochondria ($UPR^{Mt}$) (Shpilka & Haynes 2018). These stress pathways respond to the presence of misfolded proteins in various subcellular compartments (Lindquist 1986; Kozutsumi et al. 1988; Zhao et al. 2002) and are highly evolutionarily conserved, with the key proteins involved represented not only in humans and *C. elegans* but many other eukaryotes (Lindquist 1986; Powers & Balch 2013). The HSR, $UPR^{ER}$ and $UPR^{Mt}$ have been well-characterised at the cell-autonomous level. However, over the past decade increasing evidence has shown that they also have cell-non-autonomous roles which impact longevity, immunity, and the organismal protein folding environment (Taylor et al. 2014; O'Brien & van Oosten-Hawle 2016; Miles et al. 2019).

### 1.3.2 Cell-autonomous stress responses

#### 1.3.2.1 The heat shock response (HSR)

Proteins are capable of occupying multiple different structural conformations and shift between them in a highly energy-dependent manner. Temperature is therefore a significant influence on protein structure (Frauenfelder et al. 1991). Increasing temperature can promote structural changes to non-native states, exposing hydrophobic amino acids and potentially enabling aggregation (Chiti & Dobson 2009). It is therefore important for cells to increase expression of chaperones upon increased temperature, a process mediated via a mechanism called the heat shock response (HSR) (**Fig. 1.4**; Ritossa 1962; Lindquist 1986).

The key co-ordinator of the HSR is the transcription factor Heat Shock Factor 1 (HSF-1), which under non-stressful conditions is sequestered in an inactive monomeric form (Baler et al. 1993; Sarge et al. 1993). Repression of HSF-1 activity is mediated by conserved chaperones including HSP-90 and HSP-70 family members, which are thought to form a multichaperone complex with monomeric HSF-1 to inhibit its activation (Nair et al. 1996; Bharadwaj et al. 1999; Guo et al. 2001; Åkerfeld et al. 2010). Whilst association with HSP-90 prevents trimerisation and DNA binding by HSF-1, HSP-70 family chaperones repress its transactivation activity (Ali et al. 1998; Shi et al. 1998; Zou et al. 1998). In the presence of non-native proteins, such as during heat stress, these chaperones dissociate from HSF-1 to mediate protein refolding (Ananthan et al. 1986; Zou et al. 1998). This enables HSF-1 to trimerise, become active as a transcriptional regulator, and translocate to the nucleus, where it binds to heat shock elements (HSEs) in the promoters of heat shock

response genes (Baler et al. 1993; Sarge et al. 1993). HSEs take the form of inverted nGAAn repeats and are highly conserved throughout species (Pelham 1985; Lindquist 1986). Genes upregulated by HSF-1 in response to heat shock are termed heat shock proteins (HSPs) and include numerous chaperones such as HSP-70 and small HSPs (Lindquist 1986). The strong upregulation of chaperone protein expression mediated by HSF-1 promotes increased protein folding in the cell and a return to proteostasis, followed by negative feedback on HSF-1 exerted by excess chaperones (Voellmy & Boellman 2007).

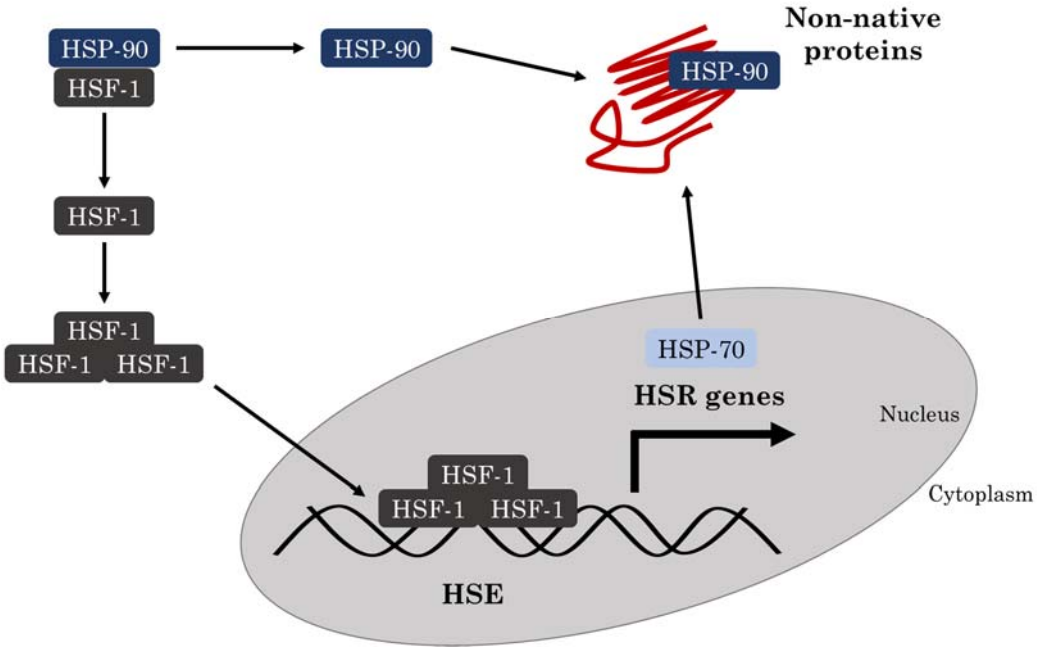


**Figure 1.4 The heat shock response (HSR)**. The transcription factor HSF-1 is normally sequestered in the cytosol by a multichaperone complex containing HSP-90. In the presence of misfolded proteins, HSP-90 dissociates to mediate refolding. HSF-1 can then trimerise, translocate to the nucleus, and bind to heat shock elements in the promoters of heat shock response genes. This promotes upregulation of chaperones such as HSP-70, which contribute to the refolding of misfolded proteins.

*C. elegans* possesses a single functional heat shock factor (HSF-1) and a single cytosolic HSP-90; but six cytosolic HSP-70 family chaperones (Brehme et al. 2014). Of these six, HSP-1 and the disaggregase HSP-110 are constitutively expressed across life stages; whilst HSP-70, F44E5.4, and F44E5.5 are not normally expressed but are heat-inducible (GuhaThakurta et al. 2002; Guisbert et al. 2013). The final cytosolic HSP-70 family member, F11F1.1, is neither constitutively expressed nor

heat-inducible; little is known of its function, but it has been suggested to be ribosomally attached (Sun et al. 2012 (a)).

Whilst dissociation of regulatory chaperones is required for HSF-1 activation, its activity is also strongly dependent on post-translational modifications (PTMs)(Berk 1989). Human HSF1 has been shown to be regulated by a combination of phosphorylation, acetylation, and SUMOylation; with the PTM 'code' determining the ability to associate with HSP90, bind DNA, or mediate transcriptional activation of heat shock response genes (Xu et al. 2012). There is therefore a great deal of scope for other cellular signalling pathways which utilise PTMs to interact with the HSR. For example, it has been shown in human cell tissue culture that the kinase Target of Rapamycin (TOR), which regulates autophagy in response to nutrient deprivation, also phosphorylates HSF1 upon heat stress to enable its activation (Bhaskar & Hay 2007; Chou et al. 2012).

An important concept relating to the HSR is the HSP-90 capacitor hypothesis. HSP-90 is a ubiquitously expressed chaperone which is considered a 'hub' protein; that is, it has many known interaction partners and is important for cellular signalling processes, both during stress and otherwise (Taipale et al. 2010; da Silva & Ramos 2012). One function of HSP-90 is to recognise and bind to non-native proteins, stabilising them in a folding-competent and aggregation-resistant state (Wiech et al. 1992; Freeman & Morimoto 1996). The capacitor hypothesis proposes that when phenotype-affecting variants arise due to sporadic mutations, HSP-90 interacts with them and prevents expression of the variant phenotype (Rutherford & Lindquist 1998; Queitsch et al. 2002). This buffering allows the widespread accumulation of variants which are held in a silenced or cryptic form, and may occur at both the genetic and epigenetic level (Sollars et al. 2003). However, if HSP-90 activity is impaired or there is an increased folding requirement such as during cell stress, these variants will no longer be silenced and expression of their phenotype will be permitted. Depending on the fitness of the resulting phenotype, a previously cryptic variant may be selected for and become independent of HSP-90 regulation; an implication of which is that cell stress can expose potentially evolutionarily beneficial variants (Rutherford & Lindquist 1998).

#### 1.3.2.2 The unfolded protein response of the endoplasmic reticulum (UPR$^{ER}$)

The endoplasmic reticulum (ER) is the main site of processing and quality control for proteins entering the secretory pathway (Vitale & Denecke 1999; Walter & Ron 2011). Such proteins undergo co-translational translocation into the ER, where they are processed by various resident chaperones (Pelham 1989). If the folding capacity of the ER is exceeded, for example due to the presence of mutant, folding-incompetent peptide chains, this constitutes ER stress and the unfolded protein response of the ER (UPR$^{ER}$) is activated (Kozutsumi et al. 1988). This promotes both increased expression of ER chaperones to bolster folding capacity, and repression of protein biosynthesis to reduce nascent chain flux (Ron & Walter 2007).

The UPR$^{ER}$ consists of three key pathways mediated by the effector proteins IRE-1, PEK-1 and ATF-6 (Shen et al. 2001, 2005). Each of these is a transmembrane protein with a cytosolic domain and an ER lumenal domain. Under non-stressful conditions, the ER lumenal domains are bound by the ER resident HSP-70 family chaperone BiP, which holds the effectors in an inactive state (Schröder & Kaufman 2005). *C. elegans* has two homologues of BiP: HSP-3 and HSP-4 (Shen et al. 2001). If levels of non-native protein increase within the ER, BiP dissociates from the UPR$^{ER}$ effectors to mediate protein refolding, enabling their activation. The three effectors then mediate signalling through complementary pathways to promote chaperone upregulation and decreased protein production (**Fig. 1.5**).

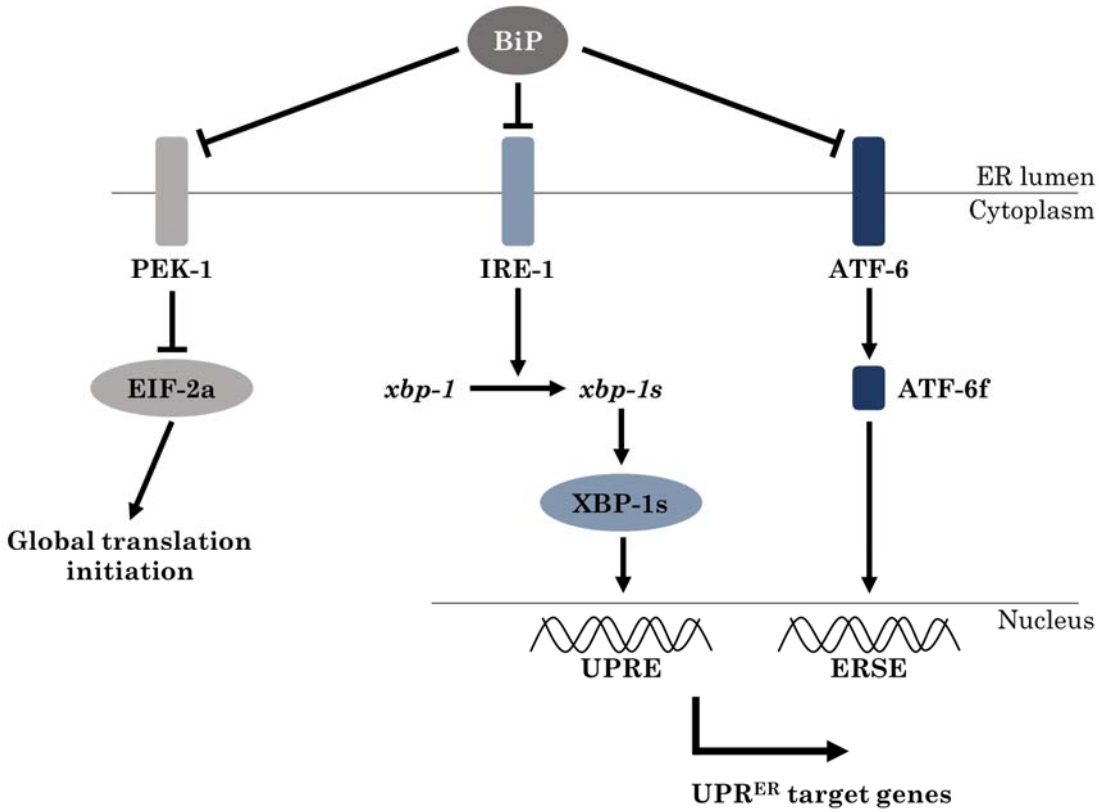


**Figure 1.5 The unfolded protein response of the endoplasmic reticulum (UPR$^{ER}$).** The ER chaperone BiP holds the UPR$^{ER}$ effectors IRE-1, PEK-1 and ATF-6 in inactive forms. If ER folding requirement increases, BiP is titrated away and the effectors become active. IRE-1 catalyses splicing of *xbp-1* mRNA into *xbp-1s*, encoding the active transcription factor XBP-1s. XBP-1s binds UPR elements (UPREs) to upregulate UPR$^{ER}$ target genes. PEK-1 promotes phosphorylation of the translation initiation factor EIF-2a, reducing global translation. ATF-6 is cleaved into a cytosolic fragment (ATF-6f), which binds ER stress elements (ERSEs) to upregulate UPR$^{ER}$ target genes.

Upon dissociation of BiP, the kinase/endonuclease IRE-1 oligomerises, undergoes trans-autophosphorylation, and becomes active (Ron & Walter 2007). Active IRE-1 mediates the alternative splicing of cytoplasmic *xbp-1* mRNA into *xbp-1s*, excising an intron to extend the open reading frame (Shen et al. 2001; Calfon et al. 2002). Translation of the spliced mRNA produces the active transcription factor XBP-1s, which binds to the UPR element (UPRE) in the promoters of UPR$^{ER}$ target genes such as BiP to activate their expression (Yamamoto et al. 2004; Shen et al. 2005). Upregulation of BiP and other ER resident chaperones then contributes to increased ER folding capacity.

The kinase PEK-1 is a homologue of human PERK (Shen et al. 2001). In a process similar to that of IRE-1, PEK-1 oligomerises and undergoes trans-autophosphorylation to become active on BiP dissociation (Ron & Walter 2007). Active PEK-1 phosphorylates the translation initiation factor EIF-2A, inhibiting its activity and leading to a global reduction in protein translation (Rhoads et al. 2006). This reduces the number of new polypeptides being produced, decreasing the demand for chaperones. However, transcripts with several short upstream open reading frames (ORFs) can still undergo translation under these conditions (Harding et al. 2000). One such transcript encodes the transcription factor ATF-4. In humans, ATF4 upregulates expression of another transcription factor, CHOP; this in turn activates expression of GADD34, which promotes dephosphorylation of eIF2A and therefore acts on the system as negative feedback (Harding et al. 2000; Marciniak et al. 2004).

The final arm of the $UPR^{ER}$ is mediated by ATF-6. Under non-stressed conditions, association of BiP with the ER lumenal domain of ATF-6 occludes a Golgi signal sequence, retaining ATF-6 in the ER membrane (Schröder & Kaufman 2005). However, when BiP dissociates, the signal sequence is exposed and ATF-6 is translocated to the Golgi body (Shen et al. 2002). Here it undergoes proteolytic cleavage, releasing a cytosolic fragment which is an active transcription factor; it is subsequently translocated to the nucleus and binds to ER stress elements (ERSEs) in the promoters of stress response genes (Chen et al. 2002; Yamamoto et al. 2004). This promotes increased expression of BiP, XBP-1, and other ER resident chaperones (Shen et al. 2005).

#### 1.3.2.3 The unfolded protein response of the mitochondria ($UPR^{Mt}$)

As the primary cellular sites of aerobic respiration and oxidative phosphorylation, mitochondria are vital for energy production in the cell. However, leakage of electrons from the electron transport chain (ETC) generates reactive oxygen species (ROS); which can react with and damage proteins, DNA and lipids (Fraga et al. 1990; Stadtman 1992). The unfolded protein response of the mitochondria ($UPR^{Mt}$) functions to increase expression of mitochondrial chaperone proteins in response to non-native proteins within the mitochondria (**Fig. 1.6**; Zhao et al. 2002; Yoneda et al. 2004).

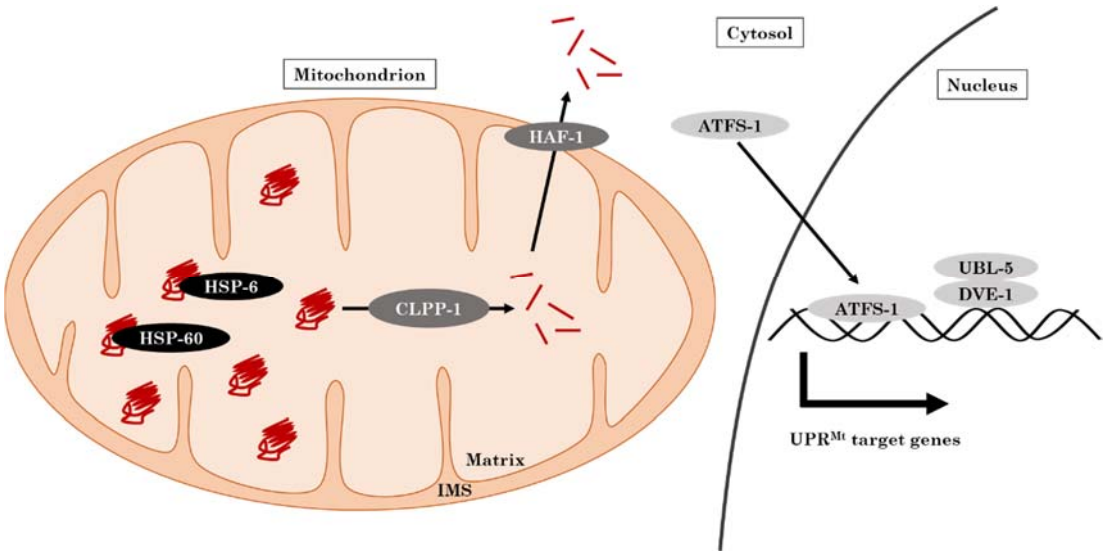


**Figure 1.6 The unfolded protein response of the mitochondria (UPR$^{Mt}$)**. If the folding capacity of mitochondrial chaperones is exceeded, the protease CLPP-1 degrades excess misfolded proteins. Peptide fragments are exported to the cytosol by HAF-1, causing nuclear translocation of the transcription factor ATFS-1. ATFS-1, along with a UBL-5/DVE-1 complex, promotes upregulation of UPR$^{Mt}$ target genes. IMS: intermembrane space.

Protein folding in the mitochondrial matrix is mediated by chaperones including HSP-60 and the mitochondrial HSP-70 family chaperone HSP-6 (Yoneda et al. 2004). If the folding capacity of mitochondrial chaperones is exceeded, excess proteins are degraded into short peptides by the mitochondrial matrix protease CLPP-1 and are then exported into the cytosol by the transporter HAF-1 (Haynes et al. 2010). This leads to activation of the transcription factor ATFS-1. ATFS-1 possesses both nuclear and mitochondrial localisation sequences, and under non-stressful conditions is imported into the mitochondria for degradation. However, if mitochondrial import is impaired such as during the UPR$^{Mt}$, ATFS-1 is instead translocated into the nucleus (Nargund et al. 2012). Nuclear ATFS-1 promotes increased expression of mitochondrial chaperones such as *hsp-6* and *hsp-60* as well as mitochondrial import machinery and detoxification enzymes, promoting restoration of mitochondrial proteostasis (Haynes et al. 2010; Nargund et al. 2012). CLPP-1 also promotes increased expression of the ubiquitin-like protein UBL-5, which forms a complex with the transcription factor DVE-1 and binds in the promoters of mitochondrial chaperone genes to upregulate their expression (Benedetti et al. 2006; Haynes et al. 2007). As the closest human orthologues of DVE-1 are chromatin-organising proteins, it has been suggested that the DVE-1/UBL-5 complex may aid expression of UPR$^{Mt}$ target genes through chromatin remodelling (Jovaisaite et al. 2014).

### 1.3.3 Cell-non-autonomous stress responses

Stress responses, and proteostasis in general, can mediate effects not only within a single cell or tissue but at the level of the whole organism (Durieux et al. 2011; Taylor & Dillin 2013; van Oosten-Hawle et al. 2013). A stress stimulus in a single cell or tissue may cause effects in distal tissues, or at the level of the whole organism. Alternatively, a stress stimulus which affects the whole organism may achieve a differential response between tissues (Fawcett et al. 1994; Prahlad et al. 2008). In addition to regulating proteostasis, this can also impact key survival processes such as immunity and longevity (Miles et al. 2019).

Maintenance of proteostasis is closely linked to the aging process. During aging, the function of the proteostasis network declines, and stress-inducible chaperone expression is impaired (Sőti & Csermely 2000; Morimoto 2008; Ben-Zvi et al. 2009). Protein aggregation therefore increases with age in a tissue-specific manner (Morley et al. 2002; David et al. 2010). Loss of proteostasis has even been classed as a 'hallmark of aging' (López-Otín et al. 2013). The decline in capacity of the proteostasis system in turn makes cells more vulnerable to proteostatic challenges and imbalance, and increasing age is consequently a key risk factor for many protein-misfolding diseases (Balch et al. 2008; Morimoto 2008). In *C. elegans*, it has been shown that the organismal weakening of stress responses during aging is in fact a programmed event, which is activated by germline signalling upon reaching reproductive maturity (Arantes-Oliveira et al. 2002; Shemesh et al. 2013; Labbadia & Morimoto 2015). Indeed, absence of the proliferating germline maintains organismal proteostasis during adulthood, and promotes longevity in adult *C. elegans* through increased lipid hydrolysis (Wang et al. 2008; Shemesh et al. 2013).

Proteostasis is therefore an organismal process closely related to longevity and innate immunity in *C. elegans*, and all three are negatively regulated by the proliferating germline (Alper et al. 2010). As producing oocytes is a highly energy-intensive process, this perhaps represents a shift at reproductive maturity from prioritising the growth and development of an individual to prioritising the health and viability of progeny. However, these processes do not act independently. Heat stress promotes increased longevity and immune resistance, and enhances dauer formation in the presence of dauer pheromone (Golden & Riddle 1984). HSF-1 is also required for the insulin-like signalling (ILS)-mediated immune response to several

pathogens (Singh & Aballay 2006). In a *C. elegans* model of polyglutamine (polyQ) disease, activation of the ILS-controlled transcription factor DAF-16 delays aggregation of disease-related proteins and ameliorates an associated motility defect (Morley et al. 2002). Suppression of insulin signalling in a mouse model of Alzheimer's disease protects against symptoms (Cohen et al. 2009); and in human lung fibroblast cells, the cytokines TGF-ß and IL-1ß promote HSF-1 activity (Sasaki et al. 2002). There is therefore a great deal of overlap in the mechanisms underlying proteostasis, aging and immunity, and the interactions between them are likely highly relevant when considering any of these processes.

#### 1.3.3.1 The cell-non-autonomous HSR

The HSR can be regulated cell-non-autonomously by neuroendocrine signalling. One of the first reports of this showed that in rats, a behavioural stressor leads to adrenal activation of the HSR through a neuroendocrine mechanism (Fawcett et al. 1994). Subsequent work in *C. elegans* identified that in this species, organismal activation of the HSR is regulated by thermosensory neurons. *C. elegans* monitor their environmental temperature through AFD neurons, thermosensory amphid neurons with ciliated finger-like endings (Perkins et al. 1986; White et al. 1986; Mori & Ohshima 1995). Within AFD neurons, heat stress promotes production of cyclic GMP by the guanylyl cyclases GCY-8, GCY-18 and GCY-23; leading to activation of a cGMP-gated ion channel composed of the subunits TAX-2 and TAX-4 (Inada et al. 2006; Ramot et al. 2008). This activates cholinergic AIY interneurons, which signal via other interneurons and motor neurons to control thermotaxis towards optimal temperatures (Mori & Ohshima 1995). In AIY interneurons, the LIM homeobox protein TTX-3 is required for thermosensation as well as control of dauer formation; possibly due to its role in specifying cholinergic terminal fate (Hobert et al. 1998; Shen et al. 2010; Zhang et al. 2014). Cholinergic neurotransmission is important in the transcellular regulation of proteostasis, and an imbalance between excitatory cholinergic and inhibitory GABAergic signalling can inhibit proteostasis in postsynaptic cells (Garcia et al. 2007).

In addition to control of thermotaxis, the AFD/AIY thermosensory circuit is required for activation of the organismal HSR upon heat stress. Upon acute heat stress, or direct optogenetic stimulation of AFD neurons, the circuit enhances serotonergic signalling which is detected by the SER-1 serotonin receptor (Prahlad et al. 2008;

Tatum et al. 2015). This activates the HSR in non-neuronal tissues, promoting increased chaperone expression, protein folding and survival (Prahlad et al. 2008; Lee & Kenyon 2009). This process also involves the G protein-coupled receptor GTR-1 in chemosensory neurons, which is required for HSR activation but not thermosensation (Maman et al. 2013). Interestingly, the thermosensory circuit also controls the organismal response to chronic proteotoxic stress, but in the opposite direction. In models overexpressing aggregation-prone proteins such as polyQ, the AFD/AIY thermosensory circuit inhibits the organismal HSR to suppress protein folding and survival (Prahlad & Morimoto 2011). This involves neurosecretory signalling mediated by the CAPS homologue UNC-31, which is required for dense core vesicle (DCV) exocytosis (Speese et al. 2007). Such differential regulation between acute and chronic proteotoxic stresses could be a mechanism to ensure that acute challenges are always met with HSR upregulation, rather than having it constantly activated during chronic stress.

The HSR is closely interlinked with ILS in the regulation of organismal processes such as immunity and longevity, and in the control of whole-organism proteostasis. HSF-1 activity is modulated by the insulin receptor-like kinase DAF-2, which promotes formation of an inhibitory DDL-1-containing HSF-1-inhibitory complex (DHIC); signalling from DAF-2 therefore suppresses the ability of HSF-1 to be activated upon heat shock (Chiang et al. 2012). In long-lived DAF-2 mutants, both DAF-16 and HSF-1 are required for increased lifespan (Hsu et al. 2003; Morley & Morimoto 2004). HSF-1 is also required for the ILS-mediated immune response, and activation of HSF-1 by heat stress increases immune resistance through HSP-90 and HSP-16 (Singh & Aballay 2006). Furthermore, inhibition of DAF-2 reduces the toxicity of amyloid ß (Aß) in a *C. elegans* model of Alzheimer's disease through increased activity of DAF-16 and HSF-1 (Cohen et al. 2006). HSF-1 mediated protein disaggregation and DAF-16 mediated aggregation of smaller, more toxic oligomeric Aß increases lifespan and ameliorates motility defects; showing that intercellular HSR and ILS signalling combine to regulate the health of the whole organism.

#### 1.3.3.2 The cell-non-autonomous UPR$^{ER}$

The UPR$^{ER}$ is an important component of immunity both in *C. elegans* and in humans. For example, UPR$^{ER}$ activity is required in the development of plasma and dendritic cells (Todd et al. 2008). In *C. elegans*, the PMK-1-mediated upregulation of

immune genes during infection with *P. aeruginosa* causes ER stress, perhaps because many immune genes are likely to be secreted antimicrobial peptides processed through the ER (Richardson et al. 2010). Survival of immune – and, interestingly, heat – stress is dependent on the ability to activate the IRE-1 and PEK-1-mediated UPR$^{ER}$ (Richardson et al. 2011). Like other stress responses, a key factor regulating UPR$^{ER}$ activity is neuronal signalling. The G protein-coupled receptor (GPCR) OCTR-1 acts in the ASH and ASI sensory neurons to suppress the PMK-1-mediated immune response to *P. aeruginosa*, downregulating the expression of both canonical and non-canonical UPR$^{ER}$ genes in non-neuronal tissues (Sun et al. 2011, 2012(b)). This is achieved at least in part by the inhibition of protein translation involving the ribosomal protein RPS-1 and the translation initiation factor EIF-3.J, which may prevent immune protein production and consequent ER stress (Liu et al. 2016).

Conversely, activation of a tissue-specific UPR$^{ER}$ can promote protective responses throughout the organism. Intestine-specific or pan-neuronal overexpression of *xbp-1s* activates the UPR$^{ER}$ in a cell-non-autonomous manner; can delay tissue-specific polyQ aggregation in the neurons, intestine or body wall muscle; and ameliorates disease phenotypes caused by polyQ or Aß aggregation (Taylor & Dillin 2013; Imanikia et al. 2019). Pan-neuronal overexpression of *xbp-1s* increases lifespan and potentiates stress responses during aging in a manner dependent on *unc-13*, a gene required for neurotransmission involving small clear vesicles (SCVs) (Richmond et al. 1999; Taylor & Dillin 2013). In addition to transcellular activation of the intestinal UPR$^{ER}$, neuronal *xbp-1s* overexpression upregulates intestine-specific expression of lysosomal genes such as aspartyl and cysteine proteases, and promotes increased lysosomal maturation and acidity (Taylor & Dillin 2013; Imanikia et al. 2019). This intestine-specific lysosome activity is required for the increased lifespan caused by pan-neuronal *xbp-1s* overexpression (Imanikia et al. 2019). In a similar recently reported mechanism, overexpression of *xbp-1s* in cephalic astrocyte-like sheath (CEPsh) glia increases lifespan and activates the intestinal UPR$^{ER}$ through *unc-31*-dependent neuropeptide signalling (Frakes et al. 2020). Interestingly, *unc-13*-mediated neuronal signalling and *unc-31*-mediated glial signalling which both activate the intestinal UPR$^{ER}$ act in distinct pathways; and overexpression of *xbp-1s* both pan-neuronally and in the CEPsh glia has an additive effect on lifespan extension and intestinal UPR$^{ER}$ activation (Frakes et al. 2020).

Beyond *C. elegans*, cell-non-autonomous UPR$^{ER}$ activity has also been demonstrated in mammals *in vitro* and *in vivo*. Murine macrophages or bone marrow-derived dendritic cells (BMDC) cultured in medium from ER-stressed murine tumour cells undergo cell-non-autonomous UPR$^{ER}$ activation, resulting in a pro-inflammatory phenotype (Mahadevan et al. 2011, 2012). This may well be a mechanism hijacked during tumorigenesis. Additionally, *in vivo* overexpression of Xbp1s in the Pomc neurons of mice results in UPR$^{ER}$ activation in the liver (Williams et al. 2014); demonstrating that neuronal control of the cell-non-autonomous UPR$^{ER}$ appears to be a theme conserved between species.

#### 1.3.3.3 The cell-non-autonomous UPR$^{Mt}$

Activation of the UPR$^{Mt}$ is also beneficial for innate immunity. Infection by *P. aeruginosa* causes mitochondrial stress and the activation of ATFS-1, which upregulates immune genes including C-type lectins and antimicrobial peptides to promote survival (Pellegrino et al. 2014). Mitochondrial damage by *P. aeruginosa* promotes increased mitophagy to suppress ROS and oxidative damage, a process which has been shown to confer cell-non-autonomous protection against ETC disruption (Kirienko et al. 2015). Treatment with the chemical rotenone causes selective loss of dopaminergic neurons due to ETC disruption; however, this also causes intestine-specific activation of the PMK-1/ATF-7 pathway to promote increased mitophagy, which is sufficient to prevent dopaminergic neuron loss (Chikka et al. 2016).

The UPR$^{Mt}$ can act cell-non-autonomously to modulate metabolism, aging and lifespan; and like the HSR and UPR$^{ER}$ is regulated at least in part by neuronal signalling. Mitochondrial stress can be induced in the neurons by pan-neuronal ETC disruption, ROS production, or proteotoxic polyQ (Dillin et al. 2002; Durieux et al. 2011; Berendzen et al. 2016; Shao et al. 2016); which activate the neuronal UPR$^{Mt}$ in an ATFS-1-dependent manner (Durieux et al. 2011; Berendzen et al. 2016; Shao et al. 2016). This promotes neuronal secretion of the Wnt homologue EGL-20 in a process requiring retromer-dependent endosomal recycling of the Wnt secretion factor MIG-14 (Zhang et al. 2018). In serotonergic neurons, EGL-20 activates UNC-31-mediated serotonin secretion (Berendzen et al. 2016; Zhang et al. 2018). However, it is not clear whether the effects of EGL-20 in the cell-non-autonomous UPR$^{Mt}$ are due solely to this action in serotonergic neurons, as *egl-20* has also been shown to be

expressed in tissues including the anal depressor muscle and cholinergic neurons (Whangbo & Kenyon 1999; Cao et al. 2017). Together with serotonin signalling, binding of secreted EGL-20 to the Wnt receptor MIG-1 promotes stabilisation of the ß-catenin homologue BAR-1 in the intestine; this enables the interaction of BAR-1 with the transcription factor POP-1 (Zhang et al. 2018). In combination with intestinal ATFS-1 and DVE-1, this causes cell-non-autonomous activation of the intestinal UPR$^{Mt}$ (**Fig. 1.7**; Berendzen et al. 2016; Shao et al. 2016; Zhang et al. 2018). If this process is activated during development before L4 stage, organismal respiration rate is reduced and lifespan is increased (Dillin et al. 2002; Zhang et al. 2018). In another neuronal signalling pathway, mitochondrial stress is detected by ASK, AWA or AWC sensory neurons, which signal to the AIA interneurons (Shao et al. 2016). Secretion of the neuropeptide FLP-2 from AIA interneurons activates the cell-non-autonomous UPR$^{Mt}$, although it is unable to promote increased lifespan (Shao et al. 2016). This suggests that the nervous system is responsible for detection of mitochondrial stress, and has an important role in co-ordination of an organismal response.

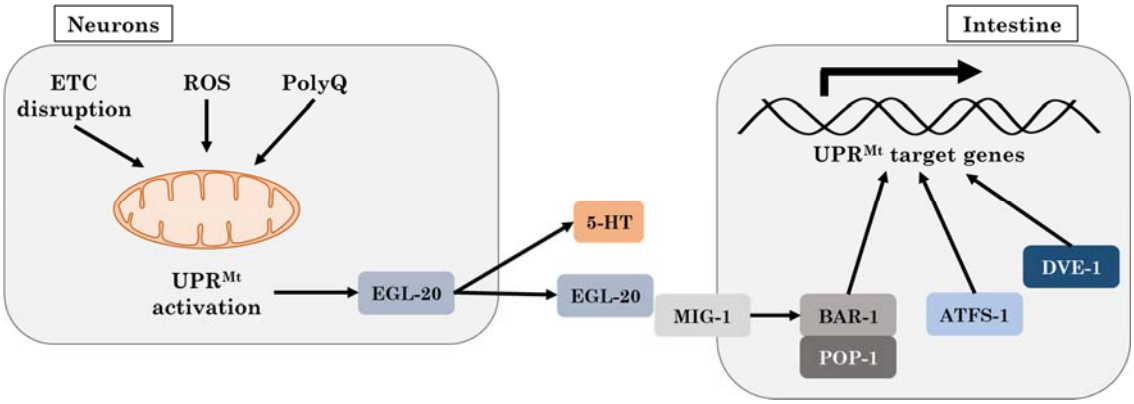


**Figure 1.7 Mitochondrial stress in neurons activates the intestinal UPR$^{Mt}$.** Pan-neuronal mitochondrial stress activates the neuronal UPR$^{Mt}$ through ATFS-1, promoting EGL-20 secretion and EGL-20-dependent serotonin (5-HT) secretion from serotonergic neurons. Secreted EGL-20 activates MIG-1, leading to BAR-1 stabilisation and interaction with POP-1. POP-1, ATFS-1 and DVE-1 promote upregulation of the intestinal UPR$^{Mt}$. ROS: Reactive oxygen species.

Cell-non-autonomous control of the UPR$^{Mt}$ has also been demonstrated in other organisms. In the fruit fly *Drosophila melanogaster*, mild or temporary disruption of the ETC (mitohormesis) in the flight muscles activates the UPR$^{Mt}$ via a redox signalling pathway, increasing lifespan and delaying age-related motor impairment

(Owusu-Ansah et al. 2013). This is partly mediated by secretion of the signalling molecule ImpL2, which represses ILS and promotes mitophagy. Furthermore, in mice and humans, genetic or pharmacological disruption of the ETC causes activation of the PERK-eIF2a-ATF4 pathway (Kim et al. 2013(b,c)). This causes upregulation of the mitokine FGF21 in the liver, leading to increased levels of circulating FGF21 in the serum or plasma and conferring protection against insulin resistance and diet-induced obesity (Suomalainen et al. 2011; Kim et al. 2013(b,c)).

#### 1.3.3.4 Organismal proteostasis and innate immunity

*C. elegans* in their natural habitat may encounter immunological challenges from various pathogens including bacteria, viruses, and fungi. In the case of viruses, RNAi is a key element of the antiviral response, and viral infection is countered by small interfering RNAi-mediated antiviral silencing (Lu et al. 2005; Schott et al. 2005; Wilkins et al. 2005). *C. elegans* lacks an adaptive immune system, but retains several conserved innate immune mechanisms including mitogen-associated protein kinase (MAPK) signalling pathways (Kim et al. 2002; Nicholas & Hodgkin 2004; Marudhupandiyan & Balamurugan 2017). *C. elegans* also demonstrate an intracellular pathogen response (IPR) in response to intracellular pathogens such as Orsay virus or *Nematocida parisii*, a fungal species of Microsporidia (Troemel et al. 2008; Félix et al. 2011). This IPR promotes resistance not only to pathogenic infection, but also to heat stress and protein aggregation; and appears to be mediated through ubiquitination, proteasome activity, and autophagy (Bakowski et al. 2014; Reddy et al. 2017). A key feature of the IPR is upregulation of ubiquitin ligase complex components such as the cullin CUL-6, which is required for the IPR's protective effects (Chen et al. 2017; Reddy et al. 2017). Expression of IPR genes is controlled by a 'molecular switch' in a mechanism which apparently balances organismal growth with stress response activation (Reddy et al. 2017, 2019), indicating that normal development and organismal stress response states may be co-ordinated centrally.

One of the mostly widely studied immune mechanisms in *C. elegans* is the insulin-like signalling (ILS) pathway which is controlled through the receptor tyrosine kinase DAF-2 (Murphy & Hu 2013). ILS is an intrinsically cell-non-autonomous signalling process co-ordinated by the nervous system (Ailion et al. 1999; Apfeld & Kenyon 1999; Wolkow et al. 2000; Kawli & Tan 2008). Under conditions beneficial

for reproductive growth, neuroendocrine insulin-like signalling promotes DAF-2 activation, leading to downstream repression of the transcription factor DAF-16 (Murphy et al. 2003; Kawli & Tan 2008). However, in conditions of scarce food or high population density, such signalling is reduced and DAF-16 becomes active. DAF-16 promotes the expression of various protective genes such as superoxide dismutase and immune response genes, but also small heat shock proteins including *hsp-16.1* (**Fig. 1.8**; Garsin et al. 2003; Lee et al. 2003; Murphy et al. 2003; Shapira et al. 2006; Troemel et al. 2006). Activation of DAF-16 also promotes longevity, and DAF-2 mutations which result in constitutive DAF-16 activation more than double lifespan (Lin et al. 1997; Ogg et al. 1997). Interestingly, ILS-mediated longevity, immunity and proteostasis are regulated not only by signals from the environment, but also from the proliferating germline. Absence or ablation of the germline causes a DAF-16-mediated increase in lifespan and immune resistance (Apfeld & Kenyon 1999; Hsin & Kenyon 1999; Miyata et al. 2008), and promotes proteotoxic stress resistance through lipophilic hormone signalling and increased activation of the proteasome subunit RPN-6 (Berman & Kenyon 2006; Vilchez et al. 2012).

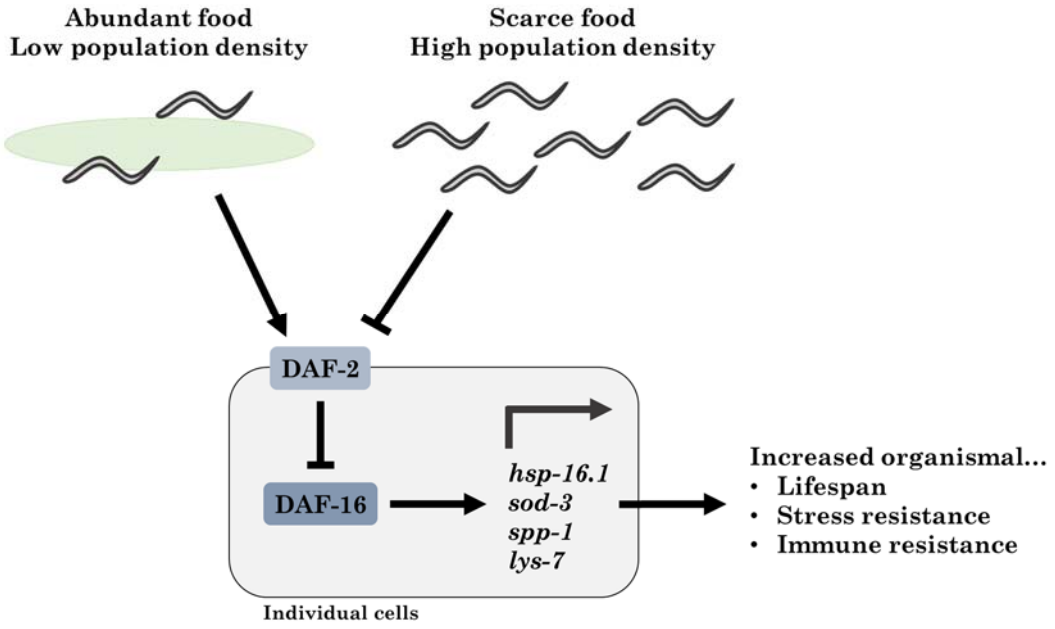


**Figure 1.8 Insulin-like signalling (ILS) promotes longevity and stress resistance**. Favourable conditions promote DAF-2 activation and suppression of DAF-16. Adverse conditions suppress DAF-2 signalling and promote DAF-16 activation. Active DAF-16 upregulates stress resistance genes such as *sod-3* or small heat shock proteins (sHSPs), and immune resistance genes such as *lys-7* or *spp-1*. This confers whole-organism benefits to promote survival.

## 1.4 Transcellular chaperone signalling (TCS) in *C. elegans*

Another cell-non-autonomous stress response in *C. elegans* is transcellular chaperone signalling (TCS), which is the focus of this research. TCS is a non-canonical mechanism of intercellular proteostasis which is closely related to the HSR but is regulated independently of HSF-1 (van Oosten-Hawle et al. 2013; O'Brien et al. 2018). It is activated by tissue-specific changes in HSP-90 expression, leading to altered expression of chaperones in distal tissues, with organismal consequences on lifespan and stress resistance. TCS can be activated by either tissue-specific overexpression or tissue-specific knockdown of HSP-90, with contrasting outcomes (**Fig. 1.9**).

### 1.4.1 TCS activated by tissue-specific *hsp-90* overexpression

Under non-stressful conditions, HSP-90 is expressed ubiquitously throughout all *C. elegans* tissues (van Oosten-Hawle et al. 2013; Cao et al. 2017). It is further upregulated upon heat stress in an HSF-1-dependent manner (Brunquell et al. 2016). However, in strains expressing temperature-sensitive alleles of *unc-54* (myosin) or *unc-15* (paramyosin), which disrupt the organisation of muscle fibres, HSP-90 is upregulated even at the permissive temperature (van Oosten-Hawle et al. 2013). Despite the fact that these strains demonstrate a muscle-specific increase in folding requirement, HSP-90 upregulation occurs not only in the body wall muscle but also in the pharynx, intestine and excretory cell (van Oosten-Hawle et al. 2013). Conversely, if HSP-90 is over-expressed pan-neuronally or in the intestine, this causes a cell-non-autonomous upregulation of HSP-90 in the pharynx and body wall muscle which can rescue muscle organisation in strains carrying temperature-sensitive UNC-54 (van Oosten-Hawle et al. 2013). Cell-non-autonomous HSP-90 upregulation through TCS can also protect against amyloid aggregation in the muscle. For example, in a *C. elegans* model of Alzheimer's disease which expresses the aggregation-prone protein amyloid beta ($A\beta_{(3\text{-}42)}$) in the body wall muscle, pan-neuronal or intestine-specific HSP-90 overexpression decreases the amount of high molecular weight Aβ oligomers and delays an associated paralysis phenotype (O'Brien et al. 2018). However, although tissue-specific HSP-90 overexpression is

protective in terms of improving the cell-non-autonomous protein folding environment, it has the detrimental effect of decreasing organismal resistance to heat stress (van Oosten-Hawle et al. 2013). Cell-non-autonomous HSP-90 upregulation leads to increased suppression of HSF-1 activity, thereby decreasing organismal expression of chaperones such as *hsp-70*, *F44E5.4* and *hsp-16.2*; it also prevents the upregulation of an *hsp-70p::mCherry* reporter upon heat stress (van Oosten-Hawle et al. 2013). This means that cells are less able to respond to heat shock and survival is decreased.

A key question when considering cell-non-autonomous mechanisms is how one cell signals to another. The transcellular upregulation of HSP-90 seen upon tissue-specific HSP-90 overexpression is not signalled by secretion of HSP-90; and is not dependent on the neuronal signalling genes *unc-13* and *unc-31* or the transcription factors *hsf-1*, *daf-16* or *skn-1* (van Oosten-Hawle et al. 2013). However, it is dependent on the transcription factor PHA-4, which is required for pharyngeal development; and *pha-4* mRNA and activity are increased in strains with tissue-specific overexpression of HSP-90 (van Oosten-Hawle et al. 2013).

TCS activated in this manner is also dependent on the paraquat-responsive transcription factor PQM-1, which recognises DAF-16-associated elements (DAEs) in DNA; although in a pathway independent of PHA-4 (Tepper et al. 2013; O'Brien et al. 2018). The nuclear localisation of PQM-1 and DAF-16 is negatively correlated, and when one is targeted to the nucleus the other is usually in the cytoplasm; this means that only one of them is transcriptionally active at any given time (Tepper et al. 2013). Whilst DAF-16 binds DBEs to promote upregulation of stress-responsive genes, PQM-1 binds DAEs to promote upregulation of developmental genes and is required for normal development (Tepper et al. 2013). In wild-type animals, PQM-1 is normally localised to the intestinal nuclei throughout development but leaves the nucleus once an animal reaches reproductive adulthood (O'Brien et al. 2018). However, when HSP-90 is overexpressed pan-neuronally or in the intestine, PQM-1 remains localised to intestinal nuclei even in adults, suggesting that it is still transcriptionally active (O'Brien et al. 2018). PQM-1 is required for the cell-non-autonomous upregulation of HSP-90 upon tissue-specific HSP-90 overexpression, and acts in the tissue in which HSP-90 is overexpressed (O'Brien et al. 2018). Although PQM-1 is required for the upregulation of HSP-90 upon heat stress, it does not directly transcriptionally regulate HSP-90; indicating that other downstream

factors are involved (O'Brien et al. 2018). The factors involved depend on the tissue in which HSP-90 is overexpressed. When HSP-90 is overexpressed pan-neuronally, PQM-1 promotes upregulation of the CUB domain protein CLEC-41, which is required neuronally for cell-non-autonomous HSP-90 upregulation (O'Brien et al. 2018). TCS activated by pan-neuronal HSP-90 overexpression is enhanced by glutamatergic signalling, but suppressed by serotonergic or octopaminergic signalling (O'Brien et al. 2018). Alternatively, when HSP-90 is overexpressed in the intestine PQM-1 promotes upregulation of the immune protein ASP-12, which is required in the intestine for cell-non-autonomous HSP-90 upregulation (O'Brien et al. 2018).

### 1.4.2 TCS activated by tissue-specific *hsp-90* knockdown

Similar to tissue-specific HSP-90 overexpression, tissue-specific knockdown of *hsp-90* in *C. elegans* activates cell-non-autonomous chaperone upregulation dependent on PHA-4 (van Oosten-Hawle et al. 2013). However, in this case the chaperone upregulated is HSP-70, which is upregulated most strongly in the body wall muscle and vulva when *hsp-90* is knocked down pan-neuronally or in the intestine (van Oosten-Hawle et al. 2013). In contrast to TCS activated by tissue-specific HSP-90 overexpression, TCS activated by tissue-specific *hsp-90* knockdown confers increased resistance to heat stress (van Oosten-Hawle et al. 2013). This may be directly due to the increased expression of protective HSP-70, or may be due to differential expression of other genes regulated by TCS. It has been shown that upon whole-organism knockdown of *hsp-90* there is an upregulation of HSP-1, small heat shock proteins, HSP-90 co-chaperones, and subunits of the TCP1 chaperonin complex (Eckl et al. 2017). This indicates that reduction of *hsp-90* promotes increased expression of chaperones, perhaps due to reduced inhibition of HSF-1. However, since this was shown using whole-animal and not tissue-specific *hsp-90* knockdown, different signalling pathways may have been activated and it may not be appropriate to directly compare results. Despite this, in the case of both whole-animal and tissue-specific *hsp-90* knockdown, animals display delayed development and aberrant phenotypes (van Oosten-Hawle et al. 2013; Eckl et al. 2017). Systemic RNAi feeding causes delayed growth and abnormal gonad development (Eckl et al. 2017). Intestine-specific *hsp-90* knockdown also causes abnormal gonad development, whilst body wall muscle-specific *hsp-90* knockdown can result in defective intestine, tail or excretory canal development (van Oosten-Hawle et al. 2013). This is

consistent with the HSP-90 capacitor hypothesis and the role of HSP-90 in suppressing cryptic mutations in wild-type animals. Finally, although TCS activated by tissue-specific HSP-90 overexpression is dependent on the transcription factor PQM-1, this is not the case for TCS activated by tissue-specific *hsp-90* knockdown (O'Brien et al. 2018).

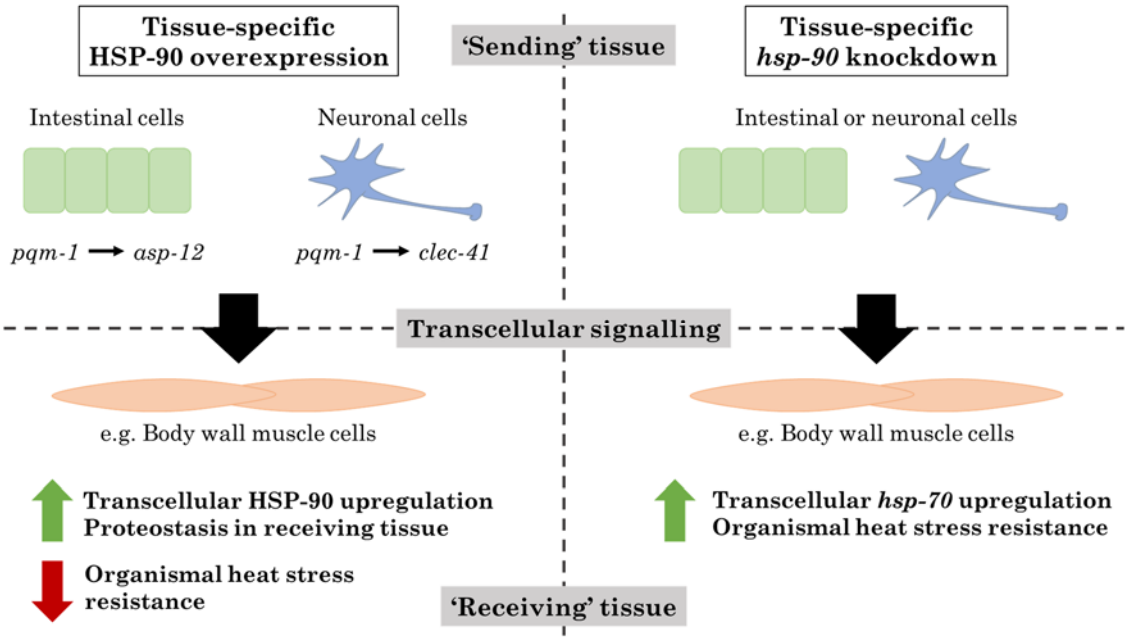


**Figure 1.9 Transcellular chaperone signalling (TCS).** Tissue-specific perturbation of HSP-90 activates transcellular signalling, leading to cell-non-autonomous chaperone upregulation with consequences for organismal proteostasis and heat stress resistance. HSP-90 overexpression in the intestine or pan-neuronally activates *pqm-1*-dependent transcellular signalling, promoting cell-non-autonomous HSP-90 upregulation and improved proteostasis, but also reduced heat stress resistance. *hsp-90* knockdown in the intestine or pan-neuronally activates cell-non-autonomous *hsp-70* upregulation and improved organismal heat stress resistance.

## 1.5 Research aims and approach

Whilst the effects of whole-organism *hsp-90* knockdown in *C. elegans* have been relatively well-studied, less is known about the systemic consequences of tissue-specific *hsp-90* depletion. This research had two key aims pertaining to the activation of TCS by tissue-specific *hsp-90* knockdown: to characterise its consequences at the organismal level, and to identify genes involved in inter-tissue signalling pathways. Organismal effects were investigated not only through longevity and stress resistance assays (**Chapter 3**), but also in terms of differential organismal gene expression (**Chapter 4**). To identify genetic components of inter-tissue signalling pathways activated by intestine-specific *hsp-90* knockdown, genetic screening was performed using both forward and reverse approaches (**Chapters 5 and 6**). An *hsp-70p::mCherry* reporter was used as a readout for these screens, as upregulation of such a reporter is a known cell-non-autonomous consequence of TCS activation (van Oosten-Hawle et al. 2013).

TCS activated by tissue-specific *hsp-90* knockdown has previously been described, using *C. elegans* strains which expressed tissue-specific *hsp-90* RNAi in extrachromosomal transgene arrays (van Oosten-Hawle et al. 2013). However, the research presented here has used strains in which the transgene arrays have been integrated into the genome for stable expression. This was necessary for the forward genetic screen carried out in **Chapter 5**, in which animals were mutagenised and visually screened for altered expression of a *hsp-70p::mCherry* reporter. Had strains carrying extrachromosomal transgenes been used, it would have been difficult to distinguish animals with mutations of interest from animals which had not inherited the transgene. As these integrated strains have not previously been described, it was necessary to first characterise them to determine whether they retained the phenotype of the strains expressing extrachromosomal arrays. Following this, the organismal effects of TCS activation in these strains were quantified in terms of longevity, heat and oxidative stress resistance, and in a model of protein-folding disease (**Chapter 3**).

Next, to characterise the effects of TCS activation at the transcriptional level, whole-organism transcriptome profiling was performed using RNA-Seq. The effect of intestine-specific or pan-neuronal *hsp-90* knockdown on differential gene expression was determined compared to controls as described in **Chapter 4**. Genes identified

as upregulated in both TCS-activated strains compared to controls were taken forward for reverse genetic screening described in **Chapter 6**, as potentially important in TCS activation by tissue-specific *hsp-90* knockdown.

To identify genes required for the cell-non-autonomous upregulation of a *hsp-70p::mCherry* reporter on tissue-specific *hsp-90* knockdown, a forward genetic screen was performed in the strain expressing intestine-specific *hsp-90* RNAi (**Chapter 5**). Random mutations were induced throughout approximately 2000 genomes and progeny screened for a phenotype of altered *hsp-70* reporter expression. Lines identified by this screen underwent whole-genome sequencing combined with CB4856 (Hawaii) SNP mapping, in order to identify which mutations were potentially causal for the phenotype of interest. Genes identified in this manner were taken forward as candidates which were potentially required for cell-non-autonomous signalling in this form of TCS.

Finally, to identify whether the candidate genes identified by RNA-Seq or forward genetic screening/whole-genome sequencing are involved in inter-tissue signalling during TCS, a tissue-specific RNAi screen was performed in the strain expressing intestine-specific *hsp-90* RNAi (**Chapter 6**). Each gene was knocked down in either the intestine (the 'sending' tissue) or the body wall muscle (the 'receiving' tissue), and the effect on *hsp-70* reporter expression quantified. Genes whose tissue-specific knockdown caused a significant effect on *hsp-70* reporter expression were identified, and the subcellular localisations of proteins encoded by these genes were predicted using the tool DeepLoc 1.0. This was then used to propose a possible novel mechanism of cell-non-autonomous *hsp-70* upregulation during TCS activated by intestine-specific *hsp-90* knockdown.

# Chapter 2. Materials & general methods

## 2.1 *C. elegans* strains and genotypes

**Table 2.1** lists all *C. elegans* strains used in this project and their genotypes. N2, CB4856, NL3321 and PS3551 strains were obtained from the *Caenorhabditis* Genetics Centre (CGC). Strains AM722 and AM994 were kindly gifted by Dr Richard Morimoto (Northwestern University, USA).

| **Strain** | **Genotype** |
|---|---|
| N2 (Bristol) | Wild-type |
| CB4856 (Hawaii) | Polymorphic alternative wild-type |
| NL3321 | *sid-1* (*pk3321*) V |
| PS3551 | *hsf-1* (*sy441*) I |
| AM722<br>'*hsp-70p::mCherry* reporter' | rmIs288 (*myo-2p::CFP*; *C12C8.1p::mCherry*) |
| AM994 ('*hsp-90*$^{control}$') | *sid-1* (*pk3321*); rmIs288 (*myo-2p::CFP*; *C12C8.1p::mCherry*) |
| PVH1<br>'*hsp-90*$^{neu}$ hp-RNAi' | *sid-1* (*pk3321*); rmIs288 (*myo-2p::CFP*; *C12C8.1p::mCherry*); pccIs001 (*rgef-1p::daf-21 RNAi::unc-54 3′-UTR*) |
| PVH2<br>'*hsp-90*$^{int}$ hp-RNAi' | *sid-1* (*pk3321*); rmIs288 (*myo-2p::CFP*; *C12C8.1p::mCherry*); pccIs002 (*vha-6p::daf-21 RNAi::unc-54 3′-UTR*) |
| PVH184<br>'*hsp-90*$^{control}$; *hsf-1*' | *sid-1* (*pk3321*); rmIs288 (*myo-2p::CFP*; *C12C8.1p::mCherry*); *hsf-1* (*sy441*) I |
| PVH190<br>'*hsp-90*$^{int}$ hp-RNAi; *hsf-1*' | *sid-1* (*pk3321*); rmIs288 (*myo-2p::CFP*; *C12C8.1p::mCherry*); pccIs002 (*vha-6p::daf-21 RNAi::unc-54 3′-UTR*); *hsf-1* (*sy441*) I |
| PVH192<br>'*hsp-90*$^{neu}$ hp-RNAi; *hsf-1*' | *sid-1* (*pk3321*); rmIs288 (*myo-2p::CFP*; *C12C8.1p::mCherry*); pccIs001 (*rgef-1p::daf-21 RNAi::unc-54 3′-UTR*); *hsf-1* (*sy441*) I |
| AM135 ('Q0') | rmIs127 *(unc-54p::*YFP*)* |
| AM167 ('Q35') | rmIs156 *(unc-54p::*Q35::YFP*)* |
| PVH113<br>'Mutant 1' | *sid-1* (*pk3321*); rmIs288 (*myo-2p::CFP*; *C12C8.1p::mCherry*); pccIs002 (*vha-6p::daf-21 RNAi::unc-54 3′-UTR*); multiple EMS-induced mutations |
| PVH114<br>'Mutant 2' | *sid-1* (*pk3321*); rmIs288 (*myo-2p::CFP*; *C12C8.1p::mCherry*); pccIs002 (*vha-6p::daf-21 RNAi::unc-54 3′-UTR*); multiple EMS-induced mutations |
| PVH115<br>'Mutant 3' | *sid-1* (*pk3321*); rmIs288 (*myo-2p::CFP*; *C12C8.1p::mCherry*); pccIs002 (*vha-6p::daf-21 RNAi::unc-54 3′-UTR*); multiple EMS-induced mutations |

| | |
|---|---|
| PVH116<br>'Mutant 4' | *sid-1* (*pk3321*); rmIs288 (*myo-2p::CFP*; *C12C8.1p::mCherry*); pccIs002 (*vha-6p::daf-21 RNAi::unc-54 3'-UTR*); multiple EMS-induced mutations |
| PVH117<br>'Mutant 5' | *sid-1* (*pk3321*); rmIs288 (*myo-2p::CFP*; *C12C8.1p::mCherry*); pccIs002 (*vha-6p::daf-21 RNAi::unc-54 3'-UTR*); multiple EMS-induced mutations |
| PVH118<br>'Mutant 6' | *sid-1* (*pk3321*); rmIs288 (*myo-2p::CFP*; *C12C8.1p::mCherry*); pccIs002 (*vha-6p::daf-21 RNAi::unc-54 3'-UTR*); multiple EMS-induced mutations |
| PVH73 ('CB4856 x N2') | Cross between N2 (Bristol) and CB4856 (Hawaii) strains |
| PVH67<br>'CB4856 x *hsp-90*$^{control}$' | *sid-1* (*pk3321*); rmIs288 (*myo-2p::CFP*; *C12C8.1p::mCherry*) |
| PVH112<br>'CB4856 x *hsp-90*$^{int}$ hp-RNAi' | *sid-1* (*pk3321*); rmIs288 (*myo-2p::CFP*; *C12C8.1p::mCherry*); pccIs002 (*vha-6p::daf-21 RNAi::unc-54 3'-UTR*) |
| PVH119<br>'CB4856 x Mutant 1' | *sid-1* (*pk3321*); rmIs288 (*myo-2p::CFP*; *C12C8.1p::mCherry*); pccIs002 (*vha-6p::daf-21 RNAi::unc-54 3'-UTR*); multiple EMS-induced mutations |
| PVH120<br>'CB4856 x Mutant 2' | *sid-1* (*pk3321*); rmIs288 (*myo-2p::CFP*; *C12C8.1p::mCherry*); pccIs002 (*vha-6p::daf-21 RNAi::unc-54 3'-UTR*); multiple EMS-induced mutations |
| PVH121<br>'CB4856 x Mutant 3' | *sid-1* (*pk3321*); rmIs288 (*myo-2p::CFP*; *C12C8.1p::mCherry*); pccIs002 (*vha-6p::daf-21 RNAi::unc-54 3'-UTR*); multiple EMS-induced mutations |
| PVH122<br>'CB4856 x Mutant 4' | *sid-1* (*pk3321*); rmIs288 (*myo-2p::CFP*; *C12C8.1p::mCherry*); pccIs002 (*vha-6p::daf-21 RNAi::unc-54 3'-UTR*); multiple EMS-induced mutations |
| PVH123<br>'CB4856 x Mutant 5' | *sid-1* (*pk3321*); rmIs288 (*myo-2p::CFP*; *C12C8.1p::mCherry*); pccIs002 (*vha-6p::daf-21 RNAi::unc-54 3'-UTR*); multiple EMS-induced mutations |
| PVH124<br>'CB4856 x Mutant 6' | *sid-1* (*pk3321*); rmIs288 (*myo-2p::CFP*; *C12C8.1p::mCherry*); pccIs002 (*vha-6p::daf-21 RNAi::unc-54 3'-UTR*); multiple EMS-induced mutations |
| PVH5 | *sid-1* (*pk3321*); pccIs005 (*myo-3p::SID-1::unc-54 3'UTR*; *myo-2p::RFP*) |
| PVH65 | *sid-1* (*pk3321*); pccIs004 (*vha-6p::SID-1::unc-54 3'UTR*; *myo-2p::RFP*) |
| PVH171 | *sid-1* (*pk3321*); rmIs288 (*myo-2p::CFP*; *C12C8.1p::mCherry*); pccIs002 (*vha-6p::daf-21 RNAi::unc-54 3'-UTR*); pccIs005 (*myo-3p::SID-1::unc-54 3'UTR*; *myo-2p::RFP*) |
| PVH172 | *sid-1* (*pk3321*); rmIs288 (*myo-2p::CFP*; *C12C8.1p::mCherry*); pccIs002 (*vha-6p::daf-21 RNAi::unc-54 3'-UTR*); pccIs004 (*vha-6p::SID-1::unc-54 3'UTR*; *myo-2p::RFP*) |

**Table 2.1 List of *C. elegans* strains used and their corresponding genotypes**.

### 2.1.1 Strain maintenance and storage

Strains were maintained at 20°C, on 60 mm NGM agar plates seeded with OP50-1 *E. coli* and sealed with parafilm to prevent contamination. Plates were viewed using a Microtec light microscope or a Leica MDG41 fluorescence microscope. Strains were not kept growing for longer than 3 months to prevent accumulation of spontaneous mutations; after this time a fresh stock was thawed from storage at -80°C.

To prepare a strain for storage at -80°C, the strain was grown on two 60 mm NGM plates until the bacterial food source was depleted and all eggs had hatched. Absence of a food source upon egg hatching causes L1-stage *C. elegans* to arrest development in a pro-survival state (Baugh & Sternberg 2006), encouraging recovery upon thawing. Worms were washed from NGM plates into a 15 mL Falcon tube using sterile M9 minimal media (20 mM $Na_2HPO_4 \cdot 7H_2O$, 20 mM $KH_2PO_4$, 90 mM NaCl, 1 mM $MgSO_4$) and pelleted using low-speed centrifugation (1 minute at 1000rpm). The pellet was washed three times with fresh M9 buffer to remove any contaminants and resuspended in 3 mL. 500 µL of the suspension was taken into each of six 1.5 mL Eppendorf tubes, to which 500 µL of sterile worm freezing solution (100 mM NaCl, 0.3 mM $MgSO_4$, 50 mM $KPO_4$ pH 6.0, 24% glycerol) was added and mixed by inversion. Tubes were wrapped in tissue paper to slow the rate of temperature decrease and stored at -80°C.

### 2.1.2 Population synchronisation by bleaching

For each strain to be synchronised, a population was grown on a 60 mm NGM plate until there was a large number of non-starved gravid adults. Worms were washed from the plate into a 1.5 mL Eppendorf tube using M9 buffer and pelleted by low-speed centrifugation. As much M9 buffer as possible was removed without disturbing the pellet, and 1 mL bleaching solution (1% sodium hypochlorite, 0.25 M NaOH) added. Tubes were placed on a rotator for 5 minutes, following which the worms were pelleted again and the bleach removed. The pellet was washed three times with M9 buffer and resuspended in 1 mL after the final wash. Tubes were placed on a rotator at 20°C overnight so that eggs from the gravid adults, which resist bleaching, would hatch and arrest in L1 stage in the absence of a food source. When these synchronised larvae were then added to NGM plates seeded with OP50-1 the following morning, they then resumed development from the same point.

### 2.1.3 Crossing strains and generation of males

To cross two strains, two L4-stage hermaphrodites of one strain were placed on a 35 mm NGM plate with seven adult males of the other strain and allowed to cross-fertilise for two days. Males were removed after two days to prevent mating with cross progeny. L4-stage hermaphrodites were used in preference to adults in order to ensure as many eggs as possible were fertilised by males rather than by self-fertilisation. A low number of hermaphrodites was used to maximise the likelihood of all hermaphrodites mating, and to prevent overcrowding of the plate by progeny.

As most of the strains used here have a very low incidence of males in a normal population, strains were subjected to heat shock to increase the probability of X chromosome non-disjunction (Rose & Baillie 1979). Three plates of 10 L4-stage hermaphrodites per strain were subjected to 35°C heat stress for 3.5 hours, followed by removal to 20°C. Plates were checked daily for male progeny. If insufficient male progeny were produced to set up a genetic cross as described above, any identified males were placed on a plate with 1-2 L4-stage hermaphrodites of the same strain and allowed to mate to increase numbers of males. An exception to the requirement of heat-shocking to generate males was the CB4856 (Hawaii) strain, which has an unusually high prevalence of males (Wegewitz et al. 2008).

Following removal of males, plates were checked daily for $F_1$ progeny with appropriate phenotypes (see **Table 2.2**). Four L4-stage hermaphrodite $F_1$ progeny were selected and allowed to self-fertilise, and the development of $F_2$ progeny checked daily. At least 20 L4-stage hermaphrodite $F_2$ progeny with appropriate phenotypes were isolated and allowed to self-fertilise, following which $F_3$ progeny were monitored to ensure phenotype homozygosity. Once a population was identified which was homozygous for all relevant phenotypes, it was considered a successful cross and a stock of the new strain was frozen at -80°C.

| Allele | Phenotype |
|---|---|
| *sid-1* (*pk3321*) V | Arrest as larvae when grown on *hsp-90* RNAi (Eckl et al. 2017) |
| *hsf-1* (*sy441*) I | Thermosensitive; do not grow at 25°C |
| rmIs288 (*myo-2p::CFP*; *C12C8.1p::mCherry*) | Constitutive expression of CFP in pharynx; upregulation of *hsp-70p::mCherry* reporter on heat stress |
| rmIs288 in addition to pccIs001 (*rgef-1p::daf-21 RNAi::unc-54 3′-UTR*) | Constitutive expression of CFP in pharynx and strong *hsp-70p::mCherry* reporter expression in body wall muscle |
| rmIs288 in addition to pccIs002 (*vha-6p::daf-21 RNAi::unc-54 3′-UTR*) | Constitutive expression of CFP in pharynx and weak *hsp-70p::mCherry* reporter expression in body wall muscle |
| pccIs004 (*vha-6p::SID-1::unc-54 3'UTR*; *myo-2p::RFP*) | Constitutive expression of RFP in pharynx |
| pccIs005 (*myo-3p::SID-1::unc-54 3'UTR*; *myo-2p::RFP*) | Constitutive expression of RFP in pharynx |

**Table 2.2 Phenotypes used to confirm genetic crossing of strains**. Animals grown on *hsp-90* RNAi arrest at L2-L3, however the *sid-1* (*pk3321*) background prevents this due to loss of dsRNA transport.

### 2.1.4 Temperature regimen for heat stress

To activate the HSR, animals were exposed to a 35°C heat stress. Expression of heat shock response genes is rapidly upregulated in animals cultivated at 35°C, and peaks after approximately 4 hours at this temperature (Jovic et al. 2017). Using the *hsp-70p::mCherry* reporter strain, which expresses the red fluorescent protein mCherry under the control of the *hsp-70* gene promoter, it was determined that one hour heat stress at 35°C followed by three hours recovery at 20°C resulted in visible upregulation of mCherry (see **Chapter 3**). This temperature regimen was therefore used in all experiments where samples are designated as 'post-heat stress (HS)'.

## 2.2 Production of Nematode Growth Medium (NGM) or RNAi plates

### 2.2.1 Preparation of NGM and NGM-RNAi agar

Nematode growth medium (NGM) agar plates were prepared as recommended by WormBook (Stiernagle 2006). Liquid agar was prepared as 1.7% agar, 50 mM NaCl and 0.25% peptone and sterilised by autoclaving; followed by supplementation with 25 mM $KPO_4$ pH 6.0, 1 mM $CaCl_2$, 1 mM $MgSO_4$, 5 µg/mL cholesterol, and 200 µg/mL streptomycin. Solutions were sterilised prior to use by autoclaving or filter-sterilisation. Liquid NGM agar was dispensed into petri dishes within the sterile field of a Bunsen burner. Plates were loosely covered with aluminium foil and left to dry at room temperature overnight. NGM plates were seeded the next morning with bacterial cultures of OP50-1 *Escherichia coli*.

NGM agar plates for experiments using gene knockdown by RNAi feeding (NGM-RNAi plates) were produced in a similar manner to NGM plates. However, streptomycin was replaced with 100 µg/mL ampicillin, and 1mM isopropyl ß-d-1-thiogalactopyranoside (IPTG) was also added to stimulate RNAi production following plate seeding with bacterial RNAi cultures.

### 2.2.2 Preparation and seeding of bacterial cultures

Glycerol stocks of bacterial cultures were produced by adding 600 µL bacterial culture to 300 µL sterile 60% glycerol, mixing well and storing at -80°C.

To grow OP50-1 *E. coli* culture from a frozen glycerol stock, a pipette tip was used to transfer a small amount of frozen stock into an appropriate volume of lysogeny broth (LB). Streptomycin was added to a final concentration of 1 mg/mL, and the mixture incubated overnight at 37°C in a shaker. Cultures were seeded onto NGM plates the following morning. 35 mm plates were seeded with 80 µL bacterial culture, 60 mm plates with 200 µL culture, and 90 mm plates with 500 µL culture. Seeded plates were loosely covered with aluminium foil and left to dry at room temperature overnight, followed by storage at 4°C once dry.

RNAi clones were obtained from a *C. elegans* RNAi clone library (Source BioScience; Kamath & Ahringer 2003) which was stored in foil-covered 96-well plates at -80°C. Each RNAi in the library consists of an *E. coli* HT115 host transformed with an L4440 (pPD129.36) vector, into which has been cloned RNAi against a specific target gene. To grow an RNAi-expressing bacterial culture from the library, an appropriate volume of LB with ampicillin added to 1 mg/mL was prepared beforehand. The correct 96-well plate was removed from the library and the foil covering cleaned with 100% ethanol, before an RNase-free filtered pipette tip was used to pierce the film over the correct well and transfer a small amount of the frozen RNAi stock into the LB. A small piece of adhesive foil was used to reseal the well, and the plate was returned to -80°C. Cultures were incubated overnight in a 37°C shaker and seeded the next morning onto NGM-RNAi plates. Seeded plates were loosely covered with aluminium foil and left to dry at room temperature overnight, followed by storage at 4°C under aluminium foil once dry.

## 2.3 Confocal microscopy

### 2.3.1 Microscope slide preparation

Imaging of strains was performed using day 1 adults synchronised by egg-laying. To prepare microscope slides, a solution of 2% agarose was mixed and dissolved. A drop of agarose was added to a glass microscope slide, and another glass slide placed on top to create a flat disc. Once the agarose had set, the glass slides were separated. 5 µL of the cholinergic agonist levamisole (5 mM) was added to the agarose pad, into which five day 1 adult worms were picked. Once all worms were fully paralysed, they were carefully aligned using a platinum wire pick and excess levamisole removed before addition of a coverslip.

### 2.3.2 Microscope settings

Images were taken using an inverted Zeiss LSM880 laser scanning confocal microscope and Zen software. Images were taken at 10x and 20x magnifications, using a 561 nm laser for mCherry fluorescence excitation. Within an experiment, all images were taken using the same settings for pinhole size and fluorescence gain to enable fair comparisons. Identical 100 nm scale bars were added to each image.

### 2.3.3 Image analysis

Image analysis was performed using ImageJ software. All analysis of fluorescence intensity was performed on images taken using a 10x objective, to ensure that all parts of the sample were within the field of view. For each image, fluorescence was measured by selecting a rectangular area covering the entirety of the fluorescence channel. This generated data including the exact size of the area selected and the mean fluorescence intensity within that area. To account for slight differences in the area selected between images, the mean fluorescence intensity for each image was normalised to the area selected. Fluorescence intensity for each image was also normalised to the length of the worms in the image.

# Chapter 3. TCS is activated in strains carrying integrated transgene arrays with organismal benefits

## 3.1 Introduction

### 3.1.1 Systemic *hsp-90* depletion

As one of the normal functions of HSP-90 is to negatively regulate HSF-1 activity (Zou et al. 1998), one would expect systemic *hsp-90* knockdown to promote increased HSF-1 activity and upregulation of target genes such as *hsp-70*. Indeed, in strains carrying *hsp-70* transcriptional reporters, feeding of systemic *hsp-90* RNAi causes reporter upregulation; particularly in the body wall muscle (Gaiser et al. 2011; van Oosten-Hawle et al. 2013). However, this does not appear to improve the muscle folding environment, as these animals display reduced motility, muscle fibre disorganisation, and formation of insoluble myosin aggregates (Gaiser et al. 2011).

Based on the capacitor hypothesis, *hsp-90* knockdown would also be expected to cause aberrant development or other phenotypes through reduced buffering of cryptic mutations. Consistent with this, *hsp-90* is an essential gene for *C. elegans* development, and null mutations or embryonic RNAi result in early larval arrest (Birnby et al. 2000; Gaiser et al. 2011). Animals which are fed *hsp-90* RNAi from L1 stage onwards exhibit delayed development into sterile adults, and display organismal upregulation of HSF-1 target genes such as *hsp-70*, small heat shock proteins (sHSPs), and HSP-90 co-chaperones (Eckl et al. 2017). These animals also demonstrate downregulation of immune genes such as C-type lectins and aspartyl proteases, particularly in the intestine – a key tissue involved in the innate immune response. Furthermore, animals fed *hsp-90* RNAi from either L1 or L4 stage have reduced lifespans, reflecting its critical role in health and longevity (Somogyvári et al. 2018).

### 3.1.2 Tissue-specific *hsp-90* depletion

It has previously been shown that constitutive tissue-specific knockdown of *hsp-90* pan-neuronally or in the intestine or body wall muscle also causes delayed development and aberrant phenotypes (van Oosten-Hawle et al. 2013). This is accompanied by cell-non-autonomous upregulation of an *hsp-70p::mCherry* reporter via TCS, particularly in the body wall muscle and vulva; increased organismal expression of *hsp-70* transcripts; and resistance to heat stress. Increased survival following heat stress may potentially be due to the upregulation of protective *hsp-70*. Although the cell-non-autonomous upregulation of *hsp-70p::mCherry* in strains expressing tissue-specific *hsp-90* RNAi has been shown to depend on the transcription factor PHA-4, little else is currently known about the intra- or intercellular mechanisms underlying this process.

To better understand the organismal effects of TCS activation by tissue-specific *hsp-90* depletion, strains carrying integrated arrays of tissue-specific *hsp-90* hairpin RNAi were first characterised in terms of *hsp-70* expression. The creation of integrated lines rather than use of the previously described lines carrying extrachromosomal arrays was for the purpose of forward genetic screening (**Chapter 5**), as mutagenised animals screened for loss of *hsp-70p::mCherry* reporter fluorescence might simply not carry the transgene. The integrated strains were then used to quantify the effect of TCS activation on longevity, stress resistance, and protein aggregation.

## 3.2 Methods

### 3.2.1 Origin of strains

Previously published results describe data from strains which express tissue-specific *hsp-90* RNAi transgenes as extrachromosomal arrays (van Oosten-Hawle et al. 2013). This research has used different strains in which such transgenes have been integrated into the genome for stable expression, followed by backcrossing five times to a control *sid-1* (*pk3321*) mutant strain. Because of these differences, the strains used here cannot be directly compared with those previously described. Additionally, as attempts to create an integrated strain expressing body wall muscle-specific *hsp-90* RNAi were unsuccessful, it was not possible to address the question of TCS activation from the body wall muscle in an integrated line.

The strains used here as controls, AM722 and AM994, were kindly gifted by Dr Richard Morimoto (Northwestern University, USA). AM722, which is subsequently referred to as '*hsp-70p::mCherry* reporter strain', enables whole-organism visualisation of *hsp-70* (*C12C8.1*) transcriptional expression due to an integrated *hsp-70p::mCherry* reporter construct. When the *hsp-70* promoter is activated, both the *hsp-70* gene and the *mCherry* fluorescent reporter should be transcriptionally upregulated. AM994, subsequently referred to as '*hsp-90*$^{control}$', was used as control strain for most experiments in this thesis. AM994 was created by genetically crossing the *hsp-70p::mCherry* reporter strain with NL3321, which carries a *sid-1* (*pk3321*) mutation. The *pk3321* allele has a D130N missense mutation causing an exonic G-A substitution, preventing the activity of SID-1 as a transmembrane transporter and resulting in loss of systemic RNAi (Winston et al. 2002). This enabled the restriction of *hsp-90* hairpin RNAi (hp-RNAi) to specific tissues in the PVH1 and PVH2 strains as discussed below. Prior to use in this project, I backcrossed the *hsp-90*$^{control}$ strain five times to NL3321.

Strains PVH1 and PVH2, subsequently referred to as '*hsp-90*$^{neu}$ hp-RNAi' and '*hsp-90*$^{int}$ hp-RNAi' respectively, were created by Dr Patricija van Oosten-Hawle (van Oosten-Hawle et al. 2013). pccIs001 and pccIs002 transgenes, expressing *hsp-90* hairpin RNAi (hp-RNAi) under the control of either the pan-neuronal *rgef-1* promoter or the intestine specific *vha-6* promoter, were microinjected into the gonad of *hsp-90*$^{control}$ animals. Transgenes were injected as complex arrays using *myo-*

*2p::CFP* as a co-injection marker. Genomic integration of extrachromosomal transgene arrays was performed by gamma irradiation. Prior to use in this project, I backcrossed both PVH1 and PVH2 five times to NL3321; however in both cases the *myo-2p::CFP* co-injection marker was lost during backcrossing. The combination of a global *sid-1* (*pk3321*) loss-of-function mutation with tissue-specific expression of *hsp-90* hp-RNAi facilitates the restriction of RNAi to the tissue of expression, as the lack of functional SID-1 prevents hp-RNAi import (Winston et al. 2002; Jose et al. 2009). To investigate the role of *hsf-1* in these strains, *hsp-90*$^{control}$, *hsp-90*$^{int}$ hp-RNAi and *hsp-90*$^{neu}$ hp-RNAi animals were crossed with the PS3551 strain. This strain carries an *hsf-1* (*sy441*) allele, in which a W585 nonsense mutation results in a truncated loss-of-function HSF-1 protein. These crosses resulted in the PVH184, PVH190 and PVH192 strains respectively (**Table 2.1**).

### 3.2.2 Survival and motility assays

#### 3.2.2.1 Lifespan assay

Lifespan assays were performed by Megan Bonsor, a former MBiol student in the van Oosten-Hawle group. One biological replicate was performed per strain. Animals were synchronised by bleaching, and 100 L4-stage animals per strain picked onto 60 mm NGM plates. Each subsequent day the numbers of alive, dead and censored animals were recorded. Animals were recorded as dead if they displayed no visually perceptible movement including pharyngeal pumping, and no response to touching with a sterilised platinum wire. Animals were censored if they had crawled onto the side of the plate and become desiccated, if they had burrowed into the agar, if they displayed internal egg hatching ('bag of worms' phenotype) or if they could not be located. During days 1-7 of adulthood live worms were transferred each day to a new NGM plate to prevent recording of progeny; from day 8 onwards live animals were transferred to new NGM plates every two days. GraphPad Prism 7 software (2018) was used to plot lifespan data as survival curves and compare them using a log-rank (Mantel-Cox) test, with comparisons considered significant if they resulted in $p < 0.05$. This would suggest a <5% chance of incorrectly rejecting the null hypothesis that there is no difference between groups; although it does not confirm that an alternative hypothesis is true, or that any difference found is not due to random chance. Confidence in an alternative hypothesis can be strengthened by testing it in several different ways using sufficiently large numbers of biological replicates.

#### 3.2.2.2 Thermotolerance assay

Three biological replicates were performed within each experiment. For each strain, three replicates of thirty gravid adults were allowed to lay eggs for 6 hours on 60 mm NGM plates. Synchronised progeny were allowed to develop to L4 stage, at which point three replicate plates of 50 L4-stage animals were picked per strain per time point. The next day, plates containing day 1 adults were incubated at 35°C for 4, 8 or 10 hours, following which they were removed to 20°C. Plates were scored for percentage survival on the following day, with animals being counted as alive if they displayed movement, pharyngeal pumping or response to light touch with sterilised platinum wire, and counted as dead otherwise. Significant differences compared to mean *hsp-90*$^{control}$ survival were determined at each time point by one-way ANOVA with multiple comparisons, with correction for multiple testing performed using the two-stage linear step-up procedure of Benjamini, Krieger and Yekutieli with a false discovery rate of 0.05.

#### 3.2.2.3 Oxidative stress assay

Three biological replicates were performed within each experiment. For each strain, three replicates of twenty gravid adults were allowed to lay eggs for 6 hours on 60 mm NGM plates. Synchronised progeny were allowed to develop to day 1 adulthood, then washed into 1.5 mL Eppendorf tubes using M9 buffer. Worms in each sample were pelleted by low-speed centrifugation and M9 buffer removed to 100 µL. 100 µL of 0.3 M paraquat was added to each sample for a final concentration of 0.15 M, and all samples were incubated at 20°C on a rotator for 6 hours. After the incubation period, each sample was again pelleted by low-speed centrifugation and the pellet washed three times with M9 buffer. After the final wash, M9 buffer was removed to 50 µl and each sample added to a 35 mm NGM plate. Percentage survival was scored the next morning using the same criteria as for thermotolerance assays. Significant differences compared to mean *hsp-90*$^{control}$ survival were determined by one-way ANOVA with multiple comparisons, with correction for multiple testing performed using the two-stage linear step-up procedure of Benjamini, Krieger and Yekutieli with a false discovery rate of 0.05. N2 and *pqm-1* (*ok485*) values were also compared using Student's t test.

#### 3.2.2.4 Paralysis assay

Three biological replicates were performed over three experiments. For each strain, two 60 mm NGM plates of twenty gravid adults were allowed to lay eggs for 6 hours. Synchronised progeny were allowed to develop to L4 stage, at which point 100 animals were picked per strain. Each subsequent day for 10 days, the numbers of animals which were mobile, paralysed or censored were recorded. Worms were considered mobile if they were able to move freely, either unprompted or when touched with a sterilised platinum wire. Worms were considered paralysed if they could not move their body normally, but still displayed some movement or pharyngeal pumping. Worms were censored if they had crawled onto the side of the plate and become desiccated, if they had burrowed into the agar, or if they could not be located. Each day, worms which were mobile were moved to a new plate. Paralysis data was plotted in GraphPad Prism software as a survival curve. Significant differences between survival curves were determined using a log-rank (Mantel-Cox) test.

### 3.2.3 Quantitative reverse transcription PCR (qRT-PCR)

#### 3.2.3.1 Sample preparation

Three independent replicate samples were prepared per strain or condition. For each sample, a mixed-age population was allowed to grow on a 60 mm NGM plate until the plate was full, but within 24 hours of the bacterial food source having been exhausted. Chilled RNase-free water was used to wash worms from the plate into a 1.5 mL RNase-free Eppendorf tube, which was kept on ice to minimise RNA degradation. The sample was pelleted by low-speed centrifugation at 4°C and washed 3 times with RNase-free water to remove any residual bacteria. Excess water was removed and the pellet frozen at -80°C.

#### 3.2.3.2 RNA extraction

Frozen samples were homogenised in TRIzol (guanidium thiocyanate) from Ambion, followed by RNA extraction using a Zymo Research Direct-Zol RNA MiniPrep kit according to the manufacturer's instructions. Samples were kept on ice at all stages of the extraction process to reduce RNA degradation. Firstly, 50 µL of TRIzol was added to each sample, followed by homogenisation with a pellet grinder. Each sample

was ground three times for 30 seconds, with at least 30 seconds on ice between each grinding. Another 150 µL of TRIzol was added, and samples vortexed at 4°C for 10 minutes to ensure tissue breakdown. Tissue debris was removed by centrifuging samples at 13000 rpm for 30 seconds and transferring the supernatant to an RNase-free Eppendorf tube. 200 µL of 100% ethanol was added to facilitate salt formation, and each sample transferred to a Zymo-Spin IICR column with collection tube. Following centrifugation at 13000 rpm for 30 seconds, flow-through was discarded and a new collection tube used. Samples were washed with RNA Wash Buffer containing the chelating agent EDTA in Tris hydrochloride, and were further treated with DNase I and DNA Digestion Buffer to remove DNA. Samples were washed again before elution with RNase-free water. RNA concentration was measured using a Thermo Scientific NanoDrop One. RNA samples were stored at -80°C.

#### 3.2.3.3 cDNA synthesis

For each sample, 100 ng of RNA was reverse transcribed into cDNA using a Bio-Rad iScript cDNA synthesis kit according to the manufacturer's instructions. Reactions contained 100 ng RNA, 4 µL iScript Reaction Mix (a combination of oligo(dT) and random hexamer primers), 1 µL reverse transcriptase, and nuclease-free water up to 20 µL. The thermal cycling profile described in **Table 3.1** was performed using an Applied Biosystems Veriti 96-Well Thermal Cycler. cDNA samples were stored at 4°C for short periods, or at -80°C for long-term storage.

| Temperature (°C) | Duration (minutes) |
|---|---|
| 25 | 5 |
| 46 | 20 |
| 95 | 1 |
| 4 | ∞ |

**Table 3.1 Thermal cycling profile used in cDNA synthesis**.

#### 3.2.3.4 qRT-PCR protocol & primers

Quantification of relative transcript expression was performed in reaction volumes of 20 µL. Each reaction contained 1 µL cDNA template, 0.5 µL 10 µM forward primer, 0.5 µL 10 µM reverse primer, 8 µL nuclease-free water, and 10 µL 2X Bio-Rad SsoAdvanced Universal SYBR Green Supermix (containing DNA polymerase,

dNTPs, SYBR green dye, and $MgCl_2$). For each gene to be quantified, forward and reverse primers were prepared beforehand with SYBR Green Supermix and nuclease-free water as a master mix to reduce pipetting errors. Sequences and suppliers of primers used are listed below in **Table 3.2**. Quantitative PCR (qPCR) was performed in a Bio-Rad CFX Connect Real-Time System using the temperature regimen described in **Table 3.3**.

| Gene | Forward primer | Reverse primer | Supplier |
|---|---|---|---|
| *cdc-42* | TGTCGGTAAAACTTGTCTCCTG | ATCCTAATGTGTATGGCTCGC | IDT |
| *hsp-70* | GATCAAGCCGCTCGTAATCC | AACCTCAACAACGGGCTTTC | IDT |
| *hsp-90* | GACCAGAAACCCAGACGATATC | GAAGAGCACGGAATTCAAGTTG | IDT |
| *mCherry* | TTGAAGGTGAAGGAGAAGGC | AGGCGAATGGTAATGGTCC | IDT |

**Table 3.2 Primers used in qPCR**. IDT: Integrated DNA Technologies.

| Step | | Temperature (°C) | Duration (seconds) |
|---|---|---|---|
| Initial denaturation | | 95 | 180 |
| 40 cycles | Denaturation | 95 | 15 |
| | Primer annealing | 56 | 30 |
| | Extension | 72 | 30 |
| Final extension | | 72 | 60 |
| Melt curve | | 55-95 (0.5°C increments) | 10 |

**Table 3.3 qPCR thermal cycling protocol**.

#### 3.2.3.5 Data analysis

Determination of relative transcript expression for each gene was performed using the comparative Ct ($2^{-\Delta\Delta Ct}$) method, in which the cycle threshold (Ct) values for each gene in each strain are normalised twice. Firstly, values for each gene of interest are normalised within each strain by the average value of a control gene, giving the $\Delta Ct$ value for each sample. Then, values for each gene are normalised across strains by the average value for that gene in a control strain, giving the $\Delta\Delta Ct$ value for each sample. Finally, the relative expression value for each sample is

calculated as ($2^{-\Delta\Delta Ct}$). The gene used as a control was the stably expressed GTPase *cdc-42* (Hoogewijs et al. 2008), and the strain used as a control was *hsp-90*$^{control}$. Three biological replicates were performed per strain. Significant differences between mean relative expression were determined by one-way ANOVA with multiple comparisons, with correction for multiple testing performed using the two-stage linear step-up procedure of Benjamini, Krieger and Yekutieli with a false discovery rate of 0.05.

## 3.3 Results

### 3.3.1 The *hsp-70p::mCherry* reporter is induced upon heat stress in controls

In *C. elegans,* heat-inducible *hsp-70* (*C12C8.1*) is not normally expressed at ambient temperature (20°C). However, it is rapidly upregulated upon heat stress at 35°C through activation of the HSR (GuhaThakurta et al. 2002; Guisbert et al. 2013). This can be visualised in the *hsp-70p::mCherry* reporter and *hsp-90*$^{control}$ strains, due to their expression of the *hsp-70p::mCherry* reporter construct. At 20°C, the *hsp-70p::mCherry* reporter and *hsp-90*$^{control}$ strains show no visible reporter expression **(Fig 3.1a)**. However, following 1 hour of heat stress at 35°C and 3 hours of recovery at 20°C, the *hsp-70* reporter is visibly expressed in various tissues including the spermatheca and posterior intestine (**Fig. 3.1a**). *hsp-70* reporter upregulation is stronger in the *hsp-90*$^{control}$ strain, which harbours a *sid-1* mutation, than in the wild-type strain expressing *hsp-70p::mCherry* (**Fig. 3.1b**). It can be seen in **Figure 3.1a** that expression in the posterior intestine is much stronger in the *hsp-90*$^{control}$ strain following heat stress. This suggests that the upregulation of *hsp-70* may be accelerated in the *hsp-90*$^{control}$ compared to the *hsp-70p::mCherry* reporter strain; potentially as a consequence of the *sid-1* (pk3321) mutation, as this is the key difference in genotype.

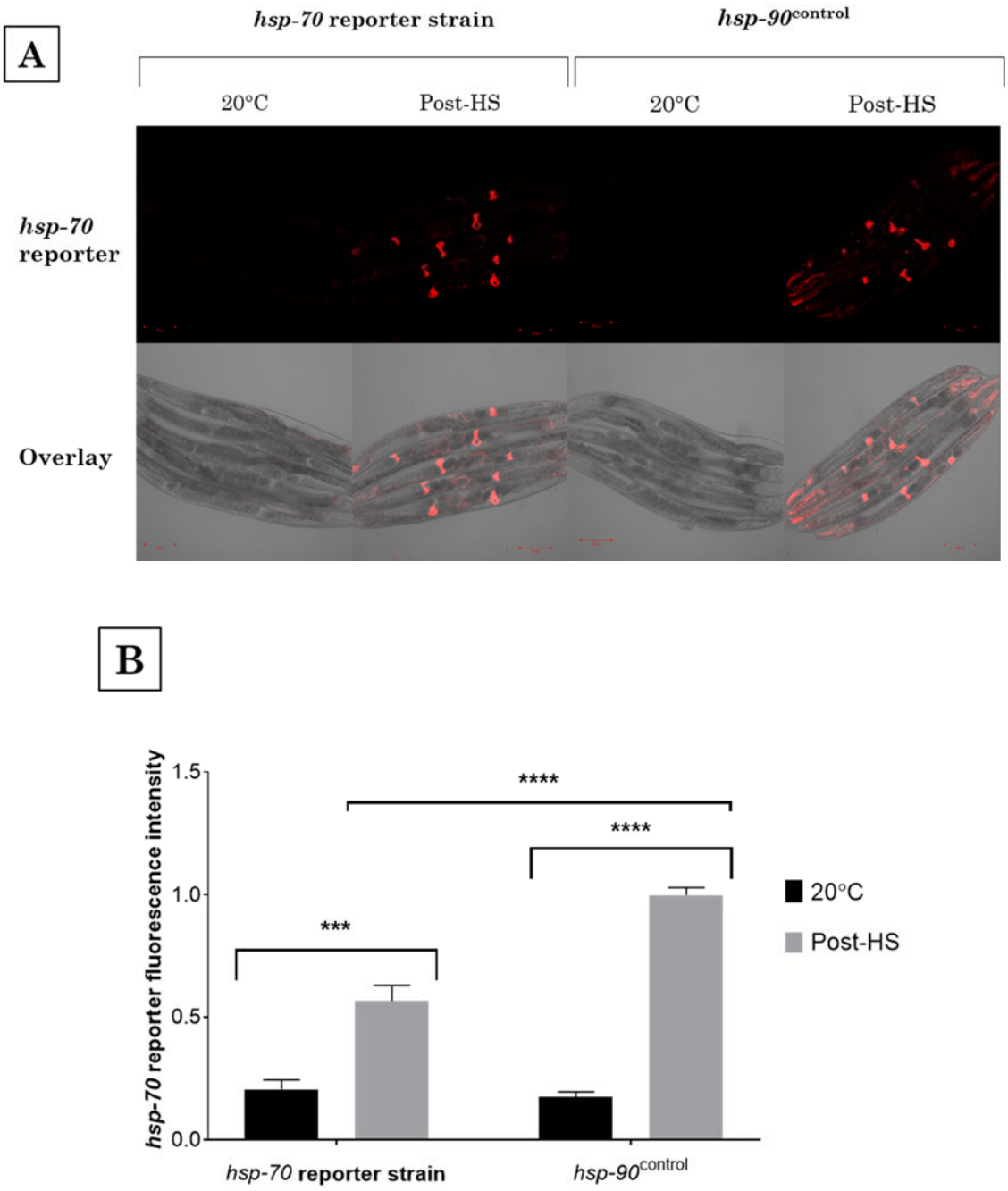


**Figure 3.1 *hsp-70p::mCherry* reporter expression in wild-type and *sid-1* mutant (*hsp-90*$^{control}$) animals**. (**A**) Images of the *hsp-70p::mCherry* reporter and *hsp-90*$^{control}$ strains at 20°C or post-heat stress (HS). Scale bars: 100µm. (**B**) Quantification of fluorescence intensity normalised by post-HS *hsp-90*$^{control}$ values. Each bar represents at least 3 biological replicates. Comparisons were made using Student's t test; error bars represent standard error of the mean (SEM). *** = p<0.001; **** = p<0.0001.

### 3.3.2 Tissue-specific *hsp-90* knockdown activates TCS in an *hsf-1*-independent manner

In agreement with published data (van Oosten-Hawle et al. 2013), strains expressing constitutive pan-neuronal or intestine-specific *hsp-90* RNAi display *hsp-70p::mCherry* reporter upregulation in the body wall muscle (**Fig. 3.2a**). However, this cell-non-autonomous reporter upregulation is considerably stronger in the *hsp-90*$^{int}$ hp-RNAi strain than in the *hsp-90*$^{neu}$ hp-RNAi strain (**Fig. 3.2b**). This differs from the published data, which showed that pan-neuronal or intestine-specific *hsp-90* knockdown caused similar upregulation of *hsp-70* mRNA. It is possible that different transgene copy numbers might have been integrated between these two strains, leading to stronger transgene expression in the strain expressing intestinal *hsp-90* RNAi. Whilst the *hsp-70p::mCherry* reporter is upregulated in control strains following heat stress (**Fig. 3.1**), this is not the case in the strains with tissue-specific *hsp-90* knockdown, and heat stress causes no further increase in reporter expression (**Figs. 3.3c,e; 3.4**). A possible explanation for this is that basal *hsp-70* levels are already increased, and so it may not be necessary to upregulate it further. Another possibility is that the ability to upregulate it further is somehow impaired.

Since *hsp-70* is a target gene of HSF-1, and depletion of *hsp-90* would be expected to increase HSF-1 activity, further experiments were performed to determine whether cell-non-autonomous upregulation of the *hsp-70* reporter is dependent on *hsf-1*. An *hsf-1* (*sy441*) loss-of-function mutation was introduced into the *hsp-90*$^{control}$, *hsp-90*$^{int}$ hp-RNAi and *hsp-90*$^{neu}$ hp-RNAi strains. In the *hsp-90*$^{control}$ strain, upregulation of the *hsp-70* reporter following heat stress was reduced by two-thirds when the *hsf-1* (*sy441*) mutation was present (**Figs. 3.3a,b; 3.4**). This would be expected for an *hsf-1*-dependent heat shock response gene such as *hsp-70*, and confirms that the *hsf-1* (*sy441*) mutation was successfully introduced. However, introduction of the *hsf-1* (*sy441*) mutation into *hsp-90*$^{int}$ hp-RNAi and *hsp-90*$^{neu}$ hp-RNAi had no effect on expression of the *hsp-70* reporter; either at 20°C or following heat stress (**Figs. 3.3c-f; 3.4**). This indicates that the cell-non-autonomous upregulation of the *hsp-70* reporter seen in these strains is not due to increased HSF-1 activity, and may therefore be *hsf-1*-independent.

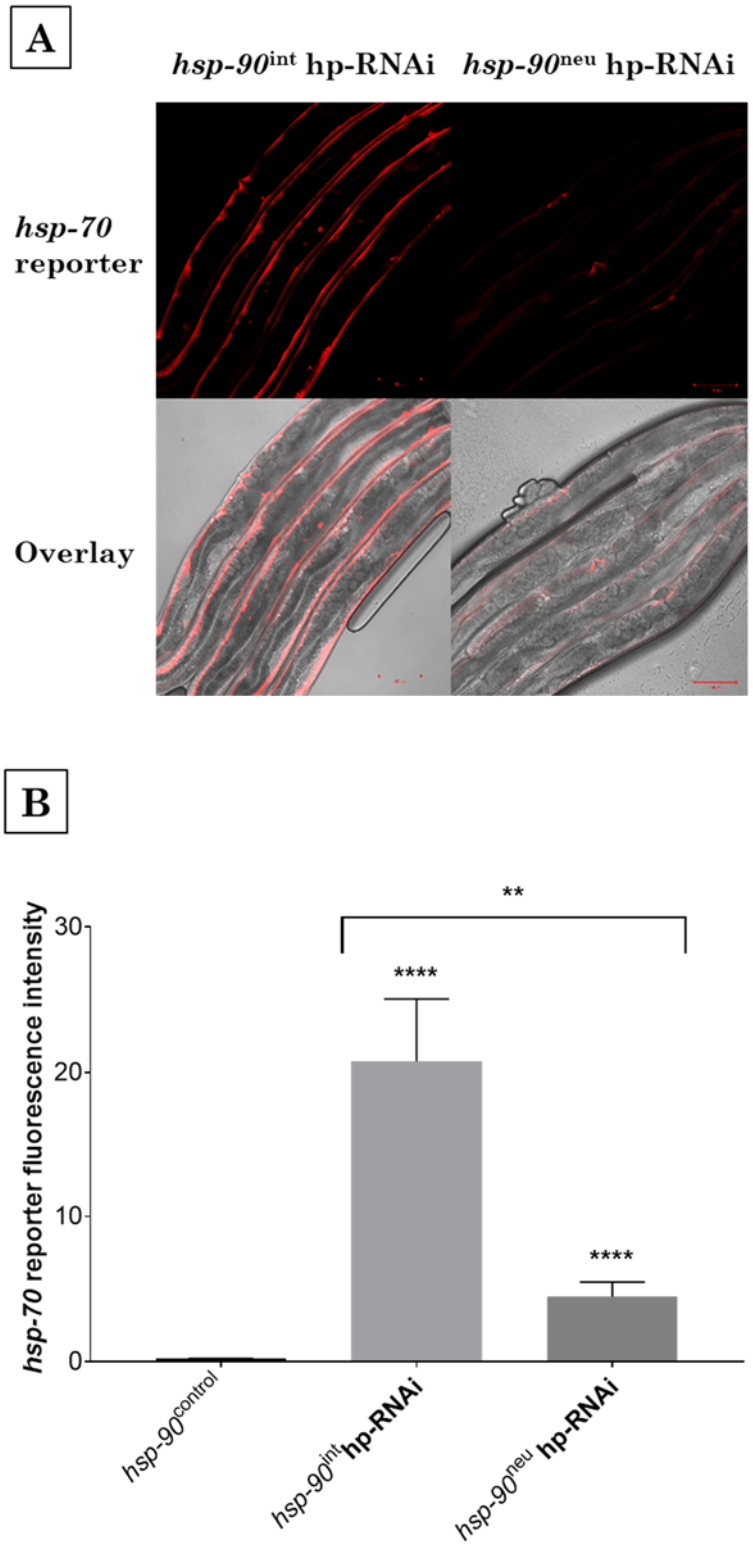


**Figure 3.2 Tissue-specific *hsp-90* knockdown causes *hsp-70* reporter upregulation.** (**A**) *hsp-70p::mCherry* reporter fluorescence in the *hsp-90*$^{int}$ hp-RNAi and *hsp-90*$^{neu}$ hp-RNAi strains at 20°C. Scale bars: 100µm. (**B**) Quantification of reporter fluorescence intensity normalised by *hsp-90*$^{control}$ values at 20°C. Each bar represents at least 3 biological replicates. Comparisons were made using Student's t test; error bars represent SEM. ** = $p<0.01$; **** = $p<0.0001$.

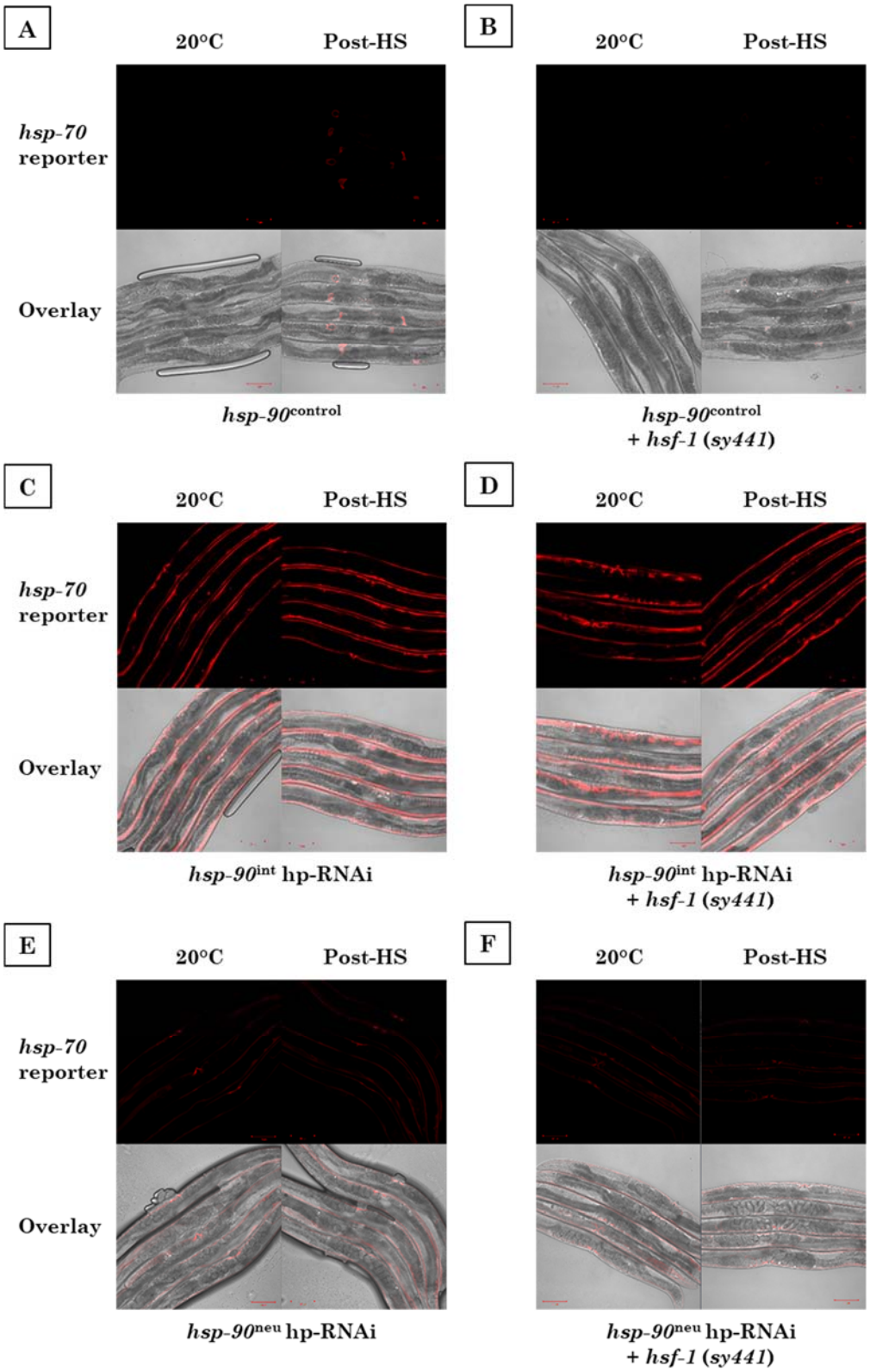


**Figure 3.3 Reporter upregulation in TCS-activated strains is not affected by heat stress or the *hsf-1* (*sy441*) allele**. Effect of heat stress (HS) on *hsp-70p::mCherry* reporter fluorescence in (**A**) *hsp-90*$^{control}$, (**B**) *hsp-90*$^{control}$; *hsf-1* (*sy441*), (**C**) *hsp-90*$^{int}$ hp-RNAi, (**D**) *hsp-90*$^{int}$ hp-RNAi; *hsf-1* (*sy441*), (**E**) *hsp-90*$^{neu}$ hp-RNAi and (**F**) *hsp-90*$^{neu}$ hp-RNAi; *hsf-1* (*sy441*). Representative 20x images; scale bars: 100µm.

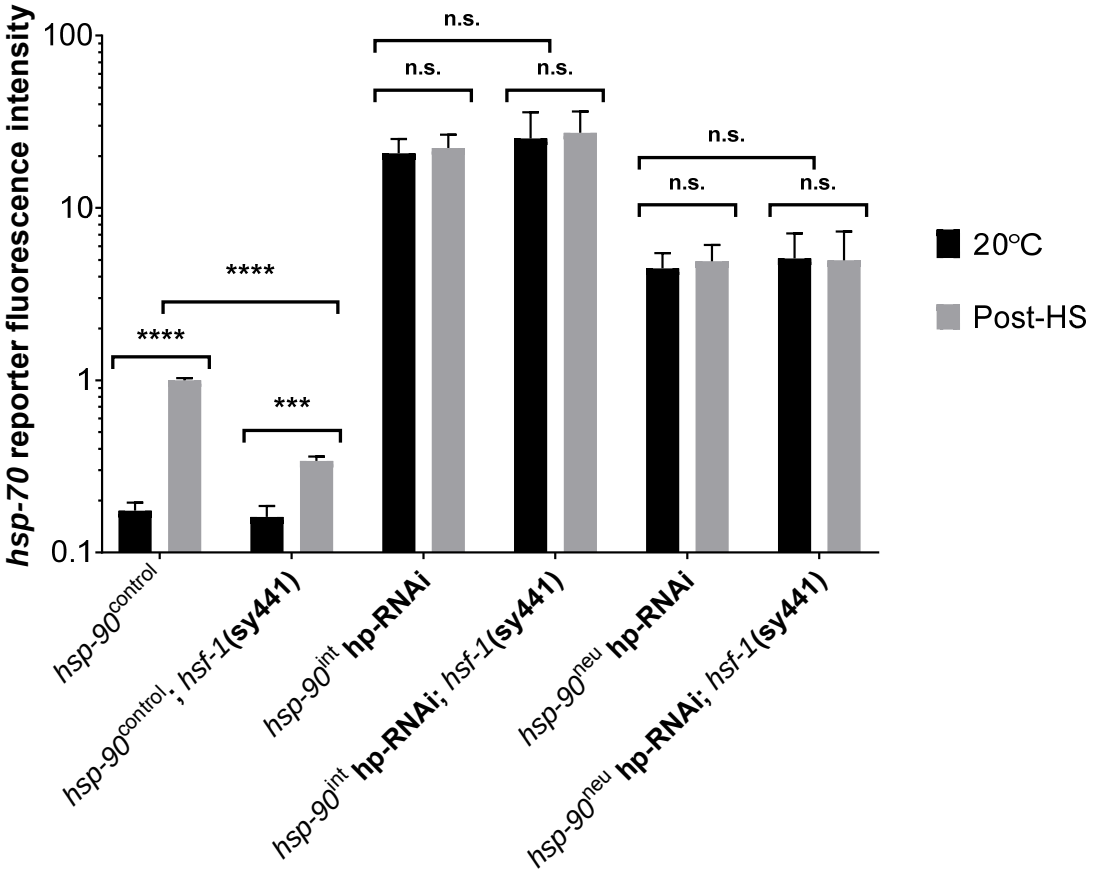


**Figure 3.4 Quantification of reporter fluorescence following heat stress and in *hsf-1* (*sy441*) mutants**. Quantification of reporter fluorescence in the *hsp-90*$^{control}$, *hsp-90*$^{int}$ hp-RNAi and *hsp-90*$^{neu}$ hp-RNAi strains at 20°C or post-heat stress (HS); in the original strains and following introduction of the *hsf-1* (*sy441*) mutation. Values were normalised by post-HS *hsp-90*$^{control}$ values. Each bar represents at least 3 biological replicates. Comparisons were made using Student's t test; error bars represent SEM. *** = $p<0.001$; **** = $p<0.0001$; n.s. = not significant ($p>0.05$).

### 3.3.3 Tissue-specific *hsp-90* knockdown causes upregulation of *hsp-70* and *mCherry* transcripts

To confirm that the *hsp-90*$^{int}$ hp-RNAi and *hsp-90*$^{neu}$ hp-RNAi strains demonstrate organismal upregulation of *hsp-70* at the transcript level, quantitative reverse transcription PCR (qRT-PCR) was performed. **Figure 3.5(a,b)** shows that at 20°C, whole-animal transcript levels of *hsp-70* and *mCherry* are not significantly different between *hsp-90*$^{control}$ and wild-type, confirming that these genes are not normally expressed in unstressed controls. However, expression of both genes is significantly increased in the *hsp-90*$^{int}$ hp-RNAi strain compared to the *hsp-90*$^{control}$ strain, indicating that *hsp-70* reporter expression reflects *hsp-70* transcriptional upregulation in this strain. In the *hsp-90*$^{neu}$ hp-RNAi strain, the expression of *mCherry* is increased over a hundred-fold whilst there is only a small increase in *hsp-70* expression (p=0.1). This could perhaps suggest a defect in the endogenous *hsp-70* promoter, or an artificial over-activation of the transgene *hsp-70* promoter. The magnitude of *hsp-70* mRNA upregulation in these strains, which harbour integrated *hsp-90* hp-RNAi arrays, is different compared to strains expressing extrachromosomal *hsp-90* hp-RNAi arrays. Extrachromosomal expression of *hsp-90*$^{int}$ hp-RNAi and *hsp-90*$^{neu}$ hp-RNAi arrays resulted in a 6-fold increase in of *hsp-70* mRNA levels (van Oosten-Hawle et al. 2013). The integrated arrays of the same transgenes used here show increases of approximately 4.5-fold or 2.5-fold in the *hsp-90*$^{int}$ hp-RNAi and *hsp-90*$^{neu}$ hp-RNAi strains respectively (**Figure 3.5a**). This indicates that TCS is not induced as strongly in these strains as in those expressing extrachromosomal arrays of tissue-specific *hsp-90* RNAi.

To determine how strongly *hsp-90* is knocked down in these strains at the whole-organism level, transcript levels of *hsp-90* were quantified (**Fig. 3.5c**). *hsp-90* expression is not significantly different in the wild-type, *hsp-90*$^{int}$ hp-RNAi or *hsp-90*$^{neu}$ hp-RNAi strains compared to the *hsp-90*$^{control}$ strain, although it is reduced by approximately 50% in the *hsp-90*$^{int}$ hp-RNAi strain (p=0.1). As a stronger knockdown of *hsp-90* suggests a stronger activation of TCS, this is potentially the reason why upregulation of *hsp-70* transcripts and the *hsp-70* reporter is weaker in these strains than in the previously described extrachromosomal strains.

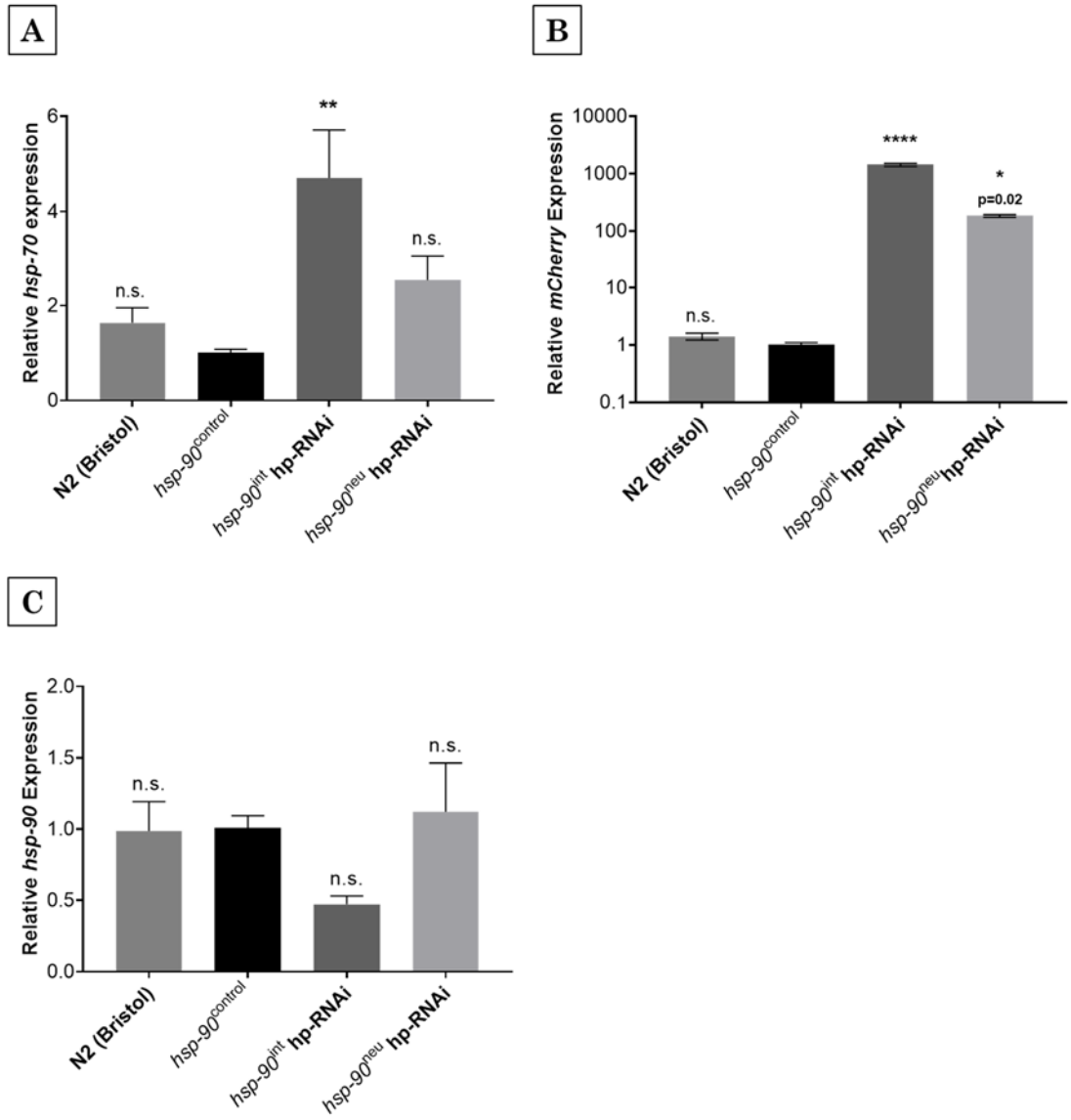


**Figure 3.5 Organismal transcript levels of *hsp-70*, *mCherry* and *hsp-90*.** Whole-animal transcript levels of (**A**) *hsp-70*, (**B**) *mCherry*, (**C**) *hsp-90* in the wild-type, *hsp-90*$^{control}$, *hsp-90*$^{int}$ hp-RNAi and *hsp-90*$^{neu}$ hp-RNAi strains at 20°C. *cdc-42* and *hsp-90*$^{control}$ were the control gene and strain used for normalisation. Each bar represents at least 3 biological replicates. Significant differences relative to *hsp-90*$^{control}$ were determined by one-way ANOVA with multiple comparisons; error bars represent SEM. * = $p<0.05$; ** = $p<0.01$; **** = $p<0.0001$; n.s. = not significant.

### 3.3.4 Intestine-specific *hsp-90* knockdown increases longevity

Decreased *hsf-1* activity, either by RNAi or by *hsf-1* (*sy441*) mutation, has been shown to reduce lifespan (Hsu et al. 2003; Morley & Morimoto 2003; Chiang et al. 2012); whereas overexpression of *hsf-1* increases lifespan (Morley & Morimoto 2003; Chiang et al. 2012). Lifespan is increased even if *hsf-1* is only overexpressed in a single tissue such as the neurons, intestine or body wall muscle (Morley & Morimoto 2003). This is thought to be partly due to increased expression of protective HSF-1 target genes such as sHSPs and *hsp-70*. Whilst RNAi against *hsp-70* does not decrease the lifespan of wild-type animals, perhaps because it is not normally expressed, knockdown of either *hsf-1* or *hsp-70* counteracts the extended lifespan seen in *age-1* mutants (Morley & Morimoto 2003). *age-1* functions in ILS to inhibit DAF-16 activation (Dorman et al. 1995). This indicates that upregulation of HSF-1 target genes such as *hsp-70* can contribute to lifespan extension. Since *hsp-70* is constitutively upregulated in the *hsp-90*$^{int}$ hp-RNAi strain, lifespan assays were performed to determine whether this also promotes increased lifespan. All lifespan assays were performed by Megan Bonsor, a former MBiol student in the van Oosten-Hawle group.

As expected, the survival curve of *hsf-1* (*sy441*) mutants was shifted significantly to the left and median lifespan was reduced compared to wild-type (**Fig. 3.6**). *sid-1* (*pk3321*) mutants demonstrated a similar effect, suggesting that *sid-1* activity may also promote longevity; although there is little published data to further support this. Whilst the survival curve of the *hsp-90*$^{control}$ strain was not significantly different to wild-type, this strain does demonstrate a reduced median lifespan, potentially due to the *sid-1* (*pk3321*) allele. The *hsp-90*$^{neu}$ hp-RNAi strain did not have a significantly different survival curve to either *hsp-90*$^{control}$ or wild-type, or a reduced median lifespan. However, the *hsp-90*$^{int}$ hp-RNAi strain had an increased median lifespan of 21 days and a significantly different survival curve compared to both *hsp-90*$^{control}$ and wild-type. This correlates with the strength of *hsp-70* upregulation. As *hsp-70* is upregulated much more strongly in the *hsp-90*$^{int}$ hp-RNAi strain than the *hsp-90*$^{neu}$ hp-RNAi strain (**Figs. 3.2b; 3.5a**), this may explain why lifespan is increased only in the former. However, it is important to note that these data represent only one biological replicate, and more replicates must be performed to increase confidence in these results.

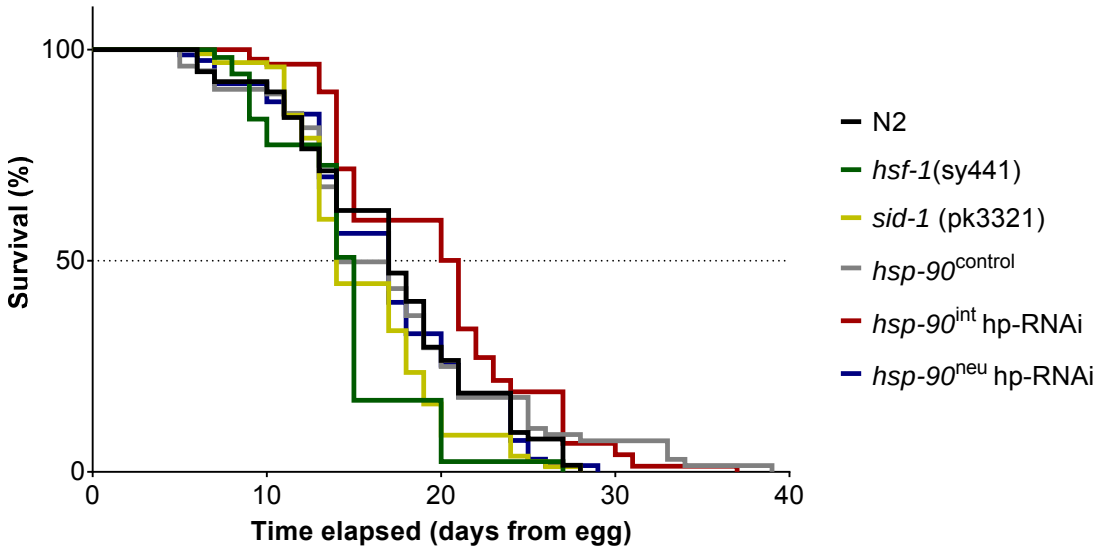


| Strain | Median Lifespan (days) | Survival curve comparisons | |
|---|---|---|---|
| | | vs N2 | vs *hsp-90*$^{control}$ |
| N2 | 17 | - | p=0.70 |
| *hsp-90*$^{control}$ | 14 | p=0.7 | - |
| *hsp-90*$^{int}$ hp-RNAi | 21 | p=0.003 | p=0.022 |
| *hsp-90*$^{neu}$ hp-RNAi | 17 | p=0.64 | p=0.44 |
| *sid-1* (*pk3321*) | 14 | p=0.027 | p=0.019 |
| *hsf-1* (*sy441*) | 15 | p=0.005 | p=0.036 |

**Figure 3.6 Lifespan is increased in the *hsp-90*$^{int}$ hp-RNAi strain**. Survival curves and median lifespan are shown for each strain based on one biological replicate. Survival curves were compared using a log-rank (Mantel-Cox) test with a significance threshold of p=0.05, comparisons meeting this threshold are highlighted in blue.

### 3.3.5 Heat stress resistance in the *hsp-90*$^{int}$ hp-RNAi and *hsp-90*$^{neu}$ hp-RNAi strains

It was previously shown that activation of TCS by pan-neuronal or intestine-specific *hsp-90* knockdown confers increased survival following 8 or 10 hours of heat stress (van Oosten-Hawle et al. 2013). To confirm whether this is also the case in the integrated *hsp-90*$^{int}$ hp-RNAi and *hsp-90*$^{neu}$ hp-RNAi strains, thermotolerance assays were performed (**Fig. 3.7**). As expected, *hsf-1* (*sy441*) mutants show strongly reduced survival following 8 or 10 hours of heat stress, likely due to an inability to upregulate heat shock response genes. The *hsp-90*$^{int}$ hp-RNAi and *hsp-90*$^{neu}$ hp-RNAi strains exhibited increased survival following 4 hours of heat stress compared to the *hsp-90*$^{control}$ strain, suggesting increased resistance to acute heat stress. However, following 8 or 10 hours of heat stress, survival of the *hsp-90*$^{int}$ hp-RNAi strain is not significantly different to the control, and survival of the *hsp-90*$^{neu}$ hp-RNAi strain is in fact reduced (**Fig. 3.7**). It is important to note here that the strains used in this research express integrated *hsp-90* hp-RNAi arrays, rather than the extrachromosomal arrays expressed in strains for which results were previously reported (van Oosten-Hawle et al. 2013); although one would expect them to show a similar effect. As the strains expressing integrated arrays do not appear to show such a strong upregulation of *hsp-70* mRNA as strains expressing extrachromosomal arrays (**Fig. 3.5a**; van Oosten-Hawle et al 2013), this could explain reduced protection against chronic heat stress.

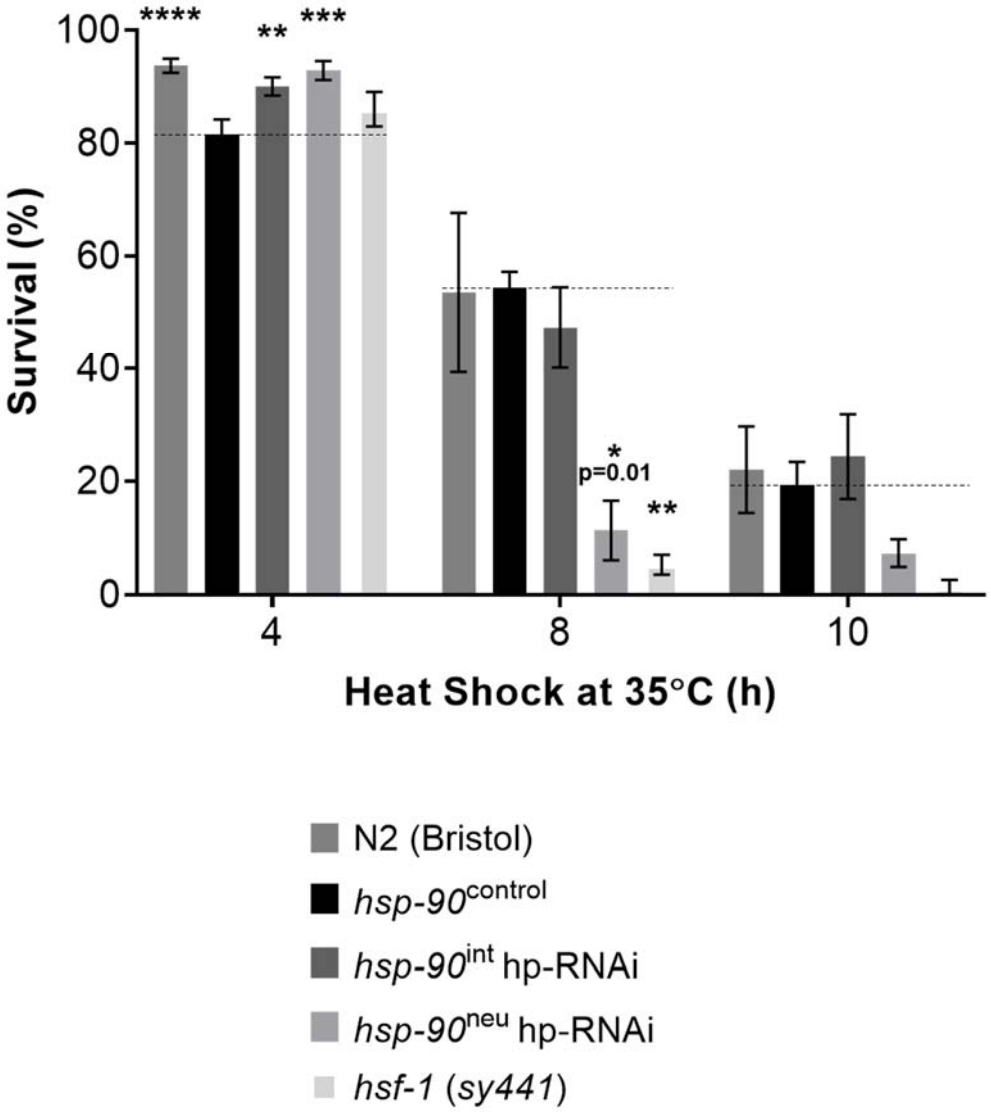


**Figure 3.7 Heat stress resistance in TCS-activated strains**. Survival was quantified the next day following 35°C heat stress. Dashed lines represent average *hsp-90*$^{control}$ survival per time point, to which mean values for other strains were compared by one-way ANOVA with multiple comparisons. Bars represent at least 3 replicates of 50 day 1 adults. Error bars represent SEM. * = $p<0.05$; ** = $p<0.01$; *** = $p<0.001$; **** = $p<0.0001$.

### 3.3.6 Pan-neuronal *hsp-90* knockdown promotes survival following oxidative stress

The oxidative stressor paraquat promotes increased ROS generation and is associated with increased activity of the paraquat-responsive transcription factor *pqm-1* (Qabazard et al. 2014). *pqm-1* is required in TCS activated by tissue-specific HSP-90 overexpression, and *pqm-1* mutant animals are also more sensitive to heat stress (O'Brien et al. 2018). To determine whether cell-non-autonomous *hsp-70* upregulation is also relevant in the case of oxidative stress, strains were exposed to paraquat and their survival quantified. As expected, animals carrying a loss-of-function *pqm-1* (*ok485*) mutation showed increased sensitivity to paraquat, with decreased survival following acute exposure (**Fig 3.8**). Surprisingly, the *hsp-90*$^{control}$ strain showed even stronger sensitivity. This may be another consequence of the *sid-1* (*pk3321*) allele. As *sid-1* is normally upregulated upon exposure to paraquat (Yee et al. 2014), this loss-of-function mutation may prevent some function relating to survival following oxidative stress. Compared to the *hsp-90*$^{control}$ strain, the *hsp-90*$^{int}$ hp-RNAi strain showed no significant difference in sensitivity to paraquat. However, the *hsp-90*$^{neu}$ hp-RNAi strain showed increased survival compared to the *hsp-90*$^{control}$ strain, indicating that resistance to oxidative stress is increased in the case of pan-neuronal *hsp-90* knockdown.

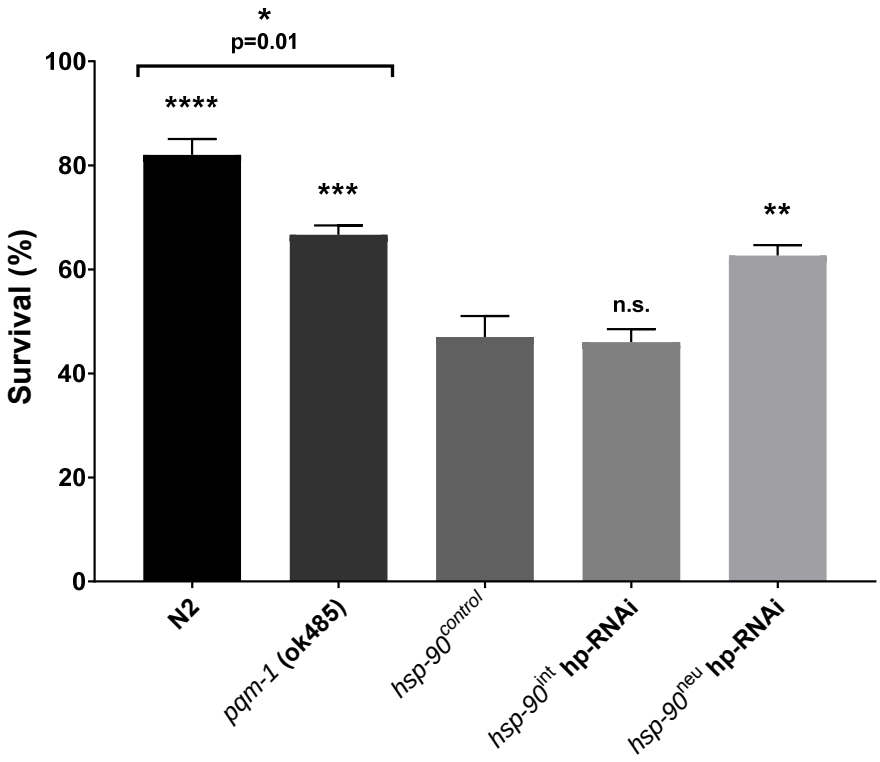


**Figure 3.8 Neuron-specific *hsp-90* knockdown increases oxidative stress survival**. Survival was quantified the next day following 6 hours exposure to 0.15M paraquat. 3 replicates of approximately 100 day 1 adults were scored per strain. Mean survival of each strain was compared to that of *hsp-90*$^{control}$ by one-way ANOVA with multiple comparisons, and N2 was also compared with *pqm-1* (*ok485*) using Student's t test. Error bars represent SEM. * = p<0.05; ** = p<0.01; *** = p<0.001; **** = p<0.0001; n.s. = not significant (p>0.05).

### 3.3.7 *hsp-70* upregulation during TCS does not ameliorate the polyQ paralysis phenotype

It has previously been shown that activation of TCS by tissue-specific HSP-90 over-expression ameliorates the paralysis phenotype seen in the CL2006 *C. elegans* model of Alzheimer's disease (O'Brien et al. 2018). In this model, which expresses amyloid beta ($A\beta_{3\text{-}42}$) in the body wall muscle, over-expression of HSP-90 in the intestine or neurons partially rescued the paralysis phenotype whilst over-expression in the body wall muscle fully rescued it. As pan-neuronal or intestine-specific over-expression of HSP-90 results in upregulation of HSP-90 in the body wall muscle by TCS (van Oosten-Hawle et al. 2013), this rescue is presumably facilitated by increased HSP-90-mediated protein folding in the body wall muscle.

To determine whether cell-non-autonomous *hsp-70* upregulation in the body wall muscle can also rescue a paralysis phenotype caused by protein misfolding in that tissue, the *hsp-90*$^{control}$ and *hsp-90*$^{int}$ hp-RNAi strains were crossed with a polyglutamine (polyQ) disease model. The disease model AM167 (termed Q35) expresses a polyQ repeat of length 35 tagged with yellow fluorescent protein (YFP), under the control of the muscle-specific *unc-54* promoter. This strain displays an age-dependent paralysis phenotype (**Fig 3.9**; Morley et al. 2002). The *hsp-90*$^{control}$ and *hsp-90*$^{int}$ hp-RNAi strains were also crossed with the control strain AM135 (termed Q0), which expresses Q0::YFP under the control of the *unc-54* promoter and does not display the paralysis phenotype. As shown in **Figure 3.9**, the paralysis rate of Q0 or Q35 animals was not affected by crossing to the *hsp-90*$^{control}$ or *hsp-90*$^{int}$ hp-RNAi strains. In Q35 animals which had been crossed to the *hsp-90*$^{int}$ hp-RNAi strain, the rate of paralysis was slightly reduced after day 6 of adulthood; however, this difference was not significant. This indicates that whilst upregulation of HSP-90 in the body wall muscle can rescue protein folding in that tissue and ameliorate a paralysis phenotype (O'Brien et al. 2018), upregulation of *hsp-70* does not appear to have the same effect. This reflects other published data in which RNAi knockdown of *hsf-1* or sHSPs, but not *hsp-70*, accelerates the aggregation of polyQ (Hsu et al. 2003). Taken together, this suggests that *hsp-70* may not be effective at preventing polyQ aggregation.

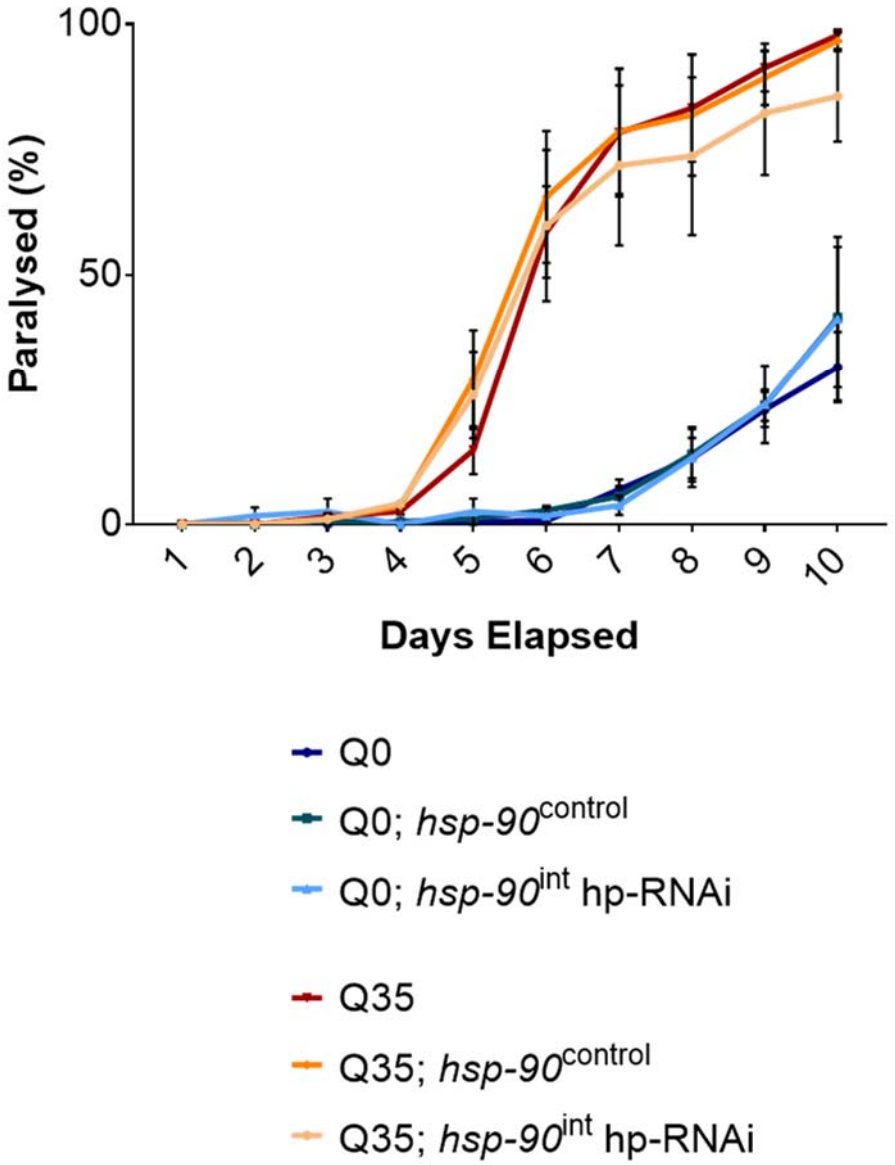


**Figure 3.9 TCS activated by intestine-specific *hsp-90* knockdown does not significantly affect the polyQ paralysis phenotype**. Paralysis assay of Q0 (control) and Q35 (polyQ disease model) strains crossed with the *hsp-90*$^{control}$ or *hsp-90*$^{int}$ hp-RNAi strain. 3 replicates of 100 animals were scored per strain; error bars represent SEM. Paralysis curves were compared using a log-rank (Mantel-Cox) test with a significance threshold of $p<0.05$; no comparisons met this threshold.

## 3.4 Discussion

### 3.4.1 Heat stress causes stronger reporter upregulation in the *hsp-90*$^{control}$ strain than in the *hsp-70p::mCherry* reporter strain

The introduction of the *sid-1* (*pk3321*) mutation appears to result in stronger upregulation of the *hsp-70* reporter following heat stress (**Fig. 3.1**). In wild-type animals fed control RNAi, *sid-1* is normally downregulated following heat stress (Brunquell et al. 2016). However, in animals fed *hsf-1* RNAi *sid-1* is upregulated, and even more strongly so following heat stress (Brunquell et al. 2016). This suggests that HSF-1 regulates SID-1 activity. Despite this, as the *hsp-90*$^{control}$, *hsp-90*$^{int}$ hp-RNAi and *hsp-90*$^{neu}$ hp-RNAi strains all share the *sid-1* (*pk3321*) loss-of-function allele, inferences from comparisons between these strains will still be fair.

### 3.4.2 TCS is activated in strains carrying integrated transgenes

Both the *hsp-90*$^{int}$ hp-RNAi and *hsp-90*$^{neu}$ hp-RNAi strains exhibit cell-non-autonomous *hsp-70* reporter upregulation, and the *hsp-90*$^{int}$ hp-RNAi strain also demonstrates increased organismal *hsp-70* transcript expression (**Figs. 3.2, 3.5a**). Reporter upregulation is considerably stronger in the *hsp-90*$^{int}$ hp-RNAi strain than in the *hsp-90*$^{neu}$ hp-RNAi strain. However, neither strain displays a significant reduction in organismal *hsp-90* transcript levels compared to controls (**Fig. 3.5c**). The *hsp-90*$^{int}$ hp-RNAi and *hsp-90*$^{neu}$ hp-RNAi strains used here carry integrated transgenes, and so differ from previously published data using strains carrying extrachromosomal arrays. It is possible that different copy numbers of each transgene were integrated into the genomes of the two strains. If it were the case that fewer transgene copies had been integrated into the *hsp-90*$^{neu}$ hp-RNAi strain than into the *hsp-90*$^{int}$ hp-RNAi strain, this could explain their differences in expression of *hsp-70* and the *hsp-70p::mCherry* reporter.

As the data in **Figure 3.5** represents whole-animal transcripts, it may be the case that neurons represent a relatively small amount of total body space, and so neuronal knockdown might not have such a large impact on organismal *hsp-90* levels. It is also possible that whilst *hsp-90* may be effectively knocked down in the

target tissue, it may be upregulated elsewhere in a compensatory mechanism. For example, in the *hsp-90*$^{neu}$ hp-RNAi strain, *hsp-90* might be effectively knocked down in the neurons but consequently upregulated in another tissue such as the body wall muscle. A straightforward way of determining this would be to cross each of the *hsp-90*$^{control}$, *hsp-90*$^{int}$ hp-RNAi and *hsp-90*$^{neu}$ hp-RNAi strains into another strain carrying a reporter for HSP-90, such as HSP-90::GFP, and to compare reporter expression patterns. Alternatively, more complex methods are available to quantify tissue-specific transcript expression. Tissue-specific transcriptome analysis has been performed by Blazie et al. (2015) using polyA-tagging and sequencing (PAT-seq); by Cao et al. (2017) using cell-specific combinatorial barcoding; and by Kaletsky et al. (2018) using tissue-specific GFP expression and fluorescence-assisted cell sorting (FACS).

### 3.4.3 *hsf-1* is not required for cell-non-autonomous *hsp-70* reporter upregulation in TCS

In the *hsp-90*$^{control}$ strain, upregulation of the *hsp-70* reporter following heat stress is lost when the *hsf-1* (*sy441*) mutation is introduced (**Fig. 3.3a,b**). This is expected as *hsp-70* is known to be upregulated following heat shock in an *hsf-1*-dependent manner (GuhaThakurta et al. 2002; Guisbert et al. 2013). However, introduction of the *hsf-1* (*sy441*) mutation into the *hsp-90*$^{int}$ hp-RNAi or *hsp-90*$^{neu}$ hp-RNAi strains does not affect expression of the *hsp-70* reporter (**Figs. 3.3c-f, 3.4**). This indicates that cell-non-autonomous *hsp-70* reporter upregulation activated by tissue-specific *hsp-90* knockdown does not require *hsf-1*, suggesting that TCS is a cell-non-autonomous stress response which is distinct from the HSR.

If *hsp-70* reporter upregulation in the *hsp-90*$^{int}$ hp-RNAi and *hsp-90*$^{neu}$ hp-RNAi strains does not require *hsf-1*, this raises the question of how *hsp-70* is transcriptionally regulated during TCS. The transcription factor *pha-4* has previously been shown to be required for *hsp-70p::mCherry* reporter upregulation in strains expressing extrachromosomal *hsp-90* hp-RNAi in the intestine, neurons or body wall muscle (van Oosten-Hawle et al. 2013). *pha-4* may therefore also be required for *hsp-70* reporter upregulation in the integrated *hsp-90*$^{int}$ hp-RNAi and *hsp-90*$^{neu}$ hp-RNAi strains. Additionally, TCS in strains with tissue-specific overexpression of HSP-90 has also been shown to be *hsf-1*-independent (van Oosten-Hawle et al. 2013), instead depending on both *pha-4* and the transcription factor

*pqm-1* (van Oosten-Hawle et al. 2013; O'Brien et al. 2018). This may indicate a possible role for *pqm-1* in the *hsp-90*$^{int}$ hp-RNAi and *hsp-90*$^{neu}$ hp-RNAi strains.

### 3.4.4 The *hsp-90*$^{int}$ hp-RNAi strain demonstrates increased *hsp-70* expression and increased lifespan

The fact that decreasing *hsf-1* activity by mutation or RNAi decreases lifespan, whilst *hsf-1* overexpression increases lifespan, suggests that HSF-1 target genes are involved in promoting longevity (Hsu et al. 2003; Morley & Morimoto 2003; Chiang et al. 2012). In addition, RNAi against *hsf-1* or *hsp-70* blunts the extended longevity of long-lived *age-1* mutants, indicating that *hsp-70* has a role in lifespan extension (Morley & Morimoto 2003). Although the stronger cell-non-autonomous *hsp-70* upregulation in the *hsp-90*$^{int}$ hp-RNAi strain does not depend on *hsf-1* (**Fig. 3.3c,d**), this strain does display increased lifespan (**Fig. 3.6**). Conversely, the *hsp-90*$^{neu}$ strain, which shows relatively weak *hsp-70* upregulation (**Figs. 3.2; 3.5a**), does not have an extended lifespan (**Fig. 3.6**). It is therefore possible that the increased lifespan seen in the *hsp-90*$^{int}$ hp-RNAi strain is due to its stronger upregulation of *hsp-70*. However, as activation of TCS likely results in the differential expression of many genes, lifespan extension may have a different cause. To determine whether increased *hsp-70* expression is responsible for this increased longevity, lifespan could be quantified in the *hsp-90*$^{control}$, *hsp-90*$^{int}$ hp-RNAi and *hsp-90*$^{neu}$ hp-RNAi strains when *hsp-70* is knocked down. However, as the *sid-1* (*pk3321*) allele prevents systemic RNAi, this would have to be done using a *hsp-70* mutant. Furthermore, to determine whether lifespan extension in the *hsp-90*$^{int}$ hp-RNAi strain is also independent of *hsf-1*, the effect of the *hsf-1* (*sy441*) mutation on the lifespan of this strain could be quantified. It should also be noted that as only one biological replicate was performed for this experiment, caution should be used in interpreting the results until more replicates are performed.

### 3.4.5 Heat stress resistance in the *hsp-90*$^{int}$ hp-RNAi and *hsp-90*$^{neu}$ hp-RNAi strains

Strains expressing pan-neuronal or intestine-specific *hsp-90* RNAi have been shown to demonstrate increased survival following heat stress (van Oosten-Hawle et al. 2013). However, whilst the *hsp-90*$^{int}$ hp-RNAi and *hsp-90*$^{neu}$ hp-RNAi strains show higher survival rates than controls following 4 hours heat stress; this is not the case

after 8 or 10 hours of heat stress (**Fig. 3.7**). The *hsp-90*$^{int}$ hp-RNAi and *hsp-90*$^{neu}$ hp-RNAi strains differ from the strains previously described in that they express integrated rather than extrachromosomal transgene arrays. Importantly, compared to published data, the integrated strains show a lower upregulation of both the *hsp-70p::mCherry* reporter and organismal *hsp-70* transcripts. This could partly explain the weaker response seen here compared to that previously reported. Tissue-specific knockdown of *hsp-90* has also previously been shown to result in aberrant phenotypes, in line with the *hsp-90* capacitor hypothesis (van Oosten-Hawle et al. 2013). It is possible that the loss of resistance to chronic heat stress is due to such an aberrant phenotype, whose expression has become possible through chronic heat stress-mediated depletion of available HSP-90. A method to address this could be to backcross each strain to the *sid-1* (*pk3321*) mutant strain again for an increased number of generations, for example 10 backcrosses instead of 5; and then to repeat thermotolerance assays immediately before cryptic variants can arise.

An alternative possibility is suggested by the fact that following heat stress, the *hsp-70* reporter is not further upregulated in the *hsp-90*$^{int}$ hp-RNAi and *hsp-90*$^{neu}$ hp-RNAi strains; that is, that these strains may be unable to detect or respond to heat stress. However, this is highly speculative. If such were the case, the increased survival of the *hsp-90*$^{int}$ hp-RNAi and *hsp-90*$^{neu}$ hp-RNAi strains after 4 hours heat stress could be due to their constitutive TCS-activated cell-non-autonomous *hsp-70* upregulation. The lack of protection against longer heat shock durations could be due to the inability to mount a response to heat stress. To investigate the dependence of thermotolerance in these strains on *hsp-70* expression, the experiment could be repeated using animals in which *hsp-70* is knocked down. In addition, the ability of these strains to activate the HSR in response to heat stress could be quantified by measuring transcript levels of other HSF-1 target genes such as sHSPs, in the presence or absence of heat shock. Alternatively, these strains might have an impaired ability to detect heat stress. As *C. elegans* prefer to remain at their cultivation temperature (Hedgecock & Russell 1975), the strains could be cultivated at a certain temperature and then placed on a temperature gradient to determine whether they can detect and return to their preferred temperature.

### 3.4.6 TCS activated by tissue-specific *hsp-90* knockdown does not rescue paralysis in the Q35 polyQ model

In the case of TCS activated by tissue-specific HSP-90 overexpression, HSP-90 is upregulated cell-non-autonomously in tissues including the body wall muscle (van Oosten-Hawle et al. 2013). This can ameliorate aggregation and paralysis phenotypes caused by body wall muscle-specific expression of the amyloidogenic protein Aß$_{(3-42)}$ (O'Brien et al. 2018). Similarly, in the *hsp-90*$^{int}$ hp-RNAi strain, intestine-specific *hsp-90* knockdown causes cell-non-autonomous *hsp-70* reporter upregulation in the body wall muscle (**Fig. 3.2a**). However, this does not rescue the paralysis phenotype of the Q35 polyQ disease model, which expresses aggregation-prone Q35::YFP in the body wall muscle (**Fig. 3.9**).

It is possible that although *hsp-70* is upregulated in the body wall muscle of the *hsp-90*$^{int}$ hp-RNAi strain, this *hsp-70* may be unable to prevent polyQ aggregation. It has previously been shown that in animals fed *hsp-90* RNAi, the folding environment of the body wall muscle is compromised even though an *hsp-70p::GFP* reporter is upregulated in that tissue (Gaiser et al. 2011). This indicates that increased *hsp-70* expression is unable to compensate for systemic *hsp-90* depletion in terms of the organismal folding environment; although it is unclear how this would be affected in the case of tissue-specific *hsp-90* depletion. Although research on TCS activated by tissue-specific *hsp-90* knockdown has so far focused largely on cell-non-autonomous *hsp-70* upregulation, there may well be transcellular effects on other aspects of proteostasis which remain to be identified.

# Chapter 4. Transcriptome profiling in *hsp-90* hp-RNAi strains

## 4.1 Introduction

It has previously been shown that when TCS is activated by pan-neuronal HSP-90 overexpression, many genes are differentially expressed compared to wild-type (O'Brien et al. 2018). It is therefore possible that TCS activated by tissue-specific *hsp-90* knockdown could also cause differential gene expression. Indeed, the *hsp-70* transcriptional reporter and organismal *hsp-70* mRNA are differentially expressed in both the *hsp-90*$^{int}$ hp-RNAi and *hsp-90*$^{neu}$ hp-RNAi strains compared to controls (**Figs. 3.2, 3.5a**). By comparing the organismal transcriptomes of the *hsp-90*$^{int}$ hp-RNAi and *hsp-90*$^{neu}$ hp-RNAi strains with those of control strains, we can identify which genes are differentially expressed during TCS depending on which tissue *hsp-90* is knocked down in. This may indicate whether certain genes are particularly strongly expressed, or whether groups of genes relating to specific biological processes are differentially regulated together. Differentially expressed genes which are common to both the *hsp-90*$^{int}$ hp-RNAi and *hsp-90*$^{neu}$ hp-RNAi strains could also potentially indicate a common signalling mechanism activated by tissue-specific *hsp-90* knockdown.

Comparison of the organismal transcriptomes of multiple strains can be performed using RNA-sequencing (RNA-Seq) (Wang et al. 2009). In this process, total RNA is extracted from each strain and reverse-transcribed to cDNA, which is fragmented into segments of a certain length and sequenced by high-throughput deep-sequencing. The resulting short sequences ('reads') are aligned to an annotated reference genome for the relevant species. The number of reads which align to each known transcript in the genome can then be quantified, identifying which transcripts were present in the original total RNA samples and their relative expression levels. Analysis of expression levels between strains can then determine whether each transcript is significantly differentially expressed between samples.

# 4.2 Methods

## 4.2.1 Sample preparation and quality control

Three biological replicates of total RNA were prepared per strain for the N2, *hsp-90*$^{control}$, *hsp-90*$^{int}$ hp-RNAi and *hsp-90*$^{neu}$ RNAi strains as described in **Sections 3.2.3.1 and 3.2.3.2**. To confirm that samples were of sufficient quality, the 260/280 and 260/230 absorbance ratios of each sample were determined using a Thermo Scientific NanoDrop spectrophotometer, and the concentration and RNA integrity number (RIN) of each sample were determined by the University of Leeds Next Generation Sequencing Facility using an Agilent 2200 TapeStation (**Table 4.1**).

| Strain | Rep. | Concentration (ng/µl) | RIN | Abs. (260/280) | Abs. (260/230) |
|---|---|---|---|---|---|
| N2 | 1 | 59.1 | 10.0 | 2.00 | 2.30 |
| | 2 | 70.4 | 10.0 | 1.99 | 2.38 |
| | 3 | 61.1 | 10.0 | 2.07 | 2.22 |
| *hsp-90*$^{control}$ | 1 | 57.0 | 10.0 | 2.00 | 2.13 |
| | 2 | 83.4 | 9.5 | 2.03 | 2.28 |
| | 3 | 83.9 | 10.0 | 2.09 | 2.41 |
| *hsp-90*$^{int}$ hp-RNAi | 1 | 72.2 | 10.0 | 2.00 | 2.21 |
| | 2 | 84.8 | 10.0 | 2.03 | 2.25 |
| | 3 | 81.9 | 9.9 | 2.01 | 2.17 |
| *hsp-90*$^{neu}$ hp-RNAi | 1 | 113.0 | 10.0 | 2.04 | 2.26 |
| | 2 | 104.0 | 10.0 | 2.07 | 2.31 |
| | 3 | 74.1 | 10.0 | 2.04 | 2.33 |

**Table 4.1 Quality control data for RNA-Seq samples**. Rep.= Replicate. Absorbance ratios (Abs.) were determined using a Thermo Scientific NanoDrop spectrophotometer. Concentration (ng/µl) and RNA Integrity Number (RIN) were determined using an Agilent 2200 TapeStation by the University of Leeds Next Generation Sequencing Facility.

### 4.2.2 RNA-Seq and data analysis performed by Novogene (Hong Kong)

RNA samples were shipped on dry ice to Novogene (Hong Kong), who performed RNA-Seq and data analysis as described below and summarised in **Figure 4.1**. All work described in **Section 4.2.2** was performed by Novogene unless otherwise specified.

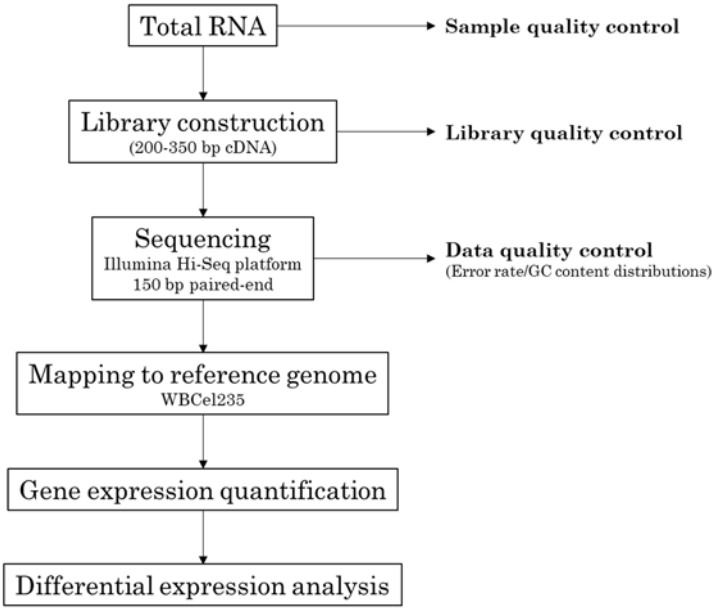


**Figure 4.1 RNA-Seq workflow performed by Novogene**.

#### 4.2.2.1 cDNA library preparation, clustering and sequencing

The process of cDNA library preparation from total RNA is summarised in **Figure 4.2**. The library was prepared using a NEBNext Ultra RNA Library Prep Kit for Illumina (New England BioLabs, USA) according to the manufacturer's instructions. Firstly, index codes were added to sequences from each sample, following which magnetic beads coated in oligo-d(T) probes were used to purify mRNA from total RNA. mRNA was fragmented using divalent cations at elevated temperature in 5X NEBNext First Strand Synthesis Reaction Buffer. First strand cDNA synthesis was mediated by reverse transcriptase with random hexamer primers, whilst second strand synthesis was mediated by DNA polymerase I with the incorporation of dUTP nucleotides. Following end repair and 3'-adenylation, Illumina-compatible NEBNext

Adaptors were ligated to cDNA fragment ends. Fragments were purified with an AMPure XP system (Beckman Coulter, USA) to size select for 150-200 base pairs, and cDNA second strands containing dUTP were degraded with USER Enzyme (NEB, USA) containing uracil DNA glycosylase (UDG). Degradation of cDNA second strands prior to PCR amplification enables the retention of directionality in amplified DNA, as amplification will only occur from the reverse-transcribed first strand. PCR was performed with Phusion High-Fidelity DNA polymerase, Universal PCR primers and index primers; following which PCR products were purified in an AMPure XP system and library quality was assessed on an Agilent Bioanalyzer 2100 system. Clonal clustering of index-coded samples was performed on a cBot Cluster Generation System, using a Hi-Seq PE Cluster Kit cBot-HS (Illumina). Cluster sequencing was performed on an Illumina Hi-Seq platform using paired-end reads of 150 bp. A paired-end strategy involves the simultaneous sequencing of each fragment from both ends, generating twice as many sequence reads and improving the accuracy of read alignment.

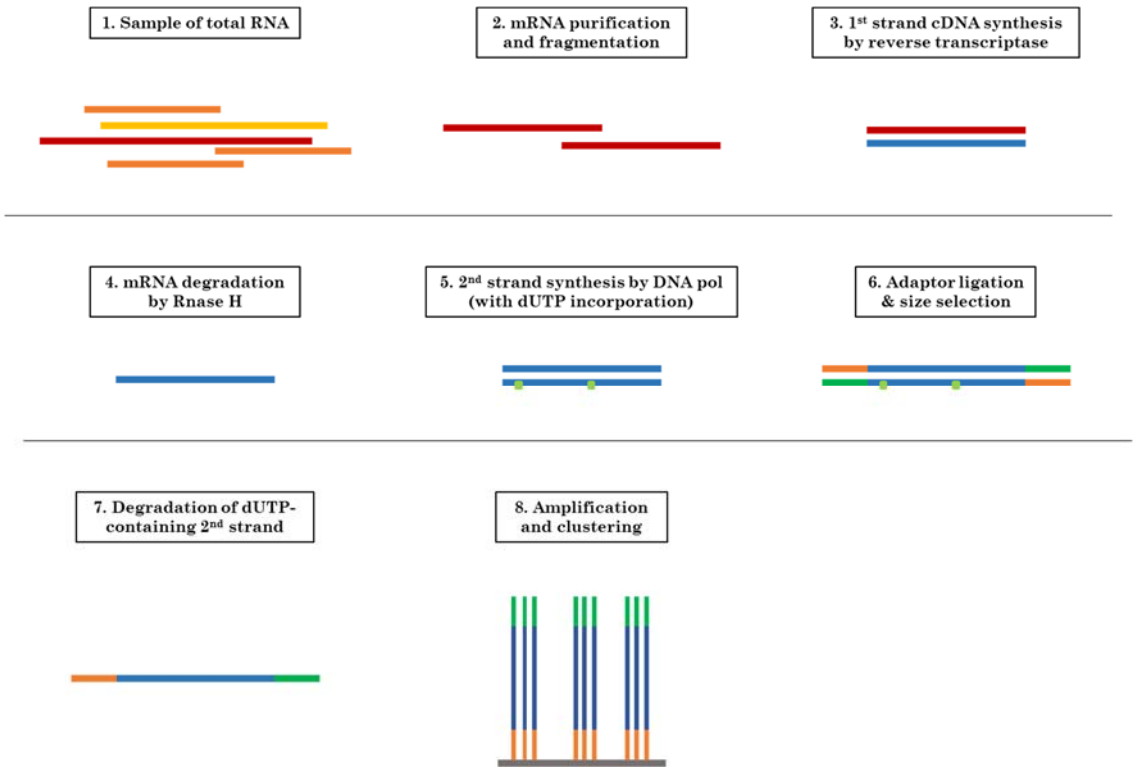


**Figure 4.2 cDNA library preparation performed by Novogene**.

#### 4.2.2.2 Analysis of RNA-Seq data

Raw sequencing reads were processed to remove low-quality reads, or those containing adaptor or poly-N (unknown base) sequences. Distributions of read classifications in each sample are given in **Table 4.2**, and indicate that at least 95% of reads generated from each sample were clean.

| Strain | Rep. | Clean | N-containing | Adaptor-containing | Low-quality |
|---|---|---|---|---|---|
| | | (%) | (%) | (%) | (%) |
| N2 | 1 | 96.80 | 0.21 | 1.86 | 1.13 |
| | 2 | 97.13 | 0.21 | 1.63 | 1.04 |
| | 3 | 96.57 | 0.21 | 2.20 | 1.02 |
| *hsp-90*$^{control}$ | 1 | 96.85 | 0.21 | 2.07 | 0.87 |
| | 2 | 95.63 | 1.92 | 1.89 | 0.56 |
| | 3 | 95.17 | 1.98 | 2.01 | 0.84 |
| *hsp-90*$^{int}$ hp-RNAi | 1 | 95.50 | 1.92 | 1.97 | 0.61 |
| | 2 | 95.93 | 1.94 | 1.59 | 0.54 |
| | 3 | 95.98 | 1.93 | 1.60 | 0.50 |
| *hsp-90*$^{neu}$ hp-RNAi | 1 | 95.61 | 1.95 | 1.87 | 0.57 |
| | 2 | 95.63 | 1.94 | 1.79 | 0.64 |
| | 3 | 95.64 | 1.94 | 1.83 | 0.58 |

**Table 4.2 Read quality distributions for RNA-Seq samples**. Rep.= Replicate. N-containing: reads with multiple unidentified nucleotides.

Bowtie software *v2.2.3* and TopHat software *v2.0.12* were used to align clean reads to the WBCel235 version of the *C. elegans* genome. The number of reads mapped to each gene was counted with HTSeq software *v0.6.1* and was used to calculate FKPM (fragments per kilobase of transcript sequence, per millions of base pairs sequenced) for each gene. Differential expression analysis was performed using the DESeq package (*v1.18.0*) in R software, which compares expression data between samples and calculates p values for fold-changes. p values were corrected for multiple testing using the Benjamini-Hochberg method with a false discovery rate of 0.05. RNA-Seq comes with inherent risks for the identification of false positive or negative results, for example due to small numbers of biological replicates, misidentification of differentially expressed isoforms of the same gene, and differences in software

packages used to identify differentially expressed genes (Leng et al. 2013; Soneson & Delorenzi 2013; Seyednasrollah et al. 2015). Candidate differentially expressed genes were therefore determined as those with both a fold-change above 1.5 and a corrected p value below 0.05, and are listed in **Tables A1-A6** in **Appendix 1**.

### 4.2.3 Gene set analysis

#### 4.2.3.1 Gene ontology (GO) term analysis

GO term analysis was performed using the Gene Ontology Resource (Ashburner et al. 2000, Mi et al. 2019, The Gene Ontology Consortium 2019). Gene lists were analysed for terms relating to biological processes, molecular functions, and cellular compartments. Only terms with a false discovery rate below 0.05 were considered.

#### 4.2.3.2 Prediction of protein subcellular localisation

To predict the subcellular localisation of a specific protein, the DeepLoc 1.0 tool was used (Armenteros et al. 2017). This tool uses an amino acid sequence as input to predict the protein's subcellular localisation, using a recurrent neural network prediction model which is trained on a protein dataset extracted from UniProt.

#### 4.2.3.3 Promoter scanning using FIMO

To identify occurrences of transcription factor consensus motifs within promoter regions of genes of interest, motif scanning was performed using the 'Find individual motif occurrences' (FIMO) tool (Bailey et al. 2009) which is part of the online MEME suite of motif analysis tools (*v5.1.1*) (Grant et al. 2011). FIMO compares input motif sequences against input promoter sequences and reports instances of overlap, allowing identification of possible transcription factor binding sites. Sequences of gene promoter regions were obtained from WormBase (Harris et al. 2010) and were determined as the 1000 nucleotides immediately upstream of the start/ATG codon. In the case of a gene having multiple possible transcripts, only one sequence pertaining to the first listed transcript was used, so as not to bias motif detection towards motifs present in multiple transcripts for a single gene. Known consensus motifs of transcription factors were identified through literature searches and the CIS-BP database of transcription factors (Weirauch et al. 2014). Consensus motifs used for analysis in this chapter are listed in **Table 4.3**.

| TF | Consensus motif | Source |
|---|---|---|
| DAF-16 | NNRWMAAYAN | Weirauch et al. 2014 |
| DAF-16 | RNHGTAAACAANHN | Matys et al. 2006 |
| DAF-16 (DBE) | GTAAACA | Furuyama et al. 2000; Murphy et al. 2003 |
| PHA-4 | GAGAGAS | Zhong et al. 2010 |
| PHA-4 | GTAAACAR | Contrino et al. 2012 |
| PHA-4 | RYAMAYAN | Heinz et al. 2010 |
| PHA-4 | TRTTKRY | Gaudet & Mango 2002 |
| PHA-4 | WRWGYAAAYA | Mathelier et al. 2014 |
| PQM-1 (DAE) | TGATAAG | Furuyama et al. 2000; Murphy et al. 2003 |

**Table 4.3 Known PHA-4 and DAF-16-related consensus DNA-binding motifs**. Motifs were identified through literature searches and the CIS-BP database (Weirauch et al. 2014). TF: Transcription factor. DBE: DAF-16 binding element. DAE: DAF-16-associated element

## 4.3 Results

### 4.3.1 Overview of differential gene expression

Following differential expression analysis by Novogene, volcano plots were generated to visualise differential gene expression in terms of fold-change and associated p value (**Fig. 4.3**). Further data analysis was then performed to determine whether each gene was differentially expressed compared to only wild-type, only the *hsp-90*$^{control}$ strain, or both the wild-type and *hsp-90*$^{control}$ strains (**Fig. 4.4**).

In terms of the numbers of differentially expressed genes, *hsp-90*$^{control}$ and wild-type are the most similar strains, with 129 genes differentially expressed between them (**Figs. 4.3a; 4.4**). Of these, 77 are upregulated and 52 downregulated in the *hsp-90*$^{control}$ strain compared to in wild-type (**Tables A1-A2**). This indicates that whilst the two control strains are indeed similar in terms of gene expression, there are differences in their transcriptomes which should be taken into consideration.

Compared to the *hsp-90*$^{control}$ strain, the *hsp-90*$^{int}$ hp-RNAi strain has 399 differentially expressed genes, with 281 upregulated and 118 downregulated (**Figs. 4.3b, 4.4; Tables A3-A4**). In contrast, the *hsp-90*$^{neu}$ hp-RNAi strain was identified as having 2251 differentially expressed genes, with 1456 upregulated and 795 downregulated (**Figs. 4.3c, 4.4; Tables A5-A6**). Despite the weaker upregulation of cell-non-autonomous *hsp-70* reporter expression and organismal *hsp-70* transcripts (**Figs. 3.2; 3.5a**), there therefore appears to be a much stronger effect in terms of the number of differentially expressed genes in the *hsp-90*$^{neu}$ hp-RNAi strain. When gene expression levels in each strain are represented as a heat map and clustered by similarity between strains (**Fig. 4.5**), it can be seen that gene expression levels in the *hsp-90*$^{neu}$ hp-RNAi strain are very different to any of the others. Not only are far more genes strongly upregulated or downregulated in the *hsp-90*$^{neu}$ hp-RNAi strain, but the direction of differential expression appears to be almost completely reversed compared to the wild-type and *hsp-90*$^{control}$ strains. That is, genes downregulated in the wild-type and *hsp-90*$^{control}$ strains are upregulated in the *hsp-90*$^{neu}$ hp-RNAi strain and *vice versa*. This suggests that pan-neuronal *hsp-90* knockdown may have a strong effect on transcriptional regulation in the *hsp-90*$^{neu}$ hp-RNAi strain, in a way which may be very different to that caused by intestine-specific *hsp-90* knockdown.

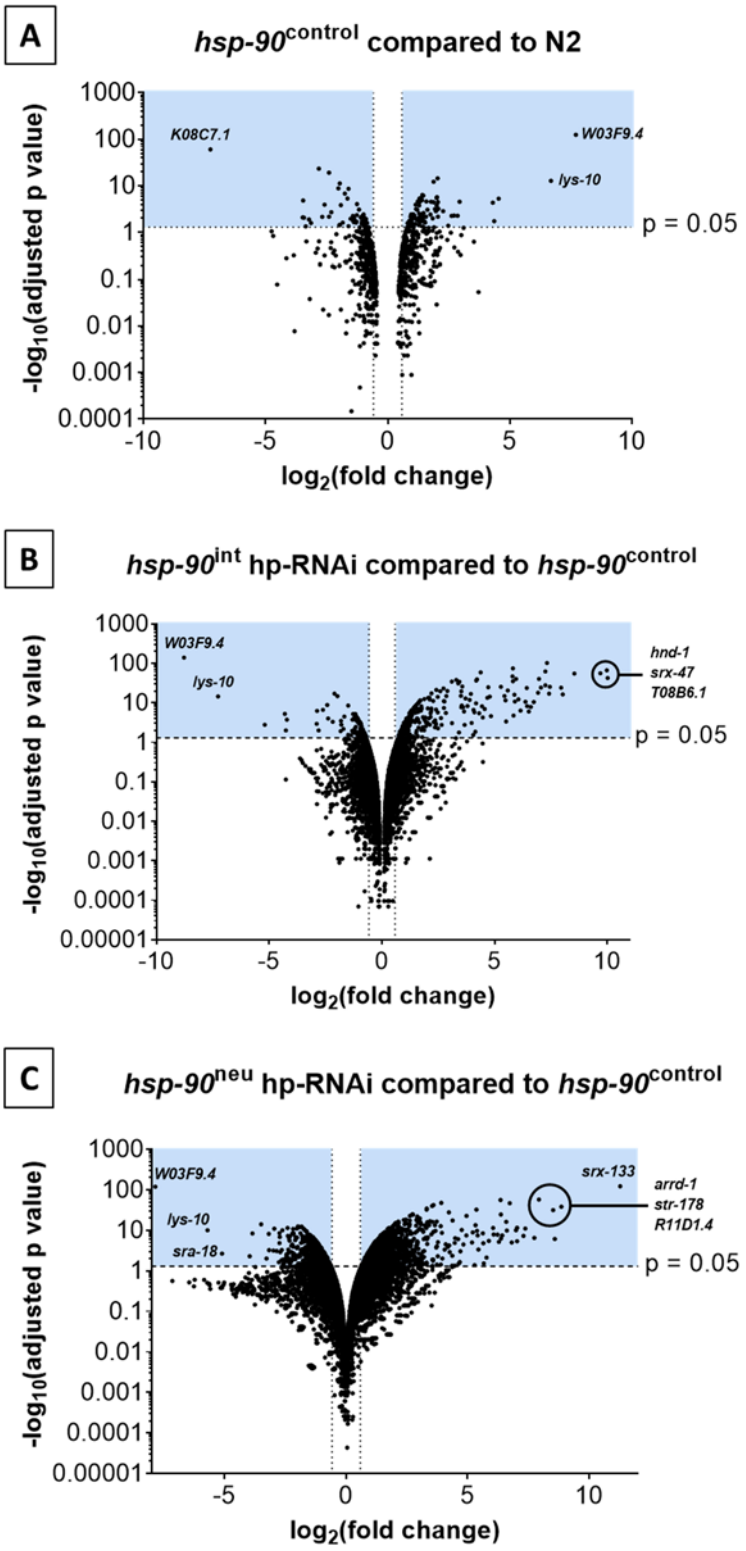


**Figure 4.3 Fold-change and p value distributions of differentially expressed genes**. Distributions are shown for genes differentially expressed between (**A**) *hsp-90*$^{control}$ and wild-type; (**B**) *hsp-90*$^{int}$ hp-RNAi and *hsp-90*$^{control}$; (**C**) *hsp-90*$^{neu}$ hp-RNAi and *hsp-90*$^{control}$. Points in the shaded upper left/right sections of each graph represent candidate differentially expressed genes; that is, their expression in that strain is at least 1.5-fold higher or lower than in the *hsp-90*$^{control}$ strain with an adjusted p value below 0.05.

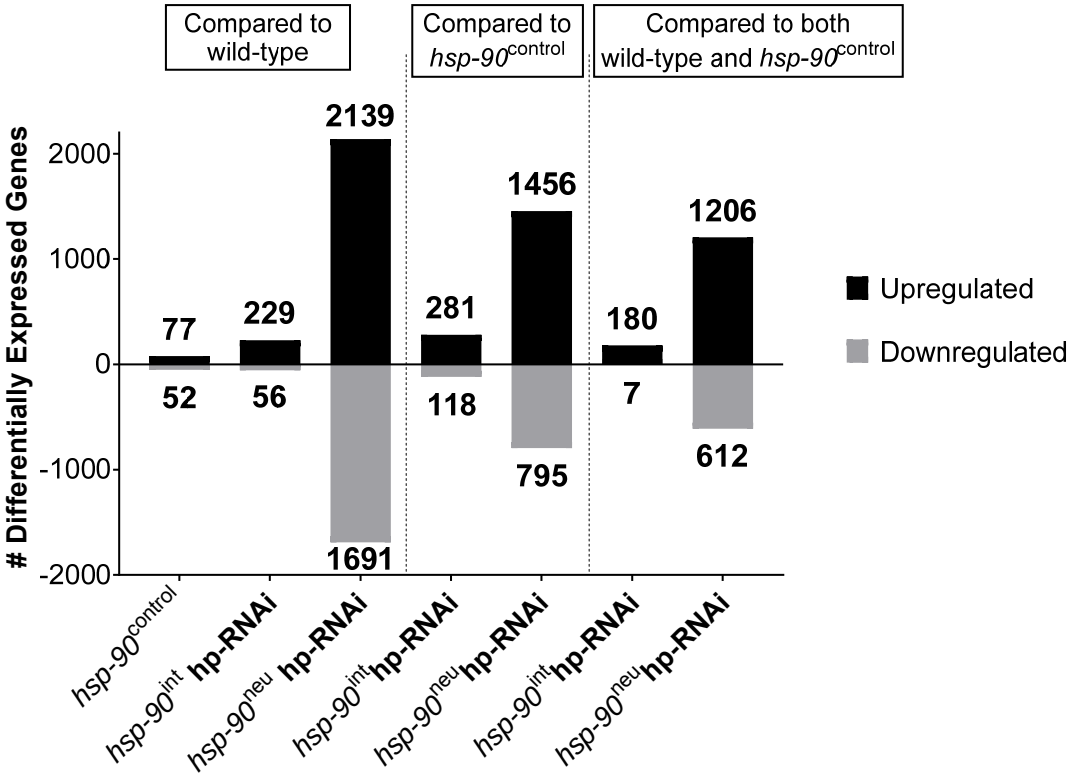


**Figure 4.4 Total number of differentially expressed genes identified by RNA-Seq**. Comparisons are split into three sections depending on whether genes are differentially expressed compared to wild-type, compared to the *hsp-90*$^{control}$ strain, or compared to both wild-type and the *hsp-90*$^{control}$ strain.

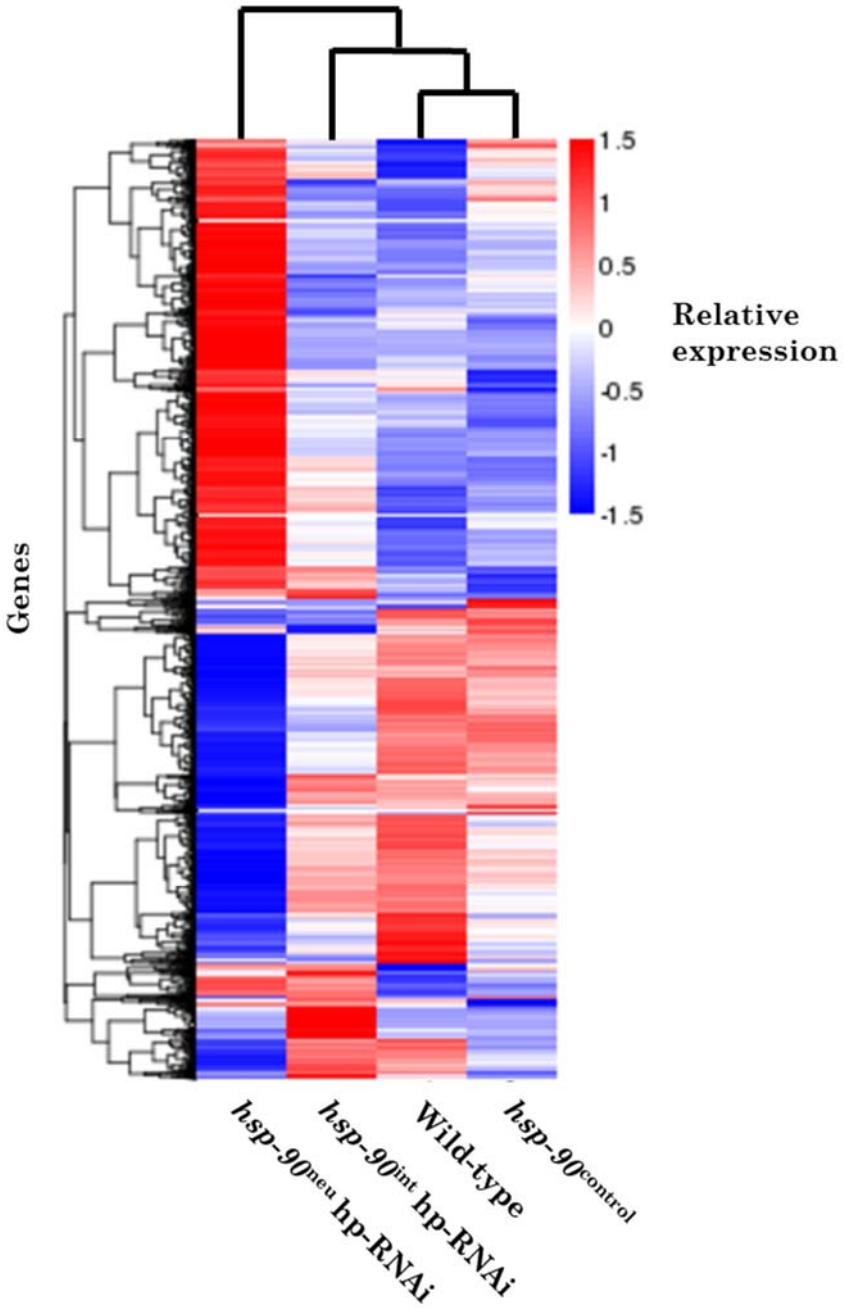


**Figure 4.5 Heat map and clustering of gene expression levels between strains**. Modified from heat map produced by Novogene.

### 4.3.2 Immune response genes are upregulated in the *hsp-90*$^{control}$ strain compared to wild-type

GO term enrichment analysis was first performed in two groups of genes: the 77 genes upregulated in the *hsp-90*$^{control}$ strain compared to wild-type, and the 52 genes downregulated between the same strains. No terms were identified as enriched amongst downregulated genes. However, terms relating to the immune response, response to stress, and lysozyme activity were enriched amongst the 77 upregulated genes (**Fig. 4.6**). This suggests that the *sid-1* (*pk3321*) allele, the key difference in genotype between the wild-type and *hsp-90*$^{control}$ strains, may promote immune response activation.

Compared to wild-type, 7 upregulated genes and 9 downregulated genes are common to each of the *hsp-90*$^{control}$, *hsp-90*$^{int}$ hp-RNAi and *hsp-90*$^{neu}$ hp-RNAi strains (**Fig. 4.7**). These genes, which are listed in **Table 4.4**, may therefore represent a core transcriptomic change from wild-type due to the inclusion of the *sid-1* (*pk3321*) allele. In keeping with the idea of an upregulated immune response, two of the shared upregulated genes (*clec-17* and *clec-38*) are c-type lectins, a gene class which is often upregulated in immune responses (Schulenburg et al. 2008). Another shared upregulated gene is the immune gene *gst-38*; and three more such upregulated genes (*scb-1*, *math-15* and *T22F7.4*) are known to interact with or be affected by the key immune regulator *daf-16* (WormBase; Harris et al. 2010). However, four shared downregulated genes (*pqn-26*, *C06G1.2*, *D2024.4* and *F40E10.5*) are also affected by *daf-16*. Two more downregulated genes (*abu-2*, *abu-4*) are involved in non-canonical UPR$^{ER}$ signalling (Urano et al. 2002); and genes of the *abu* and *pqn* classes have been shown to be commonly regulated by the sirtuin SIR-2.1 in the modulation of lifespan (Viswanathan et al. 2005). This may have some connection to the extended lifespan seen in the *hsp-90*$^{int}$ hp-RNAi strain (**Fig. 3.6**), although these genes are also downregulated in the *hsp-90*$^{control}$ and *hsp-90*$^{neu}$ hp-RNAi strains.

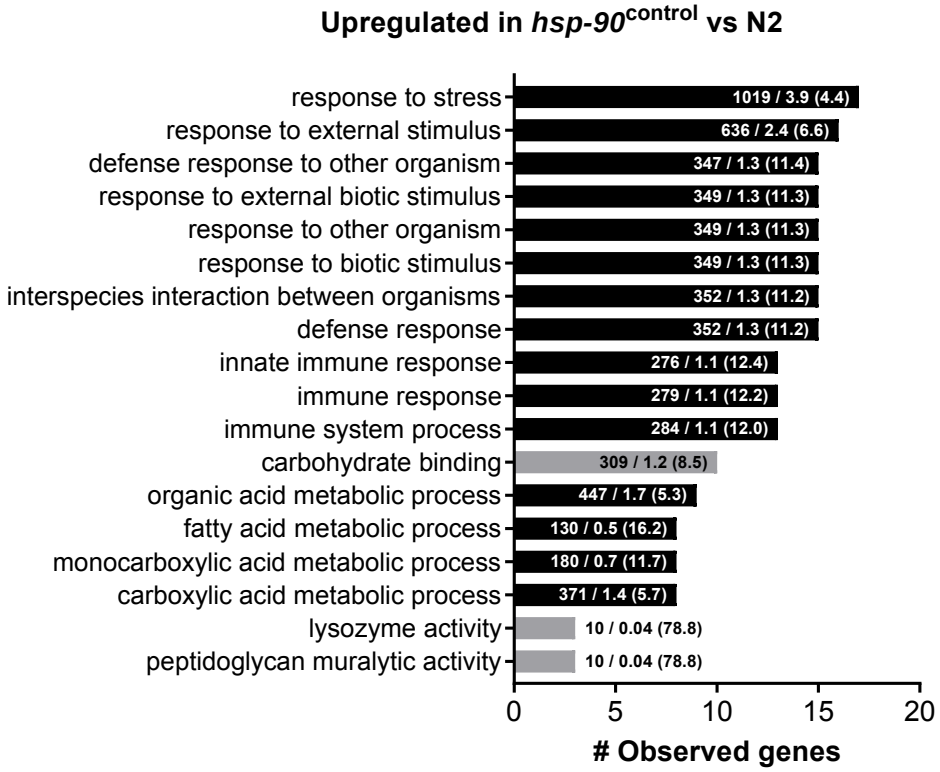


**Figure 4.6 GO terms enriched amongst genes upregulated in the *hsp-90*control strain compared to wild-type**. Labels show 'Total genes / Expected genes (Fold-enrichment)', where 'Total genes' is all genes associated with each term, 'Expected genes' is the number of genes associated with each term that you would expect from an input list of the same size, and 'Fold-Enrichment' is the number of observed genes divided by the number of expected genes. Black bars: biological process terms; grey bars: molecular function terms. FDR < 0.05 for all terms.

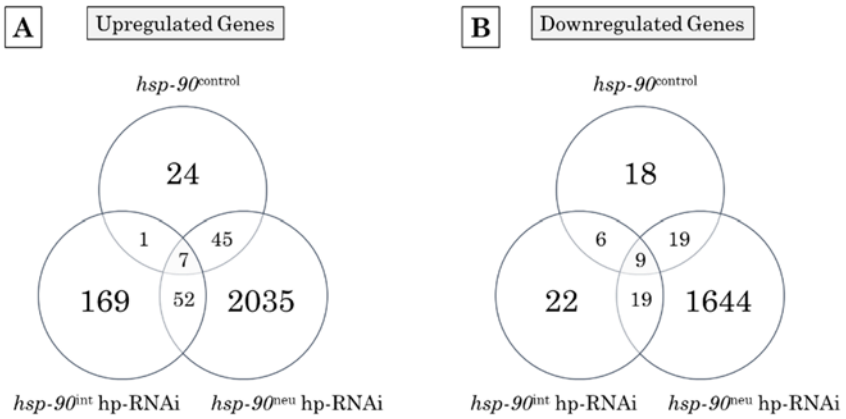


**Figure 4.7 Numbers of genes differentially expressed compared to wild-type**. (**A**) Numbers of upregulated genes in each other strain compared to wild-type, and their overlap. (**B**) Numbers of downregulated genes in each strain compared to wild-type, and their overlap. The 7 upregulated and 9 downregulated genes in the central segments are listed in **Table 4.4**.

| **Genes upregulated in all strains compared to wild-type** | | |
|---|---|---|
| **Transcript** | **Gene name** | **Function/Activity** |
| *E03H4.10* | *clec-17* | Predicted carbohydrate binding activity |
| *T25E12.10* | *clec-38* | Predicted carbohydrate binding activity |
| *F35E8.8* | *gst-38* | Involved in immunity and PERK-mediated UPR, predicted glutathione transferase |
| *C16C4.5* | *math-15* | Affected by *hsf-1*, *daf-2* and *daf-16* |
| *H19N07.3* | *scb-1* | Interacts with *daf-16* and *sod-3* |
| *T22F7.4* | | Affected by *glp-1*, *daf-2* and *daf-16* |
| *Y49G5A.1* | | Predicted serine endopeptidase inhibitor |
| **Genes downregulated in all strains compared to wild-type** | | |
| **Transcript** | **Gene name** | **Function/Activity** |
| *F19G12.7* | *abu-2* | Involved in $UPR^{ER}$ |
| *Y5H2A.3* | *abu-4* | Involved in $UPR^{ER}$ |
| *F56H6.5* | *gmd-2* | Involved in fucose biosynthesis, mannose metabolism |
| *DY3.5* | *pqn-26* | Affected by *skn-1*, *daf-2* and *daf-16* |
| *F35B3.5* | *ptrn-1* | Microtubule-binding protein |
| *C06G1.2* | | Affected by *skn-1*, *daf-2* and *daf-16* |
| *D2024.4* | | Affected by *skn-1*, *daf-2* and *daf-16* |
| *F40E10.5* | | Affected by *skn-1*, *daf-2* and *daf-16* |

**Table 4.4 Genes whose differential expression compared to wild-type is common to strains carrying the *sid-1* (*pk3321*) allele**. Compared to wild-type, 7 common genes are upregulated and 9 downregulated in each of the *hsp-90*$^{control}$, *hsp-90*$^{int}$ hp-RNAi and *hsp-90*$^{neu}$ hp-RNAi strains. Gene function information from WormBase (Harris et al. 2010).

### 4.3.3 Comparison of organismal *hsp-70* and *hsp-90* transcript quantification by qRT-PCR and RNA-Seq

**Figure 4.8** shows a comparison of organismal *hsp-70* and *hsp-90* transcript levels in the *hsp-90*$^{int}$ hp-RNAi and *hsp-90*$^{neu}$ hp-RNAi strains compared to the *hsp-90*$^{control}$ strain, as determined by either qRT-PCR or RNA-Seq. Quantification of organismal transcript expression by qRT-PCR determined that compared to the *hsp-90*$^{control}$ strain, *hsp-70* transcripts are upregulated approximately 4.5-fold in the *hsp-90*$^{int}$ hp-RNAi strain and 2.5-fold in the *hsp-90*$^{neu}$ hp-RNAi strain, but that only upregulation in the *hsp-90*$^{int}$ hp-RNAi strain is associated with a p value below 0.05 (**Fig. 3.5a**). Accordingly, RNA-Seq analysis identified that *hsp-70* is upregulated in the *hsp-90*$^{int}$ hp-RNAi strain compared to the *hsp-90*$^{control}$ strain; but is not differentially expressed in the *hsp-90*$^{neu}$ hp-RNAi strain (**Fig. 4.8a-b**). Similarly in accordance with qPCR data, RNA-Seq identified that *hsp-90* is not differentially expressed in either the *hsp-90*$^{int}$ hp-RNAi or *hsp-90*$^{neu}$ hp-RNAi strains compared to the *hsp-90*$^{control}$ strain (**Figs. 3.5c, 4.8**). However, RNA-Seq data did reflect a slight decrease in whole-organism *hsp-90* expression in the *hsp-90*$^{int}$ hp-RNAi strain identified by qPCR (**Figs. 3.5a, 4.8a**).

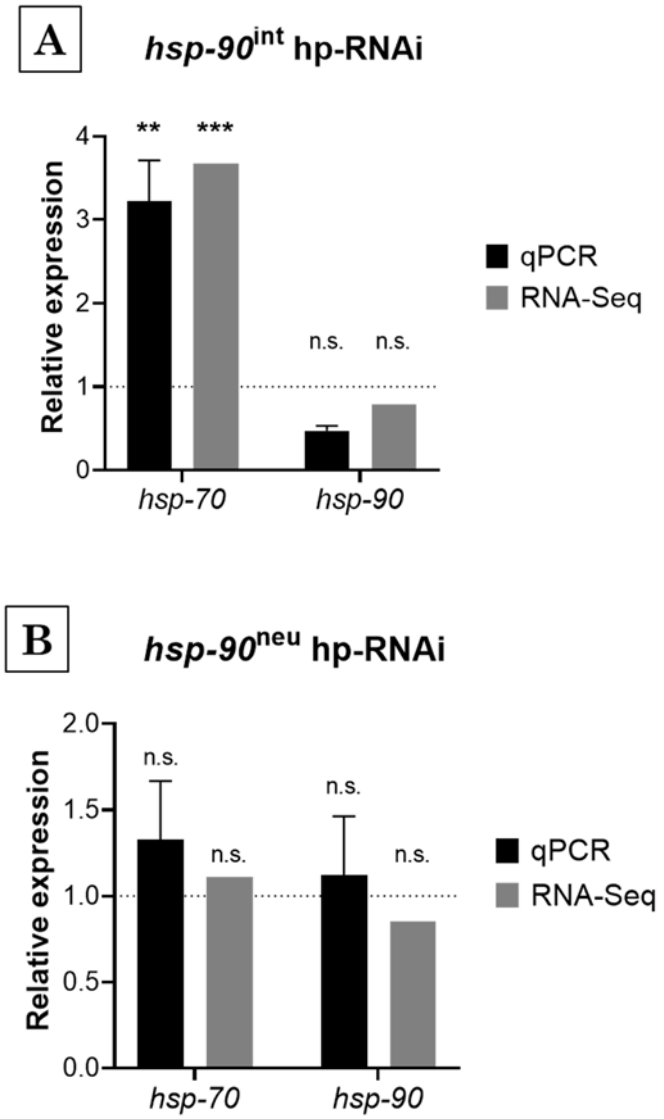


**Figure 4.8 Comparison of *hsp-70* and *hsp-90* quantification by qRT-PCR and RNA-Seq**. Organismal expression of *hsp-70* and *hsp-90* transcripts relative to the *hsp-90*$^{control}$ strain was quantified by qRT-PCR or RNA-seq, in the (**A**) *hsp-90*$^{int}$ hp-RNAi and (**B**) *hsp-90*$^{neu}$ hp-RNAi strains. Significance of qRT-PCR values was determined by one-way ANOVA with multiple comparisons, with error bars representing SEM. Significance of RNA-Seq values was determined by differential expression analysis by Novogene. * = $p<0.05$; ** = $p<0.01$; *** = $p<0.001$; n.s. = not significant.

### 4.3.4 GO terms relating to metabolism and lysosome activity are enriched amongst genes downregulated in the *hsp-90*$^{int}$ hp-RNAi strain

Compared to the *hsp-90*$^{control}$ strain, the *hsp-90*$^{int}$ hp-RNAi strain has a total of 399 differentially expressed genes. 281 genes are upregulated, and 118 downregulated (**Fig. 4.4**). GO term analysis of the 281 upregulated genes does not identify any significantly enriched terms. However, analysis of the 118 downregulated genes identifies terms relating to the metabolism of various biomolecules, and to lysosome and endopeptidase activity (**Fig. 4.9**). This suggests that in this strain there may be a general downregulation of metabolic processes.

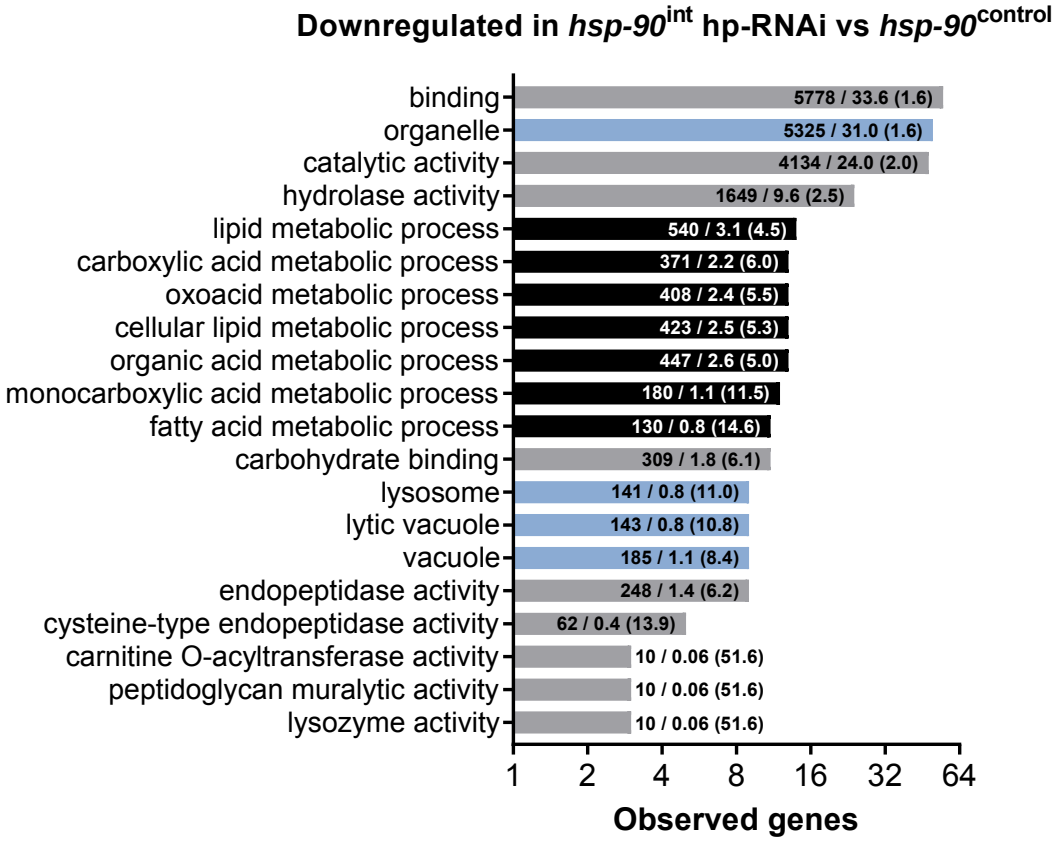


**Figure 4.9 GO terms enriched amongst genes downregulated in the *hsp-90*$^{int}$ hp-RNAi strain compared to the *hsp-90*$^{control}$ strain**. Labels show 'Total genes / Expected genes (Fold-enrichment)', where 'Total genes' is all genes associated with each term, 'Expected genes' is the number of genes associated with each term that you would expect from an input list of the same size, and 'Fold-Enrichment' is the number of observed genes divided by the number of expected genes. Black bars: biological process terms; grey bars: molecular function terms; blue bars: cellular compartment terms. FDR < 0.05 for all terms.

### 4.3.5 Defence responses are upregulated whilst protein phosphorylation is downregulated in the *hsp-90*$^{neu}$ hp-RNAi strain

Compared to the *hsp-90*$^{control}$ strain, the *hsp-90*$^{neu}$ hp-RNAi strain has 2251 differentially expressed genes. 1456 genes are upregulated and 795 downregulated (**Fig. 4.4**). GO term analysis of the 1456 upregulated genes identifies enrichments including terms relating to transmembrane transport, neuropeptide signalling, innate immunity, response to external stimuli, oxidation-reduction processes, and metal ion binding (**Fig. 4.10a**). Transmembrane transport and neuropeptide signalling could indicate that neuroendocrine signalling may be activated in response to pan-neuronal *hsp-90* knockdown. This could also relate to immune or defence processes, as neuroendocrine insulin signalling has been shown to regulate organismal immunity (Kawli & Tan 2008). The upregulation of oxidation-reduction processes may suggest oxidative stress or increased mitochondrial activity, which may relate to the increased resistance to oxidative stress displayed by this strain (**Fig. 3.8**).

Amongst the 795 genes downregulated in the *hsp-90*$^{neu}$ hp-RNAi strain compared to the *hsp-90*$^{control}$ strain, over 30 terms relating to the regulation of protein phosphorylation are identified (**Fig. 4.10b**). Many signalling mechanisms, including the HSR, ILS and PMK-1 pathways (Guettouche et al. 2005; Morris et al. 1996; Shivers et al. 2010), rely on phospho-modifications to regulate the activity of their protein components. These data may therefore suggest widespread alterations in signalling processes. In addition, several terms relating to the cuticle and extracellular matrix (ECM) are enriched amongst downregulated genes. The ECM forms the non-cellular component of tissues, and not only provides structure but also participates in the transduction of signals between cells and tissues (Frantz et al. 2010). This may indicate a role for the ECM in signal transduction during TCS.

**Figure 4.10 (Below) GO term analysis of genes differentially expressed in the *hsp-90*$^{neu}$ hp-RNAi strain compared to the *hsp-90*$^{control}$ strain.** (**A**) Enriched amongst upregulated genes. (**B**) Enriched amongst downregulated genes. Labels show 'Total genes / Expected genes (Fold-enrichment)', where 'Total genes' is all genes associated with each term, 'Expected genes' is the number of genes associated with each term that you would expect from an input list of the same size, and 'Fold-Enrichment' is the number of observed genes divided by the number of expected genes. Black bars: biological process terms; grey bars: molecular function terms; blue bars: cellular compartment terms. FDR < 0.05 for all terms.

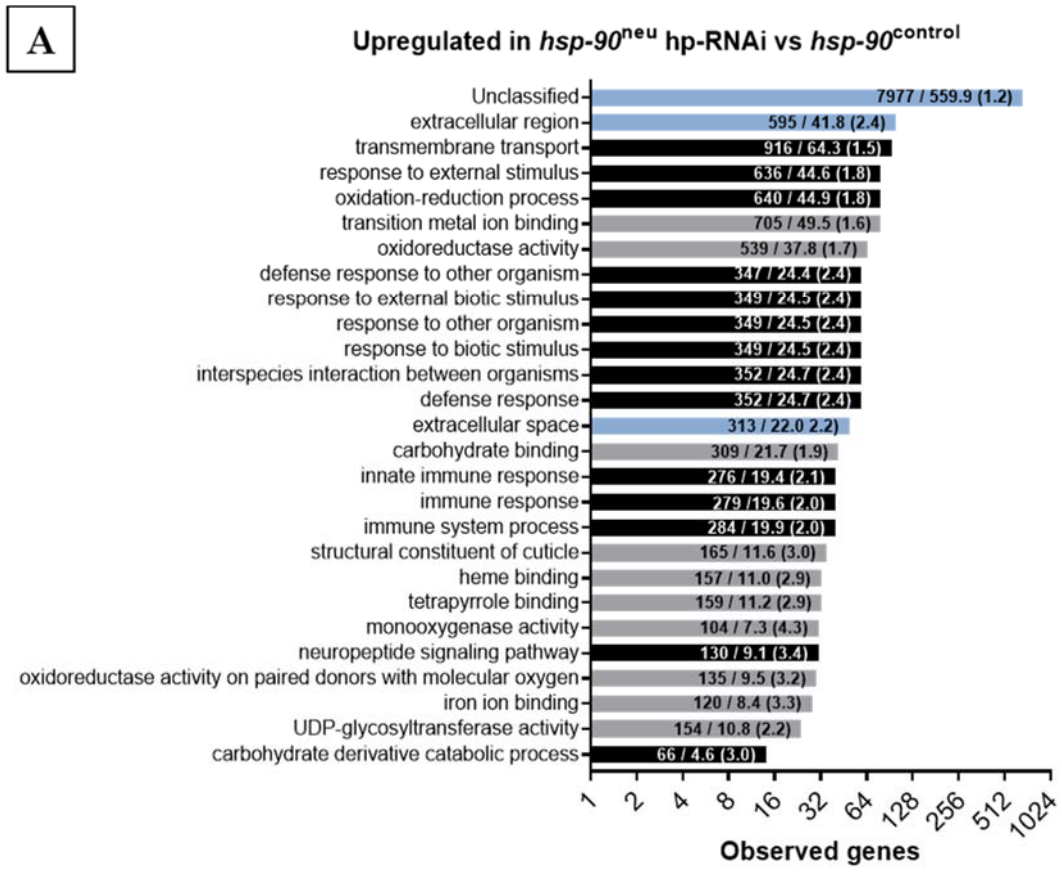

**B**

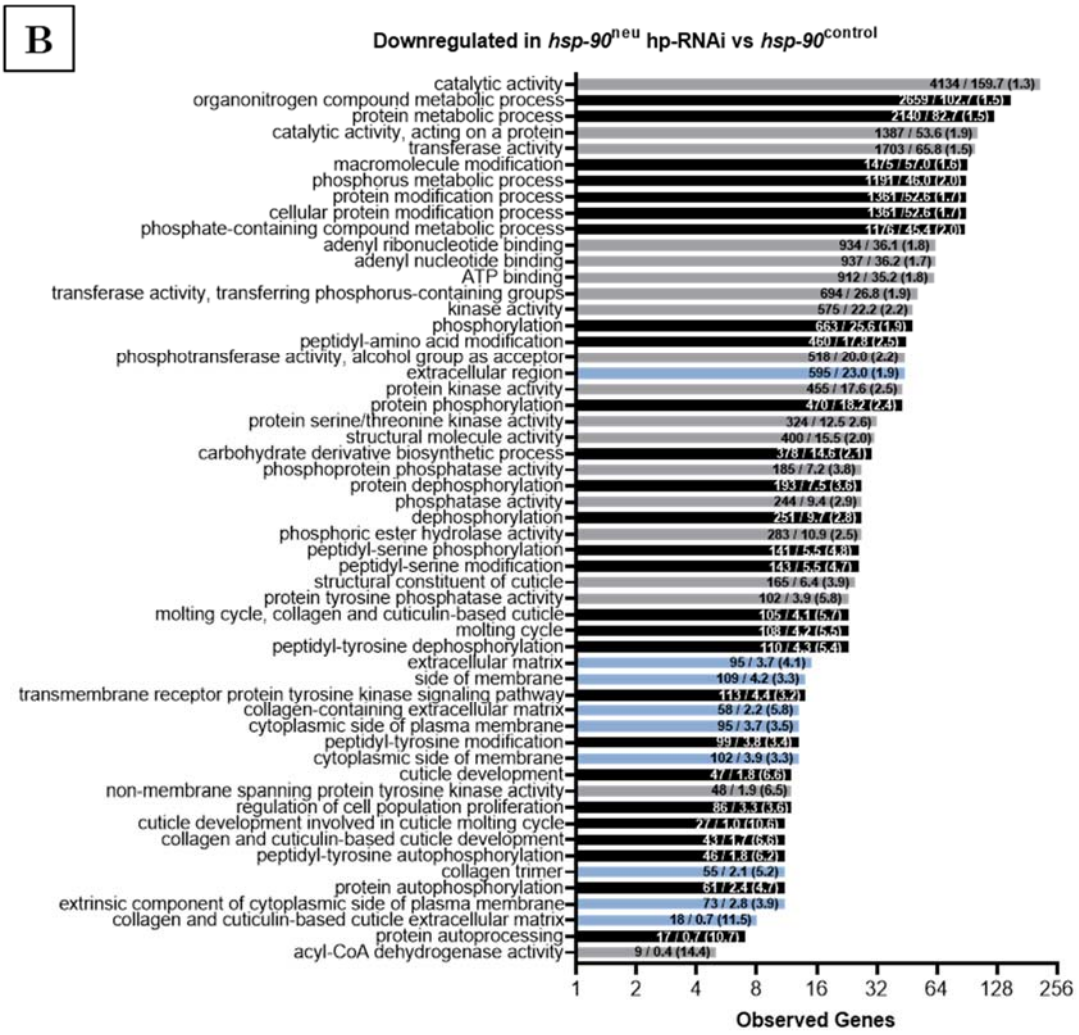
Downregulated in hsp-90neu hp-RNAi vs hsp-90control
catalytic activity
organonitrogen compound metabolic process
protein metabolic process
catalytic activity, acting on a protein
transferase activity
macromolecule modification
phosphorus metabolic process
protein modification process
cellular protein modification process
phosphate-containing compound metabolic process
adenyl ribonucleotide binding
adenyl nucleotide binding
ATP binding
transferase activity, transferring phosphorus-containing groups
kinase activity
phosphorylation
peptidyl-amino acid modification
phosphotransferase activity, alcohol group as acceptor
extracellular region
protein kinase activity
protein phosphorylation
protein serine/threonine kinase activity
structural molecule activity
carbohydrate derivative biosynthetic process
phosphoprotein phosphatase activity
protein dephosphorylation
phosphatase activity
dephosphorylation
phosphoric ester hydrolase activity
peptidyl-serine phosphorylation
peptidyl-serine modification
structural constituent of cuticle
protein tyrosine phosphatase activity
molting cycle, collagen and cuticulin-based cuticle
molting cycle
peptidyl-tyrosine dephosphorylation
extracellular matrix
side of membrane
transmembrane receptor protein tyrosine kinase signaling pathway
collagen-containing extracellular matrix
cytoplasmic side of plasma membrane
peptidyl-tyrosine modification
cytoplasmic side of membrane
cuticle development
non-membrane spanning protein tyrosine kinase activity
regulation of cell population proliferation
cuticle development involved in cuticle molting cycle
collagen and cuticulin-based cuticle development
peptidyl-tyrosine autophosphorylation
collagen trimer
protein autophosphorylation
extrinsic component of cytoplasmic side of plasma membrane
collagen and cuticulin-based cuticle extracellular matrix
protein autoprocessing
acyl-CoA dehydrogenase activity
4134 / 159.7 (1.3)
2659 / 102.7 (1.5)
2140 / 82.7 (1.5)
1387 / 53.6 (1.9)
1703 / 65.8 (1.5)
1475 / 57.0 (1.6)
1191 / 46.0 (2.0)
1385 / 52.6 (1.7)
1385 / 52.6 (1.7)
1176 / 45.4 (2.0)
934 / 36.1 (1.8)
937 / 36.2 (1.7)
912 / 35.2 (1.8)
694 / 26.8 (1.9)
575 / 22.2 (2.2)
665 / 25.6 (1.9)
460 / 17.8 (2.5)
518 / 20.0 (2.2)
595 / 23.0 (1.9)
455 / 17.6 (2.5)
470 / 18.2 (2.3)
324 / 12.5 2.6)
400 / 15.5 (2.0)
376 / 14.6 (2.1)
185 / 7.2 (3.8)
193 / 7.5 (3.6)
244 / 9.4 (2.9)
251 / 9.7 (2.8)
283 / 10.9 (2.5)
141 / 5.4 (6.8)
143 / 5.5 (6.7)
165 / 6.4 (3.9)
102 / 3.9 (5.8)
105 / 4.1 (5.7)
108 / 4.2 (5.6)
110 / 4.3 (5.4)
95 / 3.7 (4.1)
109 / 4.2 (3.3)
113 / 4.4 (3.2)
58 / 2.2 (5.8)
95 / 3.7 (3.5)
99 / 3.8 (3.4)
102 / 3.9 (3.3)
47 / 1.8 (6.8)
48 / 1.9 (6.5)
86 / 3.3 (3.8)
27 / 1.0 (10.6)
43 / 1.7 (6.6)
46 / 1.8 (6.2)
55 / 2.1 (5.2)
61 / 2.4 (4.7)
73 / 2.8 (3.9)
18 / 0.7 (11.5)
17 / 0.7 (10.7)
9 / 0.4 (14.4)
1
2
4
8
16
32
64
128
256
Observed Genes

### 4.3.6 Differential expression of chaperone genes in the *hsp-90*$^{int}$ hp-RNAi and *hsp-90*$^{neu}$ hp-RNAi strains

In response to tissue-specific *hsp-90* knockdown, the *hsp-90*$^{int}$ hp-RNAi and *hsp-90*$^{neu}$ hp-RNAi strains demonstrate cell-non-autonomous *hsp-70* reporter upregulation (**Fig. 3.2**). Tissue-specific *hsp-90* knockdown has previously been shown to cause increased resistance to heat stress (van Oosten-Hawle et al. 2013), and the *hsp-90*$^{int}$ hp-RNAi strain demonstrates increased lifespan (**Fig. 3.6**). It is possible that these benefits may involve increased expression of chaperone proteins following activation of TCS, and it has been shown that knockdown of chaperones such as small HSPs can reduce lifespan (Hsu et al. 2003). However, the cell-non-autonomous *hsp-70* reporter upregulation seen in the *hsp-90*$^{int}$ hp-RNAi and *hsp-90*$^{neu}$ hp-RNAi strains does not require functional *hsf-1* (**Figs. 3.3c-f; 3.4**). This suggests that HSF-1-mediated chaperone upregulation may not be involved in TCS. To determine which chaperone genes are differentially expressed in the *hsp-90*$^{int}$ hp-RNAi and *hsp-90*$^{neu}$ hp-RNAi strains compared to the *hsp-90*$^{control}$ strain, lists of all differentially expressed genes in these strains were compared to a list of all known *C. elegans* chaperone genes (Brehme et al. 2014). The results are shown in **Table 4.5**. No chaperone genes were identified as being downregulated in the *hsp-90*$^{int}$ hp-RNAi strains compared to the *hsp-90*$^{control}$ strain.

Four chaperone genes are upregulated in the *hsp-90*$^{int}$ hp-RNAi strain compared to the *hsp-90*$^{control}$ strain. Three of these (*hsp-70*, *F44E5.4* and *F44E5.5*) encode HSP-70 family proteins which are not normally expressed but are upregulated upon heat stress in an *hsf-1*-dependent manner (GuhaThakurta et al. 2002; Brunquell et al. 2016). Whilst this might suggest the involvement of *hsf-1*, other chaperones which are upregulated on heat stress in an *hsf-1*-dependent manner (such as *hsp-16.11*, *hsp-16.2* and *hsp-16.41*) are not upregulated in the *hsp-90*$^{int}$ hp-RNAi strain. The fourth chaperone upregulated in this strain, *ttc-36*, is a target of DAF-16 (Murphy et al. 2003). It encodes a tetratricopeptide repeat-containing (TPR) protein whose expression is upregulated on germline ablation (Ghazi et al. 2009).

In the *hsp-90*$^{neu}$ hp-RNAi strain, 12 chaperone genes are upregulated compared to the *hsp-90*$^{control}$ strain whilst 5 are downregulated. Amongst chaperones upregulated in this strain are two small HSPs (*hsp-12.3* and *hsp-12.6*) and four cadmium-responsive ER chaperones (*cdr-2*, *cdr-4*, *cdr-5* and *cdr-6*). There is also an

upregulated HSP-70 family gene, *F11F1.1*, however this gene does not appear to be regulated by *hsf-1* (Brunquell et al. 2016). Interestingly, *ttc-36* is also upregulated in this strain. As the only chaperone gene whose differential expression is common to both the *hsp-90*$^{int}$ hp-RNAi and *hsp-90*$^{neu}$ hp-RNAi strains, this may indicate that upregulation of *ttc-36* is important in TCS. Genes downregulated in the *hsp-90*$^{neu}$ hp-RNAi strain include four co-chaperones (*cdc-37*, *dpy-18*, *fkb-3* and *phy-3*) and one mitochondrial Hsp100 family gene (*K07A3.3*). As the *hsp-90*$^{neu}$ hp-RNAi strain shows higher numbers of differentially expressed chaperone genes than the *hsp-90*$^{int}$ hp-RNAi strain, and with a greater variety of functions, this may suggest that pan-neuronal *hsp-90* knockdown has a more complex effect on organismal chaperone expression.

| **Upregulated in *hsp-90*$^{int}$ hp-RNAi compared to *hsp-90*$^{control}$** | | | | |
|---|---|---|---|---|
| **Transcript** | **Gene Name** | **$log_2$(FC)** | **$p_c$** | **Description** |
| *C12C8.1* | *hsp-70* | 1.877 | 1.67E-04 | HSP-70 chaperone |
| *F44E5.4* | | 2.187 | 6.80E-08 | HSP-70 chaperone |
| *F44E5.5* | | 2.159 | 4.09E-05 | HSP-70 chaperone |
| *F52H3.5* | *ttc-36* | 1.102 | 7.10E-04 | TPR co-chaperone |
| **Upregulated in *hsp-90*$^{neu}$ hp-RNAi compared to *hsp-90*$^{control}$** | | | | |
| **Transcript** | **Gene Name** | **$log_2$(FC)** | **$p_c$** | **Description** |
| *C54D10.1* | *cdr-2* | 1.030 | 9.08E-03 | GST chaperone |
| *K01D12.11* | *cdr-4* | 0.699 | 2.57E-02 | GST chaperone |
| *K01D12.14* | *cdr-5* | 1.173 | 2.34E-02 | GST chaperone |
| *K01D12.12* | *cdr-6* | 0.702 | 2.45E-02 | GST chaperone |
| *F38E11.1* | *hsp-12.3* | 0.909 | 5.88E-03 | sHSP chaperone |
| *F38E11.2* | *hsp-12.6* | 1.290 | 8.25E-03 | sHSP chaperone |
| *R151.9* | *pfd-5* | 0.817 | 5.36E-03 | PFD chaperone |
| *D2030.2* | | 0.727 | 1.79E-02 | HSP-100/AAA+ chaperone |
| *F11F1.1* | | 0.941 | 1.98E-02 | HSP-70 chaperone |
| *F32D1.3* | | 1.100 | 3.74E-02 | TPR co-chaperone |
| *F52H3.5* | *ttc-36* | 0.964 | 2.04E-03 | TPR co-chaperone |
| *T22F3.12* | | 1.436 | 1.83E-02 | Cyclophilin co-chaperone |
| **Downregulated in *hsp-90*$^{neu}$ hp-RNAi compared to *hsp-90*$^{control}$** | | | | |
| **Transcript** | **Gene Name** | **$log_2$(FC)** | **$p_c$** | **Description** |
| *K07A3.3* | | -1.066 | 3.42E-02 | HSP-100/AAA+ chaperone |
| *W08F4.8* | *cdc-37* | -0.678 | 3.09E-02 | HSP-90 co-chaperone |
| *Y47D3B.10* | *dpy-18* | -0.681 | 2.95E-02 | co-chaperone |
| *C05C8.3* | *fkb-3* | -0.993 | 1.22E-03 | FKBP co-chaperone |
| *T20B3.7* | *phy-3* | -1.057 | 8.92E-03 | Collagen co-chaperone |

**Table 4.5 Differentially expressed chaperone genes compared to the *hsp-90*$^{control}$ strain**. Lists of differentially expressed genes in each strain were compared to a database of known *C. elegans* chaperone genes (Brehme et al. 2014). Information in the 'Description' column is also from this database. FC = fold-change compared to the *hsp-90*$^{control}$ strain. $p_c$ = corrected p value. AAA+: ATPase associated with diverse cellular activities. FKBP: FK506-binding protein. GST: Glutathione S-transferase. PFD: Prefoldin. sHSP: Small heat shock protein. TPR: Tetratricopeptide repeat-containing.

### 4.3.7 Three genes are strongly downregulated in both the *hsp-90*$^{int}$ hp-RNAi and *hsp-90*$^{neu}$ hp-RNAi strains

To determine which genes are most strongly differentially expressed upon intestine- or pan-neuronal *hsp-90* knockdown, the ten most strongly upregulated or downregulated genes were identified in the *hsp-90*$^{int}$ hp-RNAi and *hsp-90*$^{neu}$ hp-RNAi strains compared to the *hsp-90*$^{control}$ strain (**Tables 4.6, 4.7**). These lists include several genes whose differential expression compared to the *hsp-90*$^{control}$ strain is classed as 'infinite'. This means that zero transcript reads for that gene were detected by RNA-Seq in the *hsp-90*$^{control}$ strain, leading to a division by zero when calculating fold-change. The lists were therefore compiled by ranking differentially expressed genes by their corrected p value. The subcellular localisation of the protein encoded by each gene was predicted using the online tool DeepLoc 1.0 based on the amino acid sequence of the encoded protein.

In each of the *hsp-90*$^{int}$ hp-RNAi and *hsp-90*$^{neu}$ hp-RNAi strains, two of the most strongly upregulated genes encode G protein-coupled receptors (GPCRs). In the *hsp-90*$^{int}$ hp-RNAi strain, these are *srj-37* and *srx-47*; in the *hsp-90*$^{neu}$ hp-RNAi strain they are *srx-133* and *str-178*. As GPCRs often act at the cell surface in signalling pathways (Strader et al. 1994), these genes may be involved in the transduction of intercellular signals during TCS. In *hsp-90*$^{neu}$ hp-RNAi, this is further supported by the fact that five genes encoding predicted soluble extracellular proteins (*col-102*, *grl-23*, *C13A2.12*, *R11D1.4*, and *Y46G5A.23*) are also strongly upregulated (**Table 4.7**). Extracellular proteins could represent secreted signalling molecules, raising the possibility that one or more of these genes may act as a mediator of intercellular signalling.

Interestingly, the *hsp-90*$^{int}$ hp-RNAi and *hsp-90*$^{neu}$ hp-RNAi strains share three common genes amongst their ten most strongly downregulated genes: *lys-10*, *ilys-2* and *W03F9.4*. *lys-10* and *ilys-2* encode soluble extracellular lysozyme proteins predicted to be involved in the defence response to bacteria (Harris et al. 2010). This suggests that downregulation of lysozyme activity may be a common response upon tissue-specific knockdown of *hsp-90*. Such a response is also indicated by downregulation of genes relating to lysosome activity in the *hsp-90*$^{int}$ hp-RNAi strain (**Fig. 4.9**). Less is known about *W03F9.4*, but it is predicted to encode an infection-regulated transmembrane ER protein (Engelmann et al. 2011; DeepLoc 1.0).

| **10 most strongly upregulated genes in *hsp-90*$^{int}$ hp-RNAi** | | | | |
|---|---|---|---|---|
| **Transcript** | **Gene name** | **$log_2$(FC)** | **$p_c$** | **SC localisation** |
| *F48G7.1* | *srj-37* | * | 2.61E-118 | TM in cell membrane |
| *Y57A10C.9* | | 7.3 | 7.03E-103 | TM in cell membrane |
| *E02C12.3* | *srx-47* | 9.7 | 3.30E-57 | TM in cell membrane |
| *T08B6.1* | | 10.0 | 7.99E-68 | Soluble in cytoplasm |
| *T22B2.1* | | * | 1.93E-36 | Soluble in cytoplasm |
| *K08C7.1* | | 7.3 | 2.43E-63 | TM in Golgi |
| *M04D8.8* | | 7.4 | 2.94E-26 | TM in Golgi |
| *C44C10.8* | *hnd-1* | 10.0 | 1.43E-43 | Soluble in nucleus |
| *T11A5.4* | *srab-19* | 8.5 | 3.69E-56 | Pseudogene |
| *W10G11.7* | *clec-131* | * | 2.51E-26 | Pseudogene |
| **10 most strongly downregulated genes in *hsp-90*$^{int}$ hp-RNAi** | | | | |
| **Transcript** | **Gene name** | **$log_2$(FC)** | **$p_c$** | **SC localisation** |
| *T22G5.2* | *lbp-7* | -2.6 | 2.28E-07 | Soluble in cytoplasm |
| *W03F9.4* | | -8.8 | 6.99E-141 | TM in ER |
| *F17E9.11* | *lys-10* | -7.3 | 2.90E-15 | Soluble extracellular |
| *ZK218.5* | | -2.9 | 5.54E-07 | Soluble extracellular |
| *C45G7.2* | *ilys-2* | -4.3 | 5.34E-06 | Soluble extracellular |
| *F08E10.7* | *scl-24* | -2.9 | 1.18E-03 | Soluble extracellular |
| *ZK218.7* | | -5.2 | 1.59E-03 | Soluble extracellular |
| *ZK218.11* | | -2.8 | 9.72E-03 | Soluble extracellular |
| *C45G7.3* | *ilys-3* | -4.3 | 9.92E-03 | Soluble extracellular |
| *K10G4.5* | | -4.2 | 1.74E-04 | Soluble in nucleus |

**Table 4.6 The ten most strongly upregulated and downregulated genes in the *hsp-90*$^{int}$ hp-RNAi strain compared to the *hsp-90*$^{control}$ strain**. Subcellular (SC) localisation was predicted using DeepLoc 1.0 based on the amino acid sequence of the encoded protein. * = gene whose differential expression is 'infinite', and for which the fold-change therefore cannot be calculated. FC = fold-change compared to the *hsp-90*$^{control}$ strain. $p_c$ = corrected p value. TM = transmembrane.

| **10 most strongly upregulated genes in *hsp-90*$^{neu}$ hp-RNAi** | | | | |
|---|---|---|---|---|
| **Transcript** | **Gene name** | **$log_2$(FC)** | **$p_c$** | **SC localisation** |
| *F09F3.4* | *srx-133* | 11.265 | 1.6E-123 | TM in cell membrane |
| *R11D1.5* | *str-178* | 8.848 | 4.8E-39 | TM in cell membrane |
| *T04B8.3* | *arrd-1* | 7.928 | 1.7E-58 | Soluble in cytoplasm |
| *C52D10.8* | *skr-13* | 7.365 | 7.1E-12 | Soluble in cytoplasm |
| *R11D1.4* | | 8.509 | 2.0E-32 | Soluble extracellular |
| *E02A10.2* | *grl-23* | * | 4.8E-18 | Soluble extracellular |
| *C18H7.3* | *col-102* | * | 3.8E-14 | Soluble extracellular |
| *Y46G5A.23* | | * | 4.4E-14 | Soluble extracellular |
| *C13A2.12* | | 7.026 | 2.5E-12 | Soluble extracellular |
| *F37B4.14* | | * | 2.6E-28 | Pseudogene |
| **10 most strongly downregulated genes in *hsp-90*$^{neu}$ hp-RNAi** | | | | |
| **Transcript** | **Gene name** | **$log_2$(FC)** | **$p_c$** | **SC localisation** |
| *C03G5.11* | *nspc-4* | -3.497 | 8.9E-15 | Soluble extracellular |
| *F17E9.11* | *lys-10* | -5.703 | 8.9E-11 | Soluble extracellular |
| *Y68A4B.2* | *clec-242* | -3.181 | 6.7E-09 | Soluble extracellular |
| *C45G7.2* | *ilys-2* | -2.994 | 6.4E-04 | Soluble extracellular |
| *F59D8.1* | *vit-3* | * | 1.7E-03 | Soluble extracellular |
| *F28C12.2* | *sra-18* | -5.105 | 2.1E-03 | TM in cell membrane |
| *W03F9.4* | | -7.855 | 9.6E-121 | TM in ER |
| *F54D10.8* | | -3.174 | 5.6E-04 | TM in Golgi apparatus |
| *C49D10.4* | *oac-10* | -3.856 | 3.9E-09 | TM in lysosome |
| *H17B01.2* | | -3.970 | 4.9E-03 | Unable to predict |

**Table 4.7 The ten most strongly upregulated and downregulated genes in the *hsp-90*$^{neu}$ hp-RNAi strain compared to the *hsp-90*$^{control}$ strain**. Subcellular (SC) localisation was predicted using DeepLoc 1.0 based on the amino acid sequence of the encoded protein. * = gene whose differential expression is 'infinite', and for which the fold-change therefore cannot be calculated. FC = fold-change compared to the *hsp-90*$^{control}$ strain. $p_c$ = corrected p value. TM = transmembrane.

### 4.3.8 17 genes are commonly upregulated compared to both wild-type and the *hsp-90*$^{control}$ strain

Tissue-specific *hsp-90* knockdown in the neurons or intestine could result in activation of common signalling pathways, which might be key aspects of signalling during TCS. To identify genes which are differentially expressed whether TCS is activated from the neurons or intestine, differentially expressed genes were compared between the *hsp-90*$^{int}$ hp-RNAi and *hsp-90*$^{neu}$ hp-RNAi strains. Compared to the *hsp-90*$^{control}$ strain, there are 60 genes which are upregulated in both the *hsp-90*$^{int}$ hp-RNAi and *hsp-90*$^{neu}$ hp-RNAi strains (**Fig. 4.11a**), whilst 30 genes are downregulated in both strains (**Fig. 4.11b**). To determine whether the sizes of these overlaps between gene groups were greater than would be expected by chance, the probability mass function was calculated for the size of each overlap using the hypergeometric test, and in both cases was below 0.05 (shown within **Fig. 4.11**). Whilst the *hsp-90*$^{neu}$ hp-RNAi strain appears at first glance to have a very different transcriptomic profile to the *hsp-90*$^{int}$ hp-RNAi strain (**Fig. 4.5**), these shared differentially expressed genes indicate that knockdown of *hsp-90* in the neurons or intestine may nevertheless have a common transcriptional response.

Amongst the 60 genes upregulated in both strains, there is no significant enrichment for GO terms. However, amongst the 30 downregulated genes there are enrichments for terms relating to the immune system and to fatty acid metabolism (**Fig. 4.12**). As immune response-related genes are upregulated in the *hsp-90*$^{control}$ strain compared to wild-type (**Fig. 4.6**), and also in the *hsp-90*$^{neu}$ hp-RNAi strain compared to the *hsp-90*$^{control}$ strain (**Fig. 4.10a**), this shared downregulation potentially represents a different subset of immune response genes. Interestingly, one of the genes downregulated in both strains is the insulin-like neuropeptide *ins-7*, which has been shown to activate DAF-2 through neuroendocrine signalling (Murphy et al. 2003; Evans et al. 2008; Kawli & Tan 2008). Reduced ILS signalling might indicate that DAF-16 could be involved in the TCS transcriptional response.

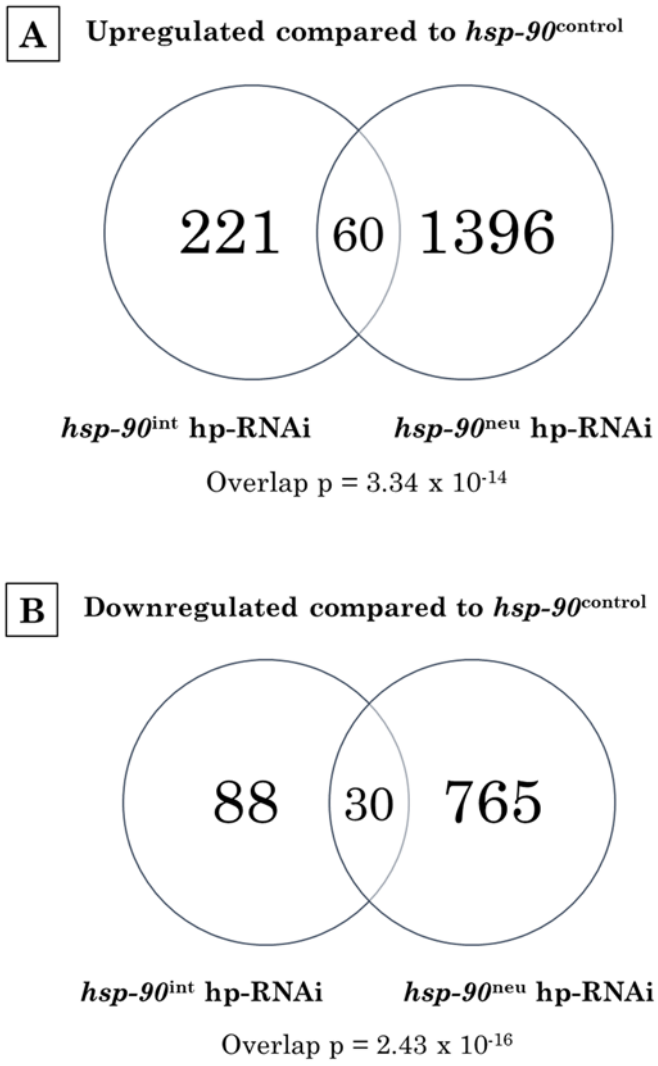


**Figure 4.11 Common differentially expressed genes compared to the *hsp-90*$^{control}$ strain**. The numbers of genes (**A**) upregulated or (**B**) downregulated in the *hsp-90*$^{int}$ hp-RNAi and *hsp-90*$^{neu}$ hp-RNAi strains compared to the *hsp-90*$^{control}$ strain, and their overlap. Overlap p: probability mass function of overlap size based on hypergeometric distribution.

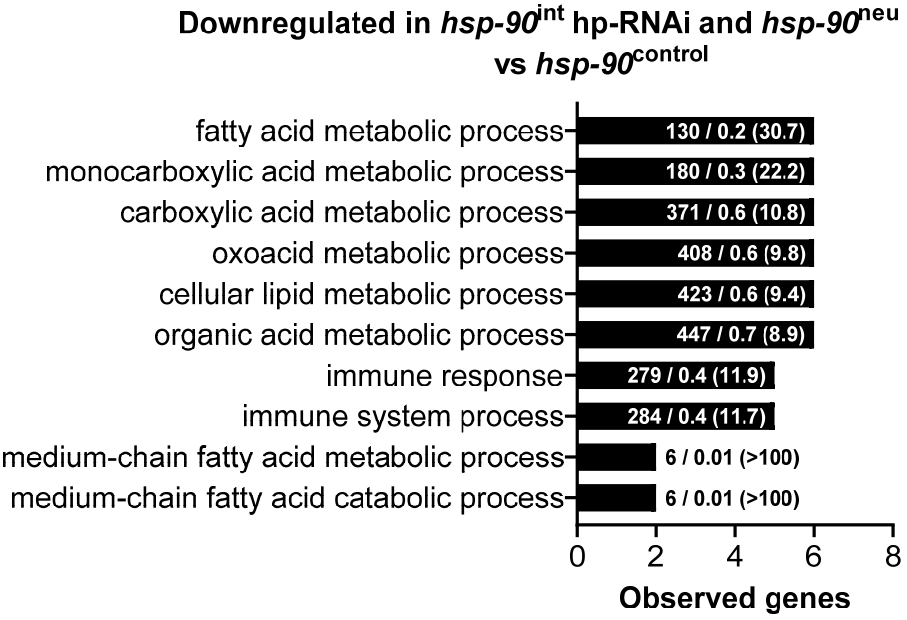


**Figure 4.12 GO terms enriched amongst genes downregulated in both TCS-activated strains compared to the *hsp-90*$^{control}$ strain**. Labels show 'Total genes / Expected genes (Fold-enrichment)', where 'Total genes' is all genes associated with each term, 'Expected genes' is the number of genes associated with each term that you would expect from an input list of the same size, and 'Fold-Enrichment' is the number of observed genes divided by the number of expected genes. All bars represent biological process terms. FDR < 0.05 for all terms.

It is possible that the differential expression of some of these commonly upregulated or downregulated genes may be due to a combinatorial effect between the tissue-specific knockdown of *hsp-90* and the presence of the *sid-1* (*pk3321*) allele. Since the wild-type strain does not carry this allele, genes were identified which were differentially expressed in both the *hsp-90*$^{int}$ hp-RNAi and *hsp-90*$^{neu}$ hp-RNAi strains when compared to both wild-type and the *hsp-90*$^{control}$ strain.

None of the 30 genes which are downregulated in both the *hsp-90*$^{int}$ hp-RNAi and *hsp-90*$^{neu}$ hp-RNAi strains when compared only to the *hsp-90*$^{control}$ strain are also downregulated when compared to wild-type. However, 17 of the 60 genes upregulated in both the *hsp-90*$^{int}$ hp-RNAi and *hsp-90*$^{neu}$ hp-RNAi strains are also upregulated compared to wild-type (**Fig. 4.13**). These 17 genes are listed in **Table 4.8** along with the predicted subcellular localisation of their encoded proteins, which was determined from protein amino acid sequences using the tool DeepLoc 1.0.

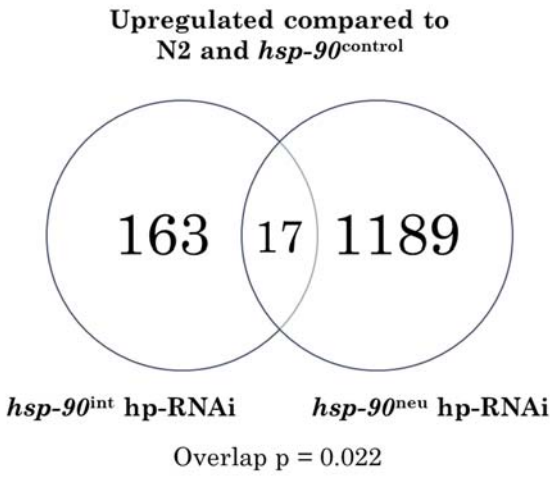


**Figure 4.13 Seventeen genes are commonly upregulated compared to both control strains**. Gene numbers upregulated in the *hsp-90*$^{int}$ hp-RNAi or *hsp-90*$^{neu}$ hp-RNAi strains compared to both wild-type and the *hsp-90*$^{control}$ strain, and their overlap. Overlap p: probability mass function of overlap size based on hypergeometric distribution.

| Transcript | Gene Name | SC Localisation | Fold-change vs *hsp-90*$^{control}$ | |
|---|---|---|---|---|
| | | | ***hsp-90***$^{int}$ | ***hsp-90***$^{neu}$ |
| *K10D11.1* | *dod-17* | Extracellular soluble | 6.14 | 5.60 |
| *T21C12.3* | *nlp-68* | Extracellular soluble | 26.32 | 3.71 |
| *C01G10.16* | | Extracellular soluble | 11.65 | 40.95 |
| *C02B8.12* | | Extracellular soluble | 4.15 | 3.07 |
| *C37C3.7* | | Extracellular soluble | 2.02 | 1.95 |
| *Y51A2D.14* | | Extracellular soluble | 9.85 | 2.84 |
| *Y9C9A.1* | | Extracellular soluble | 2.28 | 1.80 |
| *ZK262.3* | | Extracellular soluble | 2.07 | 2.13 |
| *C07G3.2* | *irg-1* | Soluble in cytoplasm | 10.82 | 2.04 |
| *Y19D10B.6* | | Soluble in ER | 6.82 | 3.83 |
| *Y38E10A.14* | | Soluble in nucleus | 4.46 | 3.11 |
| *F28H7.9* | *sre-6* | TM in cell membrane | 2.18 | 2.15 |
| *C05E4.14* | *srh-2* | TM in cell membrane | 3.17 | 1.90 |
| *F10D2.4* | *str-112* | TM in cell membrane | 3.01 | 4.91 |
| *C06A1.2* | | TM in ER | 2.36 | 4.11 |
| *W05H12.1* | | TM in ER | 7.15 | 3.34 |
| *T20D4.5* | | TM in lysosome | 2.06 | 1.58 |

**Table 4.8 Genes upregulated in both TCS-activated strains compared to both wild-type and the *hsp-90*$^{control}$ strain**. Subcellular (SC) localisation predicted from amino acid sequence using DeepLoc 1.0. TM = transmembrane.

### 4.3.9 The promoters of many shared differentially expressed genes contain PHA-4 or DAF-16 consensus motifs

It has previously been shown that cell-non-autonomous *hsp-70* reporter upregulation activated by tissue-specific *hsp-90* knockdown is dependent on the transcription factor *pha-4* (van Oosten-Hawle et al. 2013). In addition, the insulin-like signalling peptide *ins-7* is downregulated in both the *hsp-90*$^{int}$ hp-RNAi and *hsp-90*$^{neu}$ hp-RNAi strains compared to the *hsp-90*$^{control}$ strain (**Fig. 4.11b**), suggesting that DAF-16 activity may be increased in TCS. To determine whether PHA-4 or DAF-16 might be relevant to the transcriptomic changes common to the *hsp-90*$^{int}$ hp-RNAi and *hsp-90*$^{neu}$ hp-RNAi strains, motif scanning was performed in the promoters of genes which are differentially regulated in both strains.

The promoter sequences of the 60 commonly upregulated and 30 commonly downregulated genes in the *hsp-90*$^{int}$ hp-RNAi and *hsp-90*$^{neu}$ hp-RNAi strains compared to the *hsp-90*$^{control}$ strain were scanned for known PHA-4 or DAF-16 consensus motifs. As shown in **Tables 4.9 & 4.10**, 39 of these 90 genes contain a PHA-4 motif; 55 contain a DAF-16 motif; and 32 contain both. In total, 62 of the 90 genes scanned contain at least one known motif for either transcription factor. Genes whose promoters did not contain any known consensus motifs were omitted from these tables. Of the 23 genes which contained a DAF-16 motif but not a PHA-4 motif, 19 (including the *ins-7* promoter) contained a DAF-16-associated element (DAE) (**Table 4.10**). DAEs are known to be bound by the transcription factor PQM-1 (Tepper et al. 2013), which has been shown to be required for TCS activated by tissue-specific HSP-90 overexpression (O'Brien et al. 2018). It is therefore possible that PQM-1 may also act in the case of tissue-specific *hsp-90* knockdown, perhaps as a suppressor of *ins-7* and ILS.

It is important to note that the presence of a transcription factor consensus binding site in a DNA sequence does not confirm transcriptional regulation. The fact that, for example, the *ttc-36* promoter contains a PHA-4 consensus motif, does not prove that this site is actively bound or even accessible during TCS. To investigate this further, one could begin by knocking down *pha-4* in the *hsp-90*$^{int}$ hp-RNAi and *hsp-90*$^{neu}$ hp-RNAi strains by RNAi feeding, followed by qRT-PCR to see whether genes whose promoters contain a PHA-4 motif are still differentially expressed.

| | | PHA-4 | Any DAF-16 | DBE | DAE |
|---|---|---|---|---|---|
| *clec-169* | Upregulated | Y | Y | Y | Y |
| *C40H1.8* | Upregulated | Y | Y | Y | Y |
| *F45D3.4* | Upregulated | Y | Y | Y | Y |
| *K08C7.1* | Upregulated | Y | Y | Y | Y |
| *W03F9.4* | Downregulated | Y | Y | Y | Y |
| *asns-2* | Upregulated | Y | Y | Y | |
| *gst-28* | Upregulated | Y | Y | Y | |
| *lys-5* | Upregulated | Y | Y | Y | |
| *srh-2* | Upregulated | Y | Y | Y | |
| *ttc-36* | Upregulated | Y | Y | Y | |
| *ugt-26* | Upregulated | Y | Y | Y | |
| *K08C7.4* | Upregulated | Y | Y | Y | |
| *acly-1* | Downregulated | Y | Y | Y | |
| *acs-13* | Downregulated | Y | Y | Y | |
| *clec-118* | Downregulated | Y | Y | Y | |
| *ilys-2* | Downregulated | Y | Y | Y | |
| *scl-24* | Downregulated | Y | Y | Y | |
| *acs-1* | Upregulated | Y | Y | | Y |
| *irg-1* | Upregulated | Y | Y | | Y |
| *F26A3.4* | Upregulated | Y | Y | | Y |
| *F46C5.10* | Upregulated | Y | Y | | Y |
| *acdh-7* | Downregulated | Y | Y | | Y |
| *elo-2* | Downregulated | Y | Y | | Y |
| *sago-2* | Downregulated | Y | Y | | Y |
| *C06B8.7* | Downregulated | Y | Y | | Y |
| *Y46D2A.2* | Downregulated | Y | Y | | Y |
| *cyp-13A5* | Upregulated | Y | Y | | |
| *cyp-14A5* | Upregulated | Y | Y | | |
| *mxl-3* | Upregulated | Y | Y | | |
| *zig-2* | Upregulated | Y | Y | | |
| *cpl-1* | Downregulated | Y | Y | | |
| *elf-1* | Downregulated | Y | Y | | |
| *C01G10.16* | Upregulated | Y | | | |
| *C02B8.12* | Upregulated | Y | | | |
| *F08F3.4* | Upregulated | Y | | | |
| *W05H12.1* | Upregulated | Y | | | |
| *Y51A2D.14* | Upregulated | Y | | | |
| *acdh-10* | Downregulated | Y | | | |
| *F25E5.1* | Downregulated | Y | | | |

**Table 4.9 Scanned genes whose promoters contain a PHA-4 motif**. Columns indicate which motifs are present in each promoter. DBE: DAF-16 binding element. DAE: DAF-16-associated element.

| | | PHA-4 | Any DAF-16 | DBE | DAE |
|---|---|---|---|---|---|
| *clec-210* | Upregulated | | Y | | Y |
| *clec-47* | Upregulated | | Y | | Y |
| *clec-76* | Upregulated | | Y | | Y |
| *cyp-35C1* | Upregulated | | Y | | Y |
| *lbp-8* | Upregulated | | Y | | Y |
| *nhx-3* | Upregulated | | Y | | Y |
| *B0252.1* | Upregulated | | Y | | Y |
| *F45D3.3* | Upregulated | | Y | | Y |
| *F53F4.4* | Upregulated | | Y | | Y |
| *Y38E10A.14* | Upregulated | | Y | | Y |
| *Y42G9A.3* | Upregulated | | Y | | Y |
| *clec-66* | Downregulated | | Y | | Y |
| *cpr-3* | Downregulated | | Y | | Y |
| *hpo-15* | Downregulated | | Y | | Y |
| *ins-7* | Downregulated | | Y | | Y |
| *lys-10* | Downregulated | | Y | | Y |
| *lys-2* | Downregulated | | Y | | Y |
| *F01D5.3* | Downregulated | | Y | | Y |
| *K06A4.6* | Downregulated | | Y | | Y |
| *mtl-2* | Upregulated | | Y | | |
| *sre-6* | Upregulated | | Y | | |
| *C02F5.12* | Upregulated | | Y | | |
| *F33E2.5* | Downregulated | | Y | | |

**Table 4.10 Scanned genes whose promoters contain a DAF-16 but not PHA-4 motif**. Columns indicate which motifs are present in each promoter. DBE: DAF-16 binding element. DAE: DAF-16-associated element.

## 4.4 Discussion

### 4.4.1 Activation of TCS by tissue-specific *hsp-90* knockdown appears to have a complex effect on immune gene expression

Compared to wild-type, genes upregulated in the *hsp-90*$^{control}$ strain are enriched for terms relating to immune responses (**Fig. 4.6**). A key difference between these two strains is the *sid-1* (*pk3321*) allele in the *hsp-90*$^{control}$ strain. The role of *sid-1* in cellular RNAi import means that it is an important gene for immunity (Schott et al. 2005), and its homologue SIDT2 is important in human antiviral responses (Nguyen et al. 2017). Introduction of the *sid-1* (*pk3321*) allele might therefore promote upregulation of immune genes, perhaps to compensate for its reduced function.

Of the seven genes which are upregulated in the *hsp-90*$^{control}$, *hsp-90*$^{int}$ hp-RNAi and *hsp-90*$^{neu}$ hp-RNAi strains compared to wild-type, six are related to the immune response (**Fig. 4.7a, Table 4.4**). These are the c-type lectins *clec-17* and *clec-38*; the immune gene *gst-38*; and three genes affected by *daf-16*: *scb-1*, *math-15* and *T22F7.4*. This supports the idea of a common upregulation of the immune response between these strains. However, amongst genes downregulated in both the *hsp-90*$^{int}$ hp-RNAi and *hsp-90*$^{neu}$ hp-RNAi strains compared to the *hsp-90*$^{control}$ strain, there are enrichments for GO terms relating to the immune response (**Fig. 4.12**). One such downregulated gene is the neuropeptide *ins-7*, which is known to activate cell-non-autonomous ILS and suppress DAF-16 activity (Murphy et al. 2003; Evans et al. 2008; Kawli & Tan 2008). Furthermore, the lysozyme genes *lys-10* and *ilys-2* are amongst the most strongly downregulated genes in both the *hsp-90*$^{int}$ hp-RNAi and *hsp-90*$^{neu}$ hp-RNAi strains compared to the *hsp-90*$^{control}$ strain (**Tables 4.6, 4.7**). The overall effect on immune resistance in these strains therefore does not appear to be straightforward. It would be useful to quantify the resistance of these strains to infection with bacterial or viral pathogens, to determine whether the observed changes in gene expression affect the function of the immune response.

### 4.4.2 Heat-inducible *hsp-70*s are upregulated in the *hsp-90*$^{int}$ hp-RNAi strain whilst lysosome-related genes are downregulated

In the *hsp-90*$^{int}$ hp-RNAi strain, three heat-inducible *hsp-70* family genes are upregulated compared to the *hsp-90*$^{control}$ strain: *hsp-70*, *F44E5.4*, and *F44E5.5* (**Table 4.5**). The upregulation of these genes on heat stress is dependent on *hsf-1* (GuhaThakurta et al. 2002; Brunquell et al. 2016), which could indicate a role for *hsf-1* during TCS. However, *hsf-1* is not required for cell-non-autonomous *hsp-70* reporter upregulation in this strain (**Figs. 3.3c-d; 3.4**), and other *hsf-1*-dependent chaperones such as small heat shock proteins are not differentially expressed. It is interesting to note that all three heat-inducible cytoplasmic *hsp-70* family chaperones are upregulated in the *hsp-90*$^{int}$ hp-RNAi strain, which also has an increased lifespan compared to the *hsp-90*$^{control}$ strain (**Fig. 4.5; Table 3.6**). Whilst *F44E5.4* and *F44E5.5* have not been shown to modulate lifespan, their similarity to *hsp-70* could also imply a role for them in longevity. Of the other genes strongly upregulated in this strain, two (*srj-37* and *srx-47*) encode GPCRs (**Table 4.6**). GPCRs at the cell membrane are often involved in the transduction of extracellular signals to the interior (Strader et al. 1994). For example, the GPCR DCAR-1 is activated by hydroxyphenyllactic acid (HPLA) during *D. coniospora* infection, triggering the intracellular p38 MAPK cascade and promoting immune gene expression (Reboul et al. 2016). These upregulated GPCRs could therefore represent part of an intercellular pathway during TCS in the *hsp-90*$^{int}$ hp-RNAi strain.

Amongst genes downregulated in the *hsp-90*$^{int}$ hp-RNAi strain compared to the *hsp-90*$^{control}$ strain, there are enrichments for GO terms relating to metabolic activity and lysosome function (**Fig. 4.9**). This correlates with the fact that three of the most strongly downregulated genes in the *hsp90*$^{int}$ hp-RNAi strain are the lysozymes *lys-10*, *ilys-2* and *ilys-3* (**Table 4.6**). *ilys-3* has previously been shown to be upregulated in the intestine upon bacterial infection in a manner dependent on MPK-1 signalling in the pharynx (Gravato-Nobre et al. 2016), so may also be part of a cell-non-autonomous signalling pathway during TCS. It is interesting that lysosome-related genes are downregulated in this strain with intestine-specific *hsp-90* knockdown, as intestinal lysosome function has been shown to be linked to cell-non-autonomous UPR$^{ER}$ signalling (Imanikia et al. 2019). This may be related to the downregulation

of the non-canonical UPR$^{ER}$ genes *abu-2* and *abu-4* in all other strains compared to wild-type (**Table 4.4**).

### 4.4.3 Genes relating to neuropeptide signalling and innate immunity are upregulated in the *hsp-90*$^{neu}$ hp-RNAi strain

Far more genes are differentially expressed in the *hsp-90*$^{neu}$ hp-RNAi strain than in the *hsp-90*$^{int}$ hp-RNAi strain (**Figs. 4.4 and 4.5**). This suggests that pan-neuronal *hsp-90* knockdown may strongly affect gene expression throughout the organism to impact a much wider range of cellular signalling processes than intestine-specific knockdown. This would perhaps not be surprising, as adult hermaphrodites possess over 100 classes of neurons (White et al. 1986) which could potentially all respond differently upon pan-neuronal *hsp-90* depletion. In contrast, the intestine consists of only 20 cells which are clonal E blastomere descendants (Deppe et al. 1978; Sulston et al. 1983). Amongst genes upregulated in the *hsp-90*$^{neu}$ hp-RNAi strain compared to the *hsp-90*$^{control}$ strain, there are enrichments for GO terms relating to neuropeptide signalling, transmembrane transport, extracellular space, and the immune response (**Fig. 4.10a**). It is possible that the upregulation of both neuropeptide signalling and immune response genes could involve neuroendocrine regulation of organismal immunity, such as has been shown to regulate ILS (Murphy et al. 2003; Evans et al. 2008; Kawli & Tan 2008). An enrichment for genes relating to neuropeptide signalling is reflected in the fact that the *unc-31* gene, which is required for neuronal exocytosis of DCVs (Speese et al. 2007), is upregulated almost 3-fold. On another note, 76 genes relating to oxidation-reduction processes are upregulated in this strain (**Fig. 4.10a**), including the superoxide dismutase *sod-3* and over 20 cytochrome P450 (*cyp*) genes (**Table A5**). This could be an explanation for the increased resistance to oxidative stress seen in this strain (**Fig. 3.8**).

Amongst genes downregulated in the *hsp-90*$^{neu}$ hp-RNAi strain compared to the *hsp-90*$^{control}$ strain, over 30 terms relating to protein phosphorylation or dephosphorylation are enriched (**Fig. 4.10b**). Many proteins which act in signalling pathways, for example HSF-1, are regulated by the addition or removal of phosphate groups (Guettouche et al. 2005; Deribe et al. 2010). The comprehensive coverage of terms relating to these processes may indicate large-scale changes in phosphorylation-controlled signalling pathways. The fact that so many such terms are enriched amongst downregulated genes could suggest an organismal 'pause' in

protein phospho-modification; although as these data represent whole-animal transcripts it is perhaps more likely that phosphorylation is simply upregulated in some tissues but downregulated in others. There is some evidence that infection, phosphorylation pathways and HSP-90 activity are related in *C. elegans* (Balasubramaniam et al. 2019), and it is possible that neuronal *hsp-90* knockdown could therefore activate an immune response with whole-organism consequences for protein phosphorylation.

### 4.4.4 Common features of differential gene expression following tissue-specific *hsp-90* knockdown

Compared to both wild-type and the *hsp-90*$^{control}$ strain, 17 genes are upregulated in both the *hsp-90*$^{int}$ hp-RNAi and *hsp-90*$^{neu}$ hp-RNAi strains (**Fig 4.13; Table 4.8**). Of these, eight (*dod-17*, *nlp-68*, *C01G10.16*, *C02B8.12*, *C37C3.7*, *Y51A2D.14*, *Y9C9A.1* and *ZK262.3*) are predicted to encode soluble extracellular proteins and three (*sre-6*, *srh-2*, *str-112*) encode GPCRs. These may represent intercellular signalling molecules or effectors of signal transduction. Four upregulated genes are also related to immunity: the *daf-16*-regulated gene *dod-17*; the bacterial immune response gene *irg-1*; the predicted cytokine *C02B8.12*; and *C37C3.7*, which is an orthologue of a human c-type lectin and a Wnt inhibitory factor (WormBase; Harris et al. 2010). This supports the idea that tissue-specific *hsp-90* knockdown in either the neurons or intestine may influence organismal immunity.

Cell-non-autonomous *hsp-70p::mCherry* upregulation following tissue-specific *hsp-90* knockdown has previously been shown to depend on *pha-4* (van Oosten-Hawle et al. 2013). Of the 90 genes which are either upregulated in both the *hsp-90*$^{int}$ hp-RNAi and *hsp-90*$^{neu}$ hp-RNAi strains compared to the *hsp-90*$^{control}$ strain, or downregulated in both, 39 have a promoter which contains at least one PHA-4 consensus motif (**Table 4.9**). This supports the idea of PHA-4 as an important transcriptional regulator during TCS in these strains. However, the DAF-2-regulated transcription factors DAF-16 and PQM-1 may also have a role. DAF-16, which binds DBEs to promote expression of immune and stress responsive genes, is suppressed by DAF-2; whilst PQM-1, which binds DAEs to promote expression of developmental and metabolic genes, is enhanced by it (Tepper et al 2013). DAF-2 activation is mediated by neuroendocrine secretion of insulin-like neuropeptides such as INS-7 (Murphy et al. 2003; Evans et al 2008; Kawli & Tan 2008). However, *ins-7* is downregulated in

both the *hsp-90*$^{int}$ hp-RNAi and *hsp-90*$^{neu}$ hp-RNAi strains compared to the *hsp-90*$^{control}$ strain (**Tables A4, A6**), suggesting that in these strains DAF-2 signalling may be reduced and DAF-16 activity potentially increased. Of the 90 genes which are either upregulated in both the *hsp-90*$^{int}$ hp-RNAi and *hsp-90*$^{neu}$ hp-RNAi strains compared to the *hsp-90*$^{control}$ strain, or downregulated in both, 55 have a promoter which contains at least one DAF-16-related consensus motif (**Tables 4.9 & 4.10**). Both DBEs and DAEs are represented, indicating that both DAF-16 and PQM-1 could be involved in transcriptional regulation during TCS in these strains. PQM-1 has previously been shown to be involved in TCS, and is required during TCS activated by tissue-specific HSP-90 overexpression (O'Brien et al. 2018); so may also be involved in TCS activated by tissue-specific *hsp-90* knockdown.

Whilst motif scanning in the promoters of commonly differentially expressed genes yielded useful information, it would also be interesting to perform *de novo* motif discovery within each strain individually. For example, motif discovery in the promoters of the 281 genes upregulated in the *hsp-90*$^{int}$ hp-RNAi strain compared to the *hsp-90*$^{control}$ strain might identify a different transcription factor which is specifically involved in TCS activated by intestine-specific *hsp-90* knockdown.

# Chapter 5. A forward genetic screen to identify regulators of TCS in the *hsp-90*$^{int}$ hp-RNAi strain

## 5.1 Introduction

RNA-Seq identified differentially expressed genes in the *hsp-90*$^{int}$ hp-RNAi and *hsp-90*$^{neu}$ hp-RNAi strains, indicating that these genes may be involved in TCS. However, differential expression of a gene could be a consequence of TCS activation rather than due to the gene in question being a key signalling component. To identify a gene required for TCS, a forward genetics approach was taken. The *hsp-90*$^{int}$ hp-RNAi and *hsp-90*$^{neu}$ hp-RNAi strains exhibit a clear visual phenotype associated with TCS, namely the expression of the *hsp-70* reporter. The intensity of reporter fluorescence can therefore be used as a readout for the ability of the strain to activate TCS. As the reporter is expressed more strongly in the *hsp-90*$^{int}$ hp-RNAi strain than in the *hsp-90*$^{neu}$ hp-RNAi strain, facilitating visual screening, the *hsp-90*$^{int}$ hp-RNAi strain was chosen for a forward genetic screen. The aim of this screen was to identify a gene required for *hsp-70* reporter upregulation in the *hsp-90*$^{int}$ hp-RNAi strain.

Forward genetic screens are a classic method for identifying genes associated with a phenotype. One of the first *C. elegans* papers published by Brenner (Brenner 1974) described the identification by forward genetic screening of numerous genes associated with phenotypes including *uncoordinated*, *roller*, and *dumpy*. The general process of such screens involves the random introduction of mutations throughout the genome, for example by exposure to a mutagen; followed by the identification of individual mutants with a specific phenotype of interest, and the subsequent identification of specific causal mutations in these individuals. Whilst the characterisation of causal mutations has historically been time-consuming, this has been aided considerably by the sequencing of the *C. elegans* genome (The *C. elegans* Sequencing Consortium 1998) and the development of single nucleotide polymorphism (SNP) mapping (Wicks et al. 2001). Furthermore, the combination of SNP mapping with whole-genome sequencing (WGS) now enables 'one-step mapping' of previously uncharacterised mutants (Doitsidou et al. 2010), as utilised here.

## 5.2 Methods

### 5.2.1 Overview and general principles of approach

To identify genes required for cell-non-autonomous *hsp-70* upregulation in the *hsp-90*$^{int}$ hp-RNAi strain, an unbiased forward genetic screen was performed. Mutations were introduced randomly throughout the genome by exposure to the mutagen EMS, and progeny screened for a phenotype of visibly altered *hsp-70* reporter fluorescence. Animals displaying such a phenotype were isolated and allowed to self-fertilise to confirm that mutation had not caused sterility and that the phenotype was retained between generations. Organismal transcript levels of *hsp-70* and *mCherry* were also quantified in each mutant isolate by qRT-PCR, to confirm that altered fluorescence was not due to mutation of the reporter construct. Mutant isolates which satisfied these criteria were taken forward for 'one-step' WGS and SNP mapping as described below. The entire process is summarised in **Figure 5.1**.

In one-step mapping of an N2-derived mutant strain of interest, the mutant strain is first crossed with a polymorphic alternative wild-type strain such as CB4856 (Hawaii), which has over 45,000 known SNPs relative to the N2 reference genome (Hillier et al. 2008). The heterozygous $F_2$ progeny of such a 'mapping cross', which represent recombinants of mutant and CB4856 genetic material, are screened for retention of the phenotype before being isolated and allowed to self-fertilise. Populations of F3 progeny are then pooled for genomic DNA extraction and WGS (Doitsidou et al. 2010). By pooling large numbers of heterozygous progeny, one can obtain many chromosomes containing both N2-derived and CB4856-derived genetic material, which arise due to random recombination. Following WGS, analysis of data from pooled samples can then determine the ratio of CB4856 to N2 alleles in the mapping cross progeny (referred to as 'CB4856:N2 ratio') at the location of each known SNP (Minevich et al. 2012). At any position not linked to the causal mutation for the phenotype, N2 and CB4856 alleles will be approximately equally represented as recombination will be unbiased. However, any genomic regions linked to the mutation of interest must necessarily derive from the mutant strain, which has an N2 background; and so any CB4856 SNPs will be excluded from this region. By identifying genomic regions where one would expect to find a CB4856 SNP, but where the CB4856:N2 ratio is actually zero, the location of a causal mutation within the genome can be identified.

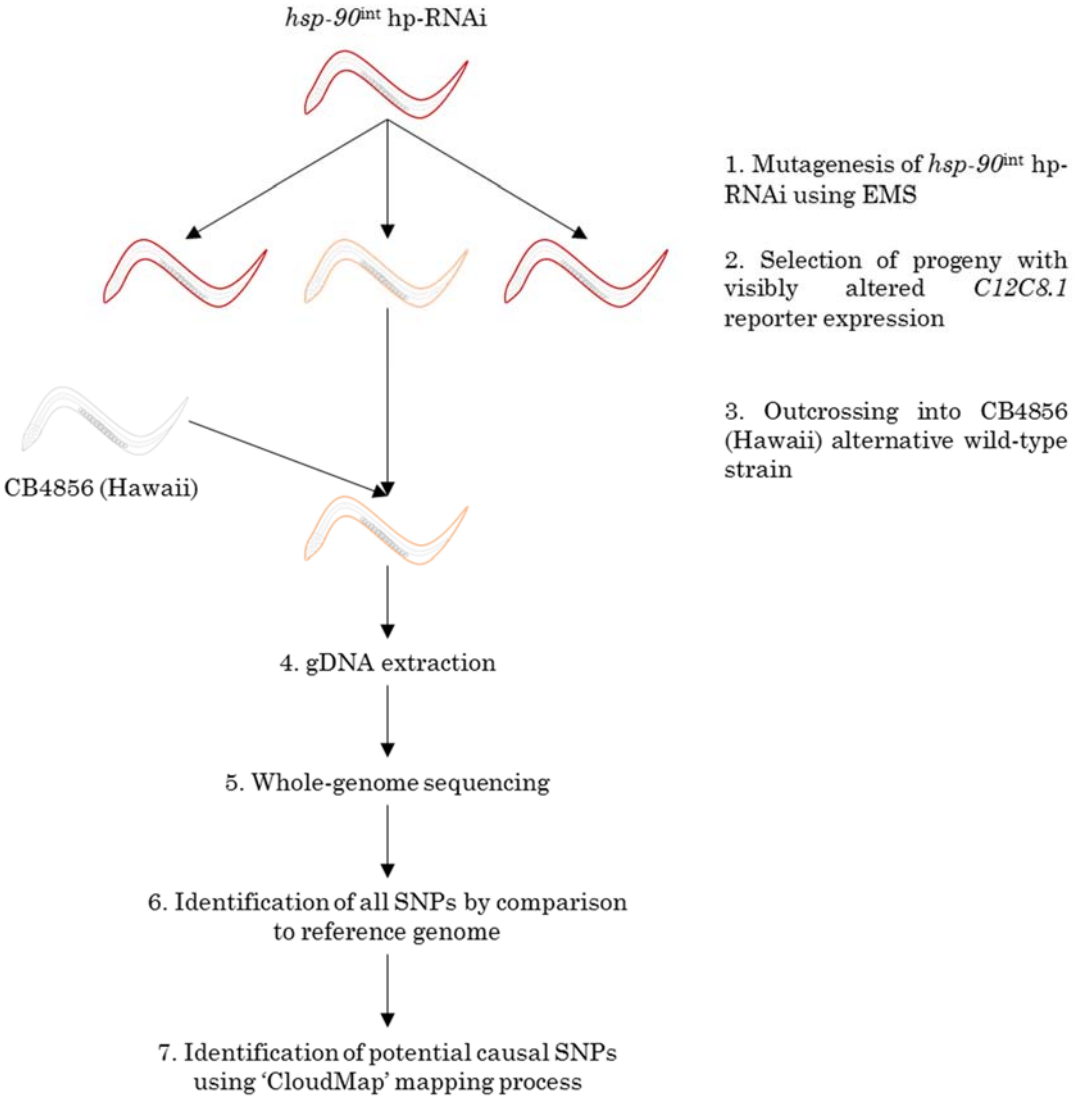


**Figure 5.1 Process to identify a gene required for *hsp-70* reporter upregulation in the *hsp-90*$^{int}$ hp-RNAi strain**. Steps 5 and 6 (whole-genome sequencing and SNP identification) were performed by Novogene (Hong Kong). gDNA: genomic DNA.

### 5.2.2 EMS mutagenesis and phenotypic screen

The *hsp-90*$^{int}$ hp-RNAi strain was grown on three 90mm NGM plates until there were large numbers of gravid adults, but some bacterial food source was still present. Worms were washed from these plates using M9 buffer, synchronised by bleaching, and the arrested L1-stage larvae distributed between five 90mm NGM plates. Synchronised worms were then allowed to develop to L4 stage.

A 100mM solution of the mutagen ethyl methanesulfonate (EMS) was prepared by mixing 0.62g of EMS stock solution in 50mL M9 buffer. All work with EMS was performed inside a fume hood, and all contaminated pipette tips and Falcon tubes soaked in EMS inactivating solution (0.1M NaOH, 20% w/v $Na_2S_2O_3$) for 24 hours before disposal. The synchronised L4-stage *hsp-90*$^{int}$ hp-RNAi animals were washed into a 15mL Falcon tube using M9 buffer and pelleted by low-speed centrifugation. M9 buffer was removed to leave a volume of 2mL, to which 2mL of 100mM EMS solution was added. The tube was wrapped securely in parafilm and incubated on a rotator for 4 hours at 20°C. Following this, worms were pelleted by low-speed centrifugation, the pellet washed three times with M9 buffer, and worms resuspended in 1mL M9 buffer. This volume was distributed between two 90mm NGM plates and allowed to dry for 1-2 hours. In total, approximately 2,000 genomes were mutagenised.

10 mutagenised adults ($P_0$ generation) were picked onto each of 200 90mm NGM plates and allowed to lay eggs ($F_1$ generation) overnight. $P_0$ adults were removed the next morning. $F_1$ eggs were allowed to mature to gravid adult stage and lay eggs ($F_2$ generation) for one day, following which adult $F_1$ animals were removed using a vacuum pump. $F_2$ animals were grown to L4 stage, at which point they were screened under a fluorescent microscope for the desired phenotype of visibly altered *hsp-70* reporter fluorescence. Individuals appearing to have a phenotype of interest were isolated on 35 mm plates and allowed to self-fertilise, and their progeny were monitored over two generations to confirm that the phenotype was homozygous and did not result in sterility. Isolates identified by this method were designated 'Mutant' strains.

### 5.2.3 Sample preparation for genomic DNA (gDNA) extraction

To facilitate one-step mapping as described in **Section 5.2.1**, each strain was first crossed to the CB4856 alternative wild-type strain. The strains crossed to CB4856 were N2 (Bristol), *hsp-90*$^{control}$, *hsp-90*$^{int}$ hp-RNAi, and EMS-generated Mutant isolates 1-6. Each mapping cross to CB4856 was combined with sample collection for gDNA extraction as shown in **Figure 5.2**. At the $F_2$ stage of such a cross, 50 $F_2$ progeny with the correct phenotype were isolated on 60mm NGM plates and allowed to self-fertilise. When these plates were full, but with some bacterial food source still available, the populations of all 50 plates were recombined into a single 50mL Falcon tube by washing plates with M9 buffer. Worms were pelleted by low-speed centrifugation and the pellet washed three times with M9 buffer, and the tube was then incubated at 20°C for 2 hours on a rotator to ensure no bacteria remained in the intestine. Worms were again pelleted by low-speed centrifugation and the pellet washed three times with M9 buffer, before the removal of as much liquid as possible without disturbing the pellet. The pellet was then frozen at -80°C.

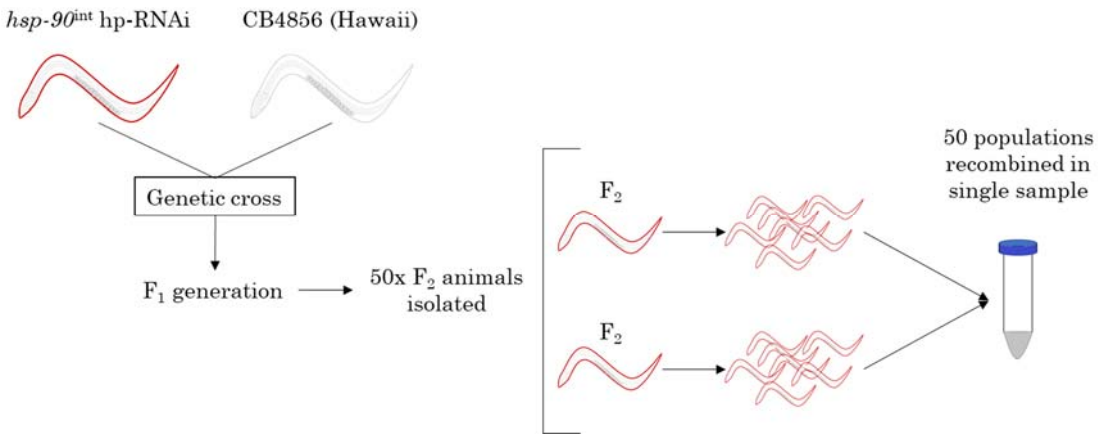


**Figure 5.2 Combining a mapping cross to CB4856 with sample collection for gDNA extraction**. The original *hsp-90*$^{int}$ hp-RNAi strain is shown here as an example.

### 5.2.4 gDNA extraction

Genomic DNA was extracted from these pellets using a Gentra PureGene Tissue Kit. Firstly, the pellet was thawed and 3 mL Cell Lysis Solution (anionic detergent with a DNA stabiliser) added along with 15 µL of 20 mg/mL proteinase K. The sample was incubated at 55°C for 3 hours to facilitate tissue lysis, then cooled to room temperature. To remove RNA, 15 µL RNase A was added and the sample incubated at 37°C for 1 hour, following which the sample was cooled on ice and 1 mL Protein Precipitation Solution added to facilitate salt precipitation. The sample was vortexed vigorously and cooled on ice for 5 minutes, before centrifugation at 2000xg for 10 minutes and removal of the supernatant to a new tube. To precipitate DNA, 3 mL isopropanol and 3 µL of the co-precipitant Pellet Paint (Merck Millipore) were added, and the sample mixed gently by inversion before incubation at -20°C for 1 hour. The sample was then centrifuged for 3 minutes at 2000xg to pellet the DNA and the supernatant was discarded. The DNA pellet was washed ten times with 3 mL of 70% ethanol and then air-dried for at least two hours until completely dry. 150 µL of DNA Hydration Solution (containing EDTA and Tris chloride) was added and the sample mixed by pipetting, followed by 1 hour incubation at 65°C. DNA concentration and absorbance ratios were measured using a Thermo Scientific NanoDrop One. Prior to shipment, gDNA samples were analysed to confirm that they were of sufficiently high concentration and purity for whole-genome sequencing. Quality control data is given below in **Table 5.1**. gDNA samples were stored at -20°C.

| Strain | [DNA] (ng/µl) | Abs. 260/280 |
|---|---|---|
| PVH73 (CB4856 x N2) | 69.5 | 1.82 |
| PVH67 (CB4856 x *hsp-90*$^{control}$) | 71.7 | 1.78 |
| PVH112 (CB4856 x *hsp-90*$^{int}$ hp-RNAi) | 115.6 | 1.77 |
| PVH119 (CB4856 x Mutant 1) | 129.1 | 1.83 |
| PVH120 (CB4856 x Mutant 2) | 276.7 | 1.85 |
| PVH121 (CB4856 x Mutant 3) | 171.4 | 1.82 |
| PVH122 (CB4856 x Mutant 4) | 312.9 | 1.85 |
| PVH123 (CB4856 x Mutant 5) | 28.6 | 1.82 |
| PVH124 (CB4856 x Mutant 6) | 289.5 | 1.84 |

**Table 5.1 Quality control data of gDNA samples used for whole-genome sequencing**. DNA concentration and absorbance (Abs.) ratios were determined using a Thermo Scientific NanoDrop spectrophotometer.

### 5.2.5 Whole-genome sequencing and data analysis performed by Novogene (Hong Kong)

gDNA samples were shipped on dry ice to Novogene (Hong Kong), who performed whole-genome sequencing and data analysis as described below and summarised in **Figure 5.3**. All work described in **Section 5.2.5** was performed by Novogene unless otherwise specified.

A DNA sequencing library was prepared using a NEBNext DNA Library Prep Kit (NEB, USA) in a similar process to that described in **Section 4.2.2.1**. DNA samples were fragmented, size selected for ~350bp fragments, and the ends repaired with 5'-phosphorylation and 3'-adenylation. NEBNext Adaptors (NEB) were ligated to fragment ends followed by PCR amplification. The resulting library was sequenced on an Illumina Hi-Seq platform using paired-end sequencing with 150bp reads.

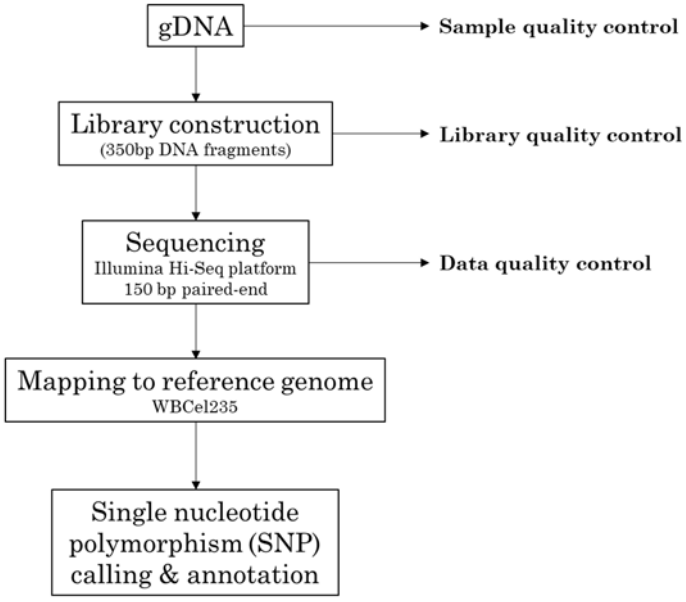


**Figure 5.3 Summary of Novogene whole-genome sequencing workflow**.

#### 5.2.5.1 Quality control of whole-genome sequencing data

Transformation of sequencing data to sequence reads was performed by base calling with CASAVA software. The resulting sequences and quality control data were stored in FASTQ files. Quality control on sequencing data was then performed to determine the distribution of sequencing quality, error rate, and read quality. Reads

were discarded if they contained Adaptor sequences, if they contained >10% unidentified nucleotides, or if they contained >50% low-quality nucleotides. Quality control data on reads from whole-genome sequencing is provided below in **Table 5.2**. This shows that for each strain sequenced, over 99.8% of data generated were classed as clean reads; over 95% of data had a Phred quality score of at least 20 (Q20) indicating at least 99% accuracy; and over 89% of data had a Phred quality score of at least 30 (Q30) indicating at least 99.9% accuracy.

Clean sequencing reads were mapped to the WBCel235 version of the *C. elegans* genome using BWA software (*v0.7.12-r1039*), and duplicate paired reads were removed using SAMtools software (*v0.1.19-44428cd*). **Table 5.3** shows the mapping coverage in each strain. Across strains, at least 98% of bases had a coverage of at least 4X, and the average depth of genome coverage was at least 27X. As an average depth of coverage of 30X is sufficient for whole-genome sequencing of a human genome (Bentley et al. 2008), which is approximately 30 times larger than the *C. elegans* genome (>3 billion base pairs compared to ~100 million), this was considered to be acceptable coverage.

| Strain | Raw reads | Raw data | Clean data | | Error rate | Q20 | Q30 | GC content |
|---|---|---|---|---|---|---|---|---|
| | (#) | (GB) | (GB) | (%) | (%) | (%) | (%) | (%) |
| PVH73 | 15097845 | 4.5 | 4.5 | 99.87 | 0.01 | 96.61 | 92.21 | 38.77 |
| PVH67 | 15424388 | 4.6 | 4.6 | 99.88 | 0.01 | 96.47 | 91.94 | 38.94 |
| PVH112 | 14414686 | 4.3 | 4.3 | 99.84 | 0.01 | 96.54 | 92.09 | 38.35 |
| PVH119 | 15331944 | 4.6 | 4.6 | 99.84 | 0.02 | 95.09 | 89.67 | 36.75 |
| PVH120 | 12360514 | 3.7 | 3.7 | 99.89 | 0.01 | 96.39 | 91.84 | 36.5 |
| PVH121 | 13384351 | 4 | 4 | 99.88 | 0.01 | 96.56 | 92.07 | 38.08 |
| PVH122 | 11939472 | 3.6 | 3.6 | 99.88 | 0.01 | 96.58 | 92.21 | 36.34 |
| PVH123 | 15938461 | 4.8 | 4.8 | 99.87 | 0.01 | 96.59 | 92.22 | 37.52 |
| PVH124 | 14539444 | 4.4 | 4.4 | 99.83 | 0.02 | 95.2 | 89.69 | 36.68 |

**Table 5.2 Quality control data for whole-genome sequencing reads**. Error: Percentage error rate. GC: Percentage GC content. Q20/Q30: Percentage of data meeting Phred score thresholds for sequence quality.

| Strain | Mapped reads (%) | Average depth (X) | Coverage >= 1X (%) | Coverage >= 4X (%) |
|---|---|---|---|---|
| PVH73 | 95.24 | 34.44 | 99.84 | 98.45 |
| PVH67 | 91.87 | 34.26 | 99.87 | 98.69 |
| PVH112 | 96.87 | 33.91 | 99.81 | 98.07 |
| PVH119 | 97.37 | 35.76 | 99.92 | 99.33 |
| PVH120 | 97.67 | 29.14 | 99.98 | 99.93 |
| PVH121 | 94.62 | 30.47 | 99.89 | 98.95 |
| PVH122 | 97.81 | 27.98 | 99.98 | 99.93 |
| PVH123 | 95.72 | 36.17 | 99.86 | 98.95 |
| PVH124 | 96.08 | 33.5 | 99.98 | 99.95 |

**Table 5.3 Mapping data for whole-genome sequencing reads**. Showing the percentage of reads for each strain which could be mapped to the reference genome, the average depth of coverage across each base in the reference genome, and the percentage of reads with at least 1X or at least 4X coverage.

#### 5.2.5.2 SNP detection and annotation

Each sequenced genome was compared to the N2 reference genome (*v. WBcel235*) in order to identify the frequency and nature of single nucleotide polymorphisms (SNPs). Detection of SNPs was performed using GATK software (*v3.8*). Annotation of transcripts in which each SNP occurred was performed with ANNOVAR software (*v2015Mar22*). **Table 5.4** shows the total number of SNPs identified in each strain.

| Strain | SNPs |
|---|---|
| PVH73 | 150958 |
| PVH67 | 195325 |
| PVH112 | 3263 |
| PVH119 | 224370 |
| PVH120 | 220058 |
| PVH121 | 220508 |
| PVH122 | 223296 |
| PVH123 | 82237 |
| PVH124 | 99113 |

**Table 5.4 Total number of SNPs identified compared to the N2 reference genome**.

### 5.2.6 Determination of CB4856 SNP density using CloudMap

To determine which SNPs might be causal for the phenotype of interest, it was necessary to calculate the ratio of N2-derived to CB4856-derived alleles (CB4856:N2 ratio) at each known SNP using data from WGS. This was performed using the 'CloudMap Hawaiian Variant Mapping with WGS and Variant Calling workflow (no candidate genes)' pipeline (Minevich et al. 2012), which is publicly available on the Galaxy data analysis platform. The workflow was followed according to the user guide available in the CloudMap data library. Using WGS data from the pooled progeny of a single cross between an N2-derived strain and the CB4856 strain, the pipeline first performs variant calling to identify all SNPs compared to a reference N2 genome. It then calculates the CB4856:N2 ratio at the positions of each identified SNP, and returns this as a data file. By this method, lists of all SNPs in each sequenced strain and their corresponding CB4856:N2 ratios were obtained.

Before considering the obtained CB4856:N2 ratios, the lists of strain-specific SNPs were further compared and refined. SNPs which were present in any of the three control strains (PVH73, PVH67 or PVH112) were discounted as potentially causal. Similarly, as the Mutant strains represented two opposing phenotypes (Phenotype 1, displaying decreased reporter expression; and Phenotype 2, displaying increased expression), any SNP which was present in one or more strains from both phenotypes was also discounted. This generated two lists of 'phenotype-specific' SNPs; that is, SNPs which occurred only within a Mutant strain or strains of a single phenotype. However, even after discounting SNPs present in control strains or in both phenotypes, there still remained a large number of phenotype-specific SNPs. **Figure 5.4** shows the number of SNPs which occurred in a phenotype-specific manner, and whether they were present in multiple Mutant strains of that phenotype. In Mutant strains 1-4, which displayed Phenotype 1, over 13000 individual phenotype-specific SNPs were detected (**Fig. 5.4a**). In contrast, only 718 individual phenotype-specific SNPs were detected in Mutant strains 5-6, which displayed Phenotype 2 (**Fig. 5.4b**).

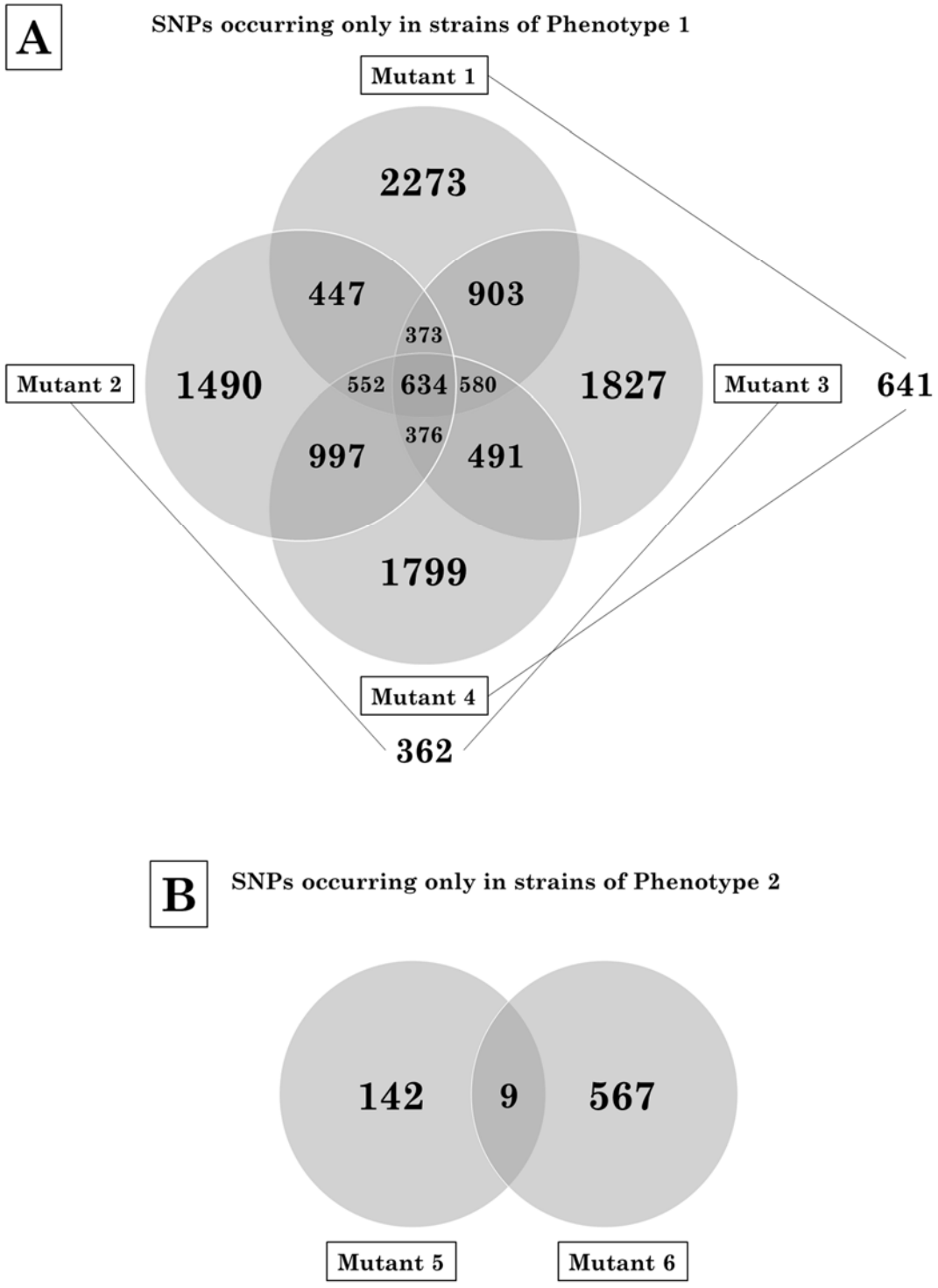


**Figure 5.4 Numbers of phenotype-specific SNPs and their overlap between strains**. SNPs were identified with the CloudMap pipeline followed by list refinement. (**A**) SNPs which occurred only in Mutant strains 1-4 of Phenotype 1, which display decreased *hsp-70* reporter expression. Lines connecting Mutants 1/4 and Mutants 2/3 indicate the number of SNPs identified in only that pair of strains. (**B**) SNPs which occurred only in Mutant strains 5-6 of Phenotype 2, which display increased *hsp-70* reporter expression.

### 5.2.7 Repetition of analysis due to outdated reference genome in CloudMap pipeline

Analysis was initially performed using the N2 reference genome provided for the CloudMap workflow in Galaxy. However, it was subsequently found that this reference genome was from WormBase version WS220, which dates from 2010 and has since been updated. The analysis was therefore repeated using the updated reference genome, from WormBase version WS266 (the WBcel235 reference genome). The analysis using version WS266 identified many more SNPs than that using version WS220, but not all SNPs identified using version WS220 were also identified using version WS266. It was therefore decided to take forward all SNPs obtained using either version, but that any SNPs which had not also been identified in Novogene's variant detection were to be excluded. This left a total of 385 SNPs from analysis using version WS220, and 13745 from version WS266 (**Fig. 5.5**). The 54 SNPs identified by analysis with version WS220 but not version WS266 might represent genomic positions where the identity of the nucleotide has been updated in the more recent WS266 version, and so no longer differs from the nucleotide identified at the same position in the sample genomes. It is therefore possible that they may have been misidentified as SNPs; however as they represented a relatively small number it was decided not to discard them as potential SNPs of interest.

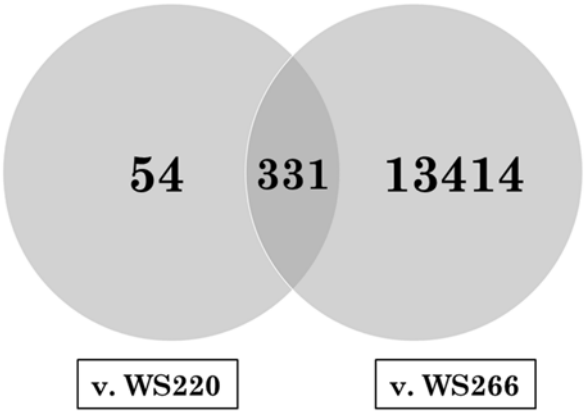


**Figure 5.5 Total number of phenotype-specific SNPs identified through CloudMap analysis**. Number and overlap of phenotype-specific SNPs detected in all Mutant strains through CloudMap analysis, using either reference genome version WS220 or version WS266.

## 5.3 Results

### 5.3.1 Identification of 6 Mutant isolates with two phenotypes of interest

Second-generation progeny of mutagenised animals were screened at L4 stage for a phenotype of visibly altered *hsp-70p::mCherry* reporter expression. This approach yielded six mutant isolates with visibly altered *hsp-70p::mCherry* reporter fluorescence, termed Mutants 1-6, which fall into two phenotypes (**Fig. 5.6**). Decreased *hsp-70* reporter fluorescence in Mutants 1-4 was denoted as 'Phenotype 1' (**Fig. 5.6a**), whilst increased fluorescence in Mutants 5 and 6 was denoted 'Phenotype 2' (**Fig. 5.6b**). Although initial statistical analysis using Student's t test identified Mutant strains 2 and 5 as having significantly altered reporter intensity, subsequent re-analysis using one-way ANOVA revealed that this is not the case after correction for multiple testing. However, as these strains also demonstrate the expected alterations in expression of *hsp-70* and *mCherry* transcripts (**Fig. 5.7a-b**), they were retained for further investigation.

As altered expression of the *hsp-70* reporter could have been caused by a mutation in the reporter construct, with actual *hsp-70* transcript expression unaffected, whole-organism transcript levels of both *hsp-70* and *mCherry* in each Mutant strain were quantified by qRT-PCR (**Fig. 5.7**). This showed that in Mutants 1-4, *hsp-70* expression is reduced by at least 50% compared to the original *hsp-90*$^{int}$ hp-RNAi strain, and is expressed at levels comparable to that of the *hsp-90*$^{control}$ strain (**Fig. 5.7a**). Organismal *mCherry* transcripts are also reduced in these strains by approximately 40% compared to the original *hsp-90*$^{int}$ hp-RNAi strain (**Fig. 5.7b**). In contrast, organismal *hsp-70* expression is more than doubled in Mutants 5 and 6 compared to the original *hsp-90*$^{int}$ hp-RNAi strain (**Fig. 5.7a**), with *mCherry* expression also significantly increased (**Fig. 5.7b**). This indicates that altered *hsp-70* reporter expression in Mutant strains 1-6 is a reflection of altered *hsp-70* transcript expression, and not due to a mutation in the reporter construct.

Whilst expression of the *hsp-70* reporter and organismal *hsp-70* transcripts is significantly reduced in Mutants 1-4, it is not completely abolished (**Figs. 5.6, 5.7a**). As the reporter is still expressed, this indicates that TCS is still activated in these strains, although to a lesser extent. This could suggest that the causative mutation

has occurred in a gene which acts as an enhancer of TCS, rather than being absolutely required. Alternatively, the causative mutation may have caused gain-of-function in a gene which acts to suppress *hsp-70* expression.

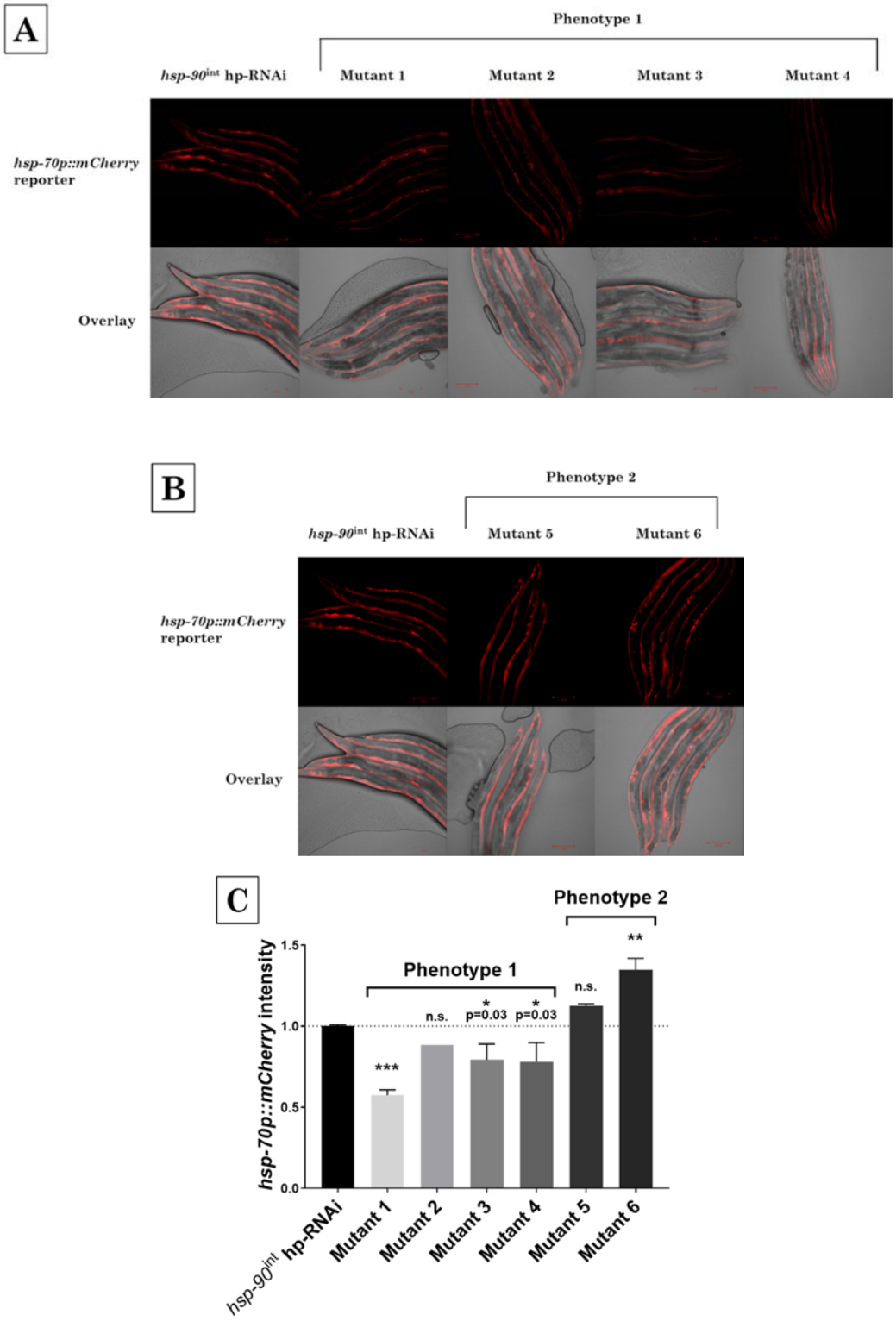


**Figure 5.6 *hsp-70* reporter fluorescence in EMS-generated Mutant strains**. Representative 20x images of Mutant strains with the *hsp-90*$^{int}$ hp-RNAi strain for comparison. Scale bars: 100nm. (**A**) Mutants 1-4 display reduced fluorescence (Phenotype 1). (**B**) Mutants 5 and 6 display increased fluorescence (Phenotype 2). (**C**) Quantification of reporter fluorescence intensity normalised by *hsp-90*$^{int}$ hp-RNAi values. Significance compared to *hsp-90*$^{int}$ hp-RNAi was determined by one-way ANOVA with multiple comparisons; error bars represent SEM. * = p<0.05; ** = p<0.01; *** = p<0.001; **** = p<0.0001.

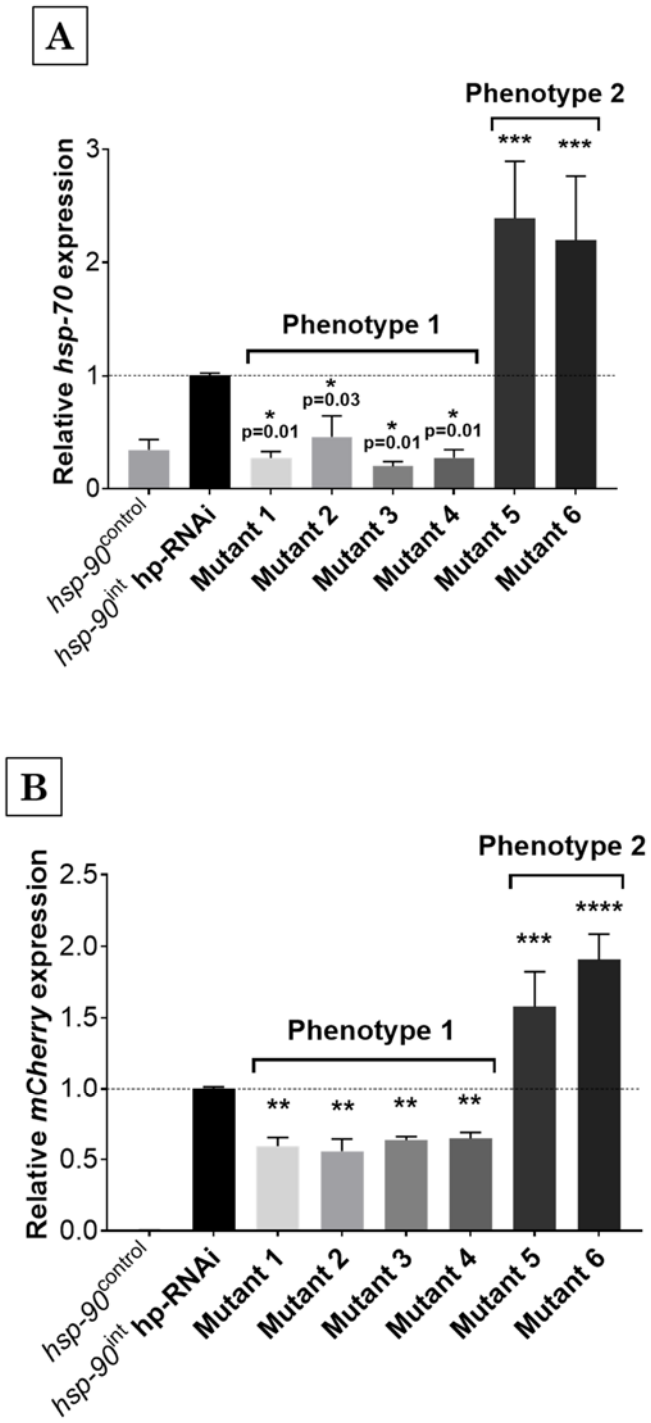


**Figure 5.7 Organismal *hsp-70* and *mCherry* transcript expression in Mutant strains**. Whole-organism transcript levels of (**A**) *hsp-70* and (**B**) *mCherry* in Mutants 1-6 and the *hsp-90*$^{control}$ and *hsp-90*$^{int}$ hp-RNAi strains. *cdc-42* and *hsp-90*$^{int}$ hp-RNAi were the control gene and strain used for normalisation. Mean expression values were compared to that of *hsp-90*$^{int}$ hp-RNAi by one-way ANOVA with multiple comparisons; error bars represent SEM. ** = $p<0.01$; *** = $p<0.001$; **** = $p<0.0001$.

### 5.3.2 Phenotypes were not caused by mutation of the *hsp-70* gene

A possible explanation for altered expression of the *hsp-70* reporter, as well as organismal *hsp-70* and *mCherry* transcripts, could have been that a mutation had occurred in the *hsp-70* gene which acted to suppress its expression. However, variant detection and annotation by Novogene did not identify any SNPs in any sequenced strain which occurred either in the *hsp-70* gene or in its promoter region. This confirms that altered reporter expression is not due to a loss-of-function mutation in the *hsp-70* gene or its promoter.

### 5.3.3 Identification of potential causal SNPs and affected genes

All phenotype-specific SNPs identified as described in **Sections 5.2.6 & 5.2.7** were ranked by their CB4856:N2 ratio. As described in **Section 5.2.1** a ratio of 0 would suggest that that SNP was required, and therefore likely causal, for the phenotype of interest. Amongst the 13,799 phenotype-specific SNPs ranked, the lowest CB4856:N2 ratio was 0.139, suggesting that no single SNP was causal for each phenotype of interest. This is not necessarily surprising, as mutagenesis introduced many SNPs throughout the genome of each strain, and each SNP which affected a gene involved in TCS had the potential to cause a gain or loss of function. Each strain is therefore likely to contain multiple SNPs in genes relevant to TCS, the effects of which combined to result in an aggregate phenotype. It was therefore necessary to select those SNPs which were most likely to be relevant, and to identify which transcripts they would affect.

As no SNP had a CB4856:N2 ratio of 0, those with the lowest CB4856:N2 ratios were considered instead. Since CloudMap analysis had been performed twice, using two different versions of the reference genome, two different threshold criteria were used. SNPs were taken forward if they had either a CB4856:N2 ratio below 0.2 according to either individual analysis; or a ratio below 0.25 according to both analyses. In total, 49 SNPs met these criteria: 45 in Phenotype 1, and 4 in Phenotype 2 (**Table 5.5**). The 42 genes predicted to be affected by each of these SNPs were identified using annotation performed by Novogene, and are listed in **Table 5.6** with any known functions.

| LG | Position | CB4856:N2 | Analysis | Gene | Location | M. |
|---|---|---|---|---|---|---|
| V | 265899 | 0.139 | WS220 | *nhr-204* | intergenic | 3 |
| II | 5638240 | 0.148 | WS266 | *F59E12.3* | upstream | 1 |
| I | 3115766 | 0.162 | WS266 | *C45E1.4* | intronic | 3 |
| II | 14986715 | 0.162 | WS266 | *Y53F4B.6* | exonic | 3 |
| I | 2773051 | 0.162 | WS266 | *sop-3* | intronic | 3 |
| I | 2773053 | 0.162 | Both | *sop-3* | intronic | 3 |
| I | 2886766 | 0.163 | WS266 | *arx-1* | intronic | 1 |
| IV | 11251604 | 0.167 | WS266 | *gtl-1* | intronic | 6 |
| V | 4604780 | 0.171 | WS266 | *Y61A9LA.11* | downstream | 2 |
| III | 10514651 | 0.175 | WS266 | *sly-1* | intronic | 3 |
| V | 20362837 | 0.177 | WS266 | *K02E2.9* | exonic | 1 |
| V | 17197315 | 0.177 | WS266 | *Y68A4A.5* | intronic | 3 |
| I | 13867553 | 0.182 | WS266 | *taf-1* | intronic | 3 |
| IV | 8981120 | 0.186 | WS266 | *C53B4.4* | exonic | 3 |
| I | 1630320 | 0.187 | WS266 | *Y73E7A.1* | intronic | 1, 3 |
| II | 416484 | 0.188 | Both | *C24H12.4* | exonic | 1 |
| IV | 1997829 | 0.189 | WS266 | *xpc-1* | intronic | 3 |
| I | 892612 | 0.190 | WS266 | *him-19* | exonic | 2, 3 |
| V | 265686 | 0.191 | WS266 | *nhr-204* | intergenic | 5 |
| II | 15240241 | 0.191 | WS266 | *Y46E12BL.2* | exonic | 3 |
| II | 5580224 | 0.192 | WS266 | *T25E4.2* | exonic | 1, 4 |
| I | 2563059 | 0.192 | WS266 | *ssp-19* | downstream | 3 |
| V | 20507856 | 0.194 | WS266 | *dct-10* | intronic | 6 |
| II | 6879237 | 0.200 | WS266 | *C44B7.7* | 3'-UTR | 4 |
| I | 2562717 | 0.200 | WS266 | *ssp-19* | exonic | 1 |
| V | 6040440 | 0.200 | WS266 | *F29G9.1* | 3'-UTR | 3 |
| IV | 14428193 | 0.200 | WS266 | *F55B11.5* | exonic | 3 |
| IV | 1513493 | 0.200 | WS266 | *K03H6.2* | intronic | 5 |
| V | 18960946 | 0.200 | WS266 | *ztf-20* | intergenic | 1 |
| IV | 15195137 | 0.200 | WS266 | *Y40H7A.15* | exonic | 1 |
| II | 13372252 | 0.200 | Both | *Y48C3A.20* | intronic | 1 |
| IV | 1180500 | 0.208 | Both | *Y104H12D.2* | intronic | 3, 4 |
| II | 510660 | 0.208 | Both | *mab-9* | intergenic | 1 |
| II | 510660 | 0.208 | Both | *srh-105* | intergenic | 1 |
| II | 416454 | 0.210 | Both | *C24H12.4* | exonic | 1, 3 |
| I | 67537 | 0.214 | Both | *csk-1* | intergenic | 3 |
| I | 67546 | 0.214 | Both | *csk-1* | intergenic | 3 |
| I | 67537 | 0.214 | Both | *Y48G1C.5* | intergenic | 3 |
| I | 67546 | 0.214 | Both | *Y48G1C.5* | intergenic | 3 |
| X | 197312 | 0.217 | Both | *T08D2.8* | intronic | 3 |
| X | 21131 | 0.219 | Both | *Y35H6.3* | intronic | 2 |
| IV | 2231205 | 0.227 | Both | *T04C4.1* | intronic | 1 |

| | | | | | | |
|---|---|---|---|---|---|---|
| II | 107742 | 0.231 | Both | *C50D2.3* | downstream | 3 |
| IV | 2815036 | 0.231 | Both | *Y54G2A.13* | exonic | 1 |
| I | 254848 | 0.238 | Both | *Y48G1BR.1* | intronic | 1 |
| I | 62253 | 0.238 | Both | *Y48G1C.5* | intronic | 4 |
| I | 36775 | 0.247 | Both | *Y74C9A.1* | intergenic | 1, 3 |
| I | 36775 | 0.247 | Both | *sesn-1* | intergenic | 1, 3 |
| I | 159472 | 0.250 | Both | *ptr-11* | downstream | 1 |

**Table 5.5 36 SNPs with low CB4856:N2 ratios and associated genes**. LG, Position: Chromosome and position of SNP. Analysis: Reference genome version with which the SNP was identified. Gene: Predicted in SNP annotation performed by Novogene. Location: Region of gene in which the SNP occurred. M.: Mutant strain in which the SNP occurred. 3'-UTR: 3' untranslated region. Upstream/downstream: indicates the SNP occurred within 1 kilobase of the gene's transcriptional start/end site.

| Gene | Known function |
|---|---|
| *arx-1* | Involved in actin nucleation |
| *gtl-1* | Involved in defecation |
| *xpc-1* | Involved in DNA damage recognition and repair |
| *taf-1* | Involved in embro development |
| *him-19* | Involved in meiotic DNA double-strand break formation |
| *ptr-11* | Involved in molting cycle |
| *sly-1* | Sec1-like protein |
| *ssp-19* | Sperm-specific protein |
| *sop-3* | Suppressor of pal-1 |
| *csk-1* | Tyrosine kinase |
| *Y73E7A.1* | Predicted coiled-coil domain protein |
| *T04C4.1* | Predicted folliculin-interacting protein |
| *C44B7.7* | Predicted gamma-glutamylcyclotransferase |
| *srh-105* | Predicted GPCR |
| *K03H6.2* | Predicted hydrolase |
| *C53B4.4* | Predicted lipid binding activity |
| *sesn-1* | Predicted oxidoreductase |
| *Y48C3A.20* | Predicted pseudouridine synthase |
| *F59E12.3* | Predicted Ser/Thr kinase |
| *mab-9* | Predicted transcription factor |
| *nhr-204* | Predicted transcription factor |
| *ztf-20* | Predicted transcription factor |
| *Y48G1C.5* | Predicted Tyr phosphatase |
| *T08D2.8* | Orthologue of cytoskeletal-associated protein |
| *C24H12.4* | Orthologue of DEAD-box helicase |
| *Y46E12BL.2* | Orthologue of rRNA-processing protein |
| *C45E1.4* | Affected by daf-16 |
| *T25E4.2* | Affected by daf-16 |
| *Y54G2A.13* | Affected by daf-2 |
| *Y61A9LA.11* | Affected by daf-2 |
| *Y74C9A.1* | Affected by daf-2 |
| *F29G9.1* | Affected by daf-2 and daf-16 |
| *Y48G1BR.1* | Affected by daf-2 and daf-16 |
| *C50D2.3* | Affected by daf-2 and hsf-1 |
| *F55B11.5* | Affected by hsf-1 |
| *Y104H12D.2* | Affected by hsf-1 |
| *dct-10* | Pseudogene |
| *K02E2.9* | Pseudogene |
| *Y35H6.3* | Pseudogene |
| *Y40H7A.15* | Pseudogene |
| *Y53F4B.6* | Pseudogene |
| *Y68A4A.5* | Pseudogene |

**Table 5.6 Known functions of genes associated with SNPs in Table 5.5**. Genes are listed along with known functions (WormBase; Harris et al. 2010).

## 5.4 Discussion

Forward genetic screening in the *hsp-90*$^{int}$ hp-RNAi strain identified six Mutant isolates with a phenotype of interest. Mutants 1-4 display Phenotype 1, which was classed as decreased expression of the *hsp-70* reporter as well as organismal *hsp-70* and *mCherry* transcripts (**Figs. 5.6a, 5.7**). Conversely, Mutants 5 and 6 display Phenotype 2, which was classed as increased expression of the *hsp-70* reporter as well as organismal *hsp-70* and *mCherry* transcripts (**Figs. 5.6b, 5.7**). Although a specific causal SNP was not identified in these strains, 49 SNPs were found to have very low CB4856:N2 ratios (**Table 5.5**). This indicates that they occurred in genomic locations which are be linked to the phenotype of interest, as a low CB4856:N2 ratio indicates that N2-derived mutant alleles were only rarely excluded during recombination in the mapping cross. This would suggest that retention of the N2 allele containing an EMS-induced SNP was important for the phenotype.

SNP annotation performed by Novogene identified the transcripts predicted to be affected by each SNP, showing that the 49 SNPs listed in **Table 5.5** are predicted to affect 42 genes (**Table 5.6**). GO term analysis amongst these genes did not identify any significantly enriched terms, indicating that mutations which affected *hsp-70* reporter expression did not all occur in genes related to a single process. This suggests that TCS may be regulated by inputs from multiple different signalling pathways. The gene predicted to be affected by the SNP with the lowest CB4856:N2 ratio was the nuclear hormone receptor *nhr-204*, which contained an intergenic SNP in Mutant 3. Interestingly, *nhr-204* was identified as also being potentially affected by another SNP with a low allele ratio, but in a Mutant strain of the opposite phenotype (**Table 5.5**). These SNPs in Mutant strains of opposing phenotypes may represent mutations in *nhr-204* which have opposing effects on gene function. As nuclear hormone receptors are transcription factors often activated by lipid-based ligands (Chawla et al. 2001), involvement of *nhr-204* could indicate the involvement of lipid signalling in TCS. Several other genes in **Table 5.6** were also predicted to be regulated by more than one identified SNP: *csk-1*, *sop-3*, *ssp-19*, *C24H12.4, and Y48G1C.5*. *csk-1* encodes a tyrosine kinase and *Y48G1C.5* a tyrosine phosphatase. The proteins encoded by these two genes could potentially even both regulate the same protein, possibly in a signalling pathway which utilises tyrosine phospho-modification.

Identifying genes through SNPs potentially causal for a phenotype of altered *hsp-70* reporter expression was particularly useful because the genes in question would not otherwise have been considered. However, identification of genes by this method does not prove involvement in TCS, and further experimental validation of each gene was required. To determine whether each gene is required for reporter expression, a tissue-specific RNAi-mediated gene knockdown approach was utilised. This process is described in **Chapter 6**.

# Chapter 6. Identification of tissue-specific genetic modulators of TCS in the *hsp-90*$^{int}$ hp-RNAi strain

## 6.1 Introduction

### 6.1.1 Rationale

Transcriptomic profiling of the *hsp-90*$^{int}$ hp-RNAi and *hsp-90*$^{neu}$ hp-RNAi strains identified 17 genes upregulated in both strains compared to controls (**Fig. 4.13, Table 4.8**). In addition, forward genetic screening combined with one-step mapping and sequencing in the *hsp-90*$^{int}$ hp-RNAi strain identified 42 genes potentially linked to *hsp-70* reporter expression (**Tables 5.5, 5.6**). To confirm whether each of these identified candidate genes has a role in TCS, the effect of gene knockdown on *hsp-70* reporter expression was determined by RNAi feeding in the *hsp-90*$^{int}$ hp-RNAi strain. To further investigate whether each gene acts in the 'sending' or 'receiving' tissue of this strain, which carries a loss-of-function mutation in the dsRNA transporter *sid-1*, functional SID-1 was re-introduced under the control of an intestine- or body wall muscle-specific promoter. This enabled tissue-specific targeting of RNAi to determine in which tissue each candidate gene might act (**Fig. 6.1**). Genes which were identified through tissue-specific RNAi screening to be tissue-specific modulators of *hsp-70* reporter expression in the *hsp-90*$^{int}$ hp-RNAi strain were denoted TCS cross (X)-Tissue (*txt*) genes.

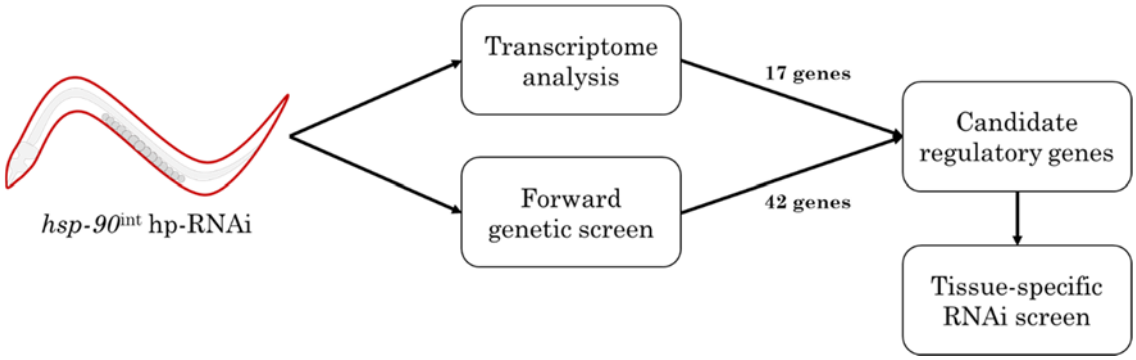


**Figure 6.1 Process to identify TCS cross (X)-Tissue (*txt*) genes**. Genes identified as candidates were screened using tissue-specific RNAi in the *hsp-90*$^{int}$ hp-RNAi strain.

### 6.1.2 Expansion of screening to include other genes from relevant signalling pathways

RNAi screening presented a valuable opportunity to identify whether a large number of candidate genes have a role in TCS, and if so in which tissue. As other genes have previously been implicated in cell-non-autonomous stress signalling or related pathways, the screen was expanded to encompass such genes, which could potentially reveal interactions between TCS and other key cell-non-autonomous signalling mechanisms. The list of all genes screened using tissue-specific RNAi in the *hsp-90*$^{int}$ hp-RNAi strain is given in **Appendix 2**.

#### 6.1.2.1 Genes previously associated with TCS

Four key genes have previously been shown to be involved in TCS: *pha-4*, *pqm-1*, *asp-12*, and *clec-41* (van Oosten-Hawle et al. 2013; O'Brien et al. 2018). In particular, *pha-4* has previously been shown to be required for *hsp-70p::mCherry* reporter upregulation in animals with tissue-specific *hsp-90* knockdown (van Oosten-Hawle et al. 2013). This identified that systemic knockdown of *pha-4* after L1 stage results in significantly decreased reporter expression in adults. *pqm-1*, *clec-41* and *asp-12* have been shown to be required for TCS activated by tissue-specific HSP-90 overexpression, in a tissue-specific manner (O'Brien et al. 2018). TCS activated by pan-neuronal HSP-90 overexpression involves signalling through neuronal *pqm-1* and *clec-41*, whilst TCS activated by intestine-specific HSP-90 overexpression involves *pqm-1* and *asp-12* (O'Brien et al. 2018). These genes were therefore included in screening to determine whether they are also required during TCS activated by tissue-specific *hsp-90* knockdown.

#### 6.1.2.2 Neuronal signalling genes which regulate cell-non-autonomous stress responses

Signalling from neurons has been shown to regulate several cell-non-autonomous stress responses. During heat stress, the genes *gcy-8* and *ttx-3* act in the AFD and AIY thermosensory circuit neurons to promote activation of the organismal HSR (Prahlad et al. 2008). This mechanism involves *tph-1*-mediated serotonin synthesis, signalling involving the DCV protein *unc-31*, and the serotonin receptor *ser-1* (Tatum et al. 2015; Prahlad & Morimoto 2011; Speese et al. 2007). Serotonergic signalling

has also been shown to regulate the organismal $UPR^{Mt}$ (Berendzen et al. 2016); whilst the $UPR^{ER}$ can be regulated cell-non-autonomously by octopaminergic signalling through the neuronal GPCR *octr-1* (Sun et al. 2011, 2012(a)). To determine whether they are also involved during cell-non-autonomous signalling in TCS, the six genes mentioned above were included in the RNAi screen. *unc-13*, which is required for synaptic vesicle fusion (Richmond et al. 1999), was also screened.

#### 6.1.2.3 Modulators of organismal proteostasis and longevity

Several other genes have been shown to act in mechanisms which regulate or interact with those of organismal stress signalling. The transcription factor *daf-16*, which is repressed by cell-non-autonomous ILS signalling, activates expression of genes promoting immune and stress resistance (Ailion et al. 1999; Wolkow et al. 2000; Murphy et al. 2003). *daf-16* acts alongside *hsf-1* in the regulation of longevity and is implicated in improved proteostasis (Morley et al. 2002; Hsu et al. 2003; Cohen et al. 2006); the transcription factor *skn-1* is also directly inhibited by ILS in parallel with *daf-16*, and contributes to ILS-mediated longevity (Tullet et al. 2008). Mutations in the genes *glp-1* and *eat-2* results in germline loss or dietary restriction respectively (Austin & Kimble 1987; Lakowski & Hekimi 1998), representing reproductive or caloric 'stressors'. Despite the differences in these stressors, both result in lifespan extension and increased proteasome activity (Lakowski & Hekimi 1998; Vilchez et al. 2012). As the signalling mechanisms involved in TCS are currently unclear, these genes were included in RNAi screening to determine whether the pathways they function in interact with those of TCS.

#### 6.1.2.4 Genes identified using protein functional association networks

As screening progressively confirmed various candidate genes as *txt* genes, protein interaction networks were generated using the GeneMania tool (Warde-Farley et al. 2010) to identify whether *txt* genes might share functional associations. This tool identified that other genes, which had not originally been identified as candidates, were nevertheless highly connected in interaction networks. As functional associations with confirmed *txt* genes could indicate a role in TCS, ten genes were included in screening based on being highly connected in protein interaction

networks. These genes were *cnd-1*, *elt-2*, *gad-1*, *hlh-10*, *hlh-2*, *hlh-25*, *lin-32*, *nhr-62*, *par-4* and *ztf-2*. Of these, all except *gad-1*, *hlh-2* and *par-4* were subsequently confirmed as *txt* genes, showing protein interaction networks to be a useful tool in identifying functionally relevant genes. As screening progressed and more candidates were confirmed as *txt* genes, updating of protein interaction networks meant that the connections identified within these networks were also updated. Some genes which were screened based on being highly connected in intermediate-stage protein networks may therefore be less highly connected in the final protein interaction networks, which were generated using lists of all *txt* genes identified by screening.

#### 6.1.2.5 Known interaction partners for a *txt* gene of particular interest

One of the first genes confirmed by RNAi screening as a *txt* gene was the predicted PDZ domain protein *C50D2.3*, which was originally identified as a candidate through forward genetic screening. *C50D2.3* was particularly interesting as it was identified as a *txt* gene acting in both the intestine and body wall muscle, and furthermore was identified as highly connected in protein functional interaction networks of *txt* genes. 10 protein interaction partners of C50D2.3 have previously been identified through yeast 2-hybrid screening (Lenfant et al. 2010). These are BTBD-10, CEH-58, DLAT-1, MCT-6, RACK-1, SWSN-9, TSCT-1, C32D5.1, Y74C10AL.2 and ZK688.9. As interactions between C50D2.3 and these partners was identified as functionally relevant amongst *txt* genes acting in the same manner as C50D2.3 (shown in **Fig. 6.6**), the interaction partners were also screened using tissue-specific RNAi.

#### 6.1.2.6 Genes identified serendipitously

Finally, 11 genes were included in the screen due to a mistake in the identification of RNAi clones. These genes are *col-20*, *gcsh-2*, *nhr-42*, *ran-5*, *C04G6.5*, *C06B8.11*, *F19F10.9*, *F20A1.10*, *F25D1.2*, *M02B1.2*, and *R02C2.6*.

## 6.2 Methods

### 6.2.1 Strains exhibiting tissue-specific RNAi sensitivity

The *hsp-90*$^{int}$ hp-RNAi strain carries a *sid-1* (*pk3321*) mutation which prevents systemic RNAi due to loss of function in the SID-1 dsRNA transporter (Winston et al. 2002; Feinberg & Hunter 2003). To enable tissue-specific RNAi targeting, functional SID-1 was reintroduced to this strain under the control of an intestine- or body wall muscle-specific promoter (*vha-6p* or *myo-3p* respectively). This was achieved by crossing the *hsp-90*$^{int}$ hp-RNAi strain to the PVH5 strain, which carries *myo-3p*::SID-1 in a *sid-1* (*pk3321*) background; or the PVH65 strain, which carries *vha-6p*::SID-1 in a *sid-1* (*pk3321*) background. This resulted in the strains PVH171 and PVH172 (**Table 2.1**), which express SID-1 in the body wall muscle or intestine respectively. This enables the tissue-specific import of ingested RNAi, and so facilitates tissue-specific gene knockdown.

The PVH5 and PVH65 strains (**Table 2.1**) were created by Dr. Patricija van Oosten-Hawle (van Oosten-Hawle et al. 2013). pccIs005 and pccIs004 transgenes, expressing wild-type SID-1 under the control of either the body wall muscle-specific promoter *myo-3* or the intestine-specific promoter *vha-6*, were microinjected into the gonad of NL3321 animals. Transgenes were injected as complex arrays using *myo-2p::mCherry* as a co-injection marker. Genomic integration of extrachromosomal transgene arrays was performed by gamma irradiation.

### 6.2.2 Screening process and data analysis

The RNAi screen was performed using NGM-RNAi plates seeded with bacterial cultures grown from an extended RNAi clone library (Source BioScience; Kamath & Ahringer 2003). For each gene screened, the PVH171 and PVH172 strains were each grown on three replicate NGM-RNAi plates for two generations to ensure that the gene had been effectively knocked down throughout development. Microscope slides were prepared using day 1 adult hermaphrodites and imaged using confocal microscopy. At least three biological replicates of 5 animals each were imaged per RNAi per strain. For each image, the intensity of *hsp-70* reporter fluorescence was measured using ImageJ software, then normalised to the average value for control RNAi (L4440) within the same experiment. Normalised fluorescence intensity values

for each RNAi were pooled, as replicates could not always be performed within the same experiment. The mean *hsp-70* reporter fluorescence intensity of each strain when grown on each RNAi was used as the screen readout, and comparison to control RNAi values was performed by one-way ANOVA with multiple comparisons. Correction for multiple testing was performed using the two-stage linear step-up procedure of Benjamini, Krieger and Yekutieli with a false discovery rate of 0.05.

The biological interpretation of the screen results is summarised in **Figure 6.2**. The process of TCS in the *hsp-90*$^{int}$ hp-RNAi strain can be considered as an intestine-specific stimulus (*hsp-90* knockdown) which activates unknown inter-tissue signalling and leads to a body wall muscle-specific response (*hsp-70* reporter expression). If a gene is knocked down by tissue-specific RNAi in the intestine, and this causes an effect on *hsp-70* reporter expression in the body wall muscle, it can be inferred that the intestinal function of that gene regulates the activation of the transcellular signalling process. On the other hand, if a gene is knocked down in the body wall muscle with a consequent change in reporter expression, it can be inferred that the activity of that gene in the body wall muscle affects the transcriptional regulation of *hsp-70* - although not necessarily directly. For each RNAi, a significantly different fluorescence intensity compared to control RNAi was interpreted as that gene acting to either enhance or suppress *hsp-70p::mCherry* expression in the relevant tissue. For example, if intestine-specific RNAi against 'Gene X' was identified as causing significantly increased *hsp-70* reporter fluorescence compared to intestine-specific control RNAi, then Gene X was considered to act in the intestine as a suppressor of transcellular signalling. Similarly, if body wall muscle-specific RNAi against 'Gene Y' resulted in decreased *hsp-70* reporter fluorescence compared to control RNAi in the same tissue, then Gene Y was considered to act in the body wall muscle as an enhancer of *hsp-70* reporter expression.

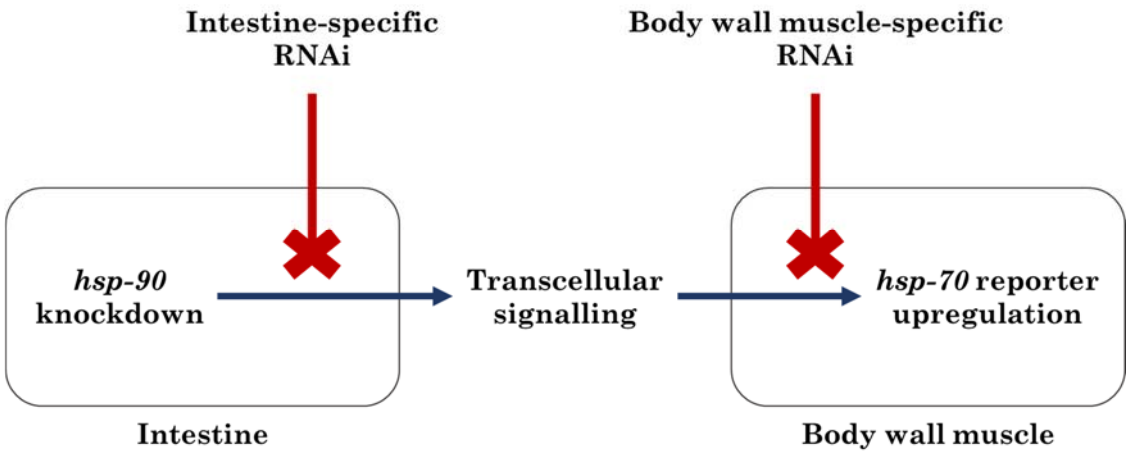


**Figure 6.2 Interpretation of tissue-specific RNAi screening results**. Intestine-specific RNAi with a resulting effect on *hsp-70* reporter expression is interpreted as modulating the activation of transcellular signalling. Body wall muscle-specific RNAi with a resulting effect on *hsp-70* reporter expression is interpreted as modulating the transcriptional regulation of *hsp-70*.

### 6.2.3 Protein interaction networks

To determine whether genes identified through transcriptome profiling encode proteins which might functionally interact, protein interaction networks were generated using the GeneMania tool (Warde-Farley et al. 2010). The particular value of this tool is to identify functionally relevant associations between input proteins and other proteins not in the input list, and to incorporate them into the output network. This potentially enables the discovery of genes involved in a pathway which might otherwise not have been identified. The networks generated by this tool are based on information drawn from published data, such as analyses of gene co-expression or protein interactions, which is then used to identify both known and predicted associations between proteins. Because of this, each identified association in a network is assigned a score between 0 and 1 denoting confidence that the association is real. Associations within networks are shown as edges, connecting nodes which represent proteins. The identified associations do not necessarily represent direct protein-protein binding; rather that two proteins are functionally associated.

### 6.2.4 Promoter scanning using FIMO

To identify occurrences of transcription factor consensus motifs within promoter regions of genes of interest, motif scanning was performed using the 'Find individual motif occurrences' (FIMO) tool (Bailey et al. 2009) which is part of the online MEME suite of motif analysis tools (*v5.1.1*) (Grant et al. 2011). FIMO compares input motif sequences against input promoter sequences and reports instances of overlap, allowing identification of possible transcription factor binding sites. Sequences of gene promoter regions were obtained from WormBase (Harris et al. 2010) and were determined as the 1000 nucleotides immediately upstream of the start/ATG codon. In the case of a gene having multiple possible transcripts, only one sequence pertaining to the first possible transcript was used, so as not to bias motif detection towards any motifs present in multiple transcripts for a single gene. Known consensus motifs of transcription factors were identified through literature searches and the CIS-BP database of transcription factors (Weirauch et al. 2014). Known consensus motifs used for analysis in this chapter are listed in **Table 6.1**.

### 6.2.5 Dual RNAi knockdown

To create NGM-RNAi plates seeded with two combined RNAi clones, RNAi cultures were initially prepared individually. Once the two cultures had been grown by overnight incubation at 37°C, they were mixed in a 1:1 ratio and the mixture seeded onto empty NGM-RNAi plates. Mixing was performed post- rather than co-incubation to prevent one bacterial clone out-competing the other prior to seeding. Dual RNAi knockdown required five controls rather than the usual one, as in addition to empty L4440 vector RNAi it was necessary to quantify the effect of each RNAi singly, and in combination with the empty vector to determine any dilution effect.

| TF | Motif | Original reference |
|---|---|---|
| CEH-58 | NNTAATTRNN | Narasimhan et al. 2015 |
| CND-1 | CAGCTG | Grove et al. 2009 |
| CND-1 | CATATG | Grove et al. 2009 |
| CND-1 | CATCTG | Grove et al. 2009 |
| DAF-16 | NNRWMAAYAN | Weirauch et al. 2014 |
| DAF-16 | RNHGTAAACAANHN | Matys et al. 2006 |
| DAF-16 (DBE) | GTAAACA | Furuyama et al. 2000; Murphy et al. 2003 |
| ELT-2 | AHTGATAARR | McGhee et al. 2007 |
| HLH-10 | CACCTG | Grove et al. 2009 |
| HLH -10 | CACGTG | Grove et al. 2009 |
| HLH -10 | CAGCTG | Grove et al. 2009 |
| HLH -10 | CATATG | Grove et al. 2009 |
| HLH -10 | CATCTG | Grove et al. 2009 |
| HLH -25 | CACACG | Grove et al. 2009 |
| HLH -25 | CACATG | Grove et al. 2009 |
| HLH -25 | CACGCG | Grove et al. 2009 |
| HLH -25 | CACGCT | Grove et al. 2009 |
| HLH -25 | CACGTG | Grove et al. 2009 |
| HLH -25 | CATACG | Grove et al. 2009 |
| HLH -25 | CATGCG | Grove et al. 2009 |
| HSF-1 | TTCYAGAA | Narasimhan et al. 2015 |
| NHR-42 | NNYGTRNYNN | Narasimhan et al. 2015 |
| PHA-4 | GAGAGAS | Zhong et al. 2010 |
| PHA-4 | GTAAACAR | Contrino et al. 2012 |
| PHA-4 | RYAMAYAN | Heinz et al. 2010 |
| PHA-4 | TRTTKRY | Gaudet & Mango 2002 |
| PHA-4 | WRWGYAAAYA | Mathelier et al. 2014 |
| PQM-1 (DAE) | TGATAAG | Furuyama et al. 2000; Murphy et al. 2003 |

**Table 6.1 Transcription factor consensus motifs used for motif scanning**. Motifs were identified by literature searches and through the CIS-BP transcription factor database (Weirauch etal. 2014). TF: Transcription factor. DBE: DAF-16 binding element. DAE: DAF-16-associated element.

## 6.3 Results

### 6.3.1 Identification of 29 tissue-specific modulators of *hsp-70* reporter expression in the *hsp-90*$^{int}$ hp-RNAi strain

Although RNAi knockdown was an essential process for screening large numbers of genes as potential regulators of TCS, a major limitation was the availability of RNAi from the clone library (Source BioScience; Kamath & Ahringer 2003). Whilst the extended library contains RNAi clones for thousands of genes including the vast majority of candidates, a number were nevertheless not represented. This meant that 16 candidate genes could not be screened: *C02B8.12*, *W05H12.1*, *Y19D10B.6* and *Y38E10A.14*, which were identified in **Chapter 4**; and *him-19*, *sop-3*, *xpc-1*, *F55B11.5*, *K02E2.9*, *T08D2.8*, *Y104H12D.2*, *Y35H6.3*, *Y40H7A.15*, *Y48G1BR.1*, *Y53F4B.6* and *Y73E7A.1*, which were identified in **Chapter 5**. Of these, *K02E2.9*, *Y35H6.3*, *Y40H7A.15* and *Y53F4B.6* are identified in WormBase as pseudogenes, which could be why no RNAi was available. An alternative method to investigate the function of these genes in TCS could have been to cross the *hsp-90*$^{int}$ hp-RNA strain into strains carrying loss-of-function gene mutations. However, this would not have been a tissue-specific approach, and investigation of each gene would have been significantly more time-consuming. It was therefore decided to continue the RNAi screen with only the genes for which RNAi clones were available, as this still presented the potential to consider a large number of candidate genes.

In total, 90 genes were screened for an effect on *hsp-70* reporter expression upon their tissue-specific knockdown in the *hsp-90*$^{int}$ hp-RNAi strain (**Appendix 6.2)**. The results of the RNAi screen are displayed in **Figure 6.3**, which shows the mean intensity of *hsp-70p::mCherry* reporter fluorescence in *hsp-90*$^{int}$ hp-RNAi animals which have been fed intestine- or body wall muscle-specific RNAi against each screened gene. Genes are ordered from lowest to highest mean intensity, with values for control RNAi shown in green. Where tissue-specific knockdown of a gene resulted in significantly decreased reporter fluorescence compared to the control, the gene was identified as acting in the relevant tissue to enhance reporter expression and is shown in blue. Conversely, where tissue-specific knockdown caused significantly increased reporter fluorescence, the gene was identified as a tissue-specific suppressor of reporter expression and is shown in red. In total, 29 of the 90 screened genes were identified as tissue-specific modulators of *hsp-70* reporter expression in

the *hsp-90*$^{int}$ hp-RNAi strain. These genes, which are listed in **Table 6.2**, have been denoted TCS cross (X)-Tissue (*txt*) genes.

Amongst the group of *txt* genes acting in the intestine to suppress *hsp-70* reporter expression (**Fig. 6.3a**), four genes (*gcsh-2*, *hlh-25, nhr-62* and *M02B1.2*) were identified as displaying increased reporter intensity but are not identified as *txt* genes. When considered individually, each of these genes would be identified as causing increased reporter fluorescence upon knockdown; however, correction for multiple testing did not identify these differences as within the false discovery rate of 0.05.

Interestingly, two *txt* genes (*C50D2.3* and *cnd-1*) were identified as acting in both the intestine and the body wall muscle to modulate reporter expression (**Figure 6.3; Table 6.2**). This may suggest that these genes have key roles in TCS. Knockdown of *C50D2.3* or *cnd-1* in the intestine causes a 15% or 17.7% respective increase in reporter intensity (**Fig. 6.3a**), whilst knockdown of either gene in the body wall muscle causes an 18% decrease (**Fig. 6.3b**). *cnd-1* encodes a basic helix-loop-helix (bHLH) transcription factor, which is a homologue of human NeuroD and is required for specification of motor neuron fate in *C. elegans* (Hallam et al. 2000). As a transcription factor, it may be involved in transcriptional regulation in intestine and body wall cells during TCS. Little is known about the function of *C50D2.3*, but it is predicted to encode a PDZ domain protein (WormBase, Harris et al. 2010). PDZ domain proteins often act as scaffolds for larger multiprotein complexes at the inner cell membrane, performing functions including transmembrane receptor organisation and vesicle trafficking (Fanning & Anderson 1996; Nourry et al. 2003; Kim & Sheng 2004). Such a function could be relevant in terms of transduction of an intercellular signal across the cell membrane.

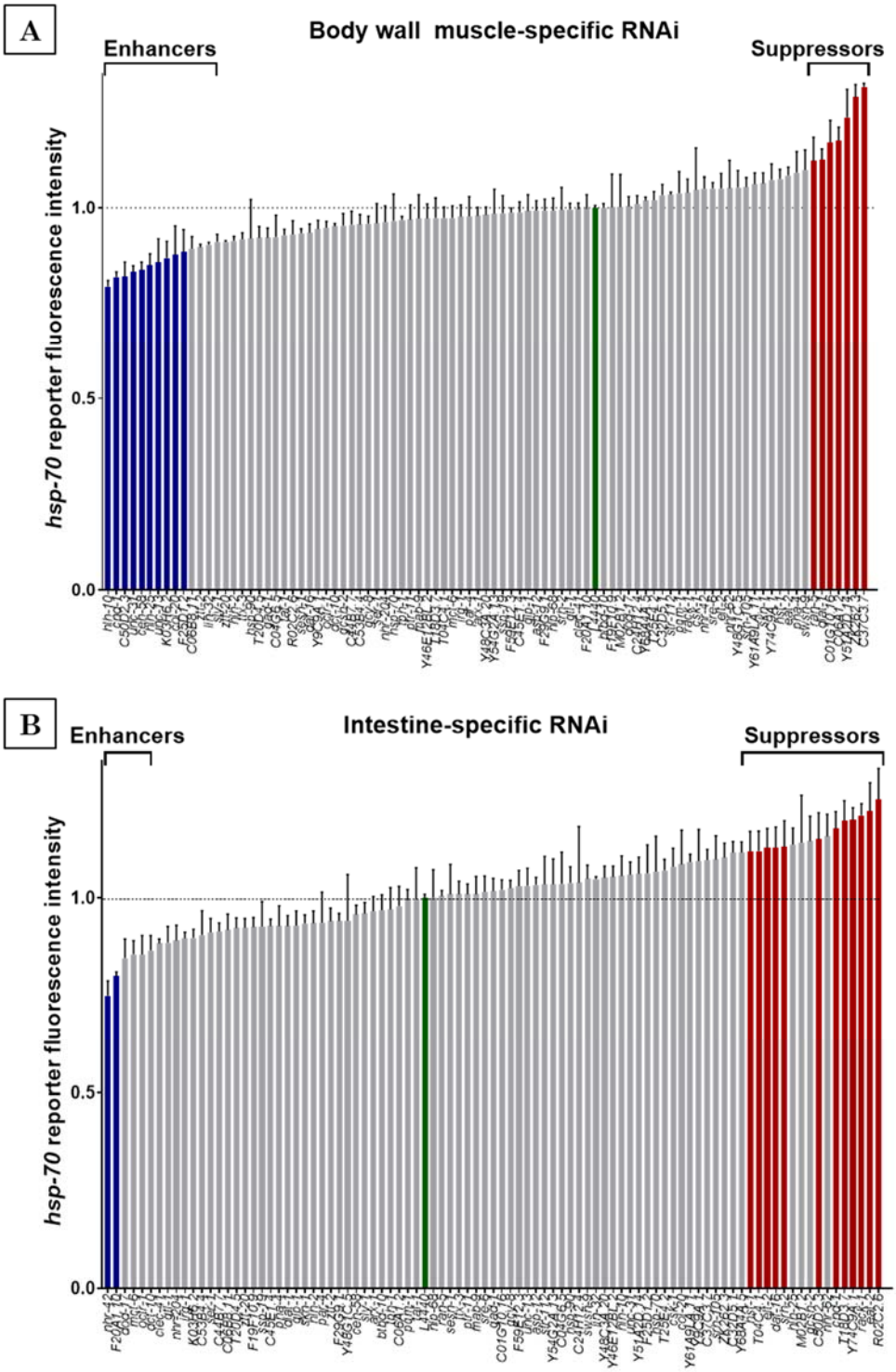


**Figure 6.3 Results of tissue-specific RNAi screening for effect of gene knockdown on *hsp-70* reporter intensity in the *hsp-90*$^{int}$ hp-RNAi strain**. Each gene was knocked down in either (**A**) the intestine or (**B**) the body wall muscle and the effect on mean *hsp-70p::mCherry* reporter fluorescence quantified. Bars for control (L4440) RNAi, to which values were normalised, are highlighted green. Bars with a significant corrected p value are highlighted blue (enhancers) or red (suppressors). Significance compared to control RNAi values was determined by one-way ANOVA with multiple comparisons; error bars represent SEM.

| ***txt* gene** | **Tissue** | **Effect** | **FC** | **$p_a$** |
|---|---|---|---|---|
| *cnd-1* | Body wall muscle | Enhancer | -18.1 | 0.0007 |
| | Intestine | Suppressor | 17.7 | 0.0311 |
| *C50D2.3* | Body wall muscle | Enhancer | -18.0 | <0.0001 |
| | Intestine | Suppressor | 15.0 | 0.0031 |
| *hlh-10* | Body wall muscle | Enhancer | -20.6 | <0.0001 |
| *unc-31* | Body wall muscle | Enhancer | -16.8 | 0.0015 |
| *ceh-58* | Body wall muscle | Enhancer | -16.3 | 0.002 |
| *hlh-25* | Body wall muscle | Enhancer | -15.0 | 0.0048 |
| *unc-13* | Body wall muscle | Enhancer | -14.3 | 0.0076 |
| *K03H6.2* | Body wall muscle | Enhancer | -13.1 | 0.0171 |
| *col-20* | Body wall muscle | Enhancer | -12.2 | 0.0014 |
| *F25D1.2* | Body wall muscle | Enhancer | -11.5 | 0.0026 |
| *ran-5* | Body wall muscle | Suppressor | 12.1 | 0.0314 |
| *dlat-1* | Body wall muscle | Suppressor | 12.5 | 0.0249 |
| *C01G10.16* | Body wall muscle | Suppressor | 16.9 | 0.0014 |
| *C06A1.2* | Body wall muscle | Suppressor | 17.5 | 0.0012 |
| *Y51A2D.14* | Body wall muscle | Suppressor | 23.6 | <0.0001 |
| *ZK262.3* | Body wall muscle | Suppressor | 28.8 | <0.0001 |
| *C37C3.7* | Body wall muscle | Suppressor | 31.5 | <0.0001 |
| *nhr-42* | Intestine | Enhancer | -25.0 | 0.0016 |
| *F20A1.10* | Intestine | Enhancer | -20.0 | 0.0144 |
| *hsf-1* | Intestine | Suppressor | 11.9 | 0.0459 |
| *fnip-2* | Intestine | Suppressor | 12.0 | 0.0459 |
| *elt-2* | Intestine | Suppressor | 12.8 | 0.0311 |
| *daf-16* | Intestine | Suppressor | 12.9 | 0.0311 |
| *srh-2* | Intestine | Suppressor | 13.1 | 0.0459 |
| *tsct-1* | Intestine | Suppressor | 19.8 | 0.0144 |
| *Y74C9A.1* | Intestine | Suppressor | 19.9 | 0.0016 |
| *rack-1* | Intestine | Suppressor | 21.1 | 0.0094 |
| *eat-2* | Intestine | Suppressor | 22.2 | 0.0058 |
| *R02C2.6* | Intestine | Suppressor | 25.2 | 0.0016 |

**Table 6.2 *txt* genes identified through tissue-specific RNAi screening in the *hsp-90*$^{int}$ hp-RNAi strain**. *cnd-1* and *C50D2.3* were identified as acting in both the body wall muscle and intestine, although with opposing effects in each tissue. FC: Fold-change in *hsp-70* reporter fluorescence intensity compared to in the same strain grown on control RNAi. $p_a$: p value after adjustment for multiple comparisons.

### 6.3.2 Visualising the subcellular localisation of *txt* genes

To visualise where each *txt* gene might act within the relevant tissue, the subcellular localisation of the protein encoded by each gene was predicted from its amino acid sequence using the DeepLoc 1.0 tool. This tool predicts firstly whether a protein is soluble or transmembrane, and secondly the organelle or region to which it is targeted. This may be the cytoplasm, nucleus, ER, mitochondria, lysosomes, cell membrane, or extracellular space. **Figure 6.4** summarises the predicted subcellular location of each *txt* gene in the tissue in which it acts. Genes predicted to encode transmembrane proteins are shown to cross the boundary of the relevant organelle or the cell membrane, whilst soluble proteins are within the appropriate compartment. Proteins predicted to be extracellularly localised are shown outside, but adjacent to, the relevant tissue. Genes acting as enhancers are shown in green whilst those acting as suppressors are shown in red.

Prediction of protein subcellular localisation identified that six *txt* genes are predicted to encode soluble extracellular proteins: *F20A1.10, K03H6.2, C37C3.7, ZK262.3, C01G10.16* and *Y51A2D.14*. Extracellular proteins could potentially represent secreted intercellular signalling molecules. Genes acting in the intestine to enhance TCS and encoding such proteins, for example *F20A1.10* (**Table 6.2; Fig. 6.4**), might therefore be responsible for the transmission of a signal between the intestine and body wall muscle during TCS. It is less clear how extracellular proteins encoded by genes acting in the body wall muscle would act; their secretion could perhaps signal back to the intestine as part of a feedback mechanism. In addition to this, four *txt* genes are predicted to encode transmembrane proteins localised to the cell membrane. These are *col-20*, *eat-2*, *R02C2.6* and *srh-2*. As the cell membrane represents a boundary across which an intercellular signal would have to be transmitted, transmembrane proteins could represent transducers of signals into or out of the cell.

Twelve genes were predicted to encode soluble proteins localised to the nucleus, with eight acting in the intestine and four in the body wall muscle (**Fig. 6.4**). The bHLH transcription factor *cnd-1* was identified as acting in both tissues (**Table 6.2**). Interestingly, most genes acting in the intestine which encode predicted nuclear proteins act to suppress reporter expression; whilst those acting in the body wall muscle act to enhance it. This could suggest that the nuclear-localised proteins in

the body wall muscle may act to promote *hsp-70* upregulation in that tissue, whilst those in the intestine may act to suppress intercellular signalling.

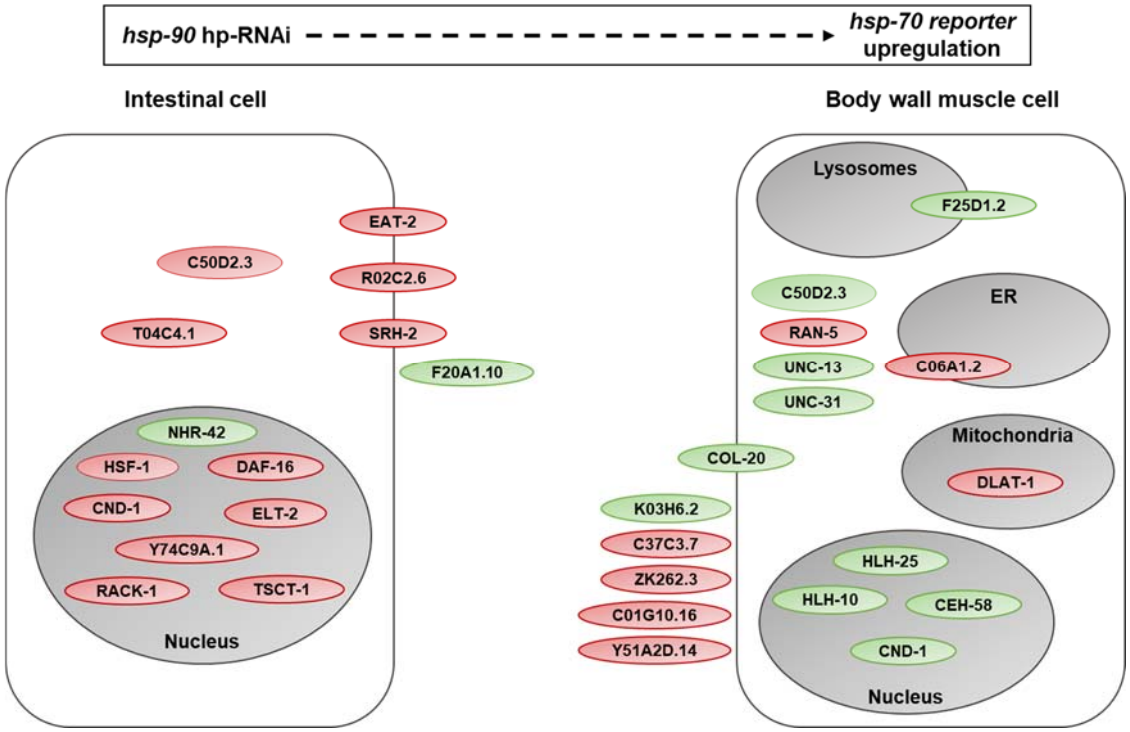


**Figure 6.4 Predicted subcellular localisation of proteins encoded by *txt* genes**. Subcellular localisation was predicted from amino acid sequence using DeepLoc 1.0. Modality of action is denoted by colour: enhancers in green, suppressors in red. Proteins shown to cross the boundary of a cell or organelle are those predicted to be transmembrane, whilst those shown outside a tissue are predicted to be soluble extracellular proteins.

### 6.3.3 Genes acting as controls

Three genes were targeted as controls or key components of TCS in the *hsp-90*$^{int}$ hp-RNAi strain: *hsf-1*, *hsp-70* and *hsp-90*. The *hsf-1* (*sy441*) mutation, which should affect *hsf-1* activity in all tissues, was shown to not affect *hsp-70* reporter upregulation in the *hsp-90*$^{int}$ hp-RNAi strain (**Figs. 3.3c-d, Fig. 3.4**). It would therefore be expected that knockdown of *hsf-1* in either the intestine or body wall muscle would also not affect reporter expression. Whilst this was shown to be the case when *hsf-1* was knocked down in the body wall muscle (**Fig. 6.3b**), *hsf-1* was identified as acting in the intestine to suppress reporter expression (**Fig. 6.3a; Table 6.2**). A possible explanation for this could be that HSF-1 in the intestine might act to restore proteostasis and ameliorate the 'stressor' of intestine-specific *hsp-90* knockdown, which might then reduce the activation of TCS and consequent *hsp-70* reporter upregulation.

The *hsp-90*$^{int}$ hp-RNAi strain already exhibits intestine-specific *hsp-90* knockdown, so further knockdown of intestinal *hsp-90* RNAi would not be expected to strongly affect the phenotype. This was shown to indeed be the case (**Fig. 6.3a**). Knockdown of *hsp-90* in the body wall muscle, which would suggest de-repression of monomeric HSF-1 in that tissue, also did not affect *hsp-70* reporter expression (**Fig. 6.3b**). This is consistent with the idea that upregulation of *hsp-70* in the body wall muscle during TCS is not dependent on *hsf-1*.

Tissue-specific knockdown of *hsp-70* in either the intestine or body wall muscle of the *hsp-90*$^{int}$ hp-RNAi strain did not affect the intensity of the *hsp-70* reporter (**Fig. 6.3**), which seems at first somewhat counter-intuitive. However, tissue-specific knockdown is achieved here using hp-RNAi, and so involves the selective degradation of *hsp-70* transcripts (Fire et al. 1998; Montgomery et al. 1998). As the *hsp-70* reporter consists of *mCherry* under the control of the *hsp-70* gene promoter, tissue-specific *hsp-70* RNAi should target *hsp-70* transcripts without affecting *mCherry*. One would therefore not expect a direct effect of *hsp-70* RNAi on reporter expression. However, tissue-specific depletion of *hsp-70* could have led to altered transcriptional regulation at the *hsp-70* promoter and modulated reporter expression indirectly. Ideally, the screen would also have included tissue-specific RNAi knockdown of *mCherry* transcripts as an additional control. However, RNAi for *mCherry* was not available.

### 6.3.4 C50D2.3 is highly connected in protein interaction networks

To determine whether any *txt* genes identified by RNAi screening were functionally associated, which could suggest a specific pathway, protein interaction networks were generated using GeneMania. **Figure 6.5a** shows the interaction network generated from an input list of the *txt* genes acting in the body wall muscle to enhance *hsp-70p::mCherry* reporter expression. In this diagram, it can be seen that the *txt* genes CND-1, COL-20, HLH-10 and HLH-25 form part of a large, highly connected subnetwork which also includes CEH-40, EGL-43, HLH-2, HLH-26, MDT-11, MLS-2 and UNC-62. All of these proteins are identified in WormBase as having activity related to DNA binding, indicating a potential role in transcriptional regulation. This network also identified the *txt* gene C50D2.3 as a highly connected node, although not one functionally associated with the larger subnetwork. This could indicate that C50D2.3 has a key role amongst *txt* genes acting in the body wall muscle, but in a different function from other genes in the network.

Interestingly, C50D2.3 is also identified as highly connected in **Figure 6.5b**, which shows the network generated from *txt* genes acting in the intestine to suppress reporter expression. In this network, the two highly connected *txt* genes DAF-16 and C50D2.3 are functionally associated through the proteins IMB-3 and DLAT-1; whilst the transcription factors CND-1 and ELT-2 are also represented in smaller subnetworks. The grouping of C50D2.3 and DAF-16 in a subnetwork may indicate that the two are functionally associated in the intestine, suggesting that C50D2.3 may interact in some way with ILS.

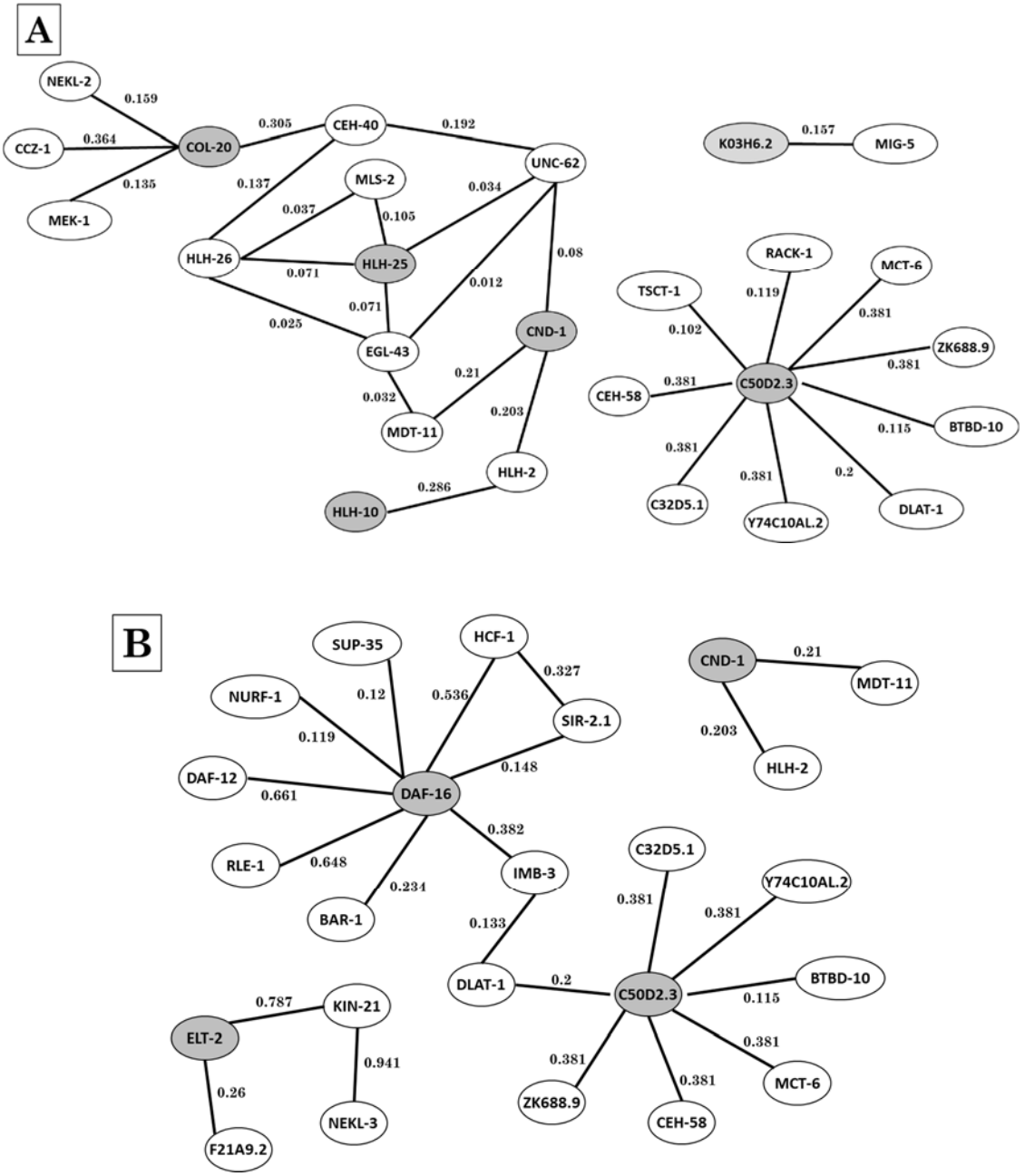


**Figure 6.5 Protein interaction networks of *txt* genes generated using GeneMania**. Networks were generated using input lists of *txt* genes acting (**A**) in the body wall muscle to enhance TCS, or (**B**) in the intestine to suppress TCS. *txt* genes present in the input list are highlighted in grey. Edge values denote the strength of confidence in the association. Genes included in the RNAi screen based on an interaction with C50D2.3 were omitted from input lists in order to avoid bias.

### 6.3.5 *C50D2.3* is required for resistance to heat stress in the *hsp-90*$^{int}$ hp-RNAi strain

The *hsp-90*$^{int}$ hp-RNAi strain, which shows stronger upregulation of *hsp-70* than the *hsp-90*$^{neu}$ hp-RNAi strain (**Figs. 3.2, 3.5a**), also demonstrates increased lifespan and survival following acute heat stress compared to controls (**Figs. 3.6, 3.7**). In the body wall muscle of the *hsp-90*$^{int}$ hp-RNAi strain, a tissue in which the *hsp-70* reporter is particularly strongly upregulated, *C50D2.3* acts to enhance this reporter expression (**Fig. 6.3b; Table 6.2**). *C50D2.3* was also identified as highly connected in a protein functional association network of *txt* genes acting in the body wall muscle to enhance reporter expression (**Fig. 6.5a**), suggesting that it may have a key role. Based on this, thermotolerance assays were performed to determine whether tissue-specific knockdown of *C50D2.3*, a gene which contributes to *hsp-70* reporter upregulation, also contributes to heat stress resistance.

**Figure 6.6b** shows that *hsp-90*$^{int}$ hp-RNAi animals grown on body wall muscle-specific *C50D2.3* RNAi have significantly reduced survival after 4 or 6 hours of heat stress, compared to animals grown on control RNAi. This suggests that heat stress resistance in this strain is due to the tissue-specific enhancement of *hsp-70* reporter expression by *C50D2.3*, and identifies *C50D2.3* as a key component of TCS acting in the body wall muscle. However, *hsp-90*$^{int}$ hp-RNAi animals grown on intestine-specific *C50D2.3* RNAi also have significantly reduced survival after 6 or 8 hours of heat stress (**Fig. 6.6a**). This indicates that it is not only the *C50D2.3*-enhanced upregulation of the *hsp-70* reporter in the body wall muscle that is important for heat stress resistance in this strain, but also a function of *C50D2.3* in the intestine. If *C50D2.3* were an intestine-specific enhancer of reporter upregulation, the intestine-specific requirement for *C50D2.3* in heat stress resistance might be explained through its involvement in promoting *hsp-70* expression. However, the action of *C50D2.3* in the intestine is to suppress reporter upregulation (**Fig. 6.3a; Table 6.2**). It is therefore unclear how by acting in the intestine to suppress *hsp-70* reporter expression, *C50D2.3* acts in the same tissue to promote heat stress resistance.

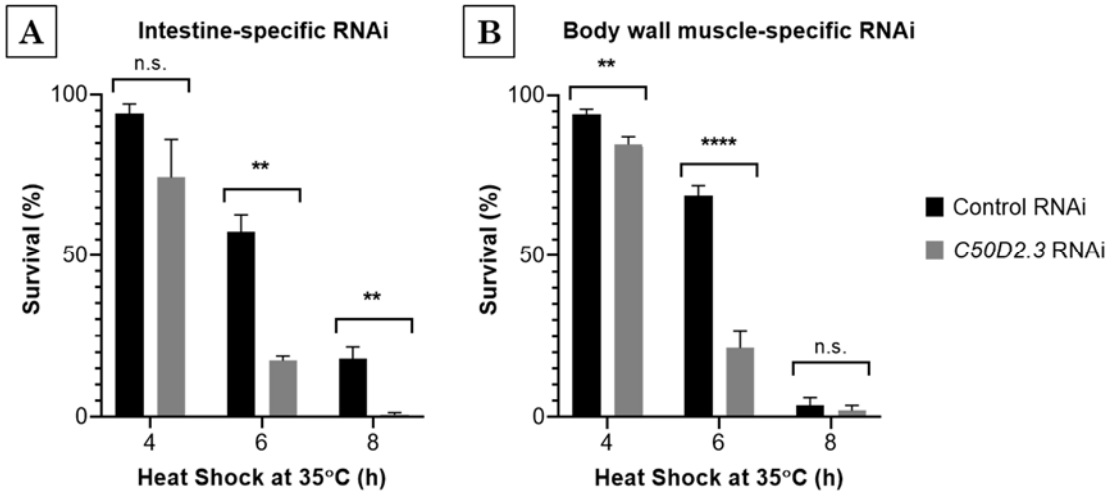


**Figure 6.6 Tissue-specific *C50D2.3* knockdown in the *hsp-90*$^{int}$ hp-RNAi strain reduces survival following heat stress**. Animals sensitive to (**A**) intestine- or (**B**) body wall muscle-specific RNAi were grown on control or *C50D2.3* RNAi for two generations, then assayed for thermotolerance. Comparisons were made using Student's t test; error bars represent SEM. ** = $p<0.01$; **** = $p<0.0001$.

To determine whether the modulation of *hsp-70* reporter expression by *C50D2.3* is specific to TCS, or whether *C50D2.3* might have a more general role in *hsp-70* upregulation and heat stress, the effect of systemic *C50D2.3* RNAi in the *hsp-70p::mCherry* reporter strain was quantified. *hsp-70p::mCherry* reporter animals were grown on control or *C50D2.3* RNAi for two generations, following which the ability of these animals to upregulate the *hsp-70* reporter was compared. As can be seen in **Figure 6.7a**, systemic *C50D2.3* RNAi in the *hsp-70p::mCherry* reporter strain does not prevent the upregulation of the *hsp-70* reporter following heat stress, indicating that *C50D2.3* is not required for *hsp-70* upregulation in general. In fact, the *hsp-70* reporter is upregulated more strongly following heat stress in animals grown on *C50D2.3* RNAi (**Fig. 6.7b**), suggesting that *C50D2.3* may act to suppress *hsp-70* expression during heat stress in wild-type animals. This indicates that the requirement during heat stress for *C50D2.3* in the intestine and body wall muscle of the *hsp-90*$^{int}$ hp-RNAi strain may be a specific feature of TCS in this strain, rather than a general role for *C50D2.3*.

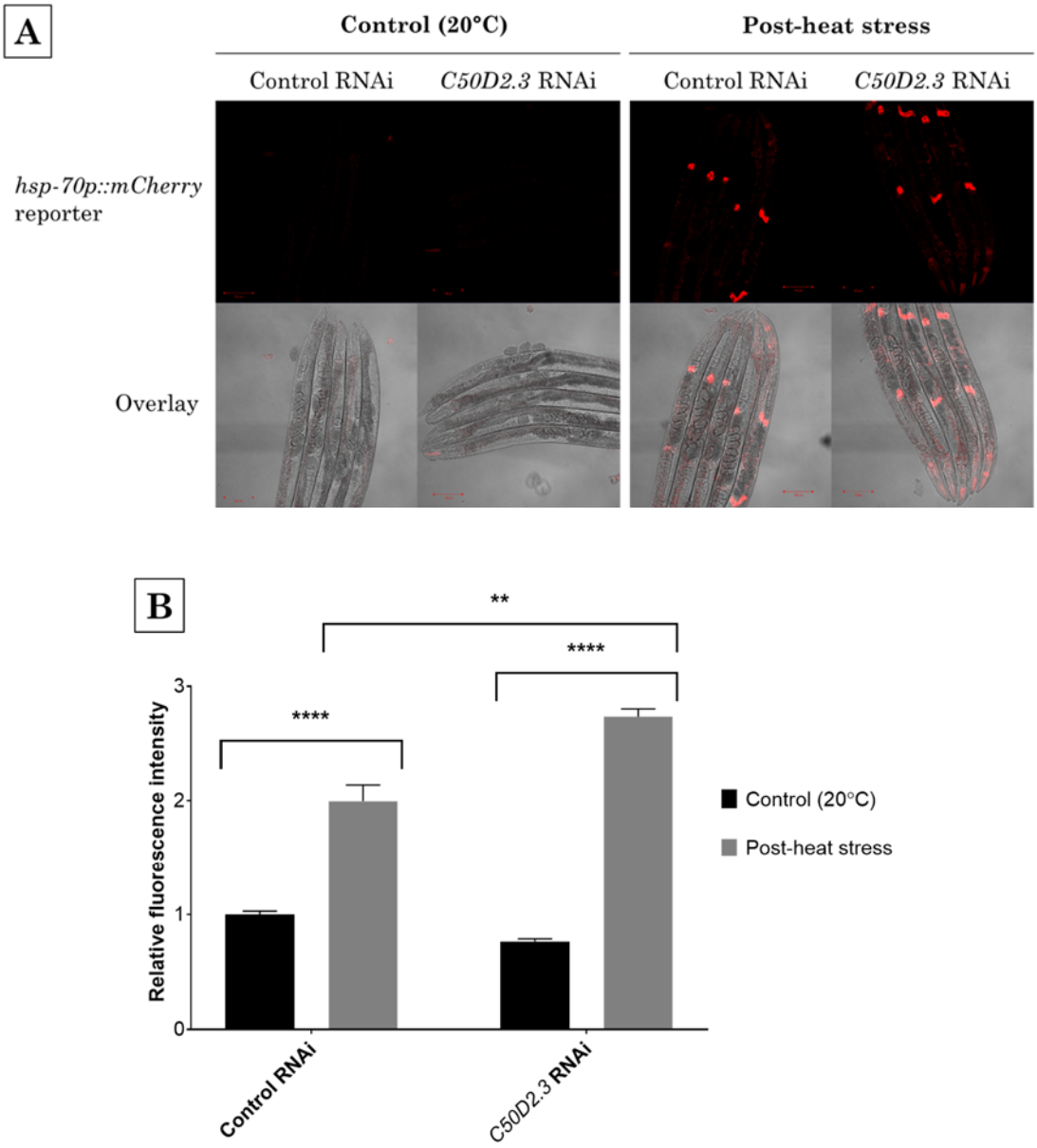


**Figure 6.7 *C50D2.3* is not required for *hsp-70* reporter upregulation following heat stress in the *hsp-70p::mCherry* reporter strain**. The *hsp-70p::mCherry* reporter strain was grown on control or *C50D2.3* RNAi for two generations. Animals were heat-shocked for 1 hour at 35°C, allowed to recover for 3 hours at 20°C, and imaged. (**A**) Representative 20x images. Scale bars: 100µm (**B**) Quantification of intensity from 10x images, normalised to that of animals on control RNAi at 20°C. Mean intensities were compared using Student's t test; error bars represent SEM. ** = $p<0.01$; **** = $p<0.0001$.

### 6.3.6 *ceh-58* and *C50D2.3* appear to act in the same pathway in the body wall muscle

*C50D2.3* was identified in protein functional association networks as a highly connected node (**Fig. 6.5**), suggesting that its interaction partners may also be relevant to TCS. Previous work has identified ten interaction partners of *C50D2.3* (Lenfant et al. 2010), of which eight were included in tissue-specific RNAi screening. This identified that four interaction partners of *C50D2.3* also act as *txt* genes: *ceh-58*, *dlat-1*, *rack-1* and *tsct-1*. Three of these modulate *hsp-70* reporter expression in a tissue-specific manner shared with *C50D2.3*: *ceh-58* acts in the body wall muscle to enhance reporter expression, whilst *rack-1* and *tsct-1* act in the intestine to suppress reporter expression (**Fig. 6.3; Table 6.2**). As *C50D2.3* and *ceh-58* both act in the body wall muscle to enhance *hsp-70* reporter expression, and the reporter is particularly strongly expressed in that tissue in the *hsp-90*$^{int}$ hp-RNAi strain (**Fig. 3.2**), this interaction was investigated further.

To determine whether an interaction between *C50D2.3* and *ceh-58* in the body wall muscle of the *hsp-90*$^{int}$ hp-RNAi strain was relevant for *hsp-70* reporter expression, dual body wall muscle-specific RNAi knockdown of these two genes was performed. The individual knockdown of *C50D2.3* in the body wall muscle causes an 18% decrease in reporter intensity, whilst knockdown of *ceh-58* causes a 16.3% decrease (**Fig. 6.3; Table 6.2**). When RNAi against either of these genes was combined with control RNAi the effect on reporter expression was not changed (**Fig. 6.8**), demonstrating that there is no dilution effect on either RNAi by combination with another. When both *C50D2.3* and *ceh-58* were simultaneously knocked down in the body wall muscle, there was no further reduction in reporter expression compared to either gene knocked down alone (**Fig. 6.8**). This indicates that the two genes act in the same pathway to enhance *hsp-70* reporter expression in the body wall muscle of the *hsp-90*$^{int}$ hp-RNAi strain.

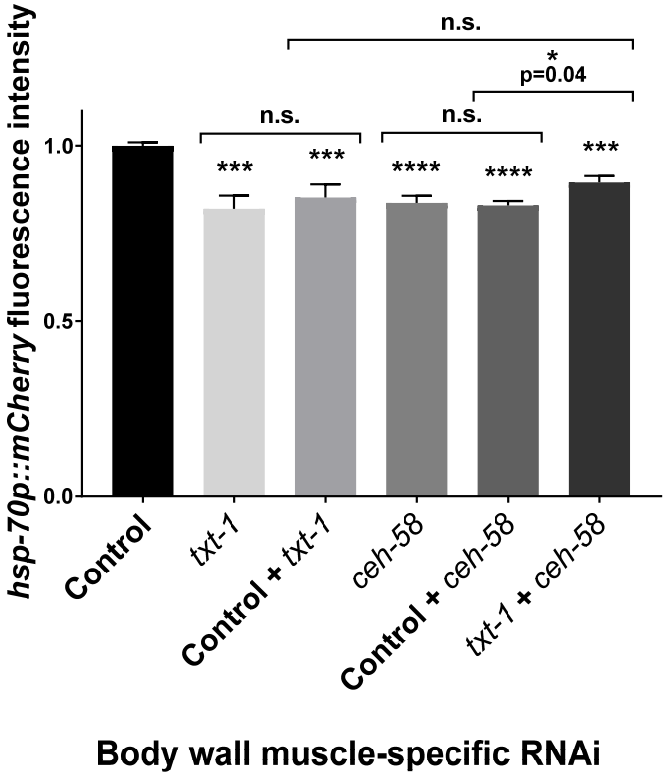


**Figure 6.8 Dual knockdown of *C50D2.3* and *ceh-58* in the body wall muscle does not have an additive effect**. The effect of single or combined body wall muscle-specific RNAi against *C50D2.3* or *ceh-58* was determined by feeding RNAi for two generations before quantification of *hsp-70* reporter intensity in day 1 adults. Values were normalised to those of animals fed control RNAi. Comparisons were made using Student's t test; error bars represent SEM. * = $p<0.05$; *** = $p<0.001$; **** = $p<0.0001$; n.s. = not significant.

### 6.3.7 The *hsp-70* promoter contains a CEH-58 consensus motif

Nine of the 29 identified *txt* genes are known or predicted to encode transcription factors: *ceh-58*, *cnd-1*, *daf-16*, *elt-2*, *hlh-10*, *hlh-25*, *hsf-1*, *nhr-42* and *tsct-1* (WormBase, Harris et al. 2010; CIS-BP database, Weirauch et al 2014). As the tissue-specific action of these genes during TCS could be due to their function in transcriptional regulation, potentially through regulation of *hsp-70* or other *txt* genes, known consensus motifs associated with these genes were identified and used to perform motif scanning in the promoters of *hsp-70* and all 29 *txt* genes. No reported consensus motif could be identified for TSCT-1. However, at least one reported consensus DNA-binding motif was identified for each of the other transcription factors using the CIS-BP transcription factor database or in literature searches (**Table 6.1**; CIS-BP database, Weirauch et al. 2014). Motifs for PHA-4 were included despite *pha-4* not being identified as a *txt* gene, as it has previously been shown that *pha-4* is required during TCS activated by tissue-specific *hsp-90* knockdown (van Oosten-Hawle et al. 2013). It is possible that *pha-4* was not identified in the RNAi screen because it is active in a tissue which was not targeted, and indeed *pha-4* is known to be strongly expressed in the pharynx where it is key for organ identity (Horner et al. 1998; Kalb et al. 1998).

**Table 6.3** shows the results of motif scanning in the promoters of *txt* genes. Genes which were not identified as having any relevant sites in their promoters are omitted from the table. Three transcription factors also did not have motifs present in any scanned promoter: CND-1, HLH-10 and HLH-25. Amongst the promoters scanned, the transcription factor with motifs in the most gene promoters was PHA-4, with motifs occurring in 12 promoters including that of *hsp-70*. This supports a role for PHA-4 in TCS in the *hsp-90*$^{int}$ hp-RNAi strain, although as it was not found to act as a TCS modulator in the same tissues as the *txt* genes which motif scanning suggests it may regulate, how it might do so is unclear. ELT-2 and HSF-1 were also identified as potentially relevant, with each having motifs in 12 of the scanned promoters. Both were identified as *txt* genes which act in the intestine to suppress *hsp-70* reporter expression (**Fig. 6.3a, Table 6.2**). *elt-2* is known to act cell-autonomously in the intestine to regulate expression of *pha-4* (Kalb et al. 1998), and so could also be relevant for the transcriptional regulation of *txt* genes whose promoters contain a PHA-4 motif.

| | PHA-4 | ELT-2 | HSF-1 | DAF-16 | DAF-16 (DBE) | CEH-58 | NHR-42 |
|---|---|---|---|---|---|---|---|
| *tsct-1* | X | X | X | | | | |
| *dlat-1* | X | X | | | | | |
| *hsp-70* | X | | X | X | X | X | |
| *ceh-58* | X | | X | | | | |
| *nhr-42* | X | | | X | | | |
| *eat-2* | X | | | X | | | |
| *srh-2* | X | | | | X | | |
| *unc-31* | X | | | | | | |
| *C01G10.16* | X | | | | | | |
| *Y51A2D.14* | X | | | | | | |
| *ran-5* | X | | | | | | |
| *rack-1* | X | | | | | | |
| *daf-16* | | X | X | X | | | |
| *elt-2* | | X | X | | | | |
| *hlh-25* | | X | X | | | | |
| *K03H6.2* | | X | | X | | X | |
| *col-20* | | X | | | | | |
| *F25D1.2* | | X | | | | | |
| *C06A1.2* | | X | | | | | |
| *unc-13* | | | X | | | | X |
| *hlh-10* | | | X | | | | |
| *cnd-1* | | | X | | | | |
| *F20A1.10* | | | | X | | X | |
| *Y74C9A.1* | | | | X | | | X |
| *hsf-1* | | | | X | | | |
| *fnip-2* | | | | | | | X |
| *C50D2.3* | | | | | | | |

**Table 6.3 Motif scanning in *txt* gene promoters identifies transcription factor consensus motifs**. A cross indicates at least one consensus site for that transcription factor was located in the relevant gene promoter. Motifs used for scanning are listed in **Table 6.1.** DBE: DAF-16-binding element.

The *hsp-70* gene promoter contains at least one known consensus motif site for each of HSF-1, DAF-16, PHA-4 and CEH-58. *hsp-70* is a well-known transcriptional target of HSF-1 and the presence of HSEs in its promoter region is conserved across species (Lindquist 1986), so one would expect to find at least one consensus motif site for HSF-1 in its promoter. In fact, motif scanning identified two canonical (nGAAn) HSEs in the *hsp-70* promoter: a TTCCAGAA sequence at 243 bp upstream of the first ATG codon, and a TTCTAGAA sequence 895 bp upstream (**Fig. 6.9b**). Motif scanning also identified a GTAAACA sequence, or DAF-16-binding element (DBE; Furuyama et al. 2000; Murphy et al. 2003), at 744 base pairs upstream of ATG (**Fig.**

**6.9b**). Activation of DAF-16 by mutation of *daf-2* does not affect *hsp-70* expression (Gao et al. 2018), and *daf-16* is not required for upregulation of *hsp-70* upon heat stress (Hsu et al. 2003). However, when a *daf-16* mutation is introduced to *daf-2* mutants, there is a significant decrease in *hsp-70* expression (McElwee et al. 2003). It is therefore possible that *hsp-70* may be a direct transcriptional target of DAF-16. One PHA-4 motif of the form GTAAACAR (Contrino et al. 2012) was also identified in the *hsp-70* promoter, as the sequence GTAAACAT which occurs 744 bp upstream of the first ATG. However, genome-wide ChIP-Seq performed throughout embryos, larvae and young adults did not identify binding of PHA-4 in the *hsp-70* promoter (Niu et al. 2011), suggesting that this motif may not be biologically relevant for transcriptional regulation of *hsp-70*.

A consensus motif was also identified in the *hsp-70* promoter for the homeobox transcription factor CEH-58 (CIS-BP database, Narasimhan et al. 2015). The consensus motif NNTAATTRNN occurs 800 base pairs before the first ATG as the sequence GGTAATTGGG (**Fig. 6.9**). The presence of a CEH-58 consensus motif in the *hsp-70* promoter suggests that *hsp-70* could be a direct transcriptional target of CEH-58, and as *ceh-58* was identified as a *txt* gene acting in the body wall muscle to enhance *hsp-70* reporter expression (**Fig. 6.3b; Table 6.2**), this suggests that *hsp-70* reporter upregulation in the body wall muscle could be directly mediated by CEH-58.

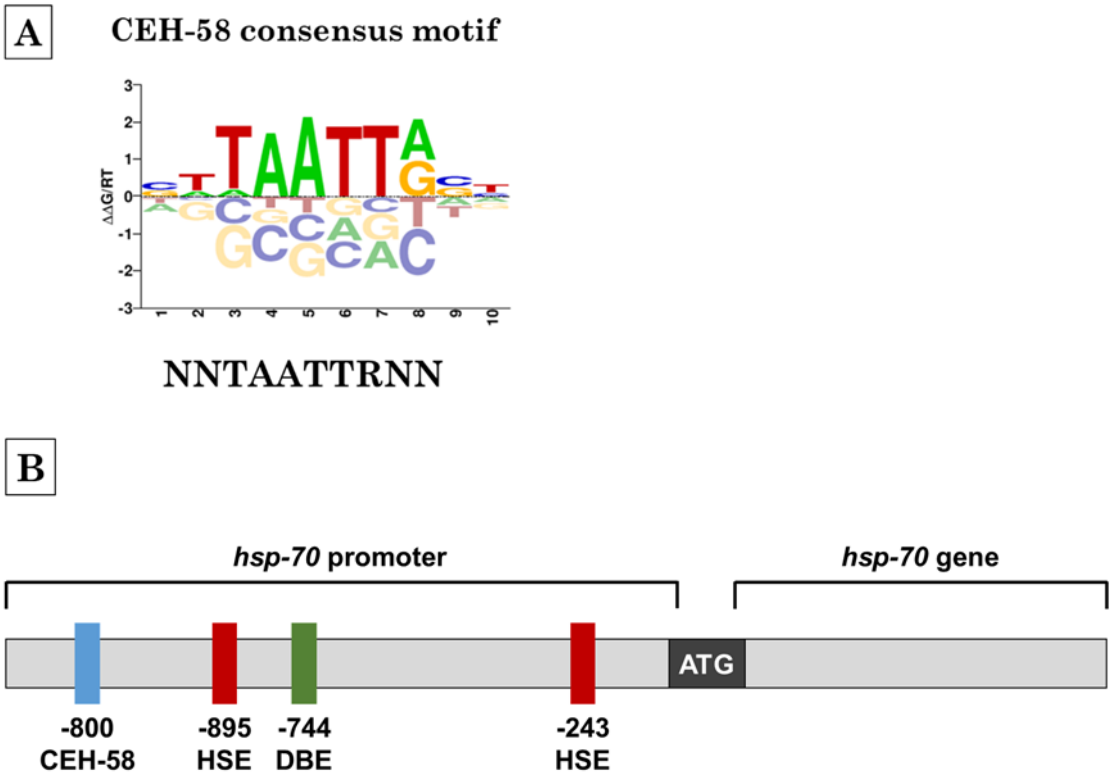


**Figure 6.9 The *hsp-70* promoter contains a CEH-58 consensus sequence**. (**A**) Consensus motif of CEH-58 (CIS-BP database, Narasimhan et al. 2015). (**B**) Locations of heat shock elements (HSEs), DAF-16-binding element (DBE) and predicted CEH-58 consensus site identified in the *hsp-70* gene promoter by motif scanning.

### 6.3.8 A possible model for *hsf-1*-independent *hsp-70* upregulation in the *hsp-90*$^{int}$ hp-RNAi strain

The *C50D2.3* gene was originally identified as a candidate for a role in TCS through forward genetic screening (**Table 5.5**), and was subsequently shown to act in the intestine of the *hsp-90*$^{int}$ hp-RNAi strain to suppress *hsp-70* reporter expression whilst acting in the body wall muscle to enhance it (**Fig. 6.3; Table 6.2**). *hsp-70* expression has previously been associated with longevity and survival following heat stress (Morley & Morimoto 2003; van Oosten-Hawle 2013). As the *hsp-70* reporter is particularly strongly upregulated in the body wall muscle of the *hsp-90*$^{int}$ hp-RNAi strain, where *C50D2.3* acts to enhance reporter expression, the role of *C50D2.3* in heat stress resistance was quantified. This showed that *C50D2.3* is required in both the intestine and body wall muscle of the *hsp-90*$^{int}$ hp-RNAi strain for heat stress survival (**Fig. 6.6**), indicating that it may have a particularly important role in TCS.

Little is known about the function of C50D2.3, but it is predicted to encode a PDZ domain protein (WormBase; Harris et al. 2010). Such proteins often act as scaffolds for larger multiprotein complexes at the inner cell membrane, performing functions including transmembrane receptor organisation and vesicle trafficking (Fanning & Anderson 1996; Nourry et al. 2003; Kim & Sheng 2004). In addition, analysis using BLAST identified the closest human homologue of C50D2.3 as the membrane-associated guanylate kinase MAGI1, which has a role in recruitment and surface presentation of signalling molecules at adherens junctions (Mizuhara et al. 2005). This suggests that the role of *C50D2.3* in the *hsp-90*$^{int}$ hp-RNAi strain may relate to signal transduction at the cell membrane, potentially of an inter-tissue signal between the intestine and body wall muscle.

Through protein interaction networks of *txt* genes with similar effects on TCS, *C50D2.3* was identified as having a large number of functional associations in each tissue (**Fig. 6.5**), suggesting that its interactions are relevant in reporter modulation. Ten interaction partners of C50D2.3 have previously been identified (Lenfant et al. 2010), of which eight were included in tissue-specific RNAi screening. This identified the *C50D2.3* interaction partners *ceh-58*, *dlat-1*, *rack-1* and *tsct-1* as *txt* genes, with the homeobox gene *ceh-58* also acting in the body wall muscle to enhance *hsp-70* reporter expression (T**able 6.2**; Hench et al. 2015). Dual knockdown of *C50D2.3* and *ceh-58* in the body wall muscle did not have an additive effect (**Fig. 6.8**), indicating

that the two genes act in the same pathway in this tissue to enhance reporter expression. Furthermore, motif scanning identified that the *hsp-70* gene promoter contains a consensus motif for CEH-58 (**Fig. 6.9**; CIS-BP database, Narasimhan et al. 2015). This indicates that CEH-58 may transcriptionally regulate *hsp-70*, which if it were the case would suggest a possible mechanism for *hsf-1*-independent upregulation of *hsp-70* in the body wall muscle of the *hsp-90*$^{int}$ hp-RNAi strain.

In the proposed model (**Fig. 6.10**), intestine-specific knockdown of *hsp-90* activates inter-tissue signalling to the body wall muscle. This is mediated through an inter-tissue signalling process which is still unclear, but which could involve *txt* genes identified as acting in the intestine. C50D2.3 in the body wall muscle mediates transduction of this inter-tissue signal into body wall muscle cells, resulting in a change in the interaction between C50D2.3 and CEH-58. This causes CEH-58 to become active as a transcriptional regulator, and through binding to its consensus motif in the *hsp-70* gene promoter, CEH-58 can then mediate the upregulation of *hsp-70* independently of HSF-1.

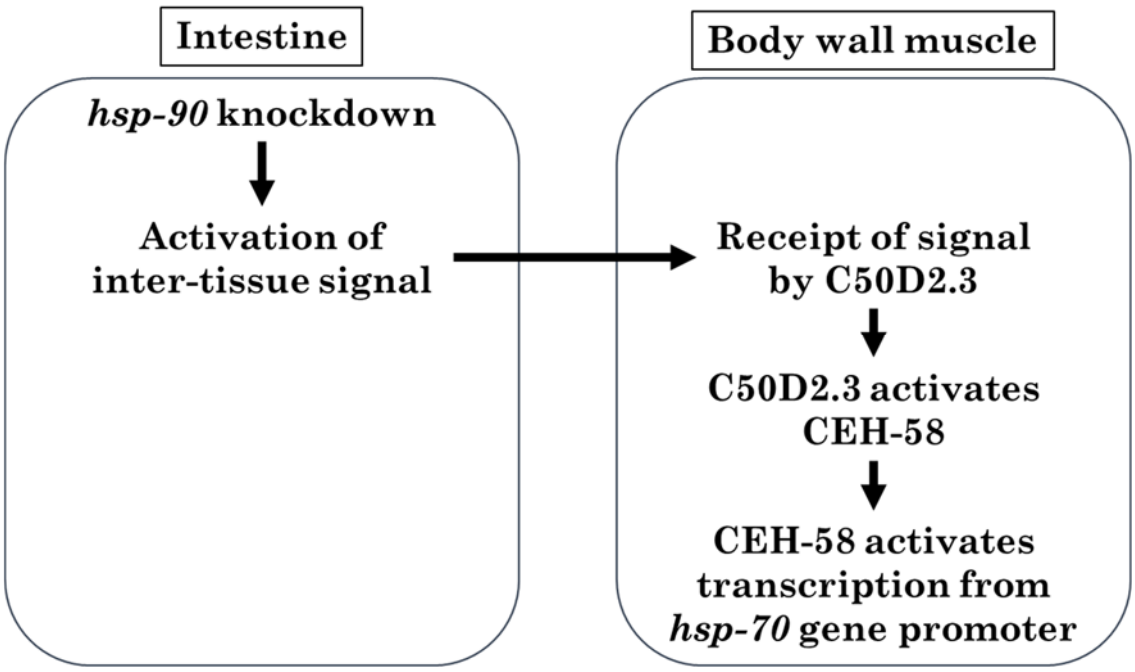


**Figure 6.10 Proposed model for *hsf-1*-independent *hsp-70* upregulation in response to intestine-specific *hsp-90* knockdown**.

## 6.4 Discussion

### 6.4.1 *daf-16* is identified as a tissue-specific modulator of *hsp-70* expression in the *hsp-90*$^{int}$ hp-RNAi strain

Tissue-specific RNAi screening confirmed that *hsf-1* expression in the body wall muscle of the *hsp-90*$^{int}$ hp-RNAi strain does not affect cell-non-autonomous *hsp-70* reporter upregulation (**Fig. 6.3b**). However, *hsf-1* was identified as acting in the intestine of this strain to suppress reporter expression (**Fig. 6.3a; Table 6.2**). A possible explanation for this might be that since *hsp-90* is a target gene of HSF-1, intestinal HSF-1 activity would promote upregulation of *hsp-90* and counteract its tissue-specific knockdown. This would reduce the 'stress' of intestinal *hsp-90* depletion and thereby potentially reduce TCS activation. In addition, motif scanning identified that an HSF-1 motif is present in the promoters of four other genes identified as acting in the intestine to suppress reporter expression: *cnd-1*, *daf-16*, *elt-2* and *tcst-1* (**Table 6.3**). The role of *hsf-1* in the intestine might therefore be to promote the expression of these genes, which could suppress TCS through downstream mechanisms.

A role for *pha-4* during TCS in the *hsp-90*$^{int}$ hp-RNAi strain was indicated by previous results, which showed that it is required for TCS activated by tissue-specific *hsp-90* knockdown (van Oosten-Hawle et al. 2013). However, tissue-specific RNAi screening in the *hsp-90*$^{int}$ hp-RNAi strain did not identify *pha-4* as acting in either the intestine or the body wall muscle to modulate *hsp-70p::mCherry* reporter expression (**Fig. 6.3**). Although *pha-4* is known to be expressed in the *C. elegans* intestine (Horner et al. 1998; Kalb et al. 1998), one of its key functions is as a pharyngeal 'organ identity factor' (Mango et al. 1994; Horner et al. 1998; Kalb et al. 1998). It is therefore possible that *pha-4* does act during TCS in the *hsp-90*$^{int}$ hp-RNAi strain, but in a different tissue such as the pharynx in which the effect of knockdown was not screened. Motif scanning also identified that 11 of the 29 identified *txt* genes, as well as *hsp-70*, have a PHA-4 consensus motif in their gene promoters (**Table 6.3**). One possibility is that by acting in another tissue such as the pharynx, *pha-4* may indirectly regulate *hsp-70* reporter expression by affecting the downstream transcriptional regulation of other genes identified as *txt* genes.

The paraquat-responsive transcription factor PQM-1 has also been shown to be involved in TCS, being required during TCS activated by tissue-specific HSP-90 overexpression (O'Brien et al. 2018). PQM-1 acts downstream of DAF-2 in a manner complementary to that of DAF-16, and both transcription factors are required for the increased longevity of DAF-2 mutants (Tepper et al 2013). Under non-stressful conditions, DAF-2 signalling inhibits DAF-16-mediated expression of immune and stress responsive genes whilst promoting PQM-1-mediated expression of developmental and metabolic genes (Tepper et al 2013). However, tissue-specific RNAi screening did not identify PQM-1 as acting in either the intestine or body wall muscle of the *hsp-90*$^{int}$ hp-RNAi strain to modulate *hsp-70* reporter expression (**Fig. 6.3**). As *pqm-1* was shown to act in the tissue from which TCS is activated in strains which overexpress HSP-90 (O'Brien et al. 2018), this suggests that *pqm-1* is not involved in TCS activated by intestine-specific *hsp-90* knockdown. However, it is possible that PQM-1 may still modulate TCS in this strain by acting in other tissues which were not screened, or that it may have a role in the *hsp-90*$^{neu}$ hp-RNAi strain.

*daf-16* was identified by screening as acting in the intestine to suppress *hsp-70* reporter expression (**Fig. 6.3a, Table 6.2**), indicating that ILS may indeed play a role in TCS activated by tissue-specific *hsp-90* knockdown. This could be further investigated by crossing the *hsp-90*$^{int}$ hp-RNAi and *hsp-90*$^{neu}$ hp-RNAi strains with *daf-2* or *daf-16* mutants, and observing the effect on *hsp-70* reporter expression. Since ILS affects longevity (Lin et al. 1997; Ogg et al. 1997), and the *hsp-90*$^{int}$ hp-RNAi strain has an increased lifespan compared to that of the *hsp-90*$^{control}$ strain, it might also be interesting to look at whether introducing such mutations would impact lifespan.

### 6.4.2 Screening identifies potential inter-tissue signalling molecules

One of the key questions relating to TCS is how the 'stress signal' activated by tissue-specific *hsp-90* depletion is transmitted from the affected tissue to elicit a cell-non-autonomous response in another tissue. A possible mechanism would be the release of an intracellular signalling molecule, which could interact with cell surface receptors on target cells and activate a signalling cascade. Alternatively, an intercellular signalling molecule could be taken up by endocytosis. It is also possible that signalling could occur by a completely different mechanism, for example

through cell-cell contacts. Whilst the mechanism of inter-tissue signalling is still unclear, the RNAi screen identified several genes which could act in intercellular signalling pathways.

The gene *F20A1.10* encodes a predicted soluble extracellular protein and acts in the intestine to enhance reporter expression (**Figs. 6.3a, 6.4; Table 6.2**). Such proteins could represent intracellular signalling molecules, which could be released from the intestine to activate reporter upregulation in the body wall muscle. In addition, the genes *K03H6.2*, *C01G10.16*, *C37C3.7*, *Y51A2D.14* and *ZK262.3* were also identified as encoding predicted soluble extracellular proteins, but as acting in the body wall muscle to modulate reporter expression. Release of extracellular proteins from the target tissue in TCS could indicate a possible feedback system, either to the intestine through paracrine signalling or between cells of the body wall muscle.

Three other genes predicted to encode transmembrane proteins at the cell membrane are *eat-2*, *srh-2* and *R02C2.6*, which were identified as acting in the intestine to suppress reporter expression (**Fig. 6.4; Table 6.2**). Proteins acting at the intestinal cell membrane to suppress reporter expression may suggest that they act in a negative feedback system, potentially by detection of signalling molecules released by the target tissue. *eat-2* is known to encode an acetylcholine (ACh)-gated cation channel which regulates pharyngeal pumping (Avery 1993) and *eat-2* mutations extend lifespan in a *daf-16*-independent manner (Lakowski & Hekimi 1998).

### 6.4.3 Two neuronal signalling-related genes enhance *hsp-70* reporter expression

Another signalling mechanism potentially involved during TCS is neuronal signalling. Although neuronal RNAi was not used in the tissue-specific RNAi screen, two genes normally involved in neuronal signalling were identified as acting in the intestine or the body wall muscle to modulate *hsp-70* reporter expression. These are *unc-13* and *unc-31,* two genes involved in vesicle exocytosis (**Table 6.2**). Whilst *unc-13* and *unc-31* are often considered in terms of their roles in neuronal signalling, they can also be expressed elsewhere; and tissue-specific transcriptomic profiling has shown that *unc-13* and *unc-31* transcripts can also be expressed in the body wall muscle (Cao et al. 2017).

*unc-13* and *unc-31* were identified as acting in the body wall muscle to enhance TCS (**Fig. 6.3b; Table 6.2**). A key function of these genes is to enable the release of SCVs and DCVs respectively during neurotransmission (Richmond et al. 1999; Speese et al. 2007). Since these genes were identified as acting in the muscle, this could suggest that retrograde synaptic signalling from the muscle to neurons may occur during TCS. Such signalling has been shown to regulate presynaptic neurotransmitter release at the *C. elegans* neuromuscular junction (NMJ) (Zhao & Nonet 2000; Doi & Iwasaki 2002), for example through the interaction of postsynaptic neurexin with presynaptic neuroligin, which suppresses presynaptic ACh release by inhibiting presynaptic calcium channels (Hu et al. 2012; Tong et al. 2017). Retrograde signalling from the body wall muscle to the neurons would imply that the nervous system may also be involved in TCS in the *hsp-90*$^{int}$ hp-RNAi strain, and possibly suggest central control of organismal TCS through the neurons. As control of systemic stress responses by the nervous system has been shown to occur in the HSR (Prahlad et al. 2008), UPR$^{ER}$ (Sun et al. 2011, 2012(a); Taylor & Dillin 2013) and UPR$^{Mt}$ (Berendzen et al. 2016), it is not implausible to consider that the same may be true for TCS.

### 6.4.4 C50D2.3 may be involved in *hsf-1*-independent regulation of *hsp-70*

The gene *C50D2.3* was originally identified as a candidate regulator of TCS through forward genetic screening (**Table 5.5**), and subsequently shown in the RNAi screen to act in the body wall muscle of the *hsp-90*$^{int}$ hp-RNAi strain to enhance *hsp-70* reporter expression whilst acting in the intestine to suppress it (**Fig. 6.3; Table 6.2**). *C50D2.3* was also identified as acting in both the intestine and body wall muscle to promote heat stress resistance (**Figure 6.6**), suggesting that its enhancement of *hsp-70* reporter expression in the body wall muscle is important for survival during TCS in this strain. As *C50D2.3* acts in the intestine to suppress *hsp-70p::mCherry* reporter expression, it seems at first counterintuitive that it should be required in the intestine to promote heat stress survival. A possible explanation might be that during TCS, *C50D2.3* could function in a cell-autonomous manner to promote *hsp-70* upregulation. In the body wall muscle, this would promote increased expression of the *hsp-70* reporter, and indeed *C50D2.3* acts in the body wall muscle to enhance reporter expression (**Fig. 6.3b; Table 6.2**). Conversely, in the intestine, upregulation of *hsp-70* might promote an improved folding environment which could reduce the

strain of depleted *hsp-90*. This could reduce the tissue-specific 'stressor', potentially leading to reduced activation of TCS. However, as *C50D2.3* knockdown does not prevent *hsp-70* reporter upregulation in the *hsp-70p::mCherry* reporter strain following heat stress (**Fig. 6.7**), *C50D2.3*-mediated enhancement of *hsp-70* reporter expression appears to be specific to TCS.

*C50D2.3* may mediate its tissue-specific effects on TCS through interactions with different, tissue-specific interaction partners. CEH-58, RACK-1 and TSCT-1 were previously identified as interaction partners of C50D2.3 (Lenfant et al. 2010), and were shown in through tissue-specific RNAi screening to act in either the body wall muscle or intestine with the same effect on *hsp-70* reporter expression as *C50D2.3* (**Fig. 6.3a; Table 6.2**). *C50D2.3* and *ceh-58* both act in the body wall muscle to enhance reporter expression, and a possible model for *hsf-1*-independent upregulation of *hsp-70* by *C50D2.3* and *ceh-58* acting in the body wall muscle has been proposed (**Section 6.3.2**). In contrast, *C50D2.3*, *rack-1* and *tsct-1* act in the intestine to suppress reporter expression. Like *C50D2.3*, little is known about *tsct-1*, but it is predicted to encode a transcription factor (Reinke et al. 2013). This is consistent with the subcellular localisation for its encoded protein, which was predicted to be soluble and localised to the nucleus (**Fig. 6.4**); and suggests that transcriptional regulation by *tsct-1* may be involved in TCS. *rack-1* is an orthologue of the human scaffold protein Receptor for Activated C Kinase and is required in *C. elegans* for resistance to *Shigella flexneri* infection (Marudhupandiyan et al. 2017). As a scaffold protein which was also predicted to be localised to the nucleus (**Fig. 6.4**), it is possible that *rack-1* may be linked to *tsct-1* function in the nucleus of intestinal cells.

To consider the regulation of *C50D2.3* itself, expression of *C50D2.3* has previously been shown to be affected by *hsf-1* and *daf-2*. A screen for genes regulated by *hsf-1* identified that expression of *C50D2.3* is reduced in animals grown on *hsf-1* RNAi (Brunquell et al. 2016). Transcriptomic analysis of *daf-2* (e1370) mutants identified that *C50D2.3* expression is also increased in these animals compared to wild-type (Gao et al. 2018). However, no consensus motifs for HSF-1 or DAF-16 were identified in the *C50D2.3* promoter (**Table 6.3**), and so these may be indirect effects.

The data presented in this chapter enabled the proposition of a model for cell-non-autonomous, *hsf-1*-independent upregulation of *hsp-70* in the body wall muscle of

the *hsp-90*$^{int}$ hp-RNAi stain (**Section 6.3.8**). However, this model requires further experimental support. Firstly, it is necessary to quantify the level of *C50D2.3* and *ceh-58* knockdown achieved by single or dual tissue-specific RNAi; and the corresponding decrease in *hsp-70* expression. This could be done by qRT-PCR using primers targeting the relevant transcripts. In order to prove that CEH-58 binds in the *hsp-70* gene promoter, a chromatin-immunoprecipitation (ChIP) coupled to qPCR could be performed (ChIP-qPCR). If CEH-58 does bind to the motif in the *hsp-70* gene promoter, it would be co-immunoprecipitated using an antibody against CEH-58. The DNA could then be amplified by qPCR with primers targeting the motif-containing region. However, if CEH-58 does not bind, the DNA will not be amplified as it will not be immunoprecipitated with CEH-58. Another alternative approach would be to use a strain that harbours a mutation or deletion of the predicted CEH-58 consensus sequence in the *hsp-70* promoter region of the *hsp-70p::mCherry* transgene.

To determine whether *C50D2.3* and *ceh-58* are required for cell-non-autonomous *hsp-70* reporter upregulation in *hsp-90*$^{int}$ hp-RNAi, it would be useful to generate mutant strains with loss-of-function mutations in *C50D2.3* or *ceh-58*, for example using CRISPR. These strains could then be crossed with *hsp-90*$^{int}$ hp-RNAi to determine the effect on reporter expression; although in this case loss of function would be systemic. Alternatively, *C50D2.3* or *ceh-58* hp-RNAi could be expressed under the control of a body wall muscle-specific promoter such as *myo-3*p, in a *sid-1* background. This would facilitate tissue-specific gene knockdown, enabling investigation of the roles of these genes within the 'receiving' tissue. If the model in **Figure 6.10** is correct, one would expect that knockdown of either *C50D2.3* or *ceh-58* in the body wall muscle would result in a loss of reporter upregulation.

# Chapter 7. Conclusions & future directions

## 7.1 Key results and conclusions

TCS activated by tissue-specific *hsp-90* hp-RNAi in extrachromosomal arrays has previously been shown to cause cell-non-autonomous *hsp-70p::mCherry* reporter expression, increased organismal *hsp-70* expression, and increased resistance to heat stress (van Oosten-Hawle et al. 2013). The research presented here aimed firstly to characterise the effects of TCS activation in strains expressing tissue-specific *hsp-90* hp-RNAi in integrated arrays, and secondly to identify genes which are required for transcellular *hsp-70* upregulation in the body wall muscle when *hsp-90* is knocked down in the intestine. In addition to the effects of TCS activation on the organismal transcriptome, effects on longevity and stress responses have been described; although further experiments are required for greater confidence in these results. Based on these results we can suggest a change in how TCS might be considered in future research. Furthermore, 29 previously unknown modulators of TCS which is activated by intestine-specific *hsp-90* knockdown have been identified, enabling a partial model to be proposed for *hsf-1*-independent *hsp-70* upregulation in this form of TCS. This may form a foundation for further investigation of this pathway.

It was firstly shown that consistent with published data (van Oosten-Hawle et al. 2013), the integrated *hsp-90*$^{int}$ hp-RNAi and *hsp-90*$^{neu}$ hp-RNAi strains used here demonstrate activation of TCS. These strains exhibit cell-non-autonomous upregulation of an *hsp-70p::mCherry* reporter (**Fig. 3.2**) in addition to whole-animal upregulation of *mCherry* and endogenous *hsp-70* transcripts (**Fig 3.5a**). The *hsp-90*$^{int}$ hp-RNAi strain, in which *hsp-70* is more strongly upregulated, demonstrates increased lifespan compared to controls (**Fig. 3.6**); whereas the *hsp-90*$^{neu}$ hp-RNAi strain demonstrates increased survival following oxidative stress (**Fig. 3.8**). This suggests that cell-non-autonomous expression of *hsp-70* may be upregulated by TCS in order to confer organismal protection against stress induced by tissue-specific *hsp-90* depletion.

It was also shown that expression of the *hsp-70* reporter in the *hsp-90*$^{int}$ hp-RNAi and *hsp-90*$^{neu}$ hp-RNAi strains does not depend on the transcription factor *hsf-1* (**Figs. 3.3c-f, 3.4**). In fact, *hsf-1* acts in the intestine of the *hsp-90*$^{int}$ hp-RNAi strain to suppress reporter expression (**Table 6.2**). This confirms that *hsp-70* upregulation in these strains does not require *hsf-1* activity, indicating that TCS acts as a cell-non-autonomous stress response which is distinct from the *hsf-1*-mediated HSR. In strains with tissue-specific *hsp-90* knockdown, *hsp-70p::mCherry* reporter expression has previously been shown to depend on the transcription factor PHA-4 (van Oosten-Hawle et al. 2013). However, tissue-specific RNAi screening in the *hsp-90*$^{int}$ hp-RNAi strain determined that *pha-4* is not required in either the intestine or the body wall muscle for *hsp-70* reporter expression in this strain (**Fig. 6.3; Table 6.3**). As PHA-4 is known to be strongly expressed in the pharynx as an 'organ identity factor' (Mango et al. 1994; Horner et al. 1998; Kalb et al. 1998), it is possible that it is instead required in this tissue for TCS.

Transcriptomic profiling in the *hsp-90*$^{int}$ hp-RNAi and *hsp-90*$^{neu}$ hp-RNAi strains proved exceedingly useful in the identification of genes which are differentially expressed during TCS (**Appendix 1**). Although weaker expression of *hsp-70* and the *hsp-70* reporter in the *hsp-90*$^{neu}$ hp-RNAi strain suggests that TCS may not be activated as strongly in this strain (**Figs. 3.2, 3.5a**), RNA-Seq identified that over 2000 genes are differentially regulated in this strain compared to the control (**Fig. 4.4**). RNA-Seq also identified that in both the *hsp-90*$^{int}$ hp-RNAi and *hsp-90*$^{neu}$ hp-RNAi strains, expression of immune genes differs from controls (**Figs. 4.10a, 4.12**). Proteostasis and immunity can both be activated during organismal stress responses (Murphy et al. 2003; Berman & Kenyon 2006; Reddy et al. 2017), and certain chaperones such as sHSPs, which are required for lifespan extension in ILS mutants (Morley & Morimoto 2004), have been shown to be regulated by both HSF-1 and DAF-16 (Hsu et al. 2003). Motif scanning in the promoters of differentially expressed genes common to both the *hsp-90*$^{int}$ hp-RNAi and *hsp-90*$^{neu}$ hp-RNAi strains also identified that many contain known consensus motifs for DAF-16 (**Tables 4.9, 4.10**), indicating that ILS and DAF-16-mediated transcriptional regulation could potentially have a role in TCS. This is supported by tissue-specific RNAi screening, which identified that DAF-16 acts in the intestine of the *hsp-90*$^{int}$ hp-RNAi strain to suppress *hsp-70* reporter expression in the muscle (**Fig. 6.2a, Table 6.2**).

A forward genetic screen with one-step mapping and sequencing in the *hsp-90*$^{int}$ hp-RNAi strain identified 49 SNPs associated with a phenotype of altered *hsp-70p::mCherry* reporter expression (**Chapter 5**), annotation of which identified 42 genes as potential regulators of reporter expression (**Tables 5.5, 5.6**). However, it was not clear which of the identified SNPs were causal for the associated phenotype, and it was therefore necessary to determine experimentally whether each gene has a role in TCS. To this end, a tissue-specific RNAi screen was performed, with the aim of identifying tissue-specific modulators of *hsp-70p::mCherry* reporter expression in animals harbouring intestine-specific *hsp-90* knockdown. In addition to the 42 genes identified using SNP mapping, the screen included as candidates 17 genes which were identified as upregulated in both the *hsp-90*$^{int}$ hp-RNAi and *hsp-90*$^{neu}$ hp-RNAi strains, and a number of other genes identified as potentially relevant to TCS. The outcome of the screen was the identification of 29 genes which act as tissue-specific modulators of transcellular *hsp-70p::mCherry* reporter expression (**Table 6.2**), and which have now been termed TCS cross (X)-Tissue (*txt*) genes. These genes were not previously known to be associated with TCS activated by tissue-specific *hsp-90* knockdown.

A key question relating to TCS is the mechanism by which the stimulus of tissue-specific *hsp-90* knockdown is transmitted between tissues to achieve *hsp-70* reporter upregulation in other tissues. Tissue-specific RNAi screening in the *hsp-90*$^{int}$ hp-RNAi strain identified six *txt* genes which are predicted to encode soluble extracellular proteins, and which may therefore represent intercellular signalling molecules in TCS (**Fig. 6.4**). One of these genes, *F20A1.10*, was identified as acting in the intestine of this strain to enhance transcellular signalling. The remaining five genes, *K03H6.2*, *C01G10.16*, *C37C3.7*, *Y51A2D.14* and *ZK262.3*, act in the body wall muscle; all were identified as suppressors of reporter expression except *K03H6.2*, which was identified as an enhancer. In addition, four *txt* genes (*col-20*, *eat-2*, *srh-2* and *R02C2.6*) were identified as encoding predicted transmembrane proteins localised to the cell membrane, and which could potentially be involved in transmembrane signal transduction during TCS (**Fig. 6.4**). Tissue-specific RNAi screening and subsequent bioinformatic analysis, such as the prediction of protein subcellular localisation, therefore proved powerful tools in identifying not only tissue-specific genetic modulators of TCS but also their possible roles within signalling pathways.

There are indications that TCS in the *hsp-90*$^{int}$ hp-RNAi and *hsp-90*$^{neu}$ hp-RNAi strains may involve neuronal signalling. Several modes of cell-non-autonomous stress signalling are co-ordinated by the nervous system in *C. elegans* (Prahlad et al. 2008; Sun et al. 2011, 2012(a); Taylor & Dillin 2013; Berendzen et al. 2016), so it is possible that this is also true for TCS. RNAi screening in the *hsp-90*$^{int}$ hp-RNAi strain identified two *txt* genes with roles in neuronal signalling: *unc-13* and *unc-31* (**Table 6.2**). These genes, which are involved in exocytosis of SCVs and DCVs respectively (Richmond et al. 1999; Speese et al. 2007), act in the body wall muscle of the *hsp-90*$^{int}$ hp-RNAi strain to enhance TCS (**Fig. 6.3b, Table 6.2**). This could indicate that retrograde synaptic signalling at the neuromuscular junction could be involved in TCS (Zhao & Nonet 2000). Genes relating to neuropeptide signalling were also identified as enriched amongst those upregulated in the *hsp-90*$^{neu}$ hp-RNAi strain (**Fig. 4.10a**); however, as TCS is activated from the neurons in this strain this is perhaps to be expected. The identification of neuronal signalling genes acting in the *hsp-90*$^{int}$ hp-RNAi strain suggests that TCS may not affect only the 'sending' and 'receiving' tissues affected by *hsp-90* knockdown or *hsp-70p::mCherry* reporter upregulation, but may also involve signalling with other tissues.

The gene *C50D2.3*, which encodes a predicted PDZ domain protein, was identified as a *txt* gene acting in both the intestine and body wall muscle of the *hsp-90*$^{int}$ hp-RNAi strain (**Fig. 6.3, Table 6.2**). Importantly, it was also shown to be required in both of these tissues for heat stress resistance in the *hsp-90*$^{int}$ hp-RNAi strain (**Fig. 6.6**). This suggests that regulation of *hsp-70* by *C50D2.3* is important for the protective effects of TCS in the *hsp-90*$^{int}$ hp-RNAi strain such as increased lifespan (**Fig. 3.6**). *C50D2.3* and a known interaction partner, the homeobox transcription factor *ceh-58* (Lenfant et al. 2010), were both shown to act in the body wall muscle of the *hsp-90*$^{int}$ hp-RNAi strain to enhance reporter expression in a non-synergistic manner (**Table 6.2**; **Fig. 6.8**). This suggests the two genes act in the same pathway during TCS. Furthermore, motif scanning revealed that the *hsp-70* gene promoter contains a known consensus motif recognised by CEH-58 (**Fig. 6.9**; CIS-BP database, Weirauch et al. 2014). Taken together, these results suggest a possible model for *hsf-1*-independent transcriptional regulation of *hsp-70* in the body wall muscle of the *hsp-90*int hp-RNAi strain (**Fig. 6.10**). In the proposed model, intestine-specific *hsp-90* knockdown activates a cell-non-autonomous signal, which is received at the body wall muscle. Receipt of this signal causes a change in the interaction between C50D2.3 and CEH-58 within the body wall muscle, which leads to transcriptional

regulation of *hsp-70* by CEH-58. This results in cell-non-autonomous upregulation of the *hsp-70* reporter in the body wall muscle in a manner independent from *hsf-1*.

## 7.2 Limitations of the research

Previous research using strains expressing tissue-specific *hsp-90* RNAi transgenes in extrachromosomal arrays identified that these strains have increased survival compared to controls following 4, 8 or 10 hours of heat shock (van Oosten-Hawle et al. 2013). However, the strains used here which express tissue-specific *hsp-90* RNAi in integrated arrays only displayed increased survival following 4 hours of heat stress (**Fig. 3.7**). After 8 or 10 hours of heat stress, the survival of integrated strains expressing intestine-specific *hsp-90* RNAi is not significantly different to controls, and that of animals expressing pan-neuronal *hsp-90* RNAi is in fact decreased. An important role of HSP-90 is in buffering mutations and it is possible that its knockdown in these strains allows the expression of mutants which would otherwise be cryptic. As these strains demonstrate increased organismal expression of *hsp-70* (**Fig. 3.5a**), the cellular folding environment might be improved sufficiently to confer resistance to an acute stress of 4 hours; but not a chronic stress of 8 or 10 hours which could compound the challenges faced by the proteostasis network. A method to address this could be to reduce the prevalence of such cryptic mutants by backcrossing to the *sid-1* (*pk3321*) mutant strain again. This could be done for an increased number of generations, for example 10 backcrosses instead of 5; and then thermotolerance assays repeated immediately before cryptic variants can arise. It would also be beneficial to repeat the experiment using the strains carrying extrachromosomal arrays as controls, to confirm that the results are reproducible and that the difference in these integrated strains is truly a consequence of transgene integration.

The one-step mapping and sequencing approach was highly useful for identifying genes which would not otherwise have been identified as modulators of TCS, including the key gene *C50D2.3*. However, this method was insufficient to identify any specific gene as required for TCS, as no SNP was identified at which no CB4856 alleles were present. It was therefore necessary to consider multiple SNPs with allele ratios below an arbitrarily 'low' threshold. It is possible that by introducing a cut-off value for the allele ratio, other relevant SNPs with an incrementally higher ratio may have been excluded. However, due to the number of SNPs identified in each phenotype, the introduction of a threshold was necessary, as it would not have been possible to screen all genes predicted to be affected otherwise.

Transcriptomic profiling and forward genetic screening together identified numerous potential genetic modulators of TCS. However, the ability to investigate whether these genes act as tissue-specific modulators of *hsp-70* reporter expression in the *hsp-90*$^{int}$ hp-RNAi strain relied on tissue-specific RNAi screening. Whilst this screen proved a powerful method for identifying which genes act as tissue-specific regulators of TCS, it was not possible to screen all the genes identified in **Chapters 4 and 5**, as clones were not available for every gene in the extended Ahringer RNAi library (Source Bioscience; Kamath & Ahringer 2003). This means that some genes which could not be screened may also act as tissue-specific modulators of TCS in the *hsp-90*$^{int}$ hp-RNAi strain. In addition, there was insufficient time to also perform tissue-specific RNAi screening in the *hsp-90*$^{neu}$ hp-RNAi strain. This means that the 29 candidate *txt* genes identified in **Chapter 6** still need to be investigated as tissue-specific modulators of TCS in animals harbouring pan-neuronal *hsp-90* knockdown.

## 7.3 Future directions

A striking observation relating to the organismal effects of TCS activation by tissue-specific *hsp-90* depletion is that when comparing the integrated strains with intestine-specific or pan-neuronal *hsp-90* knockdown, the two exhibit contrasting results for the majority of phenotypes studied here. The *hsp-90*$^{int}$ hp-RNAi strain demonstrates increased lifespan whilst the *hsp-90*$^{neu}$ hp-RNAi strain does not (**Fig. 3.6**); the *hsp-90*$^{neu}$ hp-RNAi strain appears to have exacerbated sensitivity to chronic heat stress (**Fig. 3.7**) but also increased resistance to oxidative stress (**Fig. 3.8**), neither phenotype of which is shared with the *hsp-90*$^{int}$ hp-RNAi strain; and in the *hsp-90*$^{neu}$ hp-RNAi strain hundreds more genes are differentially expressed at the whole-organism level and in an utterly contrasting pattern to that of the *hsp-90*$^{int}$ hp-RNAi strain (**Figs. 4.4, 4.5**). This suggests that rather than utilising common signalling mechanisms or sharing whole-organism consequences of TCS activation irrespective of the tissue in which *hsp-90* is knocked down, these two strains appear to represent distinct forms of TCS which perhaps ought to be considered as different phenomena. This is further supported by the fact that *pqm-1*, which is required in the case of TCS activated by tissue-specific HSP-90 overexpression (O'Brien et al. 2018), does not appear to be required for TCS in the *hsp-90*$^{int}$ hp-RNAi strain (**Figs. 6.3, 6.4**). A suggestion for future research might be a re-contextualisation of 'TCS' as a collective term referring to a group of related but distinct processes, which have differing organismal consequences and appear to act through different signalling mechanisms, and which might benefit from being considered separately from each other.

This research has identified genes which act as tissue-specific modulators of *hsp-70* reporter expression in animals with intestine-specific *hsp-90* knockdown (*txt* genes). Based on predictions of subcellular localisation for the proteins encoded by these genes, several candidates for potential inter-tissue TCS signalling molecules have been revealed. In addition, identification of two *txt* genes which appear to act in the same pathway and may transcriptionally regulate *hsp-70* has enabled the proposal of a model for *hsf-1*-independent upregulation of *hsp-70* during TCS. However, a great deal remains unknown regarding many aspects of transcellular *hsp-70* upregulation between the intestine and muscle. Key questions for future research include how knockdown of *hsp-90* in the intestine leads to the transmission of a signal beyond the cell affected. HSP-90 is a promiscuous chaperone, with over 300

known clients across various species (Picard 2002; Taipale et al. 2010; Röhl et al. 2013), and its depletion is therefore likely to have wide-ranging cellular consequences. The 14 genes identified here as acting as intestine-specific modulators of *hsp-70* expression, in animals with intestine-specific *hsp-90* knockdown (**Table 6.2**), may offer a starting point for the investigation of how TCS is initiated within the intestine.

Another interesting consideration is the potential involvement of neuronal signalling. Signalling from neurons has been shown to regulate the organismal HSR (Prahlad et al. 2008), UPR$^{ER}$ (Taylor & Dillin 2013), UPR$^{Mt}$ (Berendzen et al. 2016) and immune response (Styer et al. 2008); suggesting that central co-ordination by the nervous system may be a common theme in cell-non-autonomous stress responses. As certain sensory neurons are responsible for detecting a stressor such as adverse temperature or pathogen-derived molecules (Prahlad et al. 2008; Tatum et al. 2015; Pradel et al. 2007; Brandt & Ringstad 2015), and activating a cell-non-autonomous HSR or immune response; so too may other cell-non-autonomous stress responses such as TCS involve the activation of specific neural pathways. A possible approach to investigate this further would be to observe the effect on *hsp-70* reporter expression in animals exhibiting ablation or inactivation of individual neurons, which could identify specific neurons involved in such a process.

A more abstract question raised by TCS is its evolutionary context. In other stress responses, a biological challenge has presumably exerted evolutionary pressure on cells to the extent that a conserved stress response has been developed. For example, relevant stressors driving the HSR, UPR$^{ER}$, UPR$^{Mt}$ and immune response might include varying environmental temperature, production of large amounts of secretory proteins, high rates of aerobic respiration leading to increased ROS production, and pathological infection. But how would an organism develop a cell-non-autonomous stress response which appears to be specifically catered to perturbations in HSP-90 expression? Depletion of *hsp-90* results in developmental phenotypes (van Oosten-Hawle et al. 2013; Eckl et al. 2017) whilst overexpression results in suppression of organismal stress resistance (van Oosten-Hawle et al. 2013). Thus, a stress response which acts to correct such perturbated expression would no doubt be beneficial. But in order for such a response to arise, the 'stressor' would presumably need to occur with sufficient frequency to exert evolutionary pressure. One possibility could be that TCS has evolved as a stress response to fulfil

protein folding requirements during development, when other stress response transcription factors may be occupied with development-related functions. For example, *hsf-1* has been shown to regulate a developmental program which is distinct from the HSR (Li et al. 2016), suggesting that it may not be available to respond to heat stress during development. This could explain why TCS appears to be independent of *hsf-1* (**Figs. 3.3c-f, 3.4**; van Oosten-Hawle et al. 2013), as the two responses may in fact function in parallel.

Somewhat related to this is the question of whether TCS occurs beyond *C. elegans*. Systemic overexpression of Hsp90 in mice results in destabilisation of atherosclerotic plaques and inflammation (Mu et al. 2016), which may reflect a connection between organismal proteostasis and immune responses. Tissue-specific Hsp90 upregulation within tumour cells is implicated in cancer, with increased Hsp90 expression contributing to increased survival of tumour cells by buffering against mutations (Whitesell & Lindquist 2005). In addition to this, the presence of Hsf1 in mouse embryonic fibroblasts promotes growth and malignancy in associated cancer cells (Scherz-Shouval et al. 2014), indicating that Hsf1 is involved in the cell-non-autonomous regulation of tumour development. Furthermore, cell-non-autonomous stress signalling has also been demonstrated *in vivo*. Rats subjected to behavioural stress exhibit neuroendocrine activation of the adrenal HSR (Fawcett et al. 1994); and overexpression of Xbp1s in the Pomc neurons of mice results in cell-non-autonomous upregulation of Xbp1s and target genes in the liver (Williams et al. 2014). This indicates that control of proteostasis between tissues does occur in mammals, supporting the theory that TCS may also be conserved.

The idea that *hsp-90* modulation in one tissue can confer cell-non-autonomous benefits to stress resistance, proteostasis, or longevity has interesting implications when considered in terms of treatments for protein-misfolding disorders or the maintenance of health during aging. Could alteration of Hsp90 activity in the intestine, perhaps by oral administration of a drug, slow the progression of protein-misfolding diseases in the nervous system? Could activation of systemic proteostasis promote increased proteomic health in an aging population? These possibilities might be appealing, but they are currently only speculative. However, whilst considerable further research is still required in the field, the application of TCS may be able to change our approach to treating conditions of proteostasis.

# Appendix 1

Lists of genes identified by RNA-Seq and differential expression analysis performed by Novogene as differentially expressed compared to the *hsp-90*$^{control}$ strain (**Chapter 4**). Named genes are listed first in each table. Genes are listed in alphabetical order.

**Table A1**. Genes upregulated in the *hsp-90*$^{control}$ strain compared to N2.

| | | | | | | |
|---|---|---|---|---|---|---|
| *acly-1* | *clec-67* | *hacd-1* | *scb-1* | *C08E3.13* | *F25E5.1* | *T22F7.4* |
| *asp-12* | *clec-72* | *his-32* | *scl-24* | *C14C6.5* | *F33E2.5* | *T24B8.5* |
| *bath-47* | *col-41* | *hpo-15* | *scrm-4* | *C18D4.6* | *F33H12.7* | *W03F9.4* |
| *clec-118* | *cpr-3* | *ilys-2* | *sru-40* | *C25F9.11* | *F55G11.7* | *W07B8.4* |
| *clec-17* | *cyp-33C8* | *ilys-3* | *srw-86* | *C34H4.1* | *F59C6.18* | *Y37H2A.14* |
| *clec-265* | *dct-19* | *ins-7* | *swt-6* | *C36C5.12* | *K03D3.2* | *Y41C4A.11* |
| *clec-33* | *dlhd-1* | *irg-3* | *tba-7* | *C50D2.6* | *K05B2.4* | *Y46D2A.2* |
| *clec-38* | *ech-7* | *lys-10* | *B0205.13* | *D2063.1* | *T01D3.6* | *Y49G5A.1* |
| *clec-4* | *ech-9* | *lys-2* | *B0205.14* | *F01D5.3* | *T19D12.4* | *Y54G11A.4* |
| *clec-42* | *elo-2* | *math-15* | *B0334.3* | *F20G2.5* | *T20B3.1* | *Y68A4A.13* |
| *clec-66* | *gst-38* | *mul-1* | *B0348.2* | *F25A2.1* | *T22F7.1* | |

**Table A2**. Genes downregulated in the *hsp-90*$^{control}$ strain compared to N2.

| | | | | | | |
|---|---|---|---|---|---|---|
| *abu-2* | *col-2* | *gst-10* | *pgph-3* | *B0454.8* | *K03A1.4* | *Y71G12B.18* |
| *abu-4* | *cth-1* | *hsp-70* | *pks-1* | *C06G1.2* | *K06H6.1* | *ZC581.3* |
| *acs-1* | *cutl-5* | *lrx-1* | *plpp-1.2* | *C08B6.2* | *K08C7.1* | |
| *argk-1* | *cyp-13A4* | *myo-1* | *pqn-26* | *C40H1.8* | *M02G9.2* | |
| *cest-2.1* | *cyp-13A5* | *myo-2* | *ptrn-1* | *D2024.4* | *M60.7* | |
| *clec-169* | *cyp-35D1* | *nhr-17* | *str-7* | *F10C2.7* | *T05H4.7* | |
| *clec-258* | *gmd-2* | *nhr-175* | *ugt-63* | *F40E10.5* | *W08F4.7* | |
| *clec-47* | *grl-23* | *pgp-1* | *ugt-8* | *F45D3.4* | *Y5H2A.4* | |

**Table A3**. Genes upregulated in the *hsp-90*$^{int}$ hp-RNAi strain compared to the *hsp-90*$^{control}$ strain.

| | | | | | | |
|---|---|---|---|---|---|---|
| *acs-1* | *fbxb-83* | *nhr-214* | *srj-37* | *C04C3.6* | *F45E1.4* | *T22B2.1* |
| *acy-1* | *fbxc-31* | *nhr-217* | *srr-10* | *C04E6.8* | *F46B6.2* | *T24D5.1* |
| *aex-5* | *fbxc-33* | *nhr-290* | *sru-13* | *C06A1.2* | *F46C5.10* | *W03D8.1* |
| *akir-1* | *flp-32* | *nhx-3* | *srx-43* | *C08E8.3* | *F47B8.10* | *W03D8.7* |
| *alh-2* | *frpr-8* | *nlp-55* | *srx-47* | *C14B1.3* | *F48G7.12* | *W04C9.4* |
| *argk-1* | *gcy-25* | *nlp-68* | *srxa-2* | *C18H9.6* | *F53F4.14* | *W05H12.1* |
| *asns-2* | *gpa-7* | *nphp-2* | *srz-78* | *C26B9.3* | *F53F4.4* | *Y116F11A.6* |
| *atl-1* | *gst-10* | *npr-24* | *ssu-1* | *C26D10.3* | *F54B11.10* | *Y19D10B.6* |
| *best-21* | *gst-11* | *nspc-4* | *str-112* | *C27A7.9* | *F54C1.6* | *Y27F2A.10* |
| *brc-1* | *gst-28* | *numr-2* | *str-14* | *C27F2.9* | *F54C9.9* | *Y38E10A.14* |
| *ceh-2* | *gst-35* | *par-4* | *str-196* | *C33B4.2* | *F54E4.3* | *Y39B6A.13* |
| *cest-9.2* | *his-73* | *pat-10* | *str-230* | *C36B1.11* | *F55G11.2* | *Y39B6A.43* |
| *clec-130* | *hnd-1* | *pgp-1* | *str-7* | *C37C3.7* | *F55H12.2* | *Y41D4A.1* |
| *clec-131* | *hop-1* | *phat-5* | *str-8* | *C40H1.8* | *F56H6.9* | *Y42G9A.3* |
| *clec-161* | *hpo-18* | *phf-34* | *swt-3* | *C46C2.3* | *F58F12.4* | *Y43B11AL.1* |
| *clec-169* | *hsp-70* | *phf-5* | *syg-1* | *C49A1.5* | *F59A6.5* | *Y43F8B.20* |
| *clec-206* | *irg-1* | *plpp-1.2* | *tmed-1* | *C49C3.7* | *F59C6.8* | *Y43H11AL.1* |
| *clec-210* | *jmjd-3.3* | *prp-38* | *tni-4* | *C55C3.7* | *H04J21.1* | *Y49F6C.8* |
| *clec-218* | *lbp-8* | *rbm-3.2* | *trx-5* | *D1014.5* | *H35B03.2* | *Y51A2D.14* |
| *clec-247* | *lect-2* | *rdy-2* | *ttc-36* | *D2030.7* | *K01A12.2* | *Y52B11A.4* |
| *clec-258* | *lgc-23* | *rnh-1.0* | *twk-12* | *F07G6.2* | *K08C7.1* | *Y52E8A.6* |
| *clec-47* | *lgc-29* | *rpm-1* | *ugt-26* | *F08F3.4* | *K08C7.4* | *Y54G2A.36* |
| *clec-76* | *lgc-39* | *rrbs-1* | *ugt-30* | *F15A4.2* | *M01G12.7* | *Y57A10A.5* |
| *cnc-2* | *lgc-43* | *set-8* | *ugt-8* | *F18E3.12* | *M03B6.1* | *Y57A10C.9* |
| *cpt-4* | *lys-5* | *smcl-1* | *unc-3* | *F22B8.7* | *M04D8.8* | *Y57G11C.41* |
| *crn-2* | *math-44* | *sra-28* | *vps-37* | *F22H10.1* | *R02F2.7* | *Y6B3B.1* |
| *csn-3* | *math-46* | *srab-22* | *vps-60* | *F23D12.11* | *R04B5.6* | *Y73B3A.3* |
| *cth-1* | *miro-2* | *srbc-18* | *wago-11* | *F25H2.3* | *R05H11.1* | *Y73E7A.1* |
| *cup-4* | *mltn-2* | *srbc-58* | *xbx-3* | *F26A3.4* | *R09E12.9* | *Y73F8A.10* |
| *cyp-13A5* | *mltn-3* | *sre-26* | *zig-2* | *F26H9.5* | *R102.8* | *Y79H2A.4* |
| *cyp-14A5* | *mrpl-48* | *sre-6* | *B0252.1* | *F35E2.8* | *R107.5* | *Y7A5A.8* |
| *cyp-35B1* | *mrps-28* | *srg-59* | *B0361.9* | *F35F10.5* | *R11A5.3* | *Y95B8A.6* |
| *cyp-35C1* | *mtl-2* | *srh-184* | *B0379.1* | *F40E12.1* | *R11H6.2* | *Y9C9A.1* |
| *dhs-8* | *mxl-3* | *srh-2* | *B0563.1* | *F40G9.6* | *T05H4.3* | *ZK105.1* |
| *dod-17* | *myo-6* | *srh-207* | *B0563.18* | *F42A10.7* | *T08B6.1* | *ZK262.3* |
| *dpy-19* | *nhr-106* | *srh-246* | *C01G10.16* | *F44E5.4* | *T13C2.7* | *ZK546.14* |
| *eas-1* | *nhr-145* | *srh-258* | *C01G10.9* | *F44E5.5* | *T13G4.5* | |
| *eea-1* | *nhr-17* | *srh-69* | *C02B8.12* | *F45D3.3* | *T15B7.8* | |
| *efl-3* | *nhr-189* | *srj-25* | *C02F5.12* | *F45D3.4* | *T20D4.5* | |

**Table A4**. Genes downregulated in the *hsp-90*$^{int}$ hp-RNAi strain compared to the *hsp-90*$^{control}$ strain.

| | | | | | | |
|---|---|---|---|---|---|---|
| *acdh-10* | *clec-66* | *hacd-1* | *pab-1* | *ssl-1* | *F32B4.4* | *T21H3.1* |
| *acdh-7* | *clec-67* | *his-32* | *pde-6* | *tank-1* | *F33E2.5* | *T22F7.1* |
| *acly-1* | *clec-72* | *hpo-15* | *pho-8* | *tba-2* | *F37C4.5* | *T26C12.1* |
| *acs-13* | *clec-83* | *ilys-2* | *pisy-1* | *tba-7* | *F47G4.4* | *W03F9.4* |
| *aldo-1* | *cpl-1* | *ilys-3* | *pod-2* | *tfg-1* | *F48D6.4* | *W04B5.3* |
| *ama-1* | *cpr-1* | *ins-7* | *ppw-1* | *ubl-1* | *F55G11.7* | *Y46D2A.2* |
| *asah-1* | *cpr-3* | *itx-1* | *ppw-2* | *ugt-18* | *F58D5.5* | *Y57A10A.31* |
| *asp-1* | *cpr-5* | *klp-7* | *pqn-48* | *xpo-1* | *H02F09.3* | *Y68A4A.13* |
| *asp-12* | *dlhd-1* | *lbp-7* | *pqn-87* | *B0334.3* | *K05B2.4* | *Y71A12B.12* |
| *asp-6* | *dsc-4* | *lec-8* | *rle-1* | *B0395.3* | *K06A4.6* | *Y73B3A.1* |
| *atp-1* | *eef-1A.1* | *lido-8* | *rol-8* | *C06B8.7* | *K08D10.18* | *ZK1073.1* |
| *cbs-2* | *elf-1* | *lys-10* | *rpl-20* | *C12D12.1* | *K08D12.6* | *ZK218.11* |
| *clec-118* | *elo-2* | *lys-2* | *rpl-4* | *cTel55X.1* | *K10G4.5* | *ZK218.5* |
| *clec-174* | *fbxa-66* | *math-38* | *sago-2* | *D2063.1* | *T01D3.6* | *ZK218.7* |
| *clec-265* | *flp-33* | *nep-17* | *scl-24* | *F01D5.3* | *T04C4.1* | *ZK546.7* |
| *clec-4* | *gbf-1* | *nhr-136* | *set-26* | *F22G12.5* | *T19C9.8* | |
| *clec-65* | *gfi-1* | *nuo-5* | *sru-40* | *F25E5.1* | *T20B3.1* | |

**Table A5**. Genes upregulated in the *hsp-90*$^{neu}$ hp-RNAi strain compared to the *hsp-90*$^{control}$ strain.

| | | | | | | |
|---|---|---|---|---|---|---|
| *aagr-1* | *bcmo-2* | *clec-101* | *col-117* | *cup-16* | *dhs-19* | *fbxa-84* |
| *aat-2* | *BE10.4* | *clec-106* | *col-118* | *cup-5* | *dhs-20* | *fbxc-36* |
| *aat-7* | *best-1* | *clec-125* | *col-123* | *cut-1* | *dhs-31* | *fbxc-55* |
| *abf-5* | *best-13* | *clec-146* | *col-142* | *cutl-10* | *dhs-4* | *fbxc-7* |
| *abf-6* | *best-14* | *clec-166* | *col-144* | *cutl-16* | *dhs-8* | *fip-2* |
| *abhd-5.1* | *best-17* | *clec-167* | *col-147* | *cutl-3* | *dlc-3* | *fip-5* |
| *acc-4* | *best-24* | *clec-169* | *col-158* | *cyp-13A10* | *dmsr-12* | *fipr-1* |
| *ace-2* | *bigr-1* | *clec-17* | *col-163* | *cyp-13A11* | *dod-17* | *fipr-10* |
| *acer-1* | *btb-16* | *clec-172* | *col-164* | *cyp-13A2* | *dos-1* | *fipr-11* |
| *acl-5* | *bus-18* | *clec-204* | *col-166* | *cyp-13A3* | *dpy-6* | *fipr-2* |
| *acl-7* | *cah-3* | *clec-210* | *col-167* | *cyp-13A4* | *drd-50* | *fipr-24* |
| *acp-5* | *cah-4* | *clec-227* | *col-169* | *cyp-13A5* | *drn-1* | *fipr-3* |
| *acp-6* | *cal-2* | *clec-264* | *col-176* | *cyp-13A6* | *droe-4* | *fipr-4* |
| *acs-1* | *cal-4* | *clec-31* | *col-177* | *cyp-13A7* | *dsl-5* | *fipr-5* |
| *acs-2* | *cal-5* | *clec-37* | *col-183* | *cyp-14A1* | *efn-2* | *fipr-7* |
| *alh-5* | *cal-8* | *clec-39* | *col-185* | *cyp-14A2* | *elt-3* | *fipr-8* |
| *amt-1* | *capa-1* | *clec-42* | *col-2* | *cyp-14A3* | *epg-9* | *fipr-9* |
| *aqp-1* | *cat-4* | *clec-44* | *col-35* | *cyp-14A5* | *ethe-1* | *flp-1* |
| *aqp-4* | *cbp-3* | *clec-47* | *col-36* | *cyp-25A3* | *exos-9* | *flp-13* |
| *aqp-7* | *cdr-2* | *clec-48* | *col-37* | *cyp-29A4* | *faah-1* | *flp-15* |
| *aqp-8* | *cdr-4* | *clec-49* | *col-40* | *cyp-32B1* | *faah-6* | *flp-16* |
| *arl-3* | *cdr-6* | *clec-5* | *col-41* | *cyp-33D3* | *fahd-1* | *flp-17* |
| *arrd-1* | *ceh-20* | *clec-52* | *col-42* | *cyp-33E1* | *far-7* | *flp-18* |
| *arrd-14* | *ceh-22* | *clec-54* | *col-43* | *cyp-34A1* | *fbxa-107* | *flp-19* |
| *asah-1* | *ceh-43* | *clec-55* | *col-44* | *cyp-34A10* | *fbxa-158* | *flp-24* |
| *asah-2* | *ceh-62* | *clec-57* | *col-45* | *cyp-34A2* | *fbxa-16* | *flp-34* |
| *asb-2* | *ceh-86* | *clec-60* | *col-50* | *cyp-34A9* | *fbxa-161* | *flp-7* |
| *asns-2* | *ceh-88* | *clec-61* | *col-51* | *cyp-35C1* | *fbxa-162* | *flp-9* |
| *asp-14* | *cest-1.1* | *clec-67* | *col-54* | *cysl-2* | *fbxa-166* | *fmo-1* |
| *atg-13* | *cest-12* | *clec-7* | *col-72* | *daao-1* | *fbxa-185* | *fog-1* |
| *atg-16.1* | *cest-35.2* | *clec-72* | *col-84* | *daf-11* | *fbxa-21* | *fog-3* |
| *atm-1* | *chil-1* | *clec-75* | *col-85* | *daf-9* | *fbxa-24* | *folt-1* |
| *avr-15* | *chil-11* | *clec-76* | *col-90* | *dcn-1* | *fbxa-38* | *fozi-1* |
| *axl-1* | *chil-12* | *clec-9* | *col-98* | *dct-1* | *fbxa-44* | *fpn-1.2* |
| *bas-1* | *chil-18* | *clik-2* | *comt-5* | *ddo-2* | *fbxa-54* | *ftn-1* |
| *bath-13* | *chil-19* | *clik-3* | *cpi-1* | *decr-1.1* | *fbxa-57* | *fubl-3* |
| *bath-26* | *chil-23* | *cnc-8* | *cpn-4* | *del-5* | *fbxa-59* | *gana-1* |
| *bath-36* | *chpf-2* | *cnc-9* | *cpr-1* | *del-6* | *fbxa-61* | *gba-1* |
| *bca-1* | *ckb-2* | *col-102* | *cpr-4* | *dhp-1* | *fbxa-69* | *gba-2* |
| *bcc-1* | *clc-2* | *col-103* | *cpx-1* | *dhs-15* | *fbxa-71* | *gba-4* |
| *bcmo-1* | *clc-5* | *col-114* | *cpx-2* | *dhs-18* | *fbxa-79* | *gbb-1* |

*gcl-1*
*glb-1*
*glb-15*
*glb-3*
*glb-30*
*glb-33*
*glb-6*
*glc-1*
*glc-2*
*glna-2*
*gpa-10*
*gpa-12*
*gpa-4*
*gpx-3*
*gpx-6*
*gpx-7*
*grd-10*
*grd-13*
*grd-3*
*grd-7*
*grl-19*
*grl-20*
*grl-23*
*grl-25*
*grl-3*
*grl-9*
*grsp-3*
*gst-14*
*gst-2*
*gst-20*
*gst-24*
*gst-28*
*gst-41*
*gst-7*
*gsto-1*
*ham-1*
*hic-1*
*hil-1*
*hizr-1*
*hmbx-1*
*hmgs-1*
*hmit-1.1*
*hmit-1.3*
*hpo-26*
*hpo-36*
*hrg-2*
*hrg-3*
*hsp-12.3*
*hsp-12.6*
*ifb-2*
*igdb-2*
*igdb-3*
*igeg-1*
*ilys-5*
*ins-1*
*ins-11*
*ins-20*
*ins-24*
*ins-33*
*ins-35*
*ins-4*
*ins-5*
*inx-2*
*inx-3*
*inx-6*
*irg-1*
*irld-15*
*jmjd-5*
*kin-15*
*kin-16*
*kin-30*
*klo-2*
*klu-2*
*kqt-1*
*kynu-1*
*lact-3*
*lam-3*
*lbp-1*
*lbp-8*
*lec-2*
*lec-4*
*lec-7*
*lect-2*
*lgc-11*
*lgc-54*
*lgg-1*
*lgg-2*
*lin-46*
*lipl-1*
*lipl-3*
*lips-10*
*lips-11*
*lips-5*
*lmd-5*
*lmp-2*
*lmtr-3*
*lov-1*
*lron-5*
*lurp-1*
*lury-1*
*lys-4*
*lys-5*
*lys-6*
*mab-21*
*maf-1*
*mai-1*
*mak-1*
*mapk-15*
*marg-1*
*math-10*
*math-24*
*math-27*
*math-34*
*math-38*
*math-45*
*mct-3*
*memo-1*
*mig-21*
*mkk-4*
*mlc-1*
*mlc-2*
*mod-5*
*mpst-7*
*mrpl-28*
*mtch-1*
*mtl-1*
*mtl-2*
*mul-1*
*mxl-3*
*myo-1*
*myo-2*
*myo-6*
*nac-1*
*nas-23*
*nas-25*
*nas-3*
*nas-39*
*nas-9*
*nbet-1*
*ncam-1*
*ncs-5*
*ncx-1*
*ncx-10*
*ncx-9*
*ndnf-1*
*nep-26*
*nhr-101*
*nhr-107*
*nhr-109*
*nhr-110*
*nhr-117*
*nhr-130*
*nhr-135*
*nhr-139*
*nhr-148*
*nhr-150*
*nhr-155*
*nhr-16*
*nhr-161*
*nhr-162*
*nhr-178*
*nhr-19*
*nhr-205*
*nhr-206*
*nhr-21*
*nhr-232*
*nhr-263*
*nhr-265*
*nhr-273*
*nhr-275*
*nhr-4*
*nhr-42*
*nhr-53*
*nhr-57*
*nhr-58*
*nhr-69*
*nhr-7*
*nhr-99*
*nhx-1*
*nhx-3*
*nit-1*
*nlp-18*
*nlp-24*
*nlp-26*
*nlp-27*
*nlp-28*
*nlp-3*
*nlp-31*
*nlp-33*
*nlp-35*
*nlp-38*
*nlp-42*
*nlp-51*
*nlp-55*
*nlp-59*
*nlp-61*
*nlp-68*
*nlp-81*
*nlp-82*
*nmad-1*
*nmur-3*
*npr-10*
*npr-22*
*npr-24*
*npr-6*
*nspb-1*
*nspb-6*
*nspe-1*
*nspe-2*
*nspe-5*
*nuc-1*
*oac-14*
*oac-24*
*oac-29*
*oat-1*
*odr-10*
*oig-3*
*old-1*
*osm-6*
*otpl-6*
*pah-1*
*pals-17*
*pals-23*
*pals-24*
*pals-32*
*pals-39*
*par-5*
*parg-2*
*pcbd-1*
*pdf-1*
*pepm-1*
*pfd-5*
*pgal-1*
*pgp-1*
*pgp-10*
*pgp-14*
*pgp-5*
*pgp-6*
*pgp-7*
*phat-6*
*pho-14*
*pho-6*
*piit-1*
*plpp-1.2*
*pmt-1*
*pnp-1*
*poml-2*
*poml-3*
*poml-4*
*ppt-1*
*pqm-1*
*pqn-31*
*pqn-71*
*pqn-94*
*pqn-97*
*pqn-98*
*prmt-4*
*ptr-13*
*ptr-22*
*ptr-8*
*pud-1.2*
*pxd-1*
*pxl-1*
*rab-37*
*rbm-22*
*rgba-1*
*rgs-11*
*rgs-3*
*rhr-1*
*rhr-2*
*ric-4*
*rom-2*
*rpb-4*
*scl-11*
*scl-12*
*scl-13*
*scl-14*
*scl-2*
*scl-5*
*sdz-24*
*sdz-8*
*sftd-3*
*skr-13*
*skr-4*
*slc-17.1*
*slc-17.3*
*slc-25A21*
*slc-25A29*
*slc-36.5*
*snf-11*
*snpc-1.3*
*sod-3*
*sodh-1*
*sodh-2*
*spl-2*
*spp-18*
*spp-2*
*spp-20*
*spp-23*
*spp-3*
*spp-5*
*spp-6*
*spp-8*
*sqst-2*
*sre-6*
*srh-2*
*srh-45*
*srh-46*

| | | | | | | |
|---|---|---|---|---|---|---|
| *srp-2* | *tsp-15* | *ugt-37* | *B0478.3* | *C13A2.12* | *C34F11.8* | *C50F7.5* |
| *srp-7* | *tsp-16* | *ugt-40* | *B0524.4* | *C13A2.4* | *C35B8.3* | *C51E3.10* |
| *srr-4* | *tsp-17* | *ugt-45* | *B0546.4* | *C13A2.9* | *C35C5.8* | *C53B7.3* |
| *srr-6* | *tsp-3* | *ugt-54* | *B0554.1* | *C14C6.2* | *C35C5.9* | *C53D6.7* |
| *srsx-34* | *ttc-36* | *ugt-55* | *B0554.5* | *C14C6.3* | *C35E7.6* | *C54D1.7* |
| *srt-42* | *ttll-15* | *ugt-63* | *C01G10.16* | *C15A11.7* | *C35E7.7* | *C54D10.3* |
| *srt-43* | *ttm-2* | *ugt-8* | *C01G10.4* | *C15B12.8* | *C36B1.13* | *C54E4.4* |
| *srtx-1* | *ttr-15* | *ugt-9* | *C01G10.5* | *C15H9.11* | *C36B1.6* | *C54F6.12* |
| *sru-39* | *ttr-18* | *unc-129* | *C01G10.6* | *C16D9.1* | *C36E6.2* | *C54F6.15* |
| *srw-4* | *ttr-2* | *unc-31* | *C01G5.25* | *C16D9.6* | *C36E8.4* | *C54F6.6* |
| *srw-86* | *ttr-21* | *unc-40* | *C02B8.12* | *C16E9.1* | *C37A5.3* | *C55A6.6* |
| *srx-133* | *ttr-23* | *unc-46* | *C02F12.5* | *C17B7.4* | *C37C3.10* | *C55A6.7* |
| *srxa-10* | *ttr-26* | *unc-79* | *C02F5.12* | *C18A11.1* | *C37C3.12* | *D1005.2* |
| *srz-24* | *ttr-27* | *unc-86* | *C03G6.17* | *C18E9.4* | *C37C3.7* | *D1005.4* |
| *stdh-2* | *ttr-29* | *unc-9* | *C04A11.5* | *C18F10.2* | *C38C3.4* | *D1022.3* |
| *str-112* | *ttr-30* | *unk-1* | *C04E12.4* | *C18G1.1* | *C39B10.1* | *D1044.7* |
| *str-176* | *ttr-31* | *upp-1* | *C04E12.5* | *C18H9.5* | *C39B5.14* | *D1053.3* |
| *str-178* | *ttr-33* | *vamp-8* | *C05B5.17* | *C23G10.11* | *C39B5.2* | *D1054.18* |
| *str-181* | *ttr-37* | *vang-1* | *C05C8.7* | *C23H4.8* | *C39D10.8* | *D1054.19* |
| *str-90* | *ttr-43* | *vap-1* | *C05C8.8* | *C23H5.15* | *C39E9.8* | *D2030.2* |
| *sul-1* | *ttr-57* | *ver-2* | *C05D12.2* | *C25F9.11* | *C40H1.2* | *E02A10.4* |
| *sul-2* | *ttr-59* | *wrt-3* | *C05D9.9* | *C25F9.14* | *C40H1.7* | *E02C12.6* |
| *sul-3* | *ttr-7* | *xbp-1* | *C05G5.1* | *C25F9.6* | *C40H1.8* | *E02C12.8* |
| *sulp-2* | *ttr-8* | *xtr-1* | *C06A1.2* | *C25H3.10* | *C40H1.9* | *E02H4.4* |
| *sulp-4* | *twk-18* | *zig-2* | *C06B3.6* | *C27B7.2* | *C42D4.1* | *E02H9.4* |
| *sulp-5* | *twk-33* | *zip-8* | *C06B3.7* | *C27B7.9* | *C43F9.4* | *E03H4.8* |
| *sup-1* | *twk-34* | *zipt-2.2* | *C06E4.2* | *C28G1.2* | *C43F9.5* | *E04D5.4* |
| *swt-3* | *twk-4* | *zmp-3* | *C06E4.3* | *C29F3.3* | *C44C1.6* | *E04F6.6* |
| *swt-7* | *twk-46* | *ztf-29* | *C06E4.6* | *C29F5.8* | *C44C10.3* | *EEED8.2* |
| *tag-131* | *twk-49* | *B0001.3* | *C06G3.3* | *C29F7.1* | *C44E12.1* | *EGAP4.1* |
| *tag-209* | *tyr-1* | *B0024.4* | *C06H2.7* | *C29F7.2* | *C44H9.5* | *F01D4.8* |
| *tag-290* | *tyr-4* | *B0035.13* | *C07A9.12* | *C30F12.5* | *C45B11.6* | *F01E11.3* |
| *tag-52* | *ugt-11* | *B0222.5* | *C07B5.2* | *C30F2.3* | *C45B2.3* | *F01F1.2* |
| *tat-4* | *ugt-13* | *B0228.1* | *C07B5.4* | *C31H2.3* | *C45E5.4* | *F01F1.3* |
| *tba-8* | *ugt-14* | *B0244.4* | *C08B6.10* | *C31H5.4* | *C45G9.6* | *F02E11.7* |
| *tbb-4* | *ugt-17* | *B0244.5* | *C08B6.14* | *C32F10.4* | *C46C2.2* | *F07A11.5* |
| *tmed-13* | *ugt-18* | *B0252.1* | *C08B6.2* | *C32H11.4* | *C46H11.2* | *F07C3.3* |
| *tnc-2* | *ugt-2* | *B0294.1* | *C08D8.1* | *C33A12.19* | *C48B4.13* | *F07F6.8* |
| *tni-4* | *ugt-20* | *B0336.12* | *C08E3.13* | *C33A12.4* | *C49F5.7* | *F07G11.1* |
| *tnt-4* | *ugt-21* | *B0361.9* | *C08E8.1* | *C33D3.4* | *C49H3.12* | *F08A7.1* |
| *tps-1* | *ugt-25* | *B0393.9* | *C08F11.7* | *C33G8.13* | *C50F2.7* | *F08F3.4* |
| *trh-1* | *ugt-26* | *B0416.2* | *C09F12.2* | *C33G8.2* | *C50F4.1* | *F08F3.8* |
| *try-4* | *ugt-29* | *B0416.7* | *C09G9.1* | *C34C12.7* | *C50F4.8* | *F08G2.5* |
| *tsp-10* | *ugt-31* | *B0457.2* | *C09G9.5* | *C34D1.4* | *C50F4.9* | *F08G2.8* |

| | | | | | | |
|---|---|---|---|---|---|---|
| *F09C3.2* | *F17C11.4* | *F38E11.9* | *F54B11.11* | *H11E01.2* | *K11H3.5* | *T02G5.3* |
| *F09C6.1* | *F17C8.9* | *F40A3.2* | *F54B8.4* | *H14A12.5* | *K12B6.9* | *T03D8.7* |
| *F09C8.1* | *F18E9.3* | *F40A3.4* | *F54C1.1* | *H32K16.2* | *M01B2.13* | *T03F1.11* |
| *F09E5.16* | *F18G5.6* | *F40D4.13* | *F54D5.3* | *H38K22.4* | *M01H9.3* | *T03F7.7* |
| *F09F7.6* | *F19B6.3* | *F40H3.1* | *F55A4.7* | *H39E23.3* | *M02B1.2* | *T04B8.2* |
| *F09F9.1* | *F19H8.2* | *F40H3.2* | *F55B11.4* | *H40L08.2* | *M03A1.8* | *T04C12.11* |
| *F10A3.17* | *F20A1.6* | *F41C3.8* | *F55C9.3* | *K01A2.4* | *M04C9.1* | *T04C12.7* |
| *F10A3.4* | *F20B6.4* | *F41E6.15* | *F55C9.5* | *K01F9.2* | *M04D8.7* | *T04C12.8* |
| *F10B5.3* | *F20C5.4* | *F41E7.9* | *F55D12.1* | *K02A2.5* | *M163.8* | *T04F8.7* |
| *F10C1.9* | *F20E11.17* | *F41G3.10* | *F55G1.15* | *K02D10.4* | *M176.5* | *T04F8.8* |
| *F10D7.4* | *F20G2.1* | *F41G3.21* | *F55G11.2* | *K02E11.7* | *M6.11* | *T04G9.4* |
| *F10E9.3* | *F21C10.10* | *F42A8.1* | *F55G11.4* | *K02E7.6* | *M60.4* | *T05A1.5* |
| *F10E9.4* | *F21C10.17* | *F43C9.1* | *F55G7.4* | *K03B4.8* | *R02F11.10* | *T05A8.8* |
| *F10E9.5* | *F21D12.3* | *F43E2.1* | *F55H12.2* | *K03B8.8* | *R02F11.9* | *T05B11.1* |
| *F10E9.7* | *F21H12.7* | *F44A2.3* | *F55H12.4* | *K03H6.2* | *R02F2.8* | *T05F1.11* |
| *F11A5.15* | *F21H7.12* | *F44D12.19* | *F55H12.7* | *K04A8.20* | *R03H10.2* | *T05H10.3* |
| *F11A5.9* | *F22B7.9* | *F45D11.1* | *F56A12.2* | *K04F1.9* | *R03H10.7* | *T05H10.4* |
| *F11A6.15* | *F22E5.21* | *F45D11.14* | *F56B6.6* | *K05F1.10* | *R04A9.9* | *T05H4.15* |
| *F11C7.2* | *F23F1.7* | *F45D3.3* | *F56C4.1* | *K07A12.8* | *R04B5.5* | *T06E4.10* |
| *F11E6.11* | *F23F12.12* | *F45D3.4* | *F56C4.4* | *K07E1.1* | *R05A10.1* | *T07F12.4* |
| *F11F1.1* | *F25A2.1* | *F46A8.7* | *F56D5.3* | *K07E8.6* | *R05A10.8* | *T07G12.5* |
| *F12A10.1* | *F25B4.4* | *F46B3.23* | *F56H11.2* | *K07H8.11* | *R05D8.7* | *T08G2.2* |
| *F12E12.11* | *F25E2.3* | *F46C5.1* | *F56H9.2* | *K08B4.7* | *R05D8.9* | *T10B10.8* |
| *F13B12.2* | *F25E5.8* | *F46C5.10* | *F56H9.9* | *K08C7.1* | *R05H10.1* | *T10B5.4* |
| *F13C5.1* | *F26A3.4* | *F46G10.1* | *F57A8.1* | *K08C7.4* | *R05H11.2* | *T10C6.15* |
| *F13C5.5* | *F26F12.5* | *F47B7.1* | *F57B1.1* | *K08D8.1* | *R07A4.3* | *T10H9.8* |
| *F13D11.3* | *F28H7.2* | *F47B8.3* | *F57F4.2* | *K08F9.1* | *R09H10.3* | *T11B7.2* |
| *F13E9.15* | *F28H7.3* | *F47B8.4* | *F57G8.7* | *K08H2.7* | *R102.2* | *T11F8.12* |
| *F13E9.8* | *F31F7.1* | *F47B8.8* | *F58A3.3* | *K09C4.1* | *R102.6* | *T12B3.2* |
| *F13H6.4* | *F32D1.3* | *F47G3.4* | *F58B4.3* | *K09C4.10* | *R10D12.7* | *T12B3.3* |
| *F13H8.1* | *F32D8.12* | *F48C1.8* | *F58B4.5* | *K09C4.4* | *R10E11.5* | *T13B5.9* |
| *F14D7.10* | *F32H5.1* | *F48G7.10* | *F58B4.6* | *K09C4.5* | *R11D1.3* | *T13F3.6* |
| *F14D7.5* | *F35A5.2* | *F48G7.8* | *F58H1.7* | *K09C6.9* | *R11D1.4* | *T14A8.2* |
| *F14F9.2* | *F35B12.3* | *F49C12.10* | *F59A7.2* | *K09E2.1* | *R11G1.6* | *T15B7.1* |
| *F14F9.4* | *F35C11.7* | *F49E12.10* | *F59A7.5* | *K09H11.6* | *R11G1.7* | *T16G1.3* |
| *F14F9.8* | *F35F10.1* | *F49F1.5* | *F59B10.4* | *K09H9.5* | *R13H4.2* | *T16G1.4* |
| *F14H12.3* | *F36D1.7* | *F49H6.5* | *F59C6.16* | *K09H9.8* | *R74.10* | *T16G1.5* |
| *F14H3.12* | *F36D4.4* | *F52E1.14* | *F59D6.1* | *K10C9.1* | *T01B7.8* | *T16G1.6* |
| *F15A4.5* | *F36F2.2* | *F53A9.8* | *F59E11.5* | *K10D3.6* | *T01C3.11* | *T16G1.7* |
| *F15A4.6* | *F36G9.3* | *F53A9.9* | *F59E11.7* | *K10D6.2* | *T01C8.2* | *T16H12.9* |
| *F15E6.3* | *F36H5.14* | *F53F4.1* | *H01M10.1* | *K10D6.4* | *T01D3.3* | *T18D3.5* |
| *F16C3.2* | *F36H9.4* | *F53F4.2* | *H04M03.12* | *K10H10.12* | *T02B11.4* | *T19C3.3* |
| *F17A9.5* | *F37B4.14* | *F53F4.4* | *H05C05.4* | *K11G9.5* | *T02C12.5* | *T19C4.1* |
| *F17B5.1* | *F37H8.2* | *F53F8.4* | *H06A10.1* | *K11H12.7* | *T02G5.14* | *T19C4.24* |

*T19C4.5*
*T19E7.6*
*T19H5.4*
*T19H5.6*
*T20B5.2*
*T20D4.11*
*T20D4.13*
*T20D4.3*
*T20D4.5*
*T20G5.8*
*T21D12.12*
*T21F4.1*
*T22B11.4*
*T22E5.1*
*T22E5.6*
*T22F3.12*
*T23B12.11*
*T23B12.5*
*T23F2.3*
*T23G11.11*
*T24D3.2*
*T24E12.5*
*T25B9.1*
*T25G12.11*
*T25G12.3*
*T26C5.4*
*T26H5.10*
*T26H5.14*
*T26H5.4*
*T26H5.8*
*T26H5.9*
*T27A3.8*
*T27D12.1*
*T27E4.7*
*T28A11.19*
*T28A11.6*
*T28H11.8*
*VC5.2*
*VF13D12L.3*
*W01B11.6*
*W01C9.2*
*W01F3.2*
*W02A2.9*
*W02C12.2*
*W02D7.8*
*W02D9.4*
*W02G9.4*
*W02H5.2*
*W03F8.6*
*W03F9.11*
*W04A8.4*
*W05H12.1*
*W05H9.1*
*W06H8.2*
*W07B8.4*
*W09G12.7*
*W10C8.4*
*W10C8.6*
*Y102A11A.6*
*Y105C5A.8*
*Y105C5B.3*
*Y105C5B.5*
*Y113G7A.16*
*Y113G7B.27*
*Y119C1B.12*
*Y11D7A.3*
*Y12A6A.1*
*Y14H12A.1*
*Y14H12A.2*
*Y15E3A.4*
*Y15E3A.5*
*Y17D7C.2*
*Y17G9A.2*
*Y19D10B.6*
*Y22D7AL.15*
*Y23H5B.7*
*Y34D9A.8*
*Y34F4.1*
*Y34F4.2*
*Y34F4.6*
*Y37A1B.5*
*Y37E11B.1*
*Y37F4.8*
*Y37H2C.1*
*Y38C1AA.9*
*Y38E10A.14*
*Y38H6C.21*
*Y39A3A.4*
*Y39A3CR.8*
*Y39B6A.27*
*Y39G8B.10*
*Y39G8B.7*
*Y39G8B.9*
*Y42A5A.1*
*Y42A5A.3*
*Y42G9A.3*
*Y43C5A.3*
*Y43C5A.7*
*Y43F8B.2*
*Y44A6D.2*
*Y45F10D.6*
*Y45F3A.4*
*Y46G5A.23*
*Y46G5A.36*
*Y47G6A.21*
*Y47H9C.1*
*Y48A6B.7*
*Y48C3A.3*
*Y48E1B.8*
*Y49E10.18*
*Y4C6B.3*
*Y4C6B.7*
*Y50D4B.6*
*Y51A2D.14*
*Y51A2D.21*
*Y51H4A.25*
*Y51H4A.5*
*Y51H4A.8*
*Y51H7BR.8*
*Y51H7C.10*
*Y52B11A.12*
*Y52B11A.8*
*Y53C12B.7*
*Y53F4B.23*
*Y53F4B.39*
*Y53F4B.51*
*Y54E10A.17*
*Y54G2A.32*
*Y54G2A.7*
*Y55F3BR.11*
*Y57A10A.26*
*Y57E12B.1*
*Y57E12B.11*
*Y59E9AL.4*
*Y5H2A.1*
*Y60A3A.16*
*Y60C6A.1*
*Y60C6A.2*
*Y65A5A.1*
*Y65B4BR.1*
*Y67A10A.2*
*Y67A10A.9*
*Y69E1A.5*
*Y6D1A.2*
*Y6E2A.4*
*Y70C5C.1*
*Y70G10A.3*
*Y71F9B.1*
*Y71F9B.13*
*Y71G12B.31*
*Y73B3A.7*
*Y73B6BL.44*
*Y73F4A.2*
*Y73F4A.3*
*Y73F8A.27*
*Y75B12B.3*
*Y7A5A.7*
*Y87G2A.16*
*Y87G2A.19*
*Y97E10AL.1*
*Y97E10AR.1*
*Y9C9A.1*
*ZC116.1*
*ZC116.5*
*ZC15.5*
*ZC190.6*
*ZC196.4*
*ZC196.5*
*ZC21.3*
*ZC395.5*
*ZC412.3*
*ZC416.2*
*ZC443.1*
*ZC443.4*
*ZC449.5*
*ZC455.1*
*ZC513.14*
*ZK1290.13*
*ZK1290.14*
*ZK1320.13*
*ZK1320.2*
*ZK185.5*
*ZK218.4*
*ZK228.3*
*ZK262.2*
*ZK262.3*
*ZK355.3*
*ZK355.8*
*ZK402.3*
*ZK455.5*
*ZK512.7*
*ZK54.3*
*ZK550.6*
*ZK593.3*
*ZK622.4*
*ZK666.15*
*ZK669.3*
*ZK673.2*
*ZK742.4*
*ZK792.4*
*ZK822.5*
*ZK822.6*
*ZK856.5*
*ZK863.8*
*ZK971.1*

**Table A6**. Genes downregulated in the *hsp-90*$^{neu}$ hp-RNAi strain compared to the *hsp-90*$^{control}$ strain.

| | | | | | | |
|---|---|---|---|---|---|---|
| *aagr-4* | *cdh-8* | *cpl-1* | *fem-3* | *lact-2* | *nep-10* | *pqn-13* |
| *aat-4* | *cdh-9* | *cpn-2* | *fip-6* | *lact-8* | *nep-12* | *pqn-26* |
| *abt-1* | *cest-10* | *cpr-3* | *fipr-27* | *laf-1* | *nep-15* | *pqn-32* |
| *abt-5* | *cex-1* | *cpt-2* | *fkb-3* | *let-2* | *nep-20* | *pqn-91* |
| *abu-12* | *cey-3* | *cpz-1* | *fpn-1.1* | *let-805* | *nep-23* | *pri-2* |
| *abu-13* | *chc-1* | *cut-2* | *ftt-2* | *let-858* | *nep-8* | *prkl-1* |
| *acd-1* | *che-10* | *cutl-15* | *fut-2* | *lgc-22* | *nep-9* | *pst-1* |
| *acdh-10* | *che-13* | *cutl-8* | *fzy-1* | *lgx-1* | *nhr-234* | *ptb-1* |
| *acdh-12* | *che-14* | *cyc-2.2* | *gbf-1* | *lido-18* | *nhr-41* | *ptc-3* |
| *acdh-6* | *chk-2* | *cyn-17* | *gbh-1* | *lin-42* | *nhr-76* | *ptp-5.1* |
| *acdh-7* | *chs-2* | *dao-4* | *gly-12* | *lips-15* | *nkb-2* | *ptp-5.2* |
| *acl-13* | *cht-4* | *dct-17* | *gly-8* | *lips-9* | *nlp-30* | *ptr-1* |
| *acly-1* | *chtl-1* | *deps-1* | *grd-1* | *lon-3* | *nmy-1* | *ptr-11* |
| *acn-1* | *clec-118* | *dhhc-11* | *grd-11* | *lon-8* | *npax-2* | *ptr-16* |
| *acox-1.2* | *clec-119* | *dlg-1* | *grd-2* | *lpr-7* | *nspc-1* | *ptr-18* |
| *acp-2* | *clec-151* | *dmd-9* | *grl-15* | *ltd-1* | *nspc-4* | *ptr-19* |
| *acp-3* | *clec-175* | *dml-1* | *grl-5* | *lys-10* | *nspc-7* | *ptr-24* |
| *acs-10* | *clec-238* | *dos-2* | *grl-7* | *lys-2* | *nstp-8* | *ptr-6* |
| *acs-13* | *clec-239* | *dpy-13* | *hhat-1* | *lys-3* | *nucb-1* | *pyr-1* |
| *acs-15* | *clec-242* | *dpy-18* | *hil-5* | *mab-7* | *oac-1* | *qua-1* |
| *acs-18* | *clec-247* | *dpy-4* | *hog-1* | *mam-1* | *oac-10* | *rig-6* |
| *acs-20* | *clec-4* | *dpy-5* | *hpo-15* | *mam-2* | *oac-17* | *rnh-1.1* |
| *act-2* | *clec-45* | *dtmk-1* | *hpo-27* | *mam-3* | *oac-30* | *rnp-8* |
| *agmo-1* | *clec-66* | *dyf-7* | *ife-3* | *mbl-1* | *oac-32* | *rnr-1* |
| *alg-3* | *clec-73* | *eat-20* | *ify-1* | *mcm-2* | *oac-42* | *rnr-2* |
| *alg-4* | *cnp-2* | *ech-1.1* | *ilys-2* | *mlc-7* | *oac-54* | *rol-1* |
| *alh-13* | *col-109* | *ect-2* | *ima-2* | *mlt-10* | *oac-6* | *rol-8* |
| *apd-3* | *col-110* | *efn-3* | *ins-37* | *mlt-8* | *osr-1* | *sago-2* |
| *arrd-10* | *col-138* | *egg-6* | *ins-7* | *mlt-9* | *otpl-1* | *sams-4* |
| *arrd-9* | *col-17* | *ego-2* | *ipla-4* | *moa-1* | *paf-1* | *samt-1* |
| *bah-1* | *col-175* | *elf-1* | *irg-5* | *moe-3* | *paqr-3* | *scl-23* |
| *bed-3* | *col-182* | *elo-2* | *ivd-1* | *mpz-4* | *pash-1* | *scl-24* |
| *bgnt-1.8* | *col-38* | *elo-8* | *jmjd-1.1* | *mpz-6* | *pes-8* | *scrm-5* |
| *bli-1* | *col-48* | *emb-9* | *kel-10* | *msd-3* | *pho-12* | *sdz-27* |
| *bli-6* | *col-49* | *ets-10* | *kin-21* | *msp-74* | *phy-3* | *sec-61.A* |
| *bmk-1* | *col-63* | *exc-6* | *kin-31* | *msrp-3* | *pig-1* | *set-9* |
| *bus-4* | *col-68* | *exc-7* | *klp-10* | *msrp-4* | *plin-1* | *skpo-2* |
| *bus-8* | *col-71* | *fat-7* | *klp-18* | *msrp-5* | *pph-2* | *slcf-2* |
| *calu-1* | *col-73* | *fbxa-147* | *klp-19* | *msrp-6* | *pps-1* | *smrc-1* |
| *cdc-37* | *col-79* | *fbxa-215* | *knl-2* | *nas-15* | *ppw-1* | *snf-2* |
| *cdh-12* | *col-97* | *fbxa-96* | *laat-1* | *nep-1* | *pqn-10* | *spch-2* |

| | | | | | | |
|---|---|---|---|---|---|---|
| *spch-3* | *zyg-12* | *C24D10.2* | *C55C3.4* | *F26H11.4* | *F43C1.5* | *K01D12.15* |
| *spd-2* | *B0205.10* | *C25B8.8* | *C55C3.6* | *F27C1.3* | *F44F4.10* | *K01D12.8* |
| *spe-12* | *B0207.1* | *C25D7.1* | *C55C3.8* | *F27C8.2* | *F44G3.7* | *K02E11.10* |
| *spe-45* | *B0207.11* | *C25F6.7* | *C56C10.6* | *F27C8.5* | *F44G4.5* | *K02F6.7* |
| *spe-47* | *B0273.1* | *C26B2.2* | *CE7X_3.2* | *F28C6.5* | *F47B7.2* | *K04A8.10* |
| *spe-6* | *B0280.11* | *C27A2.12* | *D1054.9* | *F28G4.4* | *F49D11.6* | *K04G2.4* |
| *spp-13* | *B0280.7* | *C27A7.3* | *D1086.17* | *F30A10.12* | *F49E10.2* | *K04H4.2* |
| *sqt-1* | *B0348.5* | *C27D6.11* | *D2024.4* | *F30A10.2* | *F49E12.12* | *K06A4.6* |
| *sqt-2* | *B0361.11* | *C28A5.6* | *D2062.5* | *F30H5.3* | *F49E12.8* | *K07A1.5* |
| *sqt-3* | *B0393.5* | *C28D4.5* | *E01G4.6* | *F31B12.3* | *F52B5.2* | *K07A3.3* |
| *sra-18* | *B0507.1* | *C29A12.6* | *E03H12.5* | *F31F4.17* | *F52H3.6* | *K07E3.9* |
| *srd-7* | *B0511.11* | *C29H12.2* | *F01D5.10* | *F32A11.3* | *F53B1.2* | *K07F5.6* |
| *sto-1* | *B0545.4* | *C30F8.3* | *F01D5.3* | *F32B4.8* | *F53B1.4* | *K07H8.5* |
| *sups-1* | *B0554.4* | *C30G12.2* | *F01D5.6* | *F32B5.1* | *F53B2.5* | *K08C9.1* |
| *taf-11.2* | *BE10.1* | *C30G12.4* | *F09F9.2* | *F32B6.4* | *F53F4.15* | *K08C9.2* |
| *tbb-6* | *C01B10.11* | *C32E12.1* | *F13A7.1* | *F32D8.3* | *F53G12.8* | *K08E7.5* |
| *tbc-2* | *C02F4.4* | *C32H11.5* | *F13A7.12* | *F33A8.10* | *F54D10.8* | *K08F4.5* |
| *tfg-1* | *C02F5.2* | *C32H11.6* | *F13B12.4* | *F33A8.7* | *F54F11.1* | *K09C6.7* |
| *tln-1* | *C03C11.1* | *C33H5.16* | *F13C5.3* | *F33D11.2* | *F54F12.1* | *K09E4.1* |
| *tpst-1* | *C04F12.16* | *C34F11.1* | *F14E5.8* | *F33D11.7* | *F55A11.11* | *K09F6.3* |
| *trap-1* | *C04G6.2* | *C34F11.5* | *F14F7.4* | *F33D4.6* | *F55H12.3* | *K09H11.4* |
| *try-7* | *C05C12.1* | *C35A5.5* | *F15B9.8* | *F33E2.5* | *F56C9.3* | *K11C4.1* |
| *tsn-1* | *C05C9.1* | *C35E7.10* | *F15H10.8* | *F34D10.9* | *F56C9.6* | *K11D2.4* |
| *tsp-14* | *C05D12.1* | *C35E7.9* | *F16C3.4* | *F35A5.5* | *F56D3.1* | *K11H12.4* |
| *ttbk-4* | *C05E7.1* | *C36C5.12* | *F17E9.5* | *F35E12.10* | *F56D6.13* | *K12D12.4* |
| *ttbk-5* | *C06B8.7* | *C36C5.14* | *F18C5.5* | *F35E2.9* | *F57G4.11* | *K12H4.6* |
| *ttr-14* | *C06C6.8* | *C36C5.15* | *F18F11.4* | *F36A2.14* | *F58A6.9* | *M02D8.2* |
| *ttr-58* | *C06G1.2* | *C36H8.1* | *F19B10.2* | *F36H1.3* | *F58D2.2* | *M03B6.4* |
| *twk-45* | *C06G4.4* | *C37H5.14* | *F21C3.6* | *F36H12.3* | *F58E6.13* | *M05D6.3* |
| *txdc-12.1* | *C06G4.6* | *C38C6.3* | *F21D9.2* | *F36H12.5* | *F58E6.5* | *M110.7* |
| *ubc-24* | *C07A12.18* | *C40C9.3* | *F21F3.2* | *F36H2.3* | *F58H10.1* | *M117.4* |
| *uggt-2* | *C07A9.9* | *C42D4.13* | *F22B3.8* | *F36H9.5* | *F59A1.15* | *M153.1* |
| *ugt-1* | *C07E3.10* | *C45G9.4* | *F22E5.1* | *F37A4.4* | *F59E11.6* | *M162.7* |
| *ule-2* | *C08G5.3* | *C46A5.1* | *F23C8.7* | *F37H8.5* | *H03E18.1* | *M28.9* |
| *vit-1* | *C10H11.7* | *C47A4.3* | *F25E2.2* | *F38B6.4* | *H03G16.5* | *R01E6.2* |
| *vit-3* | *C14A4.13* | *C49F8.3* | *F25E5.1* | *F38B6.7* | *H04M03.3* | *R01E6.5* |
| *vrp-1* | *C14B1.7* | *C50D2.1* | *F25E5.2* | *F39F10.3* | *H05L14.1* | *R03D7.8* |
| *wago-4* | *C14C11.1* | *C50F7.3* | *F25F2.1* | *F39G3.2* | *H08M01.1* | *R03E9.2* |
| *wrt-4* | *C16C10.13* | *C52B11.5* | *F25H5.7* | *F40E10.5* | *H11L12.1* | *R05G6.9* |
| *wrt-6* | *C17E4.1* | *C52G5.2* | *F26A1.9* | *F40F12.3* | *H13N06.2* | *R05H5.4* |
| *wrt-9* | *C17F3.3* | *C53B7.2* | *F26A10.2* | *F40H3.3* | *H17B01.2* | *R07B1.13* |
| *xol-1* | *C18D4.12* | *C54F6.3* | *F26B1.1* | *F41F3.8* | *H23N18.5* | *R07E5.6* |
| *zif-1* | *C18H7.4* | *C54G4.2* | *F26F2.10* | *F41G3.3* | *H31G24.3* | *R09A1.2* |
| *zig-3* | *C23H3.9* | *C55C3.3* | *F26G1.9* | *F42C5.5* | *H42K12.3* | *R09E10.1* |

| | | | | |
|---|---|---|---|---|
| *R09E10.5* | *T22F7.4* | *Y38C1AA.7* | *Y66D12A.3* | *ZK688.10* |
| *R102.11* | *T23B3.5* | *Y38F2AR.12* | *Y67D8B.5* | *ZK783.6* |
| *R105.1* | *T23F6.3* | *Y39A1A.2* | *Y69A2AR.19* | *ZK795.2* |
| *R10D12.10* | *T24B8.5* | *Y39B6A.30* | *Y71G12A.4* | *ZK809.1* |
| *R10E4.7* | *T24C4.4* | *Y39B6A.9* | *Y71G12B.17* | *ZK829.3* |
| *R10F2.6* | *T25D3.4* | *Y39E4A.1* | *Y71G12B.22* | *ZK858.8* |
| *R11E3.1* | *T27A10.6* | *Y41C4A.7* | *Y71G12B.25* | *ZK892.3* |
| *R11G11.6* | *T27C5.12* | *Y41E3.18* | *Y71G12B.27* | |
| *R12B2.3* | *T28B8.4* | *Y44A6D.5* | *Y71G12B.30* | |
| *R13H9.6* | *T28D6.4* | *Y45F3A.1* | *Y73B6BL.23* | |
| *R151.2* | *T28H11.7* | *Y45G5AM.6* | *Y75B7AR.1* | |
| *R155.3* | *W01B6.6* | *Y46D2A.2* | *Y75B8A.28* | |
| *R74.2* | *W02A2.8* | *Y46G5A.29* | *Y76B12C.4* | |
| *T01B7.13* | *W02F12.8* | *Y47G6A.13* | *Y79H2A.2* | |
| *T01D1.4* | *W03C9.1* | *Y47G6A.15* | *Y81G3A.4* | |
| *T02B11.9* | *W03D2.9* | *Y47G6A.3* | *Y94H6A.2* | |
| *T02E1.7* | *W03D8.1* | *Y48G1C.5* | *ZC123.1* | |
| *T03D8.6* | *W03D8.3* | *Y49E10.10* | *ZC190.7* | |
| *T03F6.6* | *W03F9.4* | *Y49F6B.8* | *ZC190.8* | |
| *T04B2.7* | *W03G9.5* | *Y4C6A.1* | *ZC317.6* | |
| *T04F8.9* | *W04A4.2* | *Y4C6A.3* | *ZC434.3* | |
| *T05A7.6* | *W06D4.3* | *Y51A2B.6* | *ZC477.7* | |
| *T05B9.1* | *W06F12.3* | *Y51H7C.1* | *ZC581.10* | |
| *T05C12.1* | *W09C3.2* | *Y51H7C.13* | *ZC84.1* | |
| *T05D4.5* | *W09C3.7* | *Y52B11B.1* | *ZK1025.3* | |
| *T05F1.5* | *W09D6.4* | *Y53C10A.10* | *ZK1025.4* | |
| *T06A4.1* | *W09G12.10* | *Y53F4B.24* | *ZK1053.2* | |
| *T06A4.3* | *Y102E9.5* | *Y53F4B.25* | *ZK1225.5* | |
| *T07G12.3* | *Y105C5B.11* | *Y53F4B.27* | *ZK1248.20* | |
| *T08B6.9* | *Y116A8C.23* | *Y53H1C.3* | *ZK154.1* | |
| *T10B5.10* | *Y116A8C.33* | *Y54E2A.7* | *ZK180.6* | |
| *T11F8.4* | *Y11D7A.5* | *Y54E2A.8* | *ZK287.4* | |
| *T14G10.8* | *Y11D7A.8* | *Y54G2A.13* | *ZK353.2* | |
| *T15H9.5* | *Y11D7A.9* | *Y55B1AR.4* | *ZK354.2* | |
| *T16A1.2* | *Y14H12B.2* | *Y57A10B.7* | *ZK354.6* | |
| *T16G1.13* | *Y17G7B.19* | *Y57G11C.14* | *ZK381.2* | |
| *T19B10.2* | *Y18D10A.11* | *Y57G11C.40* | *ZK381.8* | |
| *T19C3.2* | *Y18H1A.11* | *Y57G7A.5* | *ZK470.6* | |
| *T19D12.5* | *Y22D7AR.7* | *Y62E10A.19* | *ZK484.6* | |
| *T20F5.5* | *Y32B12B.4* | *Y62H9A.12* | *ZK550.5* | |
| *T21G5.1* | *Y34B4A.10* | *Y65B4A.9* | *ZK616.61* | |
| *T22B3.3* | *Y37E11AL.2* | *Y65B4BL.4* | *ZK616.8* | |
| *T22D1.18* | *Y37E11AR.7* | *Y66C5A.1* | *ZK622.1* | |
| *T22F7.1* | *Y38A10A.2* | *Y66D12A.11* | *ZK637.12* | |

# Appendix 2

The 90 genes screened by tissue-specific RNAi for an effect on *hsp-70* reporter fluorescence intensity in the *hsp-90*$^{int}$ hp-RNAi strain (**Chapter 6**).

| | | |
|---|---|---|
| *arx-1* | *nhr-62* | *C32D5.1* |
| *asp-12* | *nlp-68* | *C37C3.7* |
| *btbd-10* | *octr-1* | *C44B7.7* |
| *ceh-58* | *par-4* | *C45E1.4* |
| *clec-41* | *pha-4* | *C50D2.3* |
| *cnd-1* | *pqm-1* | *C53B4.4* |
| *col-20* | *ptr-11* | *F19F10.9* |
| *csk-1* | *rack-1* | *F20A1.10* |
| *daf-16* | *ran-5* | *F25D1.2* |
| *dct-10* | *ser-1* | *F29G9.1* |
| *dlat-1* | *sesn-1* | *F59E12.3* |
| *dod-17* | *skn-1* | *K03H6.2* |
| *eat-2* | *sly-1* | *M02B1.2* |
| *elt-2* | *sre-6* | *R02C2.6* |
| *fnip-2* | *srh-105* | *T20D4.5* |
| *gad-1* | *srh-2* | *T25E4.2* |
| *gcsh-2* | *ssp-19* | *Y46E12BL.2* |
| *gcy-8* | *str-112* | *Y48C3A.20* |
| *glp-1* | *swsn-9* | *Y48G1C.5* |
| *gtl-1* | *taf-1* | *Y51A2D.14* |
| *hlh-10* | *tph-1* | *Y54G2A.13* |
| *hlh-2* | *tsct-1* | *Y61A9LA.11* |
| *hlh-25* | *ttx-3* | *Y68A4A.5* |
| *hsf-1* | *unc-13* | *Y74C9A.1* |
| *hsp-70* | *unc-31* | *Y9C9A.1* |
| *hsp-90* | *ztf-2* | *ZK262.3* |
| *irg-1* | *ztf-20* | |
| *lin-32* | *C01G10.16* | |
| *mab-9* | *C04G6.5* | |
| *mct-6* | *C06A1.2* | |
| *nhr-204* | *C06B8.11* | |
| *nhr-42* | *C24H12.4* | |

# Bibliography

Ailion M., Inoue T., Weaver C.I., Holdcraft R.W., Thomas J.H.; 1999. Neurosecretory control of aging in *Caenorhabditis elegans*. *PNAS* 96(13), 7394-7397

Åkerfelt M., Morimoto R.I., Sistonen L.; 2010. Heat shock factors: integrators of cell stress, development and lifespan. *Nat. Revs. Mol. Cell Biol.* 11, 545–555

Ali A., Bharadwaj S., O'Carroll R., Ovsenek N.; 1998. HSP90 Interacts with and regulates the activity of Heat Shock Factor 1 in *Xenopus* oocytes. *Mol. Cell. Biol.* 18(9), 4949–4960

Alper S., McElwee M.K., Apfeld J., Lackford B., Freedman J.H., Schwartz D.A.; 2010. The *Caenorhabditis elegans* germ line regulates distinct signalling pathways to control lifespan and innate immunity. *J. Biol. Chem.* 285, 1822-1828

Ananthan J., Goldberg A.L., Voellmy R.; 1986. Abnormal proteins serve as eukaryotic stress signals and trigger the activation of heat shock genes. *Science* 232(4749), 522-524

Anderson J.L., Morran L.T., Phillips P.C.; 2010. Outcrossing and the maintenance of males within *C. elegans* populations. *J. Heredity* 101(s1), S62-S74

Apfeld J., Kenyon C.; 1999. Regulation of lifespan by sensory perception in *Caenorhabditis elegans*. *Nature* 402, 804–809

Arantes-Oliveira N., Apfeld J., Dillin A., Kenyon C.; 2002. Regulation of life-span by germ-line stem cells in *Caenorhabditis elegans*. *Science* 295(5554), 502-505

Armenteros J.J.A., Sønderby C.K., Sønderby S.K., Nielsen H., Winther O.; 2017. DeepLoc: Prediction of protein subcellular localization using deep learning. *Bioinformatics* 33(21), 3387–3395

Ashburner M., Ball C.A., Blake J.A., Botstein D., Butler H., Cherry J.M., Davis A.P., Dolinski K., Dwight S.S., Eppig J.T., Harris M.A., Hill D.P., Issel-Tarver L., Kasarskis A., Lewis S., Matese J.C., Richardson J.E., Ringwald M., Rubin G.M., Sherlock G.; 2000. Gene Ontology: Tool for the unification of biology. *Nat. Genet*. 25, 25-29

Austin J., Kimble J.; 1987. *glp-1* is required in the germ line for regulation of the decision between mitosis and meiosis in *C. elegans*. *Cell* 51(4), 589-599

Avery L.; 1993. The genetics of feeding in *Caenorhabditis elegans*. *Genetics* 133(4), 897-917

Bailey T.L., Bodén M., Buske F.A., Frith M., Grant C.E., Clementi L., Ren J., Li W.W., Noble W.S.; 2009. MEME SUITE: Tools for motif discovery and searching. *Nucleic Acids Res*. 37, W202-W208

Bakowski M.A., Desjardins C.A., Smelkinson M.G., Dunbar T.A., Lopez-Moyado I.F., Rifkin S.A., Cuomo C.A., Troemel E.R.; 2014. Ubiquitin-mediated response to microsporidia and virus infection in *C. elegans*. *PLoS Pathog.* 10(6): e1004200

Balasubramaniam B., Vinitha T., Deepika S., JebaMercy G., VenkataKrishna L.M., Balamurugan K.; 2019. Analysis of *Caenorhabditis elegans* phosphoproteome reveals the involvement of a molecular chaperone, HSP-90 protein during *Salmonella enterica* Serovar Typhi infection. *Int. J. Biol. Macromol.* 137, 620-646

Balch W.E., Morimoto R.I., Dillin A., Kelly J.W.; 2008. Adapting proteostasis for disease intervention. *Science* 319(5865), 916-919

Baler R., Dahl G., Voellmy R.; 1993. Activation of human heat shock genes is accompanied by oligomerization, modification, and rapid translocation of heat shock transcription factor HSF1. *Mol. Cell. Biol.* 13(4), 2486-2496

Baugh L.R., Sternberg P.W.; 2006. DAF-16/FOXO Regulates Transcription of *cki-1*/Cip/Kip and Repression of *lin-4* during *C. elegans* L1 Arrest. *Current Biol.* 16(8), 780-785

Benedetti C., Haynes C.M., Yang Y., Harding H.P., Ron D.; 2006. Ubiquitin-like protein 5 positively regulates chaperone gene expression in the mitochondrial unfolded protein response. *Genetics* 174(1), 229-239

Bentley D.R., Balasubramanian S., Smith A.J., et al.; 2008. Accurate whole human genome sequencing using reversible terminator chemistry. *Nature* 456, 53–59

Ben-Zvi A., Miller E.A., Morimoto R.I.; 2009. Collapse of proteostasis represents an early molecular event in *Caenorhabditis elegans* aging. *PNAS* 106(35), 14914-14919

Berendzen K.M., Durieux J., Shao L.-W., Tian T., Kim H., Wolff S., Liu Y., Dillin A.; 2016. Neuroendocrine coordination of mitochondrial stress signalling and proteostasis. *Cell* 166(6), 1553-1563.e10

Berk A.J.; 1989. Regulation of eukaryotic transcription factors by post-translational modification. *Biochim. Biophys. Acta* 1009, 103-109

Berman J.R., Kenyon C.; 2006. Germ-cell loss extends *C. elegans* life span through regulation of DAF-16 by *kri-1* and lipophilic-hormone signalling. Cell 124(5), 1055-1068

Bharadwaj S., Ali A., Ovsenek N.; 1999. Multiple components of the HSP90 chaperone complex function in regulation of Heat Shock Factor 1 *in vivo*. *Mol. Cell. Biol.* 19(12), 8033–8041

Bhaskar P.T., Hay N.; 2007. The two TORCs and Akt. *Dev. Cell* 12(4), 487-502

Birnby D.A., Link E.M., Vowels J.J., Tian H., Colacurcio P.L., Thomas J.H.; 2000. A transmembrane guanylyl cyclase (DAF-11) and Hsp90 (DAF-21) regulate a common set of chemosensory behaviours in *Caenorhabditis elegans*. *Genetics* 155(1), 85-104

Blazie S.M., Babb C., Wilky H., Rawls A., Park J.G., Mangone M.; 2015. Comparative RNA-Seq analysis reveals pervasive tissue-specific alternative polyadenylation in *Caenorhabditis elegans* intestine and muscles. *BMC Biology* 13:4

Borkovich K.A., Farrelly F.W., Finkelstein D.B., Taulien J., Lindquist S.; 1989. Hsp82 is an essential protein that is required in higher concentrations for growth of cells at higher temperatures. *Mol. Cell. Biol.* 9(9), 3919-3930

Brandt J.P., Ringstad N.; 2015. Toll-like receptor signalling promotes development and function of sensory neurons required for a *C. elegans* pathogen-avoidance behaviour. *Current Biology* 25(17), 2228-2237

Brehme M., Voisine C., Rolland T., Wachi S., Soper J.H.Zhu Y., Orton K., Villella A., Garza D., Vidal M., Ge H., Morimoto R.I.; 2014. A chaperome subnetwork safeguards proteostasis in aging and neurodegenerative disease. *Cell Reports* 9(3), 1135-1150

Brenner S.; 1974. The genetics of *Caenorhabditis elegans*. *Genetics* 77(1), 71-94

Brunquell J., Morris S., Lu Y., Cheng F. & Westerheide S.D.; 2016. The genome-wide role of HSF-1 in the regulation of gene expression in *Caenorhabditis elegans*. *BMC Genomics* 17:559

The *C. elegans* Sequencing Consortium; 1998. Genome sequence of the nematode *C. elegans*: A platform for investigating biology. *Science* 282(5396), 2012-2018

Calfon M., Zeng H., Urano F., Till J.H., Hubbard S.R., Harding H.P., Clark S.G., Ron D.; 2002. IRE1 couples endoplasmic reticulum load to secretory capacity by processing the *XBP-1* mRNA. *Nature* 415, 92–96

Calixto A., Chelur D., Topalidou I., Chen X., Chalfie M.; 2010. Enhanced neuronal RNAi in *C. elegans* using SID-1. *Nature Methods* 7, 554–559

Cao J., Packer J.S., Ramani V., Cusanovich D.A., Huynh C., Daza R., Qiu X., Lee C., Furlan S.N., Steemers F.J., Adey A., Waterston R.H., Trapnell C., Shendure J.; 2017. Comprehensive single-cell transcriptional profiling of a multicellular organism. *Science* 357, 661-667

Cassada R.C., Russell R.L.; 1975. The dauerlarva, a post-embryonic developmental variant of the nematode *Caenorhabditis elegans*. *Dev. Biol.* 46(2), 326-342

Chávez V., Mohri-Shiomi A., Maadani A., Vega L.A., Garsin D.A.; 2007. Oxidative stress enzymes are required for DAF-16-mediated immunity due to generation of reactive oxygen species by *Caenorhabditis elegans*. *Genetics* 176(3), 1567-1577

Chávez V., Mohri-Shiomi A., Garsin D.A.; 2009. Ce-Duox1/BLI-3 generates reactive oxygen species as a protective innate immune mechanism in *Caenorhabditis elegans*. *Infection & Immunity* 77(11), 4983-4989

Chawla A., Repa J.J., Evans R.M., Mangelsdorf D.J.; 2001. Nuclear receptors and lipid physiology: Opening the X-files. *Science* 294(5548), 1866-1870

Chen X., Shen J., Prywes R.; 2002. The luminal domain of ATF6 senses endoplasmic reticulum (ER) stress and causes translocation of ATF6 from the ER to the Golgi. *J. Biol. Chem.* 277, 13045-13052

Chen K., Franz C.J., Jiang H., Jiang Y., Wang D.; 2017. An evolutionarily conserved transcriptional response to viral infection in *Caenorhabditis nematodes*. *BMC Genomics* 18: 303

Chenal J., Pierre K., Pellerin L.; 2008. Insulin and IGF□1 enhance the expression of the neuronal monocarboxylate transporter MCT2 by translational activation via stimulation of the phosphoinositide 3□kinase–Akt–mammalian target of rapamycin pathway. *Eur. J. Neurosci.* 27(1), 53-65

Chiang W.-C., Ching T.-T., Lee H.C., Mousigian C., Hsu A.-L.; 2012. HSF-1 regulators DDL-1/2 link insulin-like signalling to heat-shock responses and modulation of longevity. *Cell* 148(1-2), 322-334

Chikka M.R., Anbalagan C., Dvorak K., Dombeck K., Prahlad V.; 2016. The mitochondria-regulated immune pathway activated in the *C. elegans* intestine is neuroprotective. *Cell Reports* 16(9), 2399-2414

Chiti F., Dobson C.M.; 2009. Amyloid formation by globular proteins under native conditions. *Nature Chem. Biol.* 5, 15–22

Chou S.-D., Prince T., Gong J., Calderwood S.K.; 2012. mTOR is essential for the proteotoxic stress response, HSF1 activation and heat shock protein synthesis. *PLoS One.* 7(6): e39679

Chrousos G.P., Loriaux D.L., Gold P.W. (eds); 1988. Mechanisms of physical and emotional stress. *Adv. Exp. Med. Biol.* 245; Plenum Press, New York, 1988

Chrousos G.P.; 2009. Stress and disorders of the stress system. *Nat. Rev. Endocrinol.* 5, 374–381

Cohen F.E., Kelly J.W.; 2003. Therapeutic approaches to protein-misfolding diseases. *Nature* 426, 905–909

Cohen E., Bieschke J., Perciavalle R.M., Kelly J.W., Dillin A.; 2006. Opposing activities protect against age-onset proteotoxicity. *Science* 313(5793), 1604-1610

Cohen E., Paulsson J.F., Blinder P., Burstyn-Cohen T., Du D., Estepa G., Adame A., Pham H.M., Holzenberger M., Kelly J.W., Masliah E., Dillin A.; 2009. Reduced IGF-1 signalling delays age-associated proteotoxicity in mice. *Cell* 139(6), 1157-1169

Contrino S., Smith R.N., Butano D., Carr A., Hu F., Lyne R., Rutherford K., Kalderimis A., Sullivan J., Carbon S., Kephart E.T., Lloyd P., Stinson E.O., Washington N.L., Perry M.D., Ruzanov P., Zha Z., Lewis S.E., Stein L.D., Micklem G.; 2012. modMine: flexible access to modENCODE data. *Nucleic Acids Res.* 40(Database issue): D1082-8

da Silva V.C.H., Ramos C.H.I.; 2012. The network interaction of the human cytosolic 90 kDa heat shock protein Hsp90: A target for cancer therapeutics. *J. Proteomics* 75(10), 2790-2802

David D.C., Ollikainen N., Trinidad J.C., Cary M.P., Burlingame A.L., Kenyon C.; 2010. Widespread protein aggregation as an inherent part of aging in *C. elegans*. *PLoS Biol.* 8(8): e1000450

Deppe U., Schierenberg E., Cole T., Krieg C., Schmitt D., Yoder B., von Ehrenstein G.; 1978. Cell lineages of the embryo of the nematode *Caenorhabditis elegans*. *PNAS* 75(1), 376-380

Deribe Y.L., Pawson T., Dikic I.; 2010. Post-translational modifications in signal integration. *Nat. Struct. Mol. Biol*. 17, 666–672

Dillin A., Hsu A.-L., Arantes-Oliveira N., Lehrer-Graiwer J., Hsin H., Fraser A.G., Kamath R.S., Ahringer J., Kenyon C.; 2002. Rates of behaviour and aging specified by mitochondrial function during development. *Science* 298(5602), 2398-2401

Doi M., Iwasaki K.; 2002. Regulation of retrograde signalling at neuromuscular junctions by the novel C2 domain protein AEX-1. *Neuron* 33(2), 249-259

Doitsidou M., Poole R.J., Sarin S., Bigelow H., Hobert O.; 2010. *C. elegans* mutant identification with a one-step whole-genome-sequencing and SNP mapping strategy. *PLoS One* 5(11), e15435

Dorman J.B., Albinder B., Shroyer T., Kenyon C.; 1995. The *age-1* and *daf-2* genes function in a common pathway to control the lifespan of *Caenorhabditis elegans*. *Genetics* 141(4), 1399-1406

Durieux J., Wolff S., Dillin A.; 2011. The cell-non-autonomous nature of electron transport chain-mediated longevity. *Cell* 144(1), 79-91

Eckl J., Sima S., Marcus K., Lindemann C., Richter K.; 2017. Hsp90-downregulation influences the heat-shock response, innate immune response and onset of oocyte development in nematodes. *PLoS One* 12(10): e0186386

Engelmann I., Griffon A., Tichit L., Montañana-Sanchis F., Wang G., Reinke V., Waterston R.H., Hillier L.W., Ewbank J.J.; 2011. A comprehensive analysis of gene expression changes provoked by bacterial and fungal infection in *C. elegans*. *PLoS One* 6(5): e19055

Evans E.A., Kawli., Tan M.-W.; 2008. *Pseudomonas aeruginosa* suppresses host immunity by activating the DAF-2 insulin-like signalling pathway in *Caenorhabditis elegans*. *PLoS Pathog*. 4(10): e1000175

Fanning A.S., Anderson J.M.; 1996. Protein–protein interactions: PDZ domain networks. *Curr. Biol.* 6(11), 1385-1388

Fawcett T.W., Sylvester S.L., Sarge K.D., Morimoto R.I., Holbrook N.J.; 1994. Effects of neurohormonal stress and aging on the activation of mammalian heat shock factor 1. *J. Biol. Chem*. 269, 32272-32278

Feinberg E.H., Hunter C.P.; 2003. Transport of dsRNA into cells by the transmembrane protein SID-1. *Science* 301(5639), 1545-1547

Félix M.-A., Ashe A., Piffaretti J., Wu G., Nuez I., Bélicard T., Jiang Y., Zhao G., Franz C.J., Goldstein L.D., Sanroman M., Miska E.A., Wang D.; 2011. Natural and experimental infection of *Caenorhabditis Nematodes* by novel viruses related to nodaviruses. *PLoS Biol*. 9(1), e1000586

Félix M.-A., Duveau F.; 2012. Population dynamics and habitat sharing of natural populations of *Caenorhabditis elegans* and *C. briggsae*. *BMC Biology* 10:59

Fink A.L.; 1999. Chaperone-mediated protein folding. *Phys. Rev.* 79(2), 425-449

Fire A., Xu S., Montgomery M.K., Kostas S.A., Driver S.E., Mello C.C.; 1998. Potent and specific genetic interference by double-stranded RNA in *Caenorhabditis elegans*. *Nature* 391, 806–811

Fraga C.G., Shigenaga M.K., Park J.W., Degan P., Ames B.N.; 1990. Oxidative damage to DNA during aging: 8-hydroxy-2'-deoxyguanosine in rat organ DNA and urine. *PNAS* 87(12), 4533-4537

Frakes A.E., Metcalf M.G., Tronnes S.U., Bar-Ziv R., Durieux J., Gildea H.K., Kandahari N., Monshietehadi S., Dillin A.; 2020. Four glial cells regulate ER stress resistance and longevity via neuropeptide signalling in *C. elegans*. *Science* 367(6476), 436-440

Frantz C., Stewart K.M., Weaver V.M.; 2010. The extracellular matrix at a glance. *J. Cell Sci*. 123, 4195-4200

Frauenfelder H., Sligar S.G., Wolynes P.G.; 1991. The energy landscapes and motions of proteins. *Science* 254(5038), 1598-1603

Freeman B.C., Morimoto R.I.; 1996. The human cytosolic molecular chaperones hsp90, hsp70 (hsc70) and hdj□1 have distinct roles in recognition of a non□native protein and protein refolding. *EMBO J* 15, 2969-2979

Furuyama T., Nakazawa T., Nakano I., Mori N.; 2000. Identification of the differential distribution patterns of mRNAs and consensus binding sequences for mouse DAF-16 homologues. *Biochem. J.* 349(2), 629–634

Gaiser A.M., Kaiser C.J.O., Haslbeck V., Richter K.; 2011. Downregulation of the Hsp90 system causes defects in muscle cells of *Caenorhabditis elegans*. *PLoS One* 6(9): e25485.

Gao A.W., Smith R.L., Weeghel M., Kamble R., Janssens G.E., Houtkooper R.H.; 2018. Identification of key pathways and metabolic fingerprints of longevity in *C. elegans*. *Exp. Gerontology* 113, 128-140

Garcia S.M., Casanueva O., Silva M.C., Amara M.D., Morimoto R.I.; 2007. Neuronal signalling modulates protein homeostasis in *Caenorhabditis elegans* post-synaptic muscle cells. *Genes & Dev*. 21, 3006-3016

Garsin D.A., Sifri C.D., Mylonakis E., Qin X., Singh K.V., Murray B.E., Calderwood S.B., Ausubel F.M.; 2001. A simple model host for identifying Gram-positive virulence factors. *PNAS* 98(19), 10892-10897

Garsin D.A., Villanueva J.M., Begun J., Kim D.H., Sifri C.D., Calderwood S.B., Ruvkun G., Ausubel F.M.; 2003. Long-lived *C. elegans daf-2* mutants are resistant to bacterial pathogens. *Science* 300(5627), 1921

Gaudet J., Mango S.E.; 2002. Regulation of organogenesis by the *Caenorhabditis elegans* FoxA protein PHA-4. *Science* 295(5556), 821-825

The Gene Ontology Consortium, 2019. The Gene Ontology Resource: 20 years and still GOing strong. *Nucleic Acids Res.* 47(D1), D330-D338

Ghazi A., Henis-Korenblit S., Kenyon C.; 2009. A transcription elongation factor that links signals from the reproductive system to lifespan extension in *Caenorhabditis elegans*. *PLoS Genet.* 5(9): e1000639

Golden J.W., Riddle D.L.; 1984. The *Caenorhabditis elegans* dauer larva: Developmental effects of pheromone, food, and temperature. *Dev. Biol.* 102(2), 368-378

Grant C.E., Bailey T.L., Noble W.S.; 2011. FIMO: Scanning for occurrences of a given motif. *Bioinformatics* 27(7), 1017–1018

Gravato-Nobre M.J., Vaz F., Filipe S., Chalmers R., Hodgkin J.; 2016. The invertebrate lysozyme effector ILYS-3 is systemically activated in response to danger signals and confers antimicrobial protection in *C. elegans*. *PLoS Pathog.* 12(8): e1005826

Grove C.A., De Masi F., Barrasa I.M., Newburger D.E., Alkema M.J., Bulyk M.L., Walhout A.J.M.; 2009. A multiparameter network reveals extensive divergence between *C. elegans* bHLH transcription factors. *Cell* 138(2), 314-327

Guettouche T., Boellmann F., Lane W.S., Voellmy R.; 2005. Analysis of phosphorylation of human heat shock factor 1 in cells experiencing a stress. *BMC Biochem.* 6:4

GuhaThakurta D., Palomar L., Stormo G.D., Tedesco P., Johnson T.E., Walker D.W., Lithgow G., Kim S., Link C.D.; 2002. Identification of a novel cis-regulatory element involved in the heat shock response in *Caenorhabditis elegans* using microarray gene expression and computational methods. *Genome Res.* 12, 701-712

Guisbert E., Czyz D.M., Richter K., McMullen P.D., Morimoto R.I.; 2013. Identification of a tissue-selective heat shock response regulatory network. *PLoS Genet.* 9(4): e1003466

Guo Y., Guettouche T., Fenna M., Boellmann F., Pratt W.B., Toft D.O., Smith D.F., Voellmy R.; 2001. Evidence for a mechanism of repression of Heat Shock Factor 1 transcriptional activity by a multichaperone complex. *J. Biol. Chem.* 276, 45791-45799

Halestrap A.P., Wilson M.C.; 2016. The monocarboxylate transporter family—Role and regulation. *IUBMB Winter Sym. Joint Virtual Issue*, 109-119

Hallam S., Singer E., Waring D., Jin Y.; 2000. The *C. elegans* NeuroD homolog *cnd-1* functions in multiple aspects of motor neuron fate specification. *Development* 127, 4239-4252

Harding H.P., Novoa I., Zhang Y., Zeng H., Wek R., Schapira M., Ron D.; 2000. Regulated translation initiation controls stress-induced gene expression in mammalian cells. *Mol. Cell* 6(5), 1099-1108

Hartl F.U., Bracher A., Hayer-Hartl M.; 2011. Molecular chaperones in protein folding and proteostasis. *Nature* 475, 324–332

Harris T.W., Antoshechkin I., Bieri T., Blasiar D., Chan J., Chen W.J., De La Cruz N., Davis P., Duesbury M., Fang R., Fernandes J., Han M., Kishore R., Lee R., Müller H.M., Nakamura C., Ozersky P., Petcherski A., Rangarajan A., Rogers A., Schindelman G., Schwarz E.M., Tuli M.A., Van Auken K., Wang D., Wang X., Williams G., Yook K., Durbin R., Stein L.D., Spieth J., Sternberg P.W.; 2010. WormBase: A comprehensive resource for nematode research. *Nucleic Acids Res.* 38(S1), D463–D467

Haynes C.M., Petrova K., Benedetti C., Yang Y., Ron D.; 2007. ClpP mediates activation of a mitochondrial unfolded protein response in *C. elegans*. *Dev. Cell* 13(4), 467-480

Haynes C.M., Yang Y., Blais S.P., Neubert T.A., Ron D.; 2010. The matrix peptide exporter HAF-1 signals a mitochondrial UPR by activating the transcription factor ZC376.7 in *C. elegans*. *Mol. Cell* 37(4), 529-540

Hedgecock E.M., Russell R.L.; 1975. Normal and mutant thermotaxis in the nematode *Caenorhabditis elegans*. *PNAS* 72(10), 4061-4065

Heinz S., Benner C., Spann N., Bertolino E., Lin Y.C., Laslo P., Cheng J.X., Murre C., Singh H., Glass C.K.; 2010. Simple combinations of lineage-determining transcription factors prime cis-regulatory elements required for macrophage and B cell identities. *Mol. Cell* 38(4), 576-89

Hench J., Henriksson J., Abou-Zied A.M., Lüppert M., Dethlefsen J., Mukherjee K., Tong Y.G., Tang L., Gangishetti U., Baillie D.L., Bürglin T.R.; 2015. The homeobox genes of *Caenorhabditis elegans* and insights into their spatio-temporal expression dynamics during embryogenesis. *PLoS One* 10(5): e0126947

Hershko A., Ciechanover A.; 1998. The ubiquitin system. *Annu. Rev. Biochem.* 67, 425-479

Hillier L.W., Marth G.T., Quinlan A.R., Dooling D., Fewell G., Barnett D., Fox P., Glasscock J.I., Hickenbotham M., Huang W., Magrini V.J., Richt R.J., Sander S.N., Stewart D.A., Stromberg M., Tsung E.F., Wylie T., Schedl T., Wilson R.K., Mardis E.R.; 2008. Whole-genome sequencing and variant discovery in *C. elegans*. *Nature Methods* 5(2), 183-188

Hirsh D., Oppenheim D., Klass M.; 1976. Development of the reproductive system of *Caenorhabditis elegans*. *Dev. Biol.* 49(1), 200-219

Hobert O., D'Alberti T., Liu Y., Ruvkun G.; 1998. Control of neural development and function in a thermoregulatory network by the LIM homeobox gene *lin-11*. *J. Neurosci.* 18(6), 2084-2096

Hodgkin J., Horvitz H.R., Brenner S.; 1979. Nondisjunction mutants of the nematode *Caenorhabditis elegans*. *Genetics* 91(1), 67-94

Hong Y., Roy R., Ambros V.; 1998. Developmental regulation of a cyclin-dependent kinase inhibitor controls postembryonic cell cycle progression in *Caenorhabditis elegans*. *Development* 125, 3585-3597

Hoogewijs D., Houthoofd K., Matthijssens F., Vandesompele J., Vanfleteren J.R.; 2008. Selection and validation of a set of reliable reference genes for quantitative *sod* gene expression analysis in *C. elegans*. *BMC Mol. Biol.* 9, Article 9

Horner M.A., Quintin S., Domeier M.E., Kimble J., Labouesse M., Mango S.E.; 1998. *pha-4*, an HNF-3 homolog, specifies pharyngeal organ identity in *Caenorhabditis elegans*. *Genes & Dev.* 12, 1947-1952

Hsin H., Kenyon C.; 1999. Signals from the reproductive system regulate the lifespan of *C. elegans*. *Nature* 399, 362–366

Hsu A.-L., Murphy C.T., Kenyon C.; 2003. Regulation of aging and age-related disease by DAF-16 and heat-shock factor. Science 300(5622), 1142-1145

Hu Z., Hom S., Kudze T., Tong X.-J., Choi S., Aramuni A., Zhang W., Kaplan J.M.; 2012. Neurexin and neuroligin mediate retrograde synaptic inhibition in *C. elegans*. *Science* 337(6097), 980-984

Hunt-Newbury R., Viveiros R., Johnsen R., Mah A., Anastas D., Fang L., Halfnight E., Lee D., Lin J., Lorch A., McKay S., Okada H.M., Pan J., Schulz A.K., Tu D., Wong K., Zhao Z., Alexeyenko A., Burglin T., Sonnhammer E., Schnabel R., Jones S.J., Marra M.A., Baillie D.L., Moerman D.G.; 2007. High-throughput *in vivo* analysis of gene expression in *Caenorhabditis elegans*. *PLoS Biol.* 5(9): e237

Imanikia S., Özbey N.P., Krueger C., Casanueva M.O., Taylor R.C.; 2019. Neuronal XBP-1 activates intestinal lysosomes to improve proteostasis in *C. elegans*. *Curr. Biol.* 29(14), 2322-2338.e7

Inada H., Ito H., Satterlee J., Sengupta P., Matsumoto K., Mori I.; 2006. Identification of guanylyl cyclases that function in thermosensory neurons of *Caenorhabditis elegans*. *Genetics* 172(4), 2239-2252

Johnson J.A., Johnson D.A., Kraft A.D., Calkins M.J., Jakel R.J., Vargas M.R., Chen P.-C.; 2008. The Nrf2-ARE pathway: An indicator and modulator of oxidative stress in neurodegeneration. *Ann. N Y Acad. Sci.* 1147, 61–69.

Jose A.M., Smith J.J., Hunter C.P.; 2009. Export of RNA silencing from *C. elegans* tissues does not require the RNA channel SID-1. *PNAS* 106(7), 2283-2288

Jovaisaite V., Mouchiroud L., Auwerx J.; 2014. The mitochondrial unfolded protein response, a conserved stress response pathway with implications in health and disease. *J. Exp. Biol.* 217, 137-143

Jovic K., Sterken M.G., Grilli J., Bevers R.P.J., Rodriguez M., Riksen J.A.G., Allesina S., Kammenga J.E., Snoek L.B.; 2017. Temporal dynamics of gene expression in heat-stressed *Caenorhabditis elegans*. *PLoS ONE* 12(12): e0189445

Kalb J.M., Lau K.K., Goszczynski B., Fukushige T., Moons D., Okkema P.G., McGhee J.D.; 1998. *pha-4* is *Ce-fkh-1*, a *fork head*/HNF-3alpha, beta, gamma homolog that functions in organogenesis of the *C. elegans* pharynx. *Development* 125, 2171-2180

Kaletsky R., Yao V., Williams A., Runnels A.M., Tadych A., Zhou S., Troyanskaya O.G., Murphy C.T.; 2018. Transcriptome analysis of adult *Caenorhabditis elegans* cells reveals tissue-specific gene and isoform expression. *PLoS Genet.* 14(8): e1007559

Kamath R.S., Martinez-Campos M., Zipperlen P., Fraser A.G., Ahringer J.; 2001. Effectiveness of specific RNA-mediated interference through ingested double-stranded RNA in *Caenorhabditis elegans*. *Genome Biol.* 2(1): research0002.1–research0002.10

Kamath R.S., Ahringer J.; 2003. Genome-wide RNAi screening in *Caenorhabditis elegans*. *Methods* 30(4), 313-321

Kamath R.S., Fraser A.G., Dong Y., Poulin G., Durbin R., Gotta M., Kanapin A., Le Bot N., Moreno S., Sohrmann M., Welchman D.P., Zipperlen P., Ahringer J.; 2003. Systematic functional analysis of the *Caenorhabditis elegans* genome using RNAi. *Nature* 421, 231–237

Kawli T., Tan M.-W.; 2008. Neuroendocrine signals modulate the innate immunity of *Caenorhabditis elegans* through insulin signalling. *Nature Immunol.* 9, 1415–1424

Kim D., Ouyang H., Li G.C.; 1995. Heat shock protein hsp70 accelerates the recovery of heat-shocked mammalian cells through its modulation of heat shock transcription factor HSF1. *PNAS* 92(6) 2126-2130

Kim D.H., Feinbaum R., Alloing G., Emerson F.E., Garsin D.A., Inoue H., Tanaka-Hino M., Hisamoto N., Matsumoto K., Tan M.-W., Ausubel F.M.; 2002. A conserved p38 MAP kinase pathway in *Caenorhabditis elegans* innate immunity. *Science* 297(5581), 623-626

Kim E., Sheng M.; 2004. PDZ domain proteins of synapses. *Nat. Revs. Neurosci.* 5, 771–781

Kim Y.E., Hipp M.S., Bracher A., Hayer-Hartl M., Hartl F.U.; 2013 (a). Molecular chaperone functions in protein folding and proteostasis. *Annu. Rev. Biochem.* 82, 323-355

Kim K.H., Jeong Y.T., Kim S.H., Jung H.S., Park K.S., Lee H.-Y., Lee M.S.; 2013 (b). Metformin-induced inhibition of the mitochondrial respiratory chain increases FGF21 expression via ATF4 activation. *Biochem. Biophys. Res. Comms.* 440(1), 76-81

Kim K.H., Jeong Y.T., Oh H., Kim S.H., Cho J.M., Kim Y.-N., Kim S.S., Kim D.H., Hur K.Y., Kim H.K., Ko T.-H., Han J., Kim H.L., Kim J., Back S.H., Komatsu M., Chen H., Chan D.C., Konishi M., Itoh N., Choi C.S., Lee M.-S.; 2013 (c). Autophagy deficiency leads to protection from obesity and insulin resistance by inducing FGF21 as a mitokine. *Nature Med.* 19, 83–92

Kimble J.E., White J.G.; 1981. On the control of germ cell development in *Caenorhabditis elegans*. *Dev. Biol.* 81(2), 208-219

Kirienko N.V., Ausubel F.M., Ruvkun G.; 2015. Mitophagy confers resistance to siderophore-mediated killing by *Pseudomonas aeruginosa*. *PNAS* 112(6), 1821-1826

Kozutsumi Y., Segal M., Normington K., Gething M.-J., Sambrook J.; 1988. The presence of malfolded proteins in the endoplasmic reticulum signals the induction of glucose-regulated proteins. *Nature* 332, 462–464

Labbadia J., Morimoto R.I.; 2015. Repression of the heat shock response is a programmed event at the onset of reproduction. *Mol. Cell* 59(4), 639-650

Lakowski B., Hekimi S.; 1998. The genetics of caloric restriction in *Caenorhabditis elegans*. *PNAS* 95(22), 13091-13096

Lee S.S., Kennedy S., Tolonen A.C., Ruvkun G.; 2003. DAF-16 target genes that control *C. elegans* life-span and metabolism. *Science* 300(5619), 644-647

Lee S.-J., Kenyon C.; 2009. Regulation of the longevity response to temperature by thermosensory neurons in *Caenorhabditis elegans*. *Curr. Biol.* 19(9), 715-722

Lenfant N., Polanowska J., Bamps S., Omi S., Borg J.-P., Reboul J.; 2010. A genome-wide study of PDZ-domain interactions in *C. elegans* reveals a high frequency of non-canonical binding. *BMC Genomics* 11:671

Leng N., Dawson J.A., Thomson J.A., Ruotti V., Rissman A.I., Smits B.M.G., Haag J.D., Gould M.N., Stewart R.M., Kendziorski C.; 2013. EBSeq: An empirical Bayes hierarchical model for inference in RNA-seq experiments. *Bioinformatics* 29(8), 1035–1043

L'Hernault S.W.; 2009. The genetics and cell biology of spermatogenesis in the nematode *C. elegans*. *Mol. Cell. Endocrin.* 306(1-2), 59-65

Li J., Chauve L., Phelps G., Brielmann R.M., Morimoto R.I.; 2016. E2F coregulates an essential HSF developmental program that is distinct from the heat-shock response. *Genes & Dev.* 30, 2062-2075

Lin K., Dorman J.B., Rodan A., Kenyon C.; 1997. *daf-16*: An HNF-3/forkhead family member that can function to double the life-span of *Caenorhabditis elegans*. *Science* 278(5341), 1319-1322

Lindquist S.; 1986. The heat-shock response. *Ann. Rev. Biochem.* 55, 1151-91

Lindquist S., Craig E.A.; 1988. The heat-shock proteins. *Annu. Rev. Genet.* 22, 631-677

Liu Y., Sellegounder D., Sun J.; 2016. Neuronal GPCR OCTR-1 regulates innate immunity by controlling protein synthesis in *Caenorhabditis elegans*. *Sci. Reps*. 6: 36832

Loboda A., Damulewicz M., Pyza E., Jozkowicz A., Dulak J.; 2016. Role of Nrf2/HO-1 system in development, oxidative stress response and diseases: An evolutionarily conserved mechanism. *Cell. Mol. Life Sci.* 73, 3221–3247

López-Otín C., Blasco M.A., Partridge L., Serrano M., Kroemer G.; 2013. The hallmarks of aging. *Cell* 153(6), 1194-1217

Lu R., Maduro M., Li F., Li H.W., Broitman-Maduro G., Li W.X., Ding S.W.; 2005. Animal virus replication and RNAi-mediated antiviral silencing in *Caenorhabditis elegans*. *Nature* 436, 1040–1043

Mahadevan N.R., Rodvold J., Sepulveda H., Rossi S., Drew A.F., Zanetti M.; 2011. Transmission of endoplasmic reticulum stress and pro-inflammation from tumour cells to myeloid cells. *PNAS* 108(16), 6561-6566

Mahadevan N.R., Anufreichik V., Rodvold J.J., Chiu K.T., Sepulveda H., Zanetti M.; 2012. Cell-extrinsic effects of tumour ER stress imprint myeloid dendritic cells and impair CD8+ T cell priming. *PLoS One* 7(12): e51845

Maman M., Marques F.C., Volovik Y., Dubnikov T., Bejerano-Sagie M., Cohen E.; 2013. A neuronal GPCR is critical for the induction of the heat shock response in the nematode *C. elegans*. *J. Neurosci*. 33(14), 6102-6111

Mango S.E., Lambie E.J., Kimble J.; 1994. The *pha-4* gene is required to generate the pharyngeal primordium of *Caenorhabditis elegans*. *Development* 120, 3019-3031

Marciniak S.J., Yun C.Y., Oyadomari S., Novoa I., Zhang Y., Jungreis R., Nagata K., Harding H.P., Ron D.; 2004. CHOP induces death by promoting protein synthesis and oxidation in the stressed endoplasmic reticulum. *Genes & Dev.* 18, 3066-3077

Marudhupandiyan S., Balamurugan K.; 2017. Intrinsic JNK-MAPK pathway involvement requires *daf-16*-mediated immune response during *Shigella flexneri* infection in *C. elegans*. *Immunol. Res*. 65, 609–621

Marudhupandiyan S., Prithika U., Balasubramaniam B., Balamurugan K.; 2017. RACK-1, a multifaceted regulator is required for *C. elegans* innate immunity against *S. flexneri* M9OT infection. *Dev. Comp. Imm.* 74, 227-236

Massari M.E., Murre C.; 2000. Helix-loop-helix proteins: Regulators of transcription in eukaryotic organisms. *Mol. Cell. Biol.* 20(2), 429–440

Mathelier A., Zhao X., Zhang A.W., Parcy F., Worsley-Hunt R., Arenillas D.J., Buchman S., Chen C.Y., Chou A., Ienasescu H., Lim J., Shyr C., Tan G., Zhou M., Lenhard B., Sandelin A., Wasserman W.W..; 2014. JASPAR 2014: an extensively expanded and updated open-access database of transcription factor binding profiles. *Nucleic Acids Res.* 42(Database issue): D142-7

Matys V., Kel-Margoulis O.V., Fricke E., Liebich I., Land S., Barre-Dirrie A., Reuter I., Chekmenev D., Krull M., Hornischer K., Voss N., Stegmaier P., Lewicki-Potapov B., Saxel H., Kel A.E., Wingender E.; 2006. TRANSFAC and its module TRANSCompel: Transcriptional gene regulation in eukaryotes. *Nucleic Acids Res.* 34(Database issue): D108-10

McElwee J., Bubb K., Thomas J.H.; 2003. Transcriptional outputs of the *Caenorhabditis elegans* forkhead protein DAF□16. *Aging Cell* 2(2), 111-121

McGhee J.D., Sleumer M.C., Bilenky M., Wong K., McKay S.J., Goszczynski B., Tian H., Krich N.D., Khattra J., Holt R.A., Baillie D.L., Kohara Y., Marra M.A., Jones S.J.M., Moerman D.G., Robertson A.G.; 2007. The ELT-2 GATA-factor and the global regulation of transcription in the *C. elegans* intestine. *Dev. Biol.* 302(2), 627-645

McKay S.J., Johnsen R., Khattra J., Asano J., Baillie D.L., Chan S., Dube N., Fang L., Goszczynski B., Ha E., Halfnight E., Hollebakken R., Huang P., Hung K., Jensen V., Jones S.J.M., Kai H., Li D., Mah A., Marra M., McGhee J., Newbury R., Pouzyrev A., Riddle D.L., Sonnhammer E., Tian H., Tu D., Tyson J.R., Vatcher G., Warner A., Wong K., Zhao Z., Moerman D.G.; 2003. Gene expression profiling of cells, tissues,

and developmental stages of the nematode *C. elegans*. *Cold Spring Harb. Symp. Quant. Biol.* 68, 159-170

Meléndez A., Levine B.; 2009. Autophagy in *C. elegans*. *WormBook*, ed. The *C. elegans* Research Community

Mi H., Muruganujan A., Ebert D., Huang X., Thomas P.D.; 2019. PANTHER version 14: More genomes, a new PANTHER GO-slim and improvements in enrichment analysis tools. *Nucleic Acids Res.* 47(D1), D419-D426

Miles J., Scherz-Shouval R., van Oosten-Hawle P.; 2019. Expanding the organismal proteostasis network: Linking systemic stress signalling with the innate immune response. *Trends Biochem. Sci.* 44(11), 927-942

Minevich G., Park D.S., Blankenberg D., Poole R.J., Hobert O.; 2012. CloudMap: A cloud-based pipeline for analysis of mutant genome sequences. *Genetics* 192(4), 1249-1269

Miyata S., Begun J., Troemel E.R., Ausubel F.M.; 2008. DAF-16-dependent suppression of immunity during reproduction in *Caenorhabditis elegans*. *Genetics* 178(2), 903-918

Mizuhara E., Nakatani T., Minaki Y., Sakamoto Y., Ono Y., Takai Y.; 2005. MAGI1 recruits Dll1 to cadherin-based adherens junctions and stabilizes it on the cell surface. *J. Biol. Chem.* 280, 26499-26507

Montgomery M.K., Xu SQ., Fire A.; 1998. RNA as a target of double-stranded RNA-mediated genetic interference in *Caenorhabditis elegans*. *PNAS* 95(26), 15502-15507

Mori I., Ohshima Y.; 1995. Neural regulation of thermotaxis in *Caenorhabditis elegans*. *Nature* 376, 344–348

Morimoto R.I.; 2008. Proteotoxic stress and inducible chaperone networks in neurodegenerative disease and aging. *Genes & Dev.* 22, 1427-1438

Morley J.F., Brignull H.R., Weyers J.J., Morimoto R.I.; 2002. The threshold for polyglutamine-expansion protein aggregation and cellular toxicity is dynamic and influenced by aging in *Caenorhabditis elegans*. *PNAS* 99(16), 10417-10422

Morley J.F., Morimoto R.I.; 2003. Regulation of longevity in *Caenorhabditis elegans* by heat shock factor and molecular chaperones. *Mol. Biol. Cell* 15, 657-664

Morris J.Z., Tissenbaum H.A., Ruvkun G.; 1996. A phosphatidylinositol-3-OH kinase family member regulating longevity and diapause in *Caenorhabditis elegans*. *Nature* 382, 536–539

Mu H., Wang L., Zhao L.; 2016. HSP90 inhibition suppresses inflammatory response and reduces carotid atherosclerotic plaque formation in ApoE mice. *Cardiovasc. Ther.* 35(2): e12243

Murphy C.T., McCarroll S.A., Bargmann C.I., Fraser A., Kamath R.S., Ahringer J., Li H., Kenyon C.; 2003. Genes that act downstream of DAF-16 to influence the lifespan of *Caenorhabditis elegans*. *Nature* 424, 277-283

Murphy C.T., Hu P.J.; 2013. Insulin/insulin-like growth factor signalling in *C. elegans*. *WormBook*, ed. The *C. elegans* Research Community

Nair S.C., Toran E.J., Rimerman R.A., Hjermstad S., Smithgall T.E., Smith D.F.; 1996. A pathway of multi-chaperone interactions common to diverse regulatory proteins: Oestrogen receptor, Fes tyrosine kinase, heat shock transcription factor Hsf1, and the aryl hydrocarbon receptor. *Cell Stress Chaperones* 1(4), 237–250

Nandi D., Tahiliani P., Kumar A., Chandu D.; 2006. The ubiquitin-proteasome system. *J. Biosci.* 31, 137–155

Narasimhan K., Lambert S.A., Yang A.W.H., Riddell J., Mnaimneh S., Zheng H., Albu M., Najafabadi H.S., Reece-Hoyes J.S., Bass J.I.F., Walhout A.J.M., Weirauch M.T., Hughes T.R.; 2015. Mapping and analysis of Caenorhabditis elegans transcription factor sequence specificities. *eLife* 4: e06967

Nargund A.M., Pellegrino M.W., Fiorese C.J., Baker B.M., Haynes C.M.; 2012. Mitochondrial import efficiency of ATFS-1 regulates mitochondrial UPR activation. *Science* 337(6094), 587-590

Nguyen T.A., Smith B.R.C., Tate M.D., Belz G.T., Barrios M.H., Elgass K.D., Weisman A.S., Baker P.J., Preston S.P., Whitehead L., Garnham A., Lundie R.J., Smyth G.K., Pellegrini M., O'Keeffe M., Wicks I.P., Masters S.L., Hunter C.P., Pang K.C.; 2017. SIDT2 transports extracellular dsRNA into the cytoplasm for innate immune recognition. *Immunity* 47(3), 498-509

Nicholas H.R., Hodgkin J.; 2004. The ERK MAP kinase cascade mediates tail swelling and a protective response to rectal infection in *C. elegans*. *Curr. Biol.* 14(14), 1256-1261

Nigon V., Dougherty E.C.; 1949. Reproductive patterns and attempts at reciprocal crossing of *Rhabditis elegans maupas*, 1900, and *Rhabditis briggsae*. Dougherty and Nigon, 1949 (Nematoda: Rhabditidae). *J. Exp. Zool.* 112(3), 485-503

Niu W., Lu Z.J., Zhong M., Sarov M., Murray J.I., Brdlik C.M., Janette J., Chen C., Alves P., Preston E., Slightham C., Jiang L., Hyman A.A., Kim S.K., Waterston R.H., Gerstein M., Snyder M., Reinke V.; 2011. Diverse transcription factor binding features revealed by genome-wide ChIP-seq in *C. elegans*. *Genome Res.* 21, 245-254

Noble T., Stieglitz J., Srinivasan S.; 2013. An integrated serotonin and octopamine neuronal circuit directs the release of an endocrine signal to control *C. elegans* body fat. *Cell Met.* 18(5), 672-684

Nourry C., Grant S.G.N., Borg J.-P.; 2003. PDZ Domain Proteins: Plug and Play! *Science's STKE* 2003(179), re7

O'Brien D., van Oosten-Hawle P.; 2016. Regulation of cell-non-autonomous proteostasis in metazoans. *Essays Biochem.* 60(2), 133–142

O'Brien D., Jones L.M., Good S., Miles J., Vijayabaskar M.S., Aston R., Smith C.E., Westhead D.R., van Oosten-Hawle P.; 2018. A PQM-1-mediated response triggers

transcellular chaperone signalling and regulates organismal proteostasis. *Cell Reports* 23(13), 3905-3919

Ogg S., Paradis S., Gottlieb S., Patterson G.I., Lee L., Tissenbaum H.A., Ruvkun G.; 1997. The Fork head transcription factor DAF-16 transduces insulin-like metabolic and longevity signals in *C. elegans*. *Nature* 389, 994–999

Owusu-Ansah E., Song W., Perrimon N.; 2013. Muscle mitohormesis promotes longevity via systemic repression of insulin signalling. *Cell* 155(3), 699-712

Pelham H.; 1985. Activation of heat-shock genes in eukaryotes. *Trends Genet.*1, 31-35

Pelham H.R.B.; 1989. Control of protein exit from the endoplasmic reticulum. *Annu. Rev. Cell Biol.* 5, 1-23

Pellegrino M.W., Nargund A.M., Kirienko N.V., Gillis R., Fiorese C.J., Haynes C.M.; 2014. Mitochondrial UPR-regulated innate immunity provides resistance to pathogen infection. *Nature* 516, 414–417

Picard D.; 2002. Heat-shock protein 90, a chaperone for folding and regulation. *Cell. Mol. Life Sci.* 59, 1640–1648

Poppek D., Grune T.; 2006. Proteasomal Defence of Oxidative Protein Modifications. *Antiox. & Redox Sig.* 8(1-2) 173-184

Powers E.T., Morimoto R.I., Dillin A., Kelly J.W., Balch W.E.; 2009. Biological and chemical approaches to diseases of proteostasis deficiency. *Annu. Rev. Biochem.* 78, 959-991

Powers E.T., Balch W.E.; 2013. Diversity in the origins of proteostasis networks — a driver for protein function in evolution. *Nat. Revs. Mol. Cell Biol.* 14, 237–248

Pradel E., Zhang Y., Pujol N., Matsuyama T., Bargmann C.I., Ewbank J.J.; 2007. Detection and avoidance of a natural product from the pathogenic bacterium *Serratia marcescens* by *Caenorhabditis elegans*. *PNAS* 104(7), 2295-2300

Prahlad V., Cornelius T., Morimoto R.I.; 2008. Regulation of the cellular heat shock response in *Caenorhabditis elegans* by thermosensory neurons. *Science* 320(5877), 811-814

Prahlad V., Morimoto R.I.; 2011. Neuronal circuitry regulates the response of *Caenorhabditis elegans* to misfolded proteins. *PNAS* 108(34), 14204-14209

Qabazard B., Li L., Gruber J., Peh M.T., Ng L.F., Kumar S.D., Rose P., Tan C.-H., Dymock B.W., Wei F., Swain S.C., Halliwell B., Stürzenbaum S.R., Moore P.K.; 2014. Hydrogen sulphide is an endogenous regulator of aging in *Caenorhabditis elegans*. *Antiox. Redox Sig.* 20(16), 2621-2630

Queitsch C., Sangster T.A., Lindquist S.; 2002. Hsp90 as a capacitor of phenotypic variation. *Nature* 417, 618–624

Ramot D., MacInnis B.L., Goodman M.B.; 2008. Bidirectional temperature-sensing by a single thermosensory neuron in *C. elegans*. *Nature Neurosci.* 11, 908–915

Reboul J., Ewbank J.E.; 2016. GPCRs in invertebrate innate immunity. *Biochem. Pharmacol.* 114, 82-87

Reddy K.C., Dror T., Sowa J.N., Panek J., Chen K., Lim E.S., Wang D., Troemel E.R.; 2017. An intracellular pathogen response pathway promotes proteostasis in *C. elegans*. *Curr. Biol.* 27(22), 3544-3553.e5

Reddy K.C., Dror T., Underwood R.S., Osman G.A., Elder C.R., Desjardins C.A., Cuomo C.A., Barkoulas M., Troemel E.R.; 2019. Antagonistic paralogs control a switch between growth and pathogen resistance in *C. elegans*. *PLoS Pathog.* 15(1): e1007528

Reinke V., Krause M., Okkema P.; 2013. Transcriptional regulation of gene expression in *C. elegans*. WormBook, ed. The *C. elegans* Research Community

Rhoads R.E., Dinkova T.D., Korneeva N.L.; 2006. Mechanism and regulation of translation in *C. elegans*. WormBook: The Online Review of *C. elegans* Biology. Pasadena (CA): WormBook; 2005-2018

Richardson C.E., Kooistra T., Kim D.H.; 2010. An essential role for XBP-1 in host protection against immune activation in *C. elegans*. *Nature* 463, 1092–1095

Richardson C.E., Kinkel S., Kim D.H.; 2011. Physiological IRE-1-XBP-1 and PEK-1 signalling in *Caenorhabditis elegans* larval development and immunity. *PLoS Genet.* 7(11): e1002391

Richmond J.E., Davis W.S. Jorgensen E.M.; 1999. UNC-13 is required for synaptic vesicle fusion in *C. elegans*. *Nature Neurosci.* 2, 959-964

Ritossa F.; 1962. A new puffing pattern induced by temperature shock and DNP in *Drosophila*. *Experimentia* 18, 571–573

Röhl A., Rohrberg J., Buchner J.; 2013. The chaperone Hsp90: Changing partners for demanding clients. *Trends Biochem. Sci.* 38(5), 253-262

Ron D., Walter P.; 2007. Signal integration in the endoplasmic reticulum unfolded protein response. *Nat. Revs. Mol. Cell Biol.* 8, 519–529

Rose A.M., Baillie D.L.; 1979. The effect of temperature and parental age on recombination and non-disjunction in *Caenorhabditis elegan*s. *Genetics* 92, 409-418

Rutherford S.L., Lindquist S.; 1998. Hsp90 as a capacitor for morphological evolution. *Nature* 396, 336–342

Sammut M., Cook S.J., Nguyen K.C.Q., Felton T., Hall D.H., Emmons S.W., Poole R.J., Barrios A.; 2015. Glia-derived neurons are required for sex-specific learning in *C. elegans*. *Nature* 526, 385–390

Sarge K.D., Murphy S.P., Morimoto R.I.; 1993. Activation of heat shock gene transcription by Heat Shock Factor 1 involves oligomerization, acquisition of DNA-binding activity, and nuclear localization and can occur in the absence of stress. *Mol. Cell. Biol.* 13(3), 1392-1407

Sasaki H., Sato T., Yamauchi N., Okamoto T., Kobayashi D., Iyama S., Kato J., Matsunaga T., Takimoto R., Takayama T., Kogawa K., Watanabe N., Niitsu Y.; 2002.

Induction of heat shock protein 47 synthesis by TGF-ß and IL-1ß via enhancement of the heat shock element binding activity of heat shock transcription factor 1. *J. Immunol.* 168(10), 5178-5183

Scherz-Shouval R., Santagata S., Mendillo M.L., Sholl L.M., Ben-Aharon I., Beck A.H., Dias-Santagata D., Koeva M., Stemmer S.M., Whitesell L., Lindquist S.; 2014. The reprogramming of tumour stroma by HSF1 is a potent enabler of malignancy. *Cell* 158(3), 564-578

Schott D.H., Cureton D.K., Whelan S.P., Hunter C.P.; 2005. An antiviral role for the RNA interference machinery in *Caenorhabditis elegans*. *PNAS* 102(51), 18420-18424

Schröder M., Kaufman R.J.; 2005. ER stress and the unfolded protein response. Mutation Res. 569(1–2), 29-63

Schulenburg H., Hoeppner M.P., Weiner J., Bornberg-Bauer E.; 2008. Specificity of the innate immune system and diversity of C-type lectin domain (CTLD) proteins in the nematode *Caenorhabditis elegans*. *Immunobiol.* 213(3-4), 237-250

Seglen P.O., Bohley P.; 1992. Autophagy and other vacuolar protein degradation mechanisms. *Experientia* 48, 158–172

Seyednasrollah F., Laiho A., Elo L.L.; 2015. Comparison of software packages for detecting differential expression in RNA-seq studies. *Briefs. Bioinf.* 16(1), 59–70

Shao L.-W., Niu R., Liu Y.; 2016. Neuropeptide signals cell non-autonomous mitochondrial unfolded protein response. *Cell Res.* 26, 1182–1196

Shapira M., Hamlin B.J., Rong J., Chen K., Ronen M., Tan M.-W.; 2006. A conserved role for a GATA transcription factor in regulating epithelial innate immune responses. PNAS 103(38), 14086-14091

Shemesh N., Shai N., Ben□Zvi A.; 2013. Germline stem cell arrest inhibits the collapse of somatic proteostasis early in *Caenorhabditis elegans* adulthood. *Aging Cell* 12(5), 814-822

Shen X., Ellis R.E., Lee K., Liu C.-Y., Yang K., Solomon A., Yoshida H., Morimoto R., Kurnit D.M., Mori K., Kaufman R.J.; 2001. Complementary signalling pathways regulate the unfolded protein response and are required for *C. elegans* development. *Cell* 107(7), 893-903

Shen J., Chen X., Hendershot L., Prywes R.; 2002. ER stress regulation of ATF6 localization by dissociation of BiP/GRP78 binding and unmasking of Golgi localization signals. *Dev. Cell* 3(1), 99-111

Shen X., Ellis R.E., Sakaki K., Kaufman R.J.; 2005. Genetic interactions due to constitutive and inducible gene regulation mediated by the unfolded protein response in *C. elegans*. *PLoS Genet.* 1(3): e37

Shen L., Hu Y., Cai T., Lin X., Wang D.; 2010. Regulation of longevity by genes required for the functions of AIY interneuron in nematode *Caenorhabditis elegans*. *Mechs. Ageing Dev*. 131(11–12), 732-738

Shi Y., Mosser D.D., Morimoto R.I.; 1998. Molecular chaperones as HSF1-specific transcriptional repressors. *Genes & Dev.* 12,654-666

Shivers R.P., Pagano D.J., Kooistra T., Richardson C.E., Reddy K.C., Whitney J.K., Kamanzi O., Matsumoto K., Hisamoto N., Kim D.H.; 2010. Phosphorylation of the conserved transcription factor ATF-7 by PMK-1 p38 MAPK regulates innate immunity in *Caenorhabditis elegans*. *PLoS Genet.* 6(4): e1000892

Shpilka T., Haynes C.M.; 2018. The mitochondrial UPR: Mechanisms, physiological functions and implications in ageing. *Nat. Revs. Mol. Cell Biol.* 19, 109–120

Singh V., Aballay A.; 2006. Heat-shock transcription factor (HSF)-1 pathway required for *Caenorhabditis elegans* immunity. *PNAS* 103(35), 13092-13097

Sollars V., Lu X., Xiao L., Wang X., Garfinkel M.D., Ruden D.M.; 2003. Evidence for an epigenetic mechanism by which Hsp90 acts as a capacitor for morphological evolution. *Nature Genet.* 33, 70–74

Somogyvári M., Gecse E., Sőti C.; 2018. DAF-21/Hsp90 is required for *C. elegans* longevity by ensuring DAF16/FOXO isoform A function. *Scientific Reports* 8(12048), DOI:10.1038/s41598-018-30592-6

Soneson C., Delorenzi M.; 2013. A comparison of methods for differential expression analysis of RNA-seq data. *BMC Bioinformatics* 14:91

Sőti C., Csermely P.; 2000. Molecular chaperones and the aging process. *Biogerontology* 1, 225–233

Speese S., Petrie M., Schuske K., Ailion M., Ann K., Iwasaki K., Jorgensen E.M., Martin T.F.J.; 2007. UNC-31 (CAPS) is required for dense-core vesicle but not synaptic vesicle exocytosis in *Caenorhabditis elegans*. *J. Neurosci.* 27(23), 6150-6162

Stadtman E.R.; 1992. Protein oxidation and aging. *Science* 257(5074), 1220-1224

Stiernagle, T (2006). Maintenance of *C. elegans*. WormBook, ed. The *C. elegans* Research Community, WormBook, doi/10.1895/wormbook.1.101.1, http://www.wormbook.org

Stinchcomb D.T., Shaw J.E., Carr S.H., Hirsh D.; 1985. Extrachromosomal DNA Transformation of *Caenorhabditis elegans*. *Mol. Cell. Biol.* 5, 3484-3496

Strader C.D., Fong T.M., Tota M.R., Underwood D.; 1994. Structure and function of G protein-coupled receptors. *Ann. Rev. Biochem*. 63, 101-132

Styer K.L., Singh V., Macosko E., Steele S.E., Bargmann C.I., Aballay A.; 2008. Innate immunity in *Caenorhabditis elegans* is regulated by neurons expressing NPR-1/GPCR. *Science* 322(5900), 460-464

Sulston J.E., Brenner S.; 1974. The DNA of *Caenorhabditis elegans*. *Genetics* 77(1), 95-104

Sulston J.E., Horvitz H.R.; 1977. Post-embryonic cell lineages of the nematode, *Caenorhabditis elegans*. *Dev. Biol.* 56, 110-156

Sulston J.E., Schierenberg E., White J.G., Thomson J.N.; 1983. The embryonic cell lineage of the nematode *Caenorhabditis eleg*ans. *Dev. Biol*. 100(1), 64-119

Sun J., Singh V., Kajino-Sakamoto R., Aballay A.; 2011. Neuronal GPCR controls innate immunity by regulating noncanonical unfolded protein response genes. *Science* 332(6030), 729-732

Sun L., Edelmann F.T., Kaiser C.J.O., Papsdorf K., Gaiser A.M., Richter K.; 2012 (a). The lid domain of *Caenorhabditis elegans* Hsc70 influences ATP turnover, cofactor binding and protein folding activity. *PLoS One* 7(3): e33980

Sun J., Liu Y., Aballay A.; 2012 (b). Organismal regulation of XBP□1□mediated unfolded protein response during development and immune activation. *EMBO Rep*. 13, 855-860

Suomalainen A., Elo J.M., Pietiläinen K.H., Hakonen A.H., Sevastianova K., Korpela M., Isohanni P., Marjavaara S.K., Tyni T., Kiuru-Enari S., Pihko H., Darin N., Õunap K., Kluijtmans L.A.J., Paetau A., Buzkova J., Bindoff L.A., Annunen-Rasila J., Uusimaa J., Rissanen A., Yki-Järvinen H., Hirano M., Tulinius M., Smeitink J., Tyynismaa H.; 2011. FGF-21 as a biomarker for muscle-manifesting mitochondrial respiratory chain deficiencies: a diagnostic study. *Lancet Neurol.* 10(9), 806-818

Tabara H., Grishok A., Mello C.C.; 1998. RNAi in *C. elegans*: Soaking in the genome sequence. *Science* 282(5388), 430-431

Taipale M., Jarosz D.F., Lindquist S.; 2010. HSP90 at the hub of protein homeostasis: emerging mechanistic insights. *Nat. Revs. Mol. Cell Biol.* 11, 515–528

Tan M.-W., Mahajan-Miklos S., Ausubel F.M.; 1999. Killing of *Caenorhabditis elegans* by *Pseudomonas aeruginosa* used to model mammalian bacterial pathogenesis. *PNAS* 96(2), 715-720

Tatum M.C., Ooi F.K., Chikka M.R., Chauve L., Martinez-Velazquez L.A., Steinbusch H.W.M., Morimoto R.I., Prahlad V.; 2015. Neuronal serotonin release triggers the heat shock response in *C. elegans* in the absence of temperature increase. *Curr. Biol*. 25(2), 163-174

Tavernarakis N., Wang S.L., Dorovkov M., Ryazanov A., Driscoll M.; 2000. Heritable and inducible genetic interference by double-stranded RNA encoded by transgenes. *Nature Genet.* 24, 180–183

Taylor R.C., Dillin A.; 2013. XBP-1 is a cell-nonautonomous regulator of stress resistance and longevity. *Cell* 153(7), 1435-1447

Taylor R.C., Berendzen K.M., Dillin A.; 2014. Systemic stress signalling: understanding the cell non-autonomous control of proteostasis. *Nat. Revs. Mol. Cell Biol.* 15, 211–217

Tepper R.G., Ashraf J., Kaletsky R., Kleemann G., Murphy C.T., Bussemaker H.J.; 2013. PQM-1 complements DAF-16 as a key transcriptional regulator of DAF-2-mediated development and longevity. *Cell* 154(3), 676-690

Timmons L., Fire A.; 1998. Specific interference by ingested dsRNA. *Nature* 395, p854

Timmons L., Court D.L., Fire A.; 2001. Ingestion of bacterially expressed dsRNAs can produce specific and potent genetic interference in *Caenorhabditis elegans*. *Gene* 263(1-2), 103-112

Todd D.J., Lee A.-H., Glimcher A.H.; 2008. The endoplasmic reticulum stress response in immunity and autoimmunity. *Nat. Revs. Immunol.* 8, 663–674

Tong X.-J., López-Soto E.J. Li L., Liu H., Nedelcu D., Lipscombe D., Hu Z., Kaplan J.M.; 2017. Retrograde synaptic inhibition is mediated by α-Neurexin binding to the α2δ subunits of N-type calcium channels. *Neuron* 95(2), 326-340.e5

Troemel E.R., Chu S.W., Reinke V., Lee S.S., Ausubel F.M., Kim D.H.; 2006. p38 MAPK regulates expression of immune response genes and contributes to longevity in *C. elegans*. *PLoS Genet.* 2(11): e183

Troemel E.R., Félix M.-A., Whiteman N.K., Barrière A., Ausubel F.M.; 2008. Microsporidia are natural intracellular parasites of the nematode *Caenorhabditis elegans*. *PLoS Biol.* 6(12), 2736-2752

Tullet J.M.A., Hertweck M., An J.H., Baker J., Hwang J.Y., Liu S., Oliveira R.P., Baumeister R., Blackwell T.K.; 2008. Direct inhibition of the longevity-promoting factor SKN-1 by insulin-like signalling in *C. elegans*. *Cell* 132(6), 1025-1038

Urano F., Calfon M., Yoneda T., Yun C., Kiraly M., Clark S.G., Ron D.; 2002. A survival pathway for *Caenorhabditis elegans* with a blocked unfolded protein response. *J. Cell Biol.* 158(4), 639–646

van Oosten-Hawle P., Porter R.S., Morimoto R.I.; 2013. Regulation of organismal proteostasis by transcellular chaperone signalling. *Cell* 153, 1366-1378

Vilchez D., Morantte I., Liu Z., Douglas P.M., Merkwirth C., Rodrigues A.P.C., Manning G., Dillin A.; 2012. RPN-6 determines *C. elegans* longevity under proteotoxic stress conditions. *Nature* 489, 263–268

Viswanathan M., Kim S.K., Berdichevsky A., Guarente L.; 2005. A role for SIR-2.1 regulation of ER stress response genes in determining *C. elegans* life span. *Dev. Cell* 9(5), 605-615

Vitale A., Denecke J.; 1999. The endoplasmic reticulum - gateway of the secretory pathway. *The Plant Cell* 11, 615–628

Voellmy R., Boellmann F.; 2007. Chaperone regulation of the heat shock protein response. In: Csermely P., Vígh L. (eds.) Molecular aspects of the stress response: Chaperones, membranes and networks. *Adv. Exp. Med. Biol.* 594 (Springer, New York, NY)

Wallace E.W.J., Kear-Scott J.L., Pilipenko E.V., Schwartz M.H., Laskowski P.R., Rojek A.E., Katanski C.D., Riback J.A., Dion M.F., Franks A.M., Airoldi E.M., Pan T., Budnik B.A., Drummond D.A.; 2015. Reversible, specific, active aggregates of endogenous proteins assemble upon heat stress. *Cell* 162(6), 1286-1298

Walter P., Ron D.; 2011. The unfolded protein response: From stress pathway to homeostatic regulation. *Science* 334(6059), 1081-1086

Wang M.C., O'Rourke E.J., Ruvkun G.; 2008. Fat metabolism links germline stem cells and longevity in *C. elegans*. *Science* 322(5903), 957-960

Wang Z., Gerstein M., Snyder M.; 2009. RNA-Seq: A revolutionary tool for transcriptomics. *Nat. Revs. Genet.* 10, 57–63

Warde-Farley D., Donaldson S.L., Comes O., Zuberi K., Badrawi R., Chao P., Franz M., Grouios C., Kazi F., Lopes C.T., Maitland A., Mostafavi S., Montojo J., Shao Q., Wright G., Bader G.D., Morris Q.; 2010. The GeneMANIA prediction server: Biological network integration for gene prioritization and predicting gene function. *Nucleic Acids Res.* 38(Supp.), W214-220

Wegewitz V., Schulenburg H., Streit A.; 2008. Experimental insight into the proximate causes of male persistence variation among two strains of the androdioecious *Caenorhabditis elegans* (Nematoda). *BMC Ecology* 8(12), DOI:10.1186/1472-6785-8-12

Weirauch M.T., Yang A., Albu M., Cote A.G., Montenegro-Montero A., Drewe P., Najafabadi H.S., Lambert S.A., Mann I., Cook K., Zheng H., Goity A., van Bakel H., Lozano J.C., Galli M., Lewsey M.G., Huang E., Mukherjee T., Chen X., Reece-Hoyes J.S., Govindarajan S., Shaulsky G., Walhout A.J., Bouget F.Y., Ratsch G., Larrondo L.F., Ecker J.R., Hughes T.R.; 2014. Determination and inference of eukaryotic transcription factor sequence specificity. *Cell* 158(6), 1431-1443

Whangbo J., Kenyon C.; 1999. A Wnt signalling system that specifies two patterns of cell migration in *C. elegans*. *Mol. Cell* 4(5), 851-858

White J.G., Southgate E., Thomson J.N., Brenner S.; 1986. The structure of the nervous system of the nematode *Caenorhabditis elegans*. *Phil. Trans. Royal Soc. London; Series B, Biol. Sci.* 314(1165) 1-340

Whitesell L., Lindquist S.L.; 2005. HSP90 and the chaperoning of cancer. *Nat. Revs. Cancer* 5, 761–772

Wicks S.R., Yeh R.T., Gish W.R., Waterston R.H., Plasterk R.H.A.; 2001. Rapid gene mapping in *Caenorhabditis elegans* using a high density polymorphism map. *Nature Genetics* 28, 160–164

Wiech H., Buchner J., Zimmermann R., Jakob U.; 1992. Hsp90 chaperones protein folding *in vitro*. *Nature* 358, 169–170

Wilkins C., Dishongh R., Moore S.C., Whitt M.A., Chow M., Machaca K.; 2005. RNA interference is an antiviral defence mechanism in *Caenorhabditis elegans*. *Nature* 436, 1044–1047

Williams K.W., Liu T., Kong X., Fukuda M., Deng Y., Berglund E.D., Deng Z., Gao Y., Liu T., Sohn J.-W., Jia L., Fujikawa T., Kohno D., Scott M.M., Lee S., Lee C.E., Sun K., Chang Y., Scherer P.E., Elmquist J.K.; 2014. Xbp1s in Pomc neurons connects ER stress with energy balance and glucose homeostasis. *Cell Met.* 20(3), 471-482

Winston W.M., Molodowitch C., Hunter C.P.; 2002. Systemic RNAi in *C. elegans* requires the putative transmembrane protein SID-1. *Science* 295(5564), 2456-2459

Wolkow C.A., Kimura K.D., Lee M.-S., Ruvkun G.; 2000. Regulation of *C. elegans* life-span by insulinlike signalling in the nervous system. *Science* 290(5489), 147-150

Xu Y.-M., Huang D.-Y., Chiu J.-F., Lau A.T.Y.; 2012. Post-translational modification of human heat shock factors and their functions: A recent update by proteomic approach. *J. Proteome Res.* 11(5), 2625-2634

Yamamoto K., Yoshida H., Kokame K., Kaufman R.J., Mori K.; 2004. Differential contributions of ATF6 and XBP1 to the activation of endoplasmic reticulum stress-responsive *cis*-acting elements ERSE, UPRE and ERSE-II. *J. Biochem*. 136(3), 343–350

Yee C., Yang W., Hekimi S.; 2014. The intrinsic apoptosis pathway mediates the pro-longevity response to mitochondrial ROS in *C. elegans*. *Cell* 157(4), 897-909

Yoneda T., Benedetti C., Urano F., Clark S.G., Harding H.P., Ron D.; 2004. Compartment-specific perturbation of protein handling activates genes encoding mitochondrial chaperones. *J. Cell Sci.* 117, 4055-4066

Zhang F., Bhattacharya A., Nelson J.C., Abe N., Gordon P., Lloret-Fernandez C., Maicas M., Flames N., Mann R.S., Colón-Ramos D.A., Hobert O.; 2014. The LIM and POU homeobox genes *ttx-3* and *unc-86* act as terminal selectors in distinct cholinergic and serotonergic neuron types. *Development* 141, 422-435

Zhang J., Liu J., Norris A., Grant B.D., Wang X.; 2018. A novel requirement for ubiquitin-conjugating enzyme UBC-13 in retrograde recycling of MIG-14/Wntless and Wnt signaling. *Mol. Biol. Cell* 29(17)

Zhao H., Nonet M.L.; 2000. A retrograde signal is involved in activity-dependent remodelling at a *C. elegans* neuromuscular junction. *Development* 127, 1253-1266
Zhao Q., Wang J., Levichkin I.V., Stasinopoulos S., Ryan M.T., Hoogenraad N.J.; 2002. A mitochondrial specific stress response in mammalian cells. *EMBO J.* 21(17), 4411-4419

Zhong M., Niu W., Lu Z.J., Sarov M., Murray J.I., Janette J., Raha D., Sheaffer K.L., Lam H.Y.K., Preston E., Slightham C., Hillier LD.W., Brock T., Agarwal A., Auerbach R., Hyman A.A., Gerstein M., Mango S.E., Kim S.K., Waterston R.H., Reinke V., Snyder M.; 2010. Genome-wide identification of binding sites defines distinct functions for *Caenorhabditis elegans* PHA-4/FOXA in development and environmental response. *PLoS Genet.* 6(2): e1000848

Zou J., Guo Y., Guettouche T., Smith D.F., Voellmy R.; 1998. Repression of heat shock transcription factor HSF1 activation by HSP90 (HSP90 complex) that forms a stress-sensitive complex with HSF1. *Cell* 94(4), 471-480

Zou J., Crews F.; 2006. CREB and NF-κB transcription factors regulate sensitivity to excitotoxic and oxidative stress induced neuronal cell death. *Cell. Mol. Neurobiol.* 26, 383-403